IN VIVO IN VITRO EVALUATION OF PREDICTIVE ORAL CONTROLLED RELEASE FORMULATION TO THE LOWER INTESTINAL TRACT

A thesis submitted to the University of Strathclyde for the degree of Doctor of Philosophy in the

Faculty of Science

January, 2012

By

Mohammad Siddique Qadir

Strathclyde Institute of Pharmacy and Biomedical Sciences

University of Strathclyde

Glasgow, United Kingdom

DECLARATION OF AUTHOR'S RIGHTS

DEDICATION

To my family

ACKNOWLEDGEMENTS

In the name of Allah, the most gracious, the most merciful. I would like to thank following people for their contribution during my PhD:

I would like to express my sincerest gratitude to my supervisors, Dr Fiona McInnes and Professor Howard N.E. Stevens for supporting me throughout my PhD with their patience and knowledge whilst allowing me the room to work in my own way.

I would also like to thank my industrial supervisors Dr Paul Gellert and Dr Martin Wikberg for their constant support and useful discussions.

I would like to thank Dr Alexander Mullen for his help during the last stage of my thesis and Dr David G. Watson for his help during HPLC method development.

The technical and workshop staff of the SIPBS for all their assistance.

I am grateful to the secretarial, computer and library staff in the University of Strathclyde for assisting me in many different ways.

I am indebted to thank Astra Zeneca and Strathclyde institute of Pharmacy and Biomedical Sciences for their financial support to pursue my PhD degree.

In my daily work I have been blessed with a friendly and cheerful group of fellow students, I would like to thank my colleagues who work in SIPBS for their friendly behaviour and help.

Finally, my special appreciation goes to my family for their constant love and support throughout my life.

ABSTRACT

The aim of the current study was to design a predictable oral controlled release formulation which could be used as a pulsatile or targeted site delivery system in the large intestine using the methodology of press coating to situate a polymer barrier around an inner core tablet.

In vitro gravimetric hydration and erosion studies were initially performed on the different pharmaceutical excipients however, hydroxypropylmethyl cellulose (HPMC) or sodium CMC exhibited more cohesive gel structure compared to the other polymers and selected as potential excipients for future studies as a barrier layer. A novel Texture Analyser (TA) method was developed as a time saving approach to screen proposed formulations in terms of gel layer strength which could correlate with in vivo forces published data. A new gravimetric hydration and erosion disc method was developed and used which helped to reduce laborious and time consuming erosion studies in short time. A good correlation was demonstrated between erosion and gel strength (using TA) to quantify the performance of different HPMC grades as a rate controlling barrier layer.

In order to predict the quantity of HPMC required to form an eroding barrier layer, a new mathematical method was developed for the prediction of lag times using the polymer erosion as a main predictor. The *in vitro* dissolution of model drug theophylline from the inner core of press coated tablets having predicted lag times 180, 240 and 300 minutes revealed a reasonably good correlation between actual and predictive lag times, demonstrating that the new predictable model has a potential in future studies for pulsatile or colon delivery in press coated tablets.

Magnetic resonance imaging (MRI) was used to understand the internal processes and sequence of events that underlie the process of hydration, swelling, gelling and eventually a pulse release from pulsatile release tablets with predicted lag time 3 and 5 hours.

The press coated formulations (predictive lag time 3 and 5 hours) performed successfully in the dog using gamma scintigraphy to identify the time and site of pulse in the gastrointestinal tract.

PUBLICATIONS

M.Qadir, H.N.E. Stevens, P. Gellert, M. Wikberg , F. McInnes. Probing hydrating gel layers using the texture analyser. 36th Annual meeting and exposition of the controlled release society, 379 (2009).

M.Qadir, H.N.E. Stevens, P. Gellert, M. Wikberg , F. McInnes.Correlation between erosion and hydrating gel strength. UK-PharmSci Conference 2010. Abstract #235.

M.Qadir, H.N.E. Stevens, P. Gellert, M. Wikberg , F. McInnes.Prediction of lag time for an oral delivery system controlled by polymer erosion. FIP Pharmaceutical Sciences 2010 World Congress in Association with the AAPS Annual Meeting and Exposition. Poster#M1107.

ACRONYMS

$AUC_{0\text{-}6dis}$	Area under the curve from time of dosing to 6 hour post disintegration
CA	Colonic arrival
C_{max}	Maximum plasma concentration
CMC	Carboxymethylcellulose
CR	controlled-release
GE	Gastric emptying
GI tract	Gastrointestinal tract
H	Hour
HPMC	Hydroxypropylmethyl cellulose
IVIVC	*In vitro in vivo* correlation
K_E	Elimination rate constant
LV	Low-viscosity
MB_q	Megabecquerel
mg	Milligram
min	Minute
ml	Millilitre
mm	Millimetre
MMC	Migrating motor complex
mPa	Milli Pascal
MPa	Megapascal
MRI	Magnetic resonance imaging
N	Newton
NMR	Nuclear magnetic resonance
pa	Pascal
PC	Personal computer
pH	Potential hydrogen
PLT	Predicted lag time
rpm	Revolution per minute

SA/VOL	Surface area to volume
sec	Second
SITT	Small intestine transit time
TA	Texture analyser
T_{lag}	Time of first appearance of drug in plasma
T_{max}	Time to reach maximum concentration
USP	United States Pharmacopoeia
UV	Ultra violet
µg	Microgram
µl	Microlitre

TABLE OF CONTENTS

CHAPTER 1

GENERAL INTRODUCTION

Delivering medicine orally is the easiest, most convenient, and popular route of taking medicines. Advancements in technology and the availability of new excipients and drug entities have diversified the field of drug delivery; however per-oral drug delivery still holds its position as a main form of delivery system to the human body (Aulton, 2007).

The purpose of any route of administration is to deliver a drug to the site of action. In the case of the oral route, delivery to the target organ depends on the release of the drug from the dosage form, its subsequent solubilisation, the rate and extent of absorption and then its distribution through blood to the site of action, as opposed to intravenous route where drug is directly available for circulation and distribution (Gennaro, 2005).

Per-oral drug delivery is considered most popular route of drug delivery because of patient acceptability, economical, convenience and there is no need for sterile equipment for manufacture. Conventional dosage forms release their content immediately after administration, with the drug presumed to be instantly available for absorption to the systematic circulation. Modified release formulations are described as per-oral dosage forms which continuously release drug at rates which are sufficiently controlled to provide periods of prolonged therapeutic action following each administration of a single dose (Aulton, 2007). A variety of terms are in place to describe modified release systems. Figure 1.1 shows typical *in vivo* drug release profiles of immediate release, extended release and delayed release formulations.

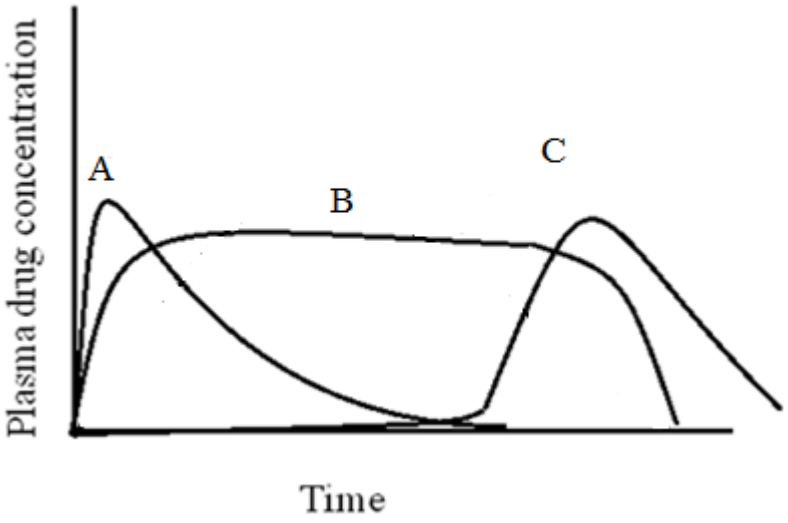

Figure 1.1 Typical drug release profiles following oral administration: A, immediate release; B, extended release; C, delayed release (Aulton, 2007).

Extended release indicates initial release to provide sufficient therapeutic dose, and then gradual release over an extended period to maintain plasma concentration. The consistent delivery of drug in an extended fashion provides some considerable benefits. Some of them are the avoidance of the typical plasma peak-trough fluctuations, reduced administration frequency, resulting improved patient compliance and lowered overall drug dose required within a given therapy.

Delayed/pulsatile release is defined as a dosage form which does not release its contents immediately; rather it liberates its drug content after a programmed lag phase starting at the time of the administration e.g. enteric coated dosage form or colonic drug delivery. At present considerable attention has been focused on colon delivery in that it could improve the treatment and prevention of inflammatory bowel disease (IBD) and colorectal adenocarcinoma. Additionally, colon delivery could be a possible strategy to increase the oral bioavailability of those drugs which are more prone to enzymatic degradation in the small intestine rather than in the large intestine. Furthermore, although having moderate absorption properties, the large

intestine is currently recognised as a gateway to the systematic circulation. The oral bioavailability of peptides, proteins, oligonucleotides, and nucleic acid has been hypothesised to be increased by colonic release due to less hostile conditions like the absence of acidic environment and proteolytic enzymes when compared to the stomach and the small intestine (Bourgeois et al., 2005). It is believed that due to the colon's longer transit time the low solubility drugs could have a better chance for dissolution and absorption if formulation happens to overcome upper GI tract barriers. Furthermore, through colonic drug delivery direct treatment at the site of action is possible with reduced systemic side effects. Additionally, the epithelium of the colon compared to the small intestine has low levels of membrane-bound metabolic enzymes known as cytochromes notably cytochrome P450, which are capable of metabolizing a host of drug molecules. This means that targeting the drugs to the colon may lead to higher bioavailability, indeed this concept was demonstrated using simvastatin. The bioavailability of simvastatin was three times higher when it was delivered to the lower gut (delayed release) compared to the upper gastrointestinal tract (immediate release) (McConnell et al., 2009).

The principle aim of this thesis will be the design of an oral controlled release formulation targeting release in the large intestine. In depth characterisation of the process of hydration and erosion will be used to define the effects of varying combinations of excipients on the timing and location of drug release. Development and use of *in vitro* models will enable the design of appropriate formulations which achieve optimised drug release and *in vivo* performance of the system. Optimised formulations will be characterised *in vivo,* in the dog model, using pharmacoscintigraphy to evaluate whether behaviour observed *in vitro* correlates with *in vivo* performance.

1.1 HUMAN DIGESTIVE SYSTEM

In order to understand the performance of oral formulations, one has to understand the human digestive system through which these formulations have to travel to reach the site of absorption. The main functions of the digestive system include: ingestion

of food, digestion and absorption of the products of digestion, transport of food through the gastrointestinal (GI) tract at a rate that allows optimal digestion and absorption, the secretion of fluid, salt, and digestive enzymes, and removal of indigestible remains from the body (defecation) (Johnson, 2000). The main anatomical features of the GI tract are shown in Figure 1.2.

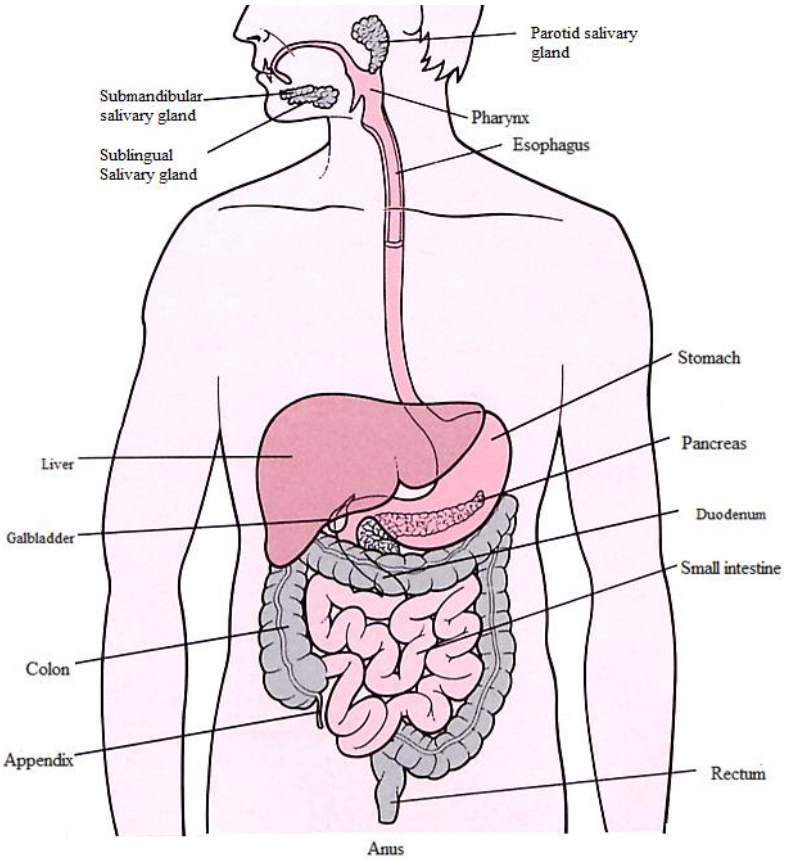

Figure 1.2 Different parts of GI tract (Youngson, 2000).

The GI tract is composed of a long muscular tube approximately 6m long with varying diameter along its length. It extends from the mouth to the anus and is anatomically composed of the oral cavity, pharynx, oesophagus, stomach, small intestine (duodenum, jejunum, and ileum), large intestine or colon (ascending, transverse, and sigmoid colon), rectum and anal canal.

1.1.1 Oesophagus

The mouth is the first contact point for most drugs but their stay is quite brief unless they are formulated as buccal or sublingual tablets. The oesophagus is the linking connection between the oral cavity and the stomach. It is about 250 mm long and 20 mm in diameter and joins at the cardiac orifice with the stomach (Barrett et al., 2006). The pH of the oesophageal lumen is usually between 5 and 6. Movement of materials in the oesophagus is due to swallowing and a single wave of peristaltic contraction. The oesophageal transit of dosage forms is extremely rapid, usually of the order of 3.2-11.5 seconds (Jorgensen et al., 1992).

1.1.2 Stomach

The stomach is located just below the oesophagus and lies on the left side of the upper abdomen. The stomach is around 25 cm long and roughly J-shaped (Barrett et al., 2006). The empty stomach has a volume of about 50ml but it can capacitate up to 4 litres in the fed state. The main anatomical features of the stomach are illustrated in Figure 1.3.

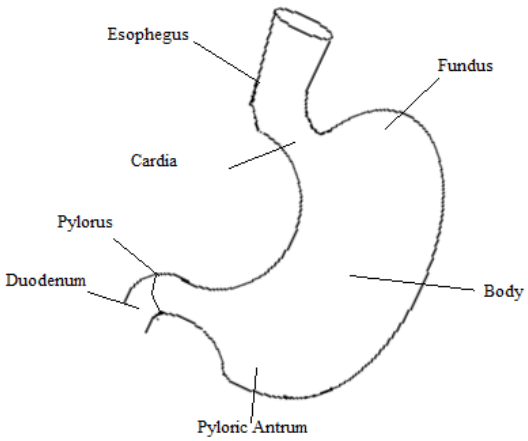

Figure 1.3 Schematic diagram of the anatomy of the stomach

The main features of the stomach are the cardia, the fundus, the body, the antrum and the pyloric region which consists of the pyloric sphincter and pylorus. The fundus and body distend in order to accommodate the large amount of food. The last part of the stomach, the pyloric sphincter controls the movement of food from the stomach to the duodenum.

The motility of the stomach acts differently under fed and fasted conditions. In the fasted state the stomach shows 4 phases of electrical activity known as the migrating motor complex (MMC), which repeats itself after every 2 hrs, and governs the transit of both food and dosage forms (Code and Marlett, 1975). In phase 1, which lasts for 40 minutes, there is no contractile activity. Phase 2 represents mixing contractions present in the stomach and the small intestine and lasts for 40-60 minutes. Phase 3 contractions are powerful propulsive contractions also called "housekeeper waves" which help to empty indigestible food from the stomach to the duodenum, and propagate till the end of the ileum. In phase 4, the contractile movements subside to resting contractions (Phase 1). During these phases, if food is eaten the stomach goes into the fed state motility.

In fed state, the antrum of the stomach performs mixing and grinding of the ingested food. All particles are propelled towards the pylorus. Smaller particles flow through the pylorus while larger particles are refluxed back and retained in the stomach. This process is repetitive in the fed state. When all food has emptied, the stomach enters the fasted state, and any undigested large particles are then swept away by the phase 3 of the MMC.

The functions of stomach include the temporary storage of food, mechanical breakdown of food into small particles, chemical digestion of protein to polypeptides by pepsins and the secretion of intrinsic factor, which is essential for the absorption of vitamin B12 (Pocock and Richards, 2006). Chyme is produced by the stomach as a consequence of mechanical and chemical action on ingested food, and is emptied into the duodenum.

The pH of the stomach in the fasted state is between 1.5 to 2.0 (Lui et al., 1986, Yakovlev, 2004). The pH of the stomach in the fed state can increase in the range of

4.3-5.4, with a peak value of 6.7. The sharp increase in gastric pH is mostly attributed to the buffering action of the ingested meal and dilution. Depending on the composition and volume of the ingested meal, gastric pH returns to fasted state value in 2 to 240 minutes (Dressman et al., 1990). In the fasted stomach fluid volumes were between 13 and 72 ml while in the fed state, the volumes of the stomach fillings were significantly higher and varied between 534 and 859 ml (Schiller et al., 2005).

1.1.3 Small intestine

The small intestine is divided into three parts: the duodenum (approximately 200-300mm in length), the jejunum (approximately 2m in length), and the ileum (approximately 3m in length). It starts from the pyloric sphincter of the stomach and ends at the ileocaecal junction. It is one of the longest parts of the GI tract and body, which is about 4-5 meter long and 5cm in diameter (Barrett et al., 2006).

The inner surface of the small intestine is covered with the folds of kerkring and the villi which are approximately 0.5-1.5mm in length and 0.1mm in diameter and well supplied with blood vessels. Each villus is further covered with approximately 600-1000 microvilli, approximately 1 micrometer in length and 0.1 micrometer in diameter which increases the effective surface area by 600 times. Villi are broad in the duodenum, slender and leaf-like in the jejunum, shorter and more finger-like in the ileum (Barrett et al., 2006). The small intestine is the major site for the absorption of food and drugs due to its large surface area.

The main mixing pattern in the small intestine is segmentation and is characteristic of the fed state. The luminal chyme moves down around a distance of 5cm through propulsive movement. The interdigestive (fasted) period is observed between the meals, when lumen is destitute of content. During such times, the phase 3 of the MMC cycle propagates from the stomach to the ileum, sweeping it clear of the debris.

The luminal pH of the small intestine varies from approximately pH 5 in duodenum to pH 7 in the ileum (Evans et al., 1988). Due to small intestine bicarbonate

secretion, pH gradually increases until it reaches the distal ileum (pH 6-7.5). The fluid volumes in the small intestinal in the fasted subjects were found extremely variable ranging between 45 and 319 ml. However, after the food, the small intestinal fluid volumes decreased and varied between 20 and 156 ml (Schiller et al., 2005).

1.1.4 The colon

The junction between the terminal ileum and the caecum is called the ileocecal junction, which regulates the movement of chyme from the small intestine into the large intestine. The anatomy of the ileocecal junction (IC junction) was initially thought as an ileocecal valve; a fold of mucosa into the lumen of caecum (Rosenberg and Didio, 1970, Kumar and Phillips, 1987). Other studies described it as a thicker wall, and so the concept of a sphincter at the IC junction was evolved (Cohen and Levitan, 1968, Nasmyth and Williams, 1985, Corazziari et al., 1991, Barberani et al., 1994, Nivatvongs and Gordon, 1999, Shafik et al., 2002). However, recent studies have suggested that the ileocecal junction is a portion of the terminal ileum which is intussuscepted into the cecum (Awapittaya et al., 2007). A region of sustained tone was identified at the IC junction in healthy volunteers. The mean pressure within the IC junction zone was 9.7±3.2 mmHg (range 8–14 mmHg) (Dinning et al., 1999).

The colon is approximately 1.5 meter in length and is composed of the ascending colon (~200mm in length), the hepatic flexure, the transverse colon (usually greater than 450mm), the splenic flexure, the descending colon (≈300mm), the sigmoid colon (≈400mm), and the rectum (Pocock and Richards, 2006).

In the colon, two different types of contractions are present namely; non-peristaltic (95%) and high amplitude propagating contractions (5%). A non-peristaltic contraction mixes the colon content back and forth without forward movements. The second type of contraction, the high amplitude propagating contraction occurs only 6-8 times per day are extremely strong contraction originating in the first part of the large intestine and ends in the rectum.

The colon does not have any villi. The main functions of the colon include the storage of food residues prior to their elimination, the secretion of mucus which lubricates the faeces, and the absorption of most of the water and electrolytes remaining in the residue (Pocock and Richards, 2006).

The colon is colonised with a large number (~10^{14} per gram of content) and variety of bacteria. This large bacterial mass is capable of several metabolic activities e.g. hydrolysis of fatty acid esters, and the reduction of inactive conjugate drugs to their active from. Their existence depends on undigested polysaccharides e.g. galactomannose in the diet and the carbohydrate component of the secretions as an energy source (Manning and Gibson, 2004). Additionally, bacteria which reside in the colon synthesise vitamin K and B. Degradation of polysaccharides caused by colonic bacteria yields short chain fatty acids (acetic acid, propioinc acid, and butyric acid), which lowers the pH of the colon. As a result, the pH of the caecum is around 6-6.5, which increases to 7-7.5 towards the end of the colon (Evans et al., 1988). In the fasting colon the volumes of the intestinal fluid were extremely variable with volumes between 1 and 44 ml available predominately in the caecal region, the ascending colon and the descending colon. In fed condition the large intestinal fluid volumes varied between 2 and 97 ml (Schiller et al., 2005).

1.2 TRANSIT TIME OF PHARMACEUTICALS IN THE GI TRACT

Some of the techniques used to measure the transit time in the animal and humans include X-ray methods using radioopaque markers (Hinton et al., 1969), gamma scintigraphy (Khosla and Davis, 1989, Wilding et al., 2001), magnetic marker monitoring (Weitschies et al., 2010), magnetic resonance imaging (Richardson et al., 2005), and AC biosusceptometry (Corá et al., 2010).

These studies revealed that material does not move uniformly in the GI tract or leave the segments of the GI tract in the same order as they arrived. As discussed above, the oral route is the major route of administration for pharmaceuticals, so it is important to understand their behaviour when they pass through the GI tract. It is

known that the small intestine is the major site of absorption in the GI tract and so the time the formulation spends in this region is extremely significant in terms of drug dissolution and absorption.

1.2.1 Gastric transit time

The gastric emptying time is very variable and depends on the type of the dosage form, administration as a liquid or solid formulation, fasted or fed state and the size of the solid form. Liquids usually leave the stomach immediately within 15±2 minutes (water) after their administration in the fasted state (Collins et al., 1983).

1.2.1.1 Gastric emptying in the fasted stomach

In the fasted stomach, the non disintegrating solid dosage forms will only empty with the phase 3 of the MMC cycle. Thus, if the timing of phase 3 of the MMC corresponds with the administration of the non-disintegrating solid dosage form, the stay of the non-disintegrating solid dosage forms could be no more than couple of minutes. On the other hand, if the administration of the oral solid dosage form does not coincide with the phase 3 of the MMC cycle it could stay up to 2 hours in the stomach. Khosla and Davis (1989) demonstrated a range of gastric emptying (GE) times of a non-disintegrating tablet (5×5mm) in the fasted state when administered on three different study days in 5 healthy volunteers. The mean GE time was 25 (range 10-35 minutes), 30 (range 10-50 minutes) and 113 minutes (range 43-230 minutes) on days 1, 2 and 3, respectively. It is worth mentioning here that some MMC cycles also originate independently in the small intestine (Rees et al., 1982), which might be another reason for longer gastric retention of modified dosage forms, especially, single-units in the fasted state which usually rely on the strong phase 3 "housekeeper waves" to undergo gastric emptying (Varum et al., 2010).

Other factors which could affect the gastric emptying are tablet density and size, however it was reported that the density of the non-disintegrating solid dosage form

is more important than the size for tablets of size 6 mm or larger (Podczeck et al., 1999, Podczeck et al., 2007b). Podczeck et al., (1999) demonstrated that increasing the density of a 12 mm non-disintegrating tablet in fasting healthy volunteers from 1.5 to 3.7 gcm^{-3} extended the gastric emptying time of the tablet (Table 1.1).

Table 1.1 The effect of tablet density and size on gastric emptying in fasted healthy volunteers

Tablet size (mm)	Density (gcm^{-3})	GE, Median (minutes)
12	1.50	14.8
	3.70	24.6
6.6	1.41	58.0
	2.85	82.0
3.2	1.38	94.0
	2.86	156

Similar results were observed for non-disintegrating 6.6 mm light 1.41 gcm^{-3} and dense 2.85 gcm^{-3} tablets (Table 1.1) (Podczeck et al., 2007b). Interestingly, they found that tablets with a larger size (12 mm) emptied faster than those of a smaller size (6.6 mm). More interestingly, in later studies Podczeck et al., (2007a) observed that non-disintegrating tablet 3.2 mm in size displayed variable and longer GE in comparison to 6.6 and 12 mm diameter tablets (Table 1.1). This is contradictory to a previous study where Park et al., (1984) reported no effect of size (spherical 6 mm to 12.7 mm or capsule shaped 7×9.8 mm to 9.5×17.6 mm) or shape (spherical and capsular) on GE of enteric coated tablet.

1.2.1.2 Gastric emptying in the fed stomach

The gastric emptying time with reference to a meal is of importance for two reasons. Firstly, in order to achieve desirable therapeutic action in some disease conditions it is important that the drug should release with the meal, such as in case of enzyme replacement therapy or bile salt replacement. Secondly, in some controlled release formulation it is desirable to achieve maximum contact time with the absorption site in the upper part of the intestine by delaying its gastric emptying (Dressman, 1986).

In the fed state, stomach mills and mixes the ingested material into chyme and release its content with an appropriate rate into duodenum. Therefore, the duodenum also plays an important role in gastric emptying in the fed state. The higher the osmotic pressure and energy content of digested food; the lower is the amount transferred to the duodenum (Hunt, 1983). In the fed state stomach emptying is mostly controlled by the meal properties (food composition low or high calorie and its timing) and the size of the dosage forms.

It was demonstrated by Davis et al., (1984a) that the gastric emptying of pellets (mean GE 79 minutes, range 30-150 minutes) was faster than the single unit tablet (mean GE 164 minutes, range 30-600 minutes) when given with a light breakfast. A similar trend was also observed by another author (Abrahamsson et al., 1996) where pellets (size 0.7 mm, compressed as tablets) administered after a heavy breakfast (2800 kJ) were found to clear from the stomach 6 hours earlier than the non-disintegrating tablets (size 9 mm). Gastric emptying of multiple-units (pellets 3 mm) (light breakfast mean GE 77.8±8.2, range 55-99 and heavy breakfast GE 170±10.5, range 130-198) has also been shown to be progressively delayed as caloric content of the food ingested increased (Davis et al., 1987). In another study by the same authors (Davis et al., 1984b), it was found that the gastric emptying was delayed for both pellets and an osmotic device when a heavy breakfast (3600KJ) was eaten compared to a light breakfast (1500KJ). However, the delay was more pronounced for tablets, which failed to empty in volunteers consuming a high caloric meal (3600 kJ) for up to 10 hours post dosing. The physical form of the food also dictates the GE of the dosage form. It has also been demonstrated that a liquid meal containing the same caloric content as solid meal emptied faster from the stomach (Feinle et al., 1999).

The higher content of fat in the food could also result in delaying of the GE because addition of fat increases the caloric content of the food (Houghton et al., 1990).

With respect to size of the dosage form Khosla et al., (1989) demonstrated that non-disintegrating tablets of different sizes (3–7 mm diameter) emptied from the stomach into small intestine with food. However, in later studies Khosla and Davis (1990) found that 7 and 11 mm tablets were emptied in fed state with food while the emptying of a 13 mm tablet was delayed, concluding that the cut-off size of solid dosage form from the stomach is 12.8±7 mm, similar in diameter to the aperture of the resting pylorus. This is because large dosage forms empty from the stomach in a phase 3 of the MMC, which occurs only after the return of the fasted state in the stomach. However, Smith and Feldman (1986) reported the gastric emptying of 2 and 10 mm radio-opaque markers after the emptying of food. Similarly, Podczeck et al., (2007c) reported that the emptying of 3.2 mm and 10.2 mm tablets only occurred after the emptying of food.

Another factor which could affect the clearance of the dosage form from the stomach is the time of the day at which dosage form is taken. Coupe et al., (1992b) demonstrated that the gastric residence time of a radiotelemetric capsule (day: median 2.97 hour, and night: median 7.5 hour) and radiolabelled tablet (day: median 0.98 hour, and night: median 4.25 hour) was significantly higher in night compared to day.

It is evident from this discussion that gastric emptying is a complex process which is affected and influenced by various factors.

1.2.2 Small intestine and colon transit

The transit time in small intestine was found to be similar for tablets, pellets and liquids when compared in 201 individuals, and was reported to be 3-4 hours (Davis et al., 1986). The authors concluded that only gastric emptying was affected by the nature of the dosage form and the presence of food in the stomach. No effect of dosage form and fed state was found on the measured intestinal transit time. Several

other studies performed on pellets or single unit tablets using gamma scintigraphy also found the mean small intestinal transit times to be closed to 3–4 hours. Coupe et al., (1991) reported a mean value of 3.5 ± 1.0 hours with pellets administered after a light breakfast, while Yuen et al., (1993) reported a mean value of 4.2 ± 2.9 hours with pellets administered under fasted conditions, and 3.9 ± 2.4 h when administered after a meal. Similar values were obtained by Billa et al., (2000) for single units who reported a mean value of 3.1 ± 0.7 hour when the tablets were administered after an overnight fast and 3.2 ± 0.4 h when given after a standard meal. However, it is worth noting that individual data for small intestine transit time is quite variable with values ranging from 0.5 to 9.5 h (Davis et al., 1986, Sugito et al., 1990, Coupe et al., 1991). Data from Davis et al (1986) reveals that the values for small intestinal transit time can range from less than 1 hour to around 6 hours for tablets, between 1-9 hours for pellets and 2-6 hours for solutions.

There is some evidence that the transit time of the small intestine can be influenced by some excipients present in the dosage form. For example, lactulose (an unabsorbable disaccharide used in the treatment of chronic constipation), has been shown to accelerate small intestinal transit (Read et al., 1982). The influence of polyethylene glycol 400 (PEG 400), a commonly used solvent or co-solvent in pharmaceutical formulations, on gastrointestinal transit was investigated by the Basit et al., (2001). The small intestinal transit time of a liquid preparation comprising 10g of PEG 400 in 150 ml of orange juice was found to be reduced by 35%. However, the presence of PEG 400 did not influence the transit time of non-disintegrating pellets administered simultaneously with the liquid preparation. This discrepancy was attributed to the more rapid gastric emptying of the liquid preparation compared to the pellets. Thus, the liquid containing the PEG passed into small intestine in front of the pellets and exercised no effect on the pellets which were left behind. In contrast, pellets that were emptied concurrently with the PEG 400 containing liquid from the stomach demonstrated a short small intestinal transit time (though not statistically significant) when the pellets were administered with the PEG 400 containing liquid. In subsequent studies by the same authors (Basit et al., 2002) it was demonstrated that the bioavailability of the ranitidine from an immediate release pellets was reduced by 37% when administered with PEG 400 containing liquid. This

effect was caused by the significant shortening of the small intestinal transit time (31%) due to the presence of the PEG 400.

Many studies have shown that the small intestinal transit time of various dosage forms is not affected by the fed state (Davis et al., 1986, Yuen et al., 1993, Billa et al., 2000). However, Fadda et al., (2009) investigated the influence of timing of tablet and food administration on the small intestinal transit time in ten human volunteers. Three feeding regimens were investigated; namely fasted, fed and pre-feed. The small intestinal transit times of tablets under fasted and fed conditions were not significantly different, which is in accordance with the findings of previous studies having median values of 204 minutes and 210 minutes, respectively. In the case of pre-feed the tablet was administered 45 minutes before the breakfast. A significant reduction in the small intestinal transit time (median 100 minutes) in six volunteers was observed where the tablet had emptied from the stomach before arrival of the meal. In the other four volunteers, the presence of the tablet in the stomach after 45 minutes when food was served resulted in the transit behaviour of the tablet being essentially similar to that of the fed state. This shows that the timing of the ingested food has an important influence on the performance of the dosage form in terms of its transit and bioavailability.

Both single-unit (tablets) and multiple-unit (pellets) dosage forms exhibit the phenomenon of the stagnation and accumulate at the IC junction for a variable period of time (Abrahamsson et al., 1996, Wilding et al., 2001). Khosla et al., (1989) demonstrated that this stagnation of dosage form is usually affected by the meal size. However, meal composition does not seem to have any effect on this process (Price et al., 1993). Transit through the colon is a lengthy process and reported around 20 hours (Davis, 2005). Abrahamsson et al., (1996) reported that the single-unit dosage forms have a shorter colonic transit time than multiple-units (Figure 1.4).

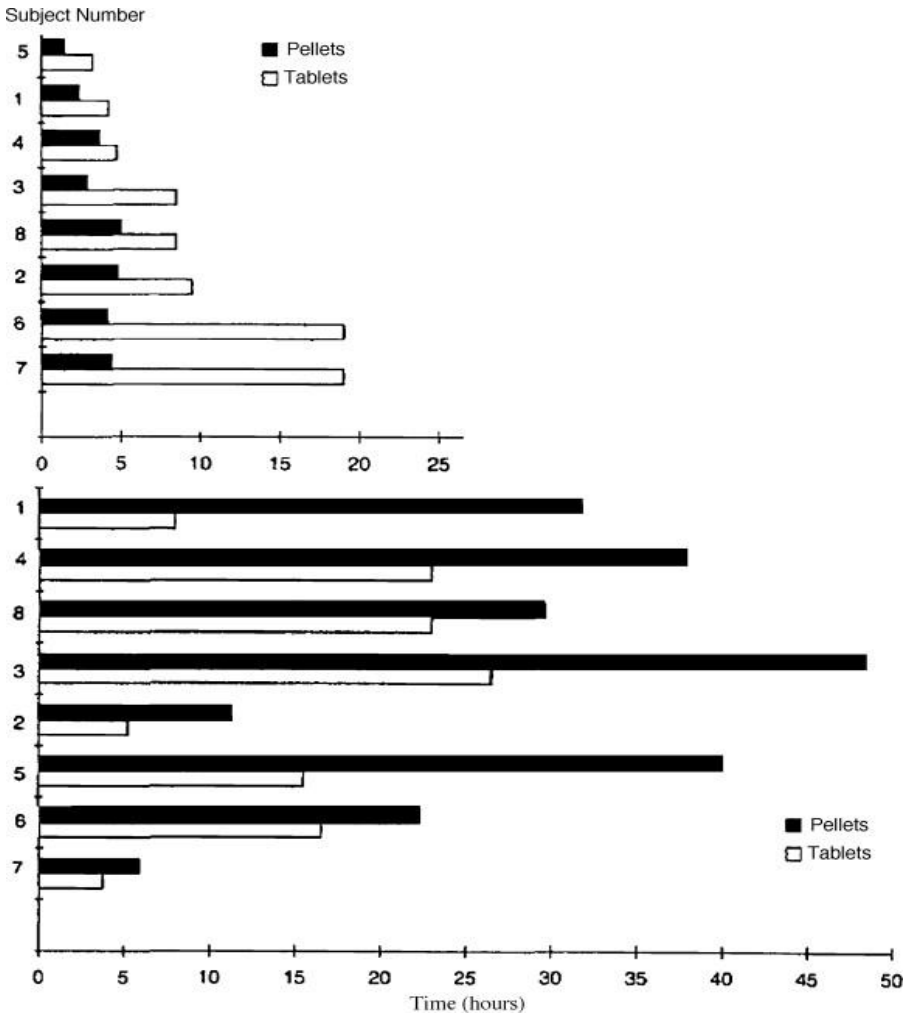

Figure 1.4 Gastric emptying (top) and colonic transit (bottom) of single-unit (9 mm tablets) and multiple-unit (0.5 mm pellets) systems in the presence of food (Abrahamsson et al., 1996).

Similarly, in another study simultaneous administration of tablet and pellets compressed as a tablet formulation showed in gamma scintigraphic imaging that the tablet moved ahead of the pellets in the colon (Davis et al., 1984a). Additionally it was found that after administration, pellets have been found to be dispersed in the colon, mainly in the ascending colon (up to 14 hours) and transverse colon (up to 48 hours), whereas transit through distal parts was relatively fast (Abrahamsson et al., 1996). Comparative study of a gelatine capsule containing 200 mg Amberlite IR-

120 (H) pellets with co-administered radiotelemetry device 25 mm long × 9 mm diameter was performed to observe the transit time in the colon (Hardy et al., 1985). It was noticed that the gastric emptying and small intestinal transit time was similar for both formulations though colon transit was faster in case of radiotelemetry device. The transit time varied in ascending colon in the range of 0.7-7.5 hours while in transverse colon it was 10 to more than 25 hours. The time of the dose is also found to affect the total gastrointestinal transit of non-disintegrating tablets. Dosing in morning resulted in tablet being excreted the next morning (24 hours total transit time) (Sathyan et al., 2000). However, with the night dosing it was found that the tablet excretion was delayed to the following morning (36 hours). This can be related to the pattern of bowel movement (Coupe et al., 1992a). On contrary, presence of pellets were recently reported in the large intestine 5 days after morning dosing (Basit et al., 2009).

Gastrointestinal transit can also be altered by the disease state of the gut when compared to healthy subjects. An accelerated intestinal transit, particularly through the proximal colon was found in patients with irritable bowel syndrome (Vassallo et al., 1992). Similarly, significantly faster intestinal and colonic transit (Davis et al., 1991, Hebden et al., 2000) was observed in patients with active ulcerative colitis.

1.3 GASTROINTESTINAL FORCES

In addition to the variable chemical environment faced by the dosage form during its transit through the gastrointestinal tract, the importance of gastrointestinal forces has also been noticed by some researchers who have tried to quantify them. Aoyagi el al., (1982) suggested that there is a deaggregation force present in the gastrointestinal tract of humans and beagle dogs. Katori el al., (1995) designed hydrophilic matrix based controlled release paracetamol tablets with the aim that one of the tablets would release at low paddle speeds (0 to 10 rpm), while the other at high paddle speeds (50 to 100rpm). It was observed that the *in vivo* disintegration in humans corresponded to that at *in vitro* paddle speeds of 10 rpm, while in dogs it corresponded to *in vitro* paddle speed of 100 rpm. It was postulated that the *in*

vitro/in vivo relationship for a solid dosage form is dependent upon the interaction between sensitivity to formulation erosion and destructive forces within the GI tract. In conclusion, Katori et al., (1995) stated that "the presence of destructive and hydrodynamic forces is essential conditions for establishing a useful dissolution testing system".

Abrahamsson et al., (1998b) highlighted that the main source of variability in their results could be attributed to the mechanical agitation present in the *in vivo* conditions. Similarly, McInnes et al., (2008) suggested that the mechanical destructive forces within the GI tract of the dogs was responsible for dose dumping from a hydroxypropylmethyl cellulose (HPMC) matrix tablet. Dose dumping is a phenomenon of rapid unplanned release of the drug from an extended release product.

Kamba et al., (2000) identified the limitation in the tablets used in the Katori et al., (1995) studies. A hydrophilic matrix tablet was used in the previous studies where the crushing strength of the dosage forms decreased with an increase in soaking time in the GI fluid. Thus it was impossible to determine the exact destructive force applied when the dosage forms were crushed in the GI tract. Therefore, Kamba et al., (2000) developed a novel destructive force dependent release system (DDRS) (Figure 1.5) which was used to evaluate the destructive forces within the gastrointestinal tract.

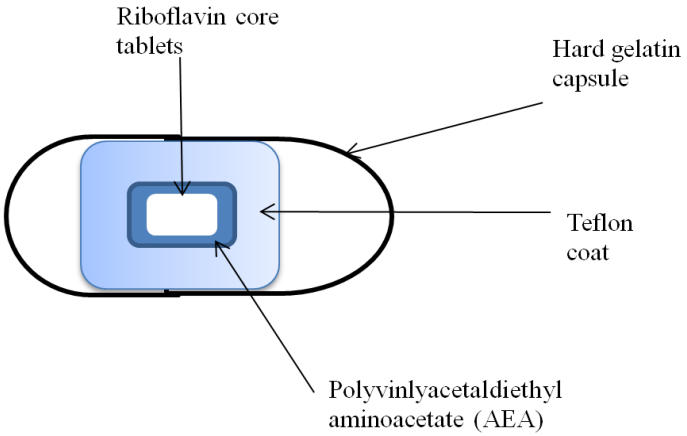

Figure 1.5 Schematic diagram of destructive force dependent release system (Kamba et al., 2000).

The DDRS was a press-coated tablet consisting of a core tablet (riboflavin and carboxymethyl cellulose) and an outer Teflon layer coated with Polyvinlyacetaldiethylaminoacetate (AEA) film. The AEA dissolves only in acidic environments and it does not dissolve in environments of pH over 4. The DDRS was further encapsulated in a gelatin capsule. The crushing strength of tablets was controlled by changing both the Teflon grade and the tablet compression pressure.

Initially, the DDRS of 1.89N strength was administered in both fed (n=6) and fasted conditions (n=5). In the fed state only 2 out of 6 subjects crushed the 1.89N DDRS system, which were then administered with 3.04N DDRS which they failed to crush. The remaining 4 subjects who failed to crush 1.89N DDRS in fed state were administered with lower strength tablet of 1.5N, which they were able to successfully crush (Figure 1.6).

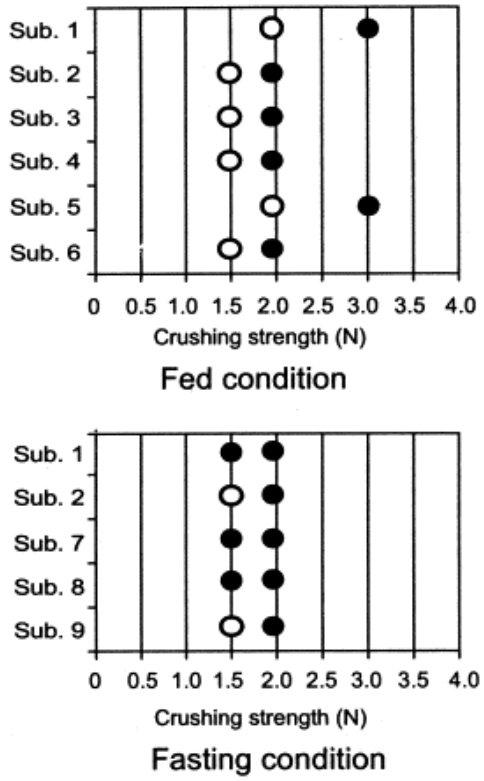

Figure 1.6 Crushing strength in the human stomach under fed and fasting conditions, symbols: (○) crushed, (•) not crushed (Kamba et al., 2000)

Under fasting conditions, none of the 5 subjects were able to crush the 1.89N DDRS however, 2 out of 5 were able to crush the 1.5N DDRS in the next administration (Figure 1.6). Therefore, it was concluded that the human stomach imparts a crushing strength of 1.89N under fed conditions. Under similar conditions, the dog stomach exhibited a crushing force of 3.2N in both fed and fasted conditions (Kamba et al., 2001). It was observed that the crushing force in the dog's stomach is potentially higher than in humans. Due to the absence of visualisation technique in their studies it was difficult to locate the position of the DDRS during its destruction within the stomach and establish a correlation with the mechanical forces.

A year later Kamba et al., (2002) attempted to determine the mechanical destructive forces in the human and dog small intestine using the same method as outlined above. However, in this case the AEA was not used, rather a starch capsule was coated with hydroxypropylmethyl cellulose phthalate (HPMCP) HP-55 to ensure its

intact delivery into the small intestine. HPMCP HP-55 only dissolves in environments of pH above 5.5 and does not dissolve in acidic environments.

In the dog study all dogs were able to crush 0.8N and 0.9N DDRS tablets except one which did not crush the 0.8N DDRS tablet but did crush 0.9N. However, only one dog crushed 1.2N DDRS tablet while no disintegration was observed when 1.7N DDRS tablets were administered (Figure 1.7).

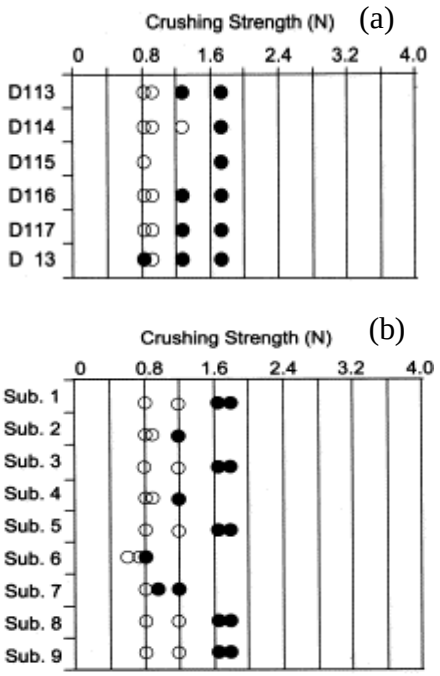

Figure 1.7 Destructive forces in dog (a) and (b) human small intestine. Symbols: (○) crushed, (●) not crushed (Kamba et al., 2002).

In the human small intestine, five of the eight subjects crushed the 1.2N DDRS tablets and no subject crushed the DDRS tablet 1.7N (Figure 1.7). These results showed that the small intestine of the human and dog can potentially crush tablet that have a crushing strength of 1.2 N, although inter-subject variability in human does exist ranging from 0.8N to 1.2N.

1.4 PULSATILE DRUG DELIVERY SYSTEMS

There has been growing interest and advancement in the field of pulsatile delivery system (Maroni et al., 2010). This delivery system is tailored to provide a rapid release of active pharmaceutical compounds as a pulse after predefined lag time as shown in Figure 1.8.

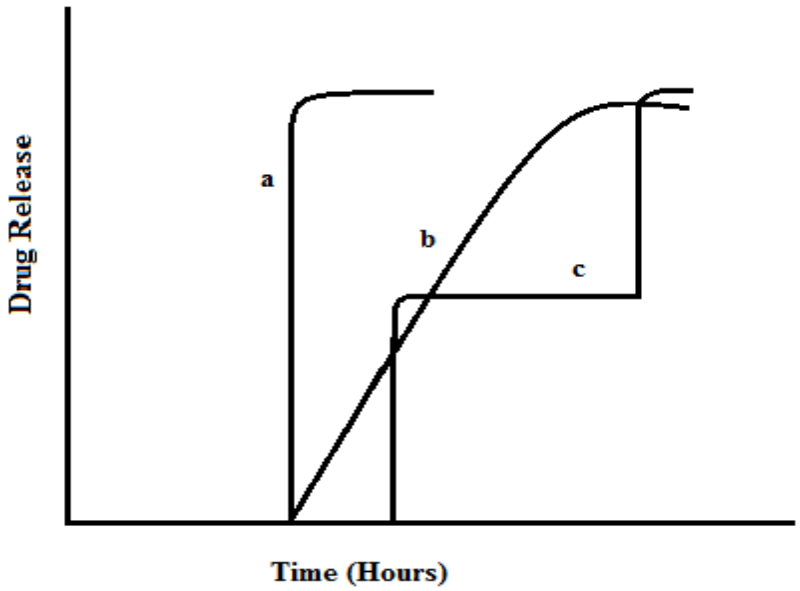

Figure 1.8 Example drug release profiles of pulsatile drug delivery systems with a) immediate b) prolonged and c) repeated drug release after the lag phase.

Pulsatile delivery systems are gaining a lot of interest for chronopharmaceutics and site specific delivery systems, especially to the lower intestinal tract. Chronopharmaceutics is a branch of pharmaceutics which deals with the design and evaluation of drug delivery systems specifically made to deliver the pharmaceutically active material according to the rhythmical need of the biological system in disease conditions (Gazzaniga et al., 2008). For instance, patients suffering from osteoarthritis are more prone to pain in the evening, while rheumatoid arthritis

patient suffering is higher early in the morning. Therefore, the best drug delivery system for an osteoarthritis patient is the one which provides a peak plasma concentration of pain killers like paracetamol at evening time and for rheumatoid arthritis patient at morning times just before the patient wakes up. Pulsatile drug delivery provides an opportunity to address these issues, however their use has also been found tremendously beneficial in delivering medicine to the lower intestinal tract and colon.

Pulsatile drug delivery to the colon is based on a time dependent approach that relies on the relatively consistent small intestinal transit time (3-4 hours) of dosage forms (Stevens et al., 2002, Gazzaniga et al., 2006). In order to overcome the unpredictable gastric emptying an enteric coat is usually applied to the pulsatile delivery system. Many design strategies have been published to achieve pulsatile release. In order to achieve pulsatile release several capsular, osmotic, multi-particulate and tablet formulations have been described in literature and brief description is given below.

1.4.1 Capsules

In this delivery system a drug formulation is sealed by a hydrophilic matrix plug in an impermeable capsular body. Contact with aqueous fluid starts the dissolution of the gelatine cap, which ultimately allows the gradual swelling of the plug until its expulsion from the body, thus allowing the drug to be released (Figure 1.9).

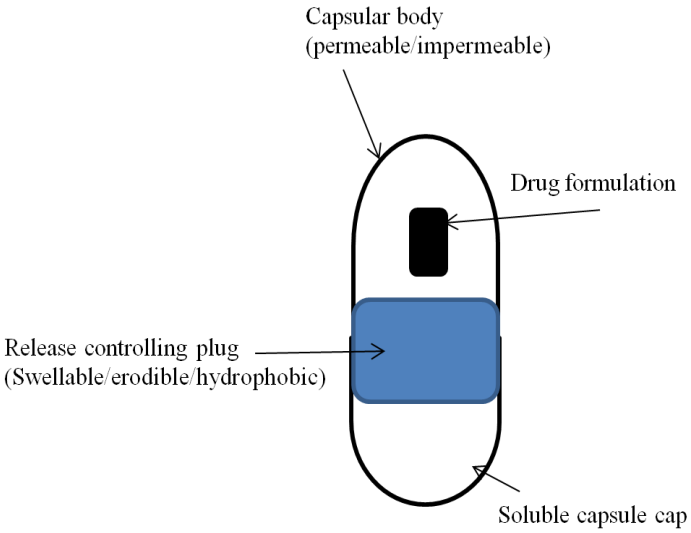

Figure 1.9 Oral pulsatile delivery system based on capsule

The time needed to remove the plug dictates the lag phase and its duration is dependent on the physical-chemical nature, size and position of the plug itself. The first one of its type was started with Pulsincap (TM) which contained cross-linked polyethylene glycol (PEG) 8000 hydrogel (Binns et al., 1996, Stevens et al., 2002), and the suitability of this device was extensively studied by human imaging investigations. However, in recent years cross-linked polyethylene glycol was substituted with other polymers like hydroxypropylmethyl cellulose (HPMC) of various grades, polyvinyl alcohol (PVA), polyethylene oxide, guar gum, and sodium alginate as an alternative to prepare the release controlling plug (Ross et al., 2000, Gohel and Sumitra 2002, Mastiholimath et al., 2007, McConville et al., 2009). A release controlling plug was also prepared by erodible plug using Gelucire® (polyglycolated glyceride) with sodium dodecyl sulphate (SDS) (Krogel and Bodmeier, 1998). The erodible plug was prepared by the melt method and directly poured and congealed within the capsular body, thereby offering a tight contact between capsule body and plug. Erosion of the plug was controlled by the hydrophilic-lipophilic balance (HLB) value of the Gelucire® or the concentration of the added surfactant which in turn modulated the lag time of this capsular device. In a later study, the same group prepared another plug from a pectin/pectinase mixture

(Krogel and Bodmeier, 1999). Egalet ® technology has recently been introduced as a pulsatile delivery system. Briefly, a drug core is embedded in a hollow impermeable shell with an injection-moulded erodible plug (PEO, high molecular weight PEG), at both ends. Different lag times were achieved by varying the size and composition of the plug (Bar-Shalom et al., 2009). The disadvantage of these systems is that the manufacturing process is quite difficult and mostly performed manually.

An alternative pulsatile drug delivery system consisting of a drug-containing hard gelatine capsule coated with a swelling layer of Croscarmellose sodium plus polyvinylpyrrolidone and a coated barrier layer (ethyl cellulose and HPMC) was reported by Bussemer et al., (2003). The lag time was controlled by the expansion of the swelling polymer and subsequent rupturing of the polymer coat. In later studies the same approach was applied to coat soft gelatine capsules (Bussemer and Bodmeier, 2003), and performance was compared to the pulsatile hard gelatin capsules. The lag time was longer with hard gelatine than with soft gelatine capsules at the same coating level, both having the same composition of the swelling and coating layer. The reason for the shorter lag times with the soft gelatine capsules resides in the different degree of fillings of hard and soft gelatine capsules. Soft gelatine capsules were completely filled with liquid, therefore the pressure developed by the swelling layer is directed primarily towards the outer polymer layer. In comparison, hard gelatine capsules were not completely filled with powder due to air inside the capsule. As a result the pressure of the swelling layer is not exclusively towards the outer coating but also directed towards the capsule core. However, no *in vivo* data is available to evaluate the performance of this system.

1.4.2 Osmotic pumps

Most osmotic pump delivery systems consist of a bipartite core tablet, including an expandable polymeric compartment and a drug compartment (Gupta et al, 1996, Prisant et al., 2003). The core is entirely coated with a semi-permeable film with laser drilled opening as shown in Figure 1.10.

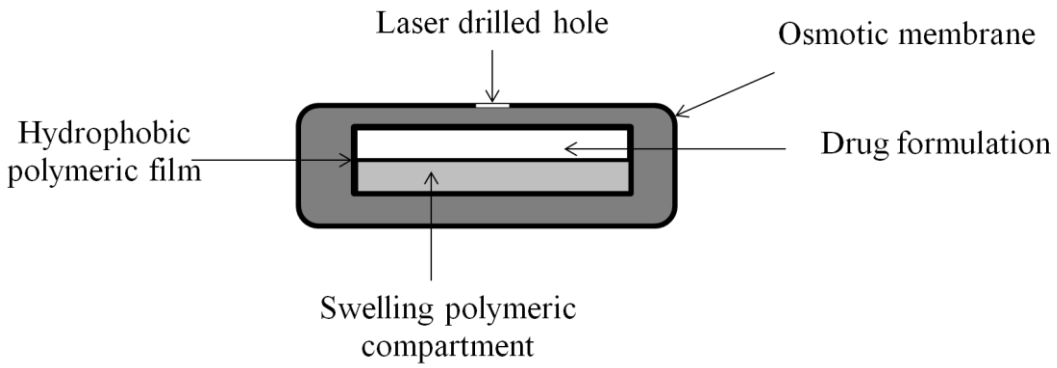

Figure 1.10 Pulsatile delivery system based on osmotic pump

A hydrophobic coat between the core and the outer membrane further prolongs the onset of the release. The ingress of water starts the dissolution of the active ingredient and the push compartment starts swelling. Thus the drug solution is pumped out at constant rate. The suitability of this system has been assessed for verapamil hydrochloride in controlled-onset extended release COER-24 as a clinical trial for chronic stable angina pectoris (Cutler et al., 1995). A chronopharmaceutical product named Covera-HS^{TM} from Pfizer is available in the USA market utilising this technology for the management of hypertension and angina. A main disadvantage associated with these osmotic systems is that the manufacturing requires sophisticated techniques and equipment.

1.4.3 Multi-particulate

Multi-particulate pulsatile release systems in the form of pellets offer some typical advantages which are not often achieved from the single unit pulsatile release systems. These systems have reproducible gastric emptying time, less dose dumping and pellets with different composition can be blend together to achieve desired release. However, the disadvantage resides in their lengthy manufacturing process. Ueda et al., (1994) used this approach as a time-controlled explosion system (TES) (Figure 1.11) to achieve pulsatile release.

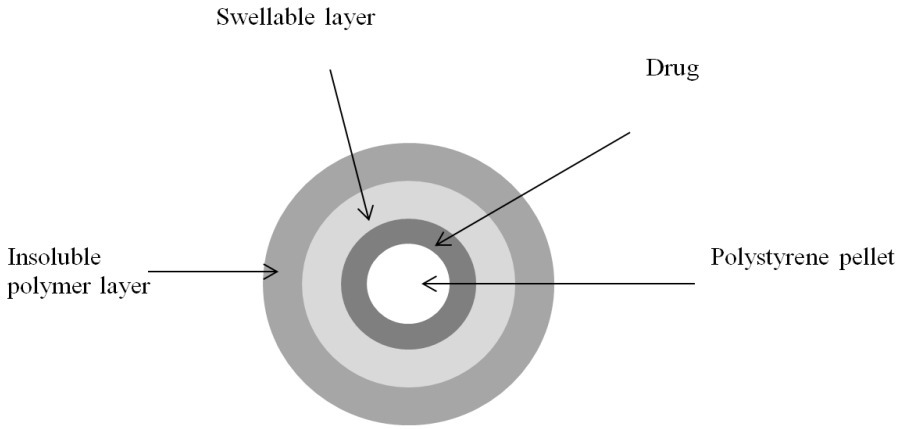

Figure 1.11 Oral pulsatile time controlled explosion system

The TES consists of four layers: polystyrene pellets, drug (metoprolol), swellable polymer (L-HPC) and an outer water insoluble membrane (ethyl cellulose). The penetration of water through the outer membrane results in swelling of the L-HPC which eventually ruptures the outer membrane after a predetermined lag time. The lag time was modulated by controlling the thickness of the ethyl cellulose. The lag time prior to the release was independent of the pH of the dissolution medium, solubility of the drug and the pellet size.

1.4.4 Tablets

The pulsatile tablets consists of solid core either immediate or sustained release, coated with one or more barrier layers. The schematic diagram of the representative pulsatile release tablet is shown in Figure 1.12.

Figure 1.12 Oral pulsatile release system based on tablets

The purpose of the barrier layer is to prevent the ingress of the fluid into the core for a predetermined period, thereby providing a desired lag time before rapid/sustained drug release from the inner core tablet. The composition of the barrier layer (s) is either coated with liquid coating, dry coated (compression coated or press coated) or through specialised coating such as 3 dimensional printing (3 DP) coating. 3 DP is solid free-form fabrication techniques where computer assisted inject printers fabricate 3D layers by depositing a liquid binder or drug excipients. The procedure allows to spatially deposit multiple components with fine resolution within the tablets (Katstra et al., 2000). *In vitro* drug release profile shows that different lag times are achievable by having higher polymer content. The main disadvantage of this technique is that it requires sophisticated manufacturing instrumentation, which is not easily available. In addition to that the large scale manufacturing cost is still unknown. Therefore, spray coating and compression coating is extensively reported techniques in the literature to manufacture pulsatile release system.

Sangalli et al., (2001) used aqueous spray coating technique to coat the tablet core with HPMC E50 and polyethylene glycol (PEG) 400 to obtained different lag times by having different coated thicknesses. The same formulation having another gastro-resistant coat of Eudragit® L30D were also tested for colon specific delivery system in healthy volunteers. However, spray coating technique especially the aqueous coating might not be a feasible technique for moisture sensitive drugs while spray coating using organic solvents is mostly discouraged due to the presence of residual solvents in the tablet which raises safety issues.

However, the press coating technique is extensively reported approach to develop a time delayed system and has been widely investigated (Fukui et al., 2000b, Ishino et al., 1992, Fukui et al., 2001b, Sawada et al., 2004, Ghimire et al., 2007). A press coated tablet consists of a core tablet containing an active ingredient and an outer shell capable of delaying the drug release to achieve the required lag time. The press coating technique differs from the liquid coating as it does not use any solvents and allows greater weight gain to the core tablet. It has been also used for physical separation of incompatible materials. Manufacturing of press coated tablet is not an easy procedure and accurate centralising of the inner core tablet could be a major challenge for a large scale industrial manufacturing. However, Ozeki et al (2004) recently reported a new compression coating method where the manufacturing of the inner core tablet and press coating can be performed in a single-step process. This is a positive sign towards scale up processing and overcomes some of the drawbacks in the press coating technique as mentioned earlier. However, this equipment is not readily available.

The composition of the barrier layer in coated tablets manufactured by any technique (3 DP, liquid coating or compression coating) is of paramount importance as it defines the magnitude of the lag time and the mechanism by which it is produced. In general, thicker the barrier layer longer would be the lag time, while composition of the barrier layer controls the mechanism of lag time (Fukui et al., 2000b, Ozeki et al., 2004, Sungthongjeen et al., 2004).

Hydrophobic materials such as castor oil has been reported as a barrier layer component for press coated tablets (Ishino et al., 1992). Due to their hydrophobic nature these materials are usually admixed with hydrophilic excipients (lactose, PEG, HPMC). The lag time can be modulated by changing the ratio of these excipients. Ishino et al., (1992) achieved different lag times in press coated tablets by controlling the thickness of the barrier layer, and selecting an appropriate mix of hydrogenated castor oil and hydrophilic excipients lactose and polyethyleneglycol 600. The granules for the outer shell were prepare by the melt granulation method and coated on the rapidly disintegrating isoniazid core. The lag time prior to the drug release from the core was a result of the channels created by the water soluble excipients.

Thus, higher the hydrophilic excipients in the barrier layer lower will be the lag time prior to the drug release.

Lin et al., (2001) used water insoluble polymer ethyl cellulose (EC) as a barrier layer component in press coated tablets, the mechanism of lag time from these is similar to the TES (Figure 1.11). The mechanism involves the penetration of the water through the insoluble polymer layer followed by expansion of the swelling layer and eventually rupturing of the barrier layer. The lag time can be increased by using the small particle size of the EC or by increasing the compression pressure which led to the decreased porosity resulting in slow water penetration. It was observed that the tablets broke into two half through lateral surfaces during dissolution. The authors suggested that it was due to loosely packed EC particles in the lateral side compared to upper and lower surfaces. However, mixture of HMPC or lactose with EC as barrier layer demonstrated a complete breakdown of the barrier layer (Lin et al., 2004). The addition of the lactose decreased the lag time due to channels caused by the water soluble lactose, while addition of HPMC retarded the water penetration due to gel formation. The order of lag time prior to the drug release from press coated tablet was lactose plus EC < EC plus HPMC< EC in the barrier layer (Lin et al., 2004).

Hydrophilic polymers such as HPMC (Ozeki et al., 2004), polyethylene oxide (Sawada et al., 2003b) or hydroxypropyl cellulose (HPC) (Fukui et al., 2000a), with or without other excipients are commonly used as a barrier layer components. These hydrophilic polymers upon exposure to fluid, swell and subsequently the barrier layer dissolve and/or erode, allowing the fluid access to the inner core. Generally, the lag time increase with higher viscosity of the polymer, due to the formation of stronger gel layer which is resistant to erosion.

Sawada et al., (2003b) demonstrated the potential application of a press coated tablet having PEO as a barrier layer to avoid the drug-drug interaction of diltiazem when concomitantly administered with a midazolam aqueous solution. The diltiazem release was delayed for 2-3 hours which allowed sufficient time for midazolam to be absorbed from the GI tract which otherwise would have caused inhibition of the CYP3A4-mediated metabolism due to their interaction. In case of inhibition of the

midazolam metabolism, the concentration of midazolam could significantly increase (3.3 fold) in the blood resulting in its higher anaesthetic effect and ultimately death of the patient.

Fukui et al., (2000b) manufactured press coated tablets using different viscosity grades of HPC (SL, L, M, and H) to achieve the desired lag time. The lag time was found to be dependent on the viscosity of the HPC i.e. increasing the viscosity of the HPC resulted in increase in lag times. Additionally, the lag time could also be controlled by changing the quantity of the L-HPC in the outer shell. In later studies from the same author (Fukui et al., 2000a) the same press coated tablet was enteric coated and tested in beagle dogs, where they demonstrated a good *in vivo* correlation with their *in vitro* data proposing its potential use as a colon targeting delivery system.

1.5 COLONIC DRUG DELIVERY

The function of the colon is to absorb electrolyte and water, and help in the formation of stool and to act as temporary storage for stool. However, in the last two decades its usefulness as a drug delivery site has been established quite widely. It provides better treatment for the pathologies of the colon e.g. diarrhoea, constipation, inflammatory bowel disease (ulcerative colitis, and Crohn's disease) and potential use in the chemoprevention of colorectal adenocarcinoma (third deadliest cancer in both man and woman) (Takayama et al., 2009). Despite of moderate absorption properties, the large intestine is currently recognised as a gateway to the systematic circulation and be used for the oral bioavailability of peptides, proteins, oligonucleotides, and nucleic acid (Bourgeois et al., 2005). Furthermore, through colonic drug delivery direct treatment at the site of action is possible with reduced systemic side effects.

The colon is the last part of the GI tract and in order for a formulation to reach at such a distal part and deliver its content, it has to pass through and retard all the diverse and hostile conditions of stomach and small intestine. In the colon a dosage

form has to face a low water environment and high mucous content which will hinder its dissolution and release of the drug from the formulation. Many approaches have been developed in order to overcome these challenges to achieve colonic drug delivery. One conventional approach to deliver medicaments to the colon is the use of suppositories and enemas. They have been used both for local and systematic effects, although these formulation have rarely reached beyond descending colon. Moreover, they are unacceptable and inconvenient for most patients, leaving the oral route as a suitable means of drug administration.

Different exploitable GI tract features which could be used to approach the colon include pH, transit time, pressure, and bacteria, (Basit, 2005). The time dependent approach has already been discussed in Section 1.4 and will not be discussed further.

1.5.1 Approaches for colon drug delivery through the oral route

1.5.1.1 pH dependent delivery

The GI tract has a different pH gradient in its different regions which ranges from 1.2 in stomach to 6.6 in the proximal small intestine to peak of 7.6 in the distal small intestine (Evans et al., 1988). Enteric coated delivery system use this difference in pH to deliver drugs to the small intestine. Mostly polymers which are resistant at lower pH values e.g. pH 4.5 are frequently used for this purpose. Therefore, it is possible to deliver the drugs to the terminal ileum or colon using the same concept by those polymers which show high resistant to these pH changes and dissolve at high pH values. The most widely used polymers in this category are copolymer of methacrylic acid with its derivatives. On the basis of this, Eudragit ® S (copolymer of methyl methacrylate and methacrylic acid) has been used, which dissolves above pH 7, to deliver 5-Aminosalicylic acid for the treatment of ulcerative colitis (Bruce et al., 2005) (Asacol ®, Ipacol ®, Claversal ®). However, pH of the proximal colon is about 6.4, which is slightly lower than the small intestine. This suggests that premature release or variable release could occur in ileum/ileocecal junction which

was seen by Ashford et al., (1993b) through scintigraphic evaluation of Eudragit® S made tablets.

In another study newly developed polymer Eudragit ® FS (copolymer of methyl acrylate, methacrylic acid, and methyl methacrylate) which dissolves at slightly lower pH 6.8 was investigated by the Ibekwe et al., (2006) as a pH responsive polymer in comparison with Eudragit ® S for colonic drug delivery. Tablet cores containing the prednisolone as an active were coated with Eudragit ® S (aqueous and organic dispersion) and Eudragit ® FS (aqueous dispersion), and studied in male healthy volunteers. Tablets coated with aqueous Eudragit ® S were disintegrated prematurely in 7 out of 8 volunteer in the proximal and mid small intestine, and in 1 tablet was disintegrated in the distal small intestine while tablets coated with organic Eudragit ® S were failed to disintegrate in 3 out of 8 volunteers. In contrast, tablets coated with Eudragit ® FS disintegrated in all subjects, predominantly at the ileo-cecal junction or in the ascending colon with more consistent intra-subject performance.

1.5.1.2 Pressure dependent delivery devices

The first pressure-controlled colon delivery capsule (PCDC) was described by Takada (1997) and later on by the other researchers (Takaya et al., 1997). This novel drug delivery device utilises the pressure which develops in the colon due to re-absorption of water and electrolyte in the lumen of the colon (Takaya et al., 1997). In the PCDC, drug is dispersed in polyethylene glycol (PEG) 1000 which is then covered by the hydrophobic polymer ethyl cellulose (insoluble in water, alkali and acid). After ingestion of these devices, normal body temperature will melt the base, however the ethyl cellulose covering protects it from leaking and releasing its content in the stomach and small intestine. As soon as it crosses the ileocecal junction, under the higher colonic pressure, this PCDC burst its contents in the colon (Takada, 1997). Further *in vivo* studies have been done on human and beagle dogs to correlate the appearance of drug in the colon through saliva and biomagnetic measurement analysis (Hu et al., 2000b, Hu et al., 2000a, Shibata et al., 2001).

However, no studies have been done using gamma scintigraphy which would provide exact location and time of capsule disintegration during its transit through colon.

1.5.1.3 Micro-floral dependent delivery systems

The colon is the house of a large number of bacteria and they are estimated to be 10^{12} per gram colonic content and consist of >400 species which are predominantly anaerobic in nature. These bacteria produce wide range of enzymes such as beta-glucuronidase, beta-xylosidase, alpha-L-arabinosidase, beta-galactosidase, nitroreductase, azoreductase, deaminase and urea dehydroxylase (Kinget et al., 1998). The first system based on the use of the micro-flora of the large intestine was marketed for ulcerative colitis using sulphasalazine, a pro-drug comprises of 5-aminosalicylic acid (5-ASA), linked by an azo-bond to sulphapyridine (Khan et al., 1977). This azo-bond is cleaved by intestinal bacterial (azoreductase) to release 5-ASA for localised effect in the large intestine. This opens new ways of targeting drugs to the colon and since 1977 many delivery systems have been reported using this approach, such as styrene and hydroxyethylmethacrylate polymers cross linked with an azo-aromatic group of divinylazobenzene reported in 1986 to coat pellets and to deliver insulin to the colon in rats (Saffran et al., 1986). Due to potential carcinogenicity of azo-aromatic compounds, their potential use has been decreased in recent years.

The upper GI tract has limited intrinsic capacity to digest dietary polysaccharides. Therefore, undigested polysaccharides such as cellulose, xylan, and undigested starch, pass into the distal regions of the small intestine (ileum) and colon. Micro-flora of the colon has the ability to degrade the naturally occurring polysaccharides through various enzymes such as galactosidase and arabinosidase. This makes polysaccharides a suitable substrate for these bacteria.

Polysaccharides are regularly used by the pharmaceutical and food industries and generally considered as safe. Many of these polysaccharides are hydrophilic in nature and swell in the upper GI tract conditions which could result in premature drug

release. In order to prevent this polysaccharides are chemically modified such as cross-linked galactomannan and calcium pactinate or mixed with hydrophobic insoluble polymers such as ethylcellulose. Examples of some of these polysaccharides include pectin (Ashford et al., 1993a, Berliner and Nacht, 1997, Lerner et al., 2000), amylose (Basit, 2000), chitosan (Nunthanid et al., 2008), chondroitin sulphate (Rubinstein et al., 1992), dextran (Simonsen et al., 1995), guar gum (Bayliss and Houston, 1984), and inulin (Vervoort and Kinget, 1996), etc. The combination of amylose and water insoluble polymer ethylcellulose has been exploited as film coating for colon targeting, which has shown series of successful results under *in vitro* and *in vivo* studies (Basit, 2005).

It is clear from above discussion that the choice of delivery system to the colon depends on many factors and entirely depends on formulator to choose a suitable combination for reliable performance.

1.6 FORMULATION STRATEGY

The approach adopted in this study utilises the methodology of press coating (previously discussed in Section 1.4.4) to situate a polymer barrier around an inner core tablet, containing an active pharmaceutical ingredient as an immediate release formulation (Figure 1.13).

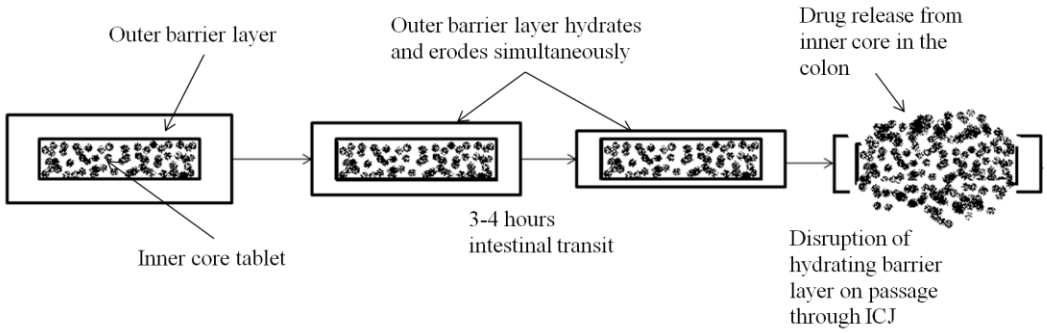

Figure 1.13 A schematic diagram outlining the proposed design for pulsatile/colon delivery.

It is proposed that the polymer barrier layer, once in contact with the dissolution medium or the intestinal fluid will hydrate and form a cohesive and mechanically strong gel, affording erosion over 3-5 hours, while at the same time keeping the inner core tablet intact. A literature review earlier in Section 1.3 indicated that the destructive forces in the human stomach under fed and fasting conditions are 1.9N and 1.5N respectively, and in the human small intestine it is potentially around 1.2N (Kamba et al., 2000, Kamba et al., 2002). For any formulation to successfully reach the lower GI tract intact, it must maintain sufficient mechanical strength and integrity to resist breakdown by these forces. Due to the process of erosion and mechanical shear forces presented in the GI tract the barrier gel layer would get weaker and weaker during its passage through the small intestine. Therefore, it is assumed that already weaken barrier gel layer would burst its content in the colon as soon as it passes through the ileo-cecal junction (Figure 1.13). There is some scintigraphic evidence that the ileo-cecal junction may exert a significant mechanical pressure on the dosage form as it transits from ileum to colon (Wilson, 2010). Takada (Takada, 1997) designed such a delivery system utilising the pressure at ileo-cecal junction as a trigger for the colon delivery as discussed in Section 1.5.1.2.

Therefore, a press coated tablet which would pulse after a pre-determined lag time is designed which could be used as a pulsatile delivery system or it could also be used in colon delivery pulsing after 3-5 hours post stomach (normal small intestine transit

time). The effect of variable gastric emptying (as discussed in Section 1.2.1) can be avoided by having an enteric coat to avoid any premature release in the stomach.

1.7 AIMS AND OBJECTIVES

The main aim of the current study was to design a predictable oral controlled release formulation which could be used as a pulsatile or targeted site specific delivery system in the large intestine using the time delayed approach.

In order to achieve this aim following objectives were defined.

1. To investigate the hydration, gel formation and gel strength and subsequent erosion of suitable excipients to be used as the coating layer component.
2. To develop appropriate screening methods for characterisation of formulation performance.
3. To characterise in depth the process of hydration and erosion and establish their correlation with analytical screening method in order to select appropriate excipients for time delayed delivery.
4. To develop a mathematical method to accurately predict a desired lag time and evaluate its *in vitro* behaviour.
5. To determine the *in vitro* and *in vivo* performance of the time delayed system.

CHAPTER 2

MATERIALS AND EQUIPMET

2.1 MATERIALS

2.1.1 Formulation excipients

Acacia (molecular weight 250000)	Sigma Aldrich, Dorset, UK
Activated charcoal	Merck, Leicestershire, UK.
Carbopol-934P-NF	Goodrich, Cleveland, UK
Carboxymethyl cellulose sodium (CMC sodium) 100, 1000, 1000/07, 20,000 and 40,000 viscosity grades	Dow Wolf Cellulose GmbH, Germany.
Chitin-7170	Sigma Aldrich, Louis, USA
Hydroxypropylmethyl cellulose (HPMC), Methocel E5LV, E6LV, E15LV, E50LV, E4MCR, E10MCR, K4M PREM, K100M	Dow Chemical Company, USA
Hydroxypropylmethyl cellulose (HPMC) Metolose 60SH-2910	Shin-Etsu Chemical, Tokyo, Japan.
Kappa-carrageenan	Dow Chemical Company, USA.
Lactose (Pharmatose, DCL11)	DMV-Fonterra, Goch, Germany.

Low hydoxypropyl cellulose-11 (L-HPC-11)	Shin-Etsu Chemical, Tokyo, Japan.
Magnesium stearate	Pfizer R&D, Kent, UK
Microcrystalline cellulose, Avicel® PH102	FMC BioPolymer, Girvan, UK.
Potato starch	Fluka Chemie GmbH, Buchs, Switzerland.
Poly(butyl methacrylate, (2-dimethylaminoethyl) methacrylate, methyl methacrylate) 1 : 2 : 1 (Eudragit® EPO)	Evonik Industries AG, Darmstadt Germany
Poly(methacrylic acid, methyl methacrylate) 1 : 1 (Eudragit® L100)	Evonik Industries AG, Darmstadt Germany
PVP Cross linked	ISP Technologies, New Jersey, USA.
Sodium alginate (viscosity of 2% solution 25 °C, ≈1400 cps)	BDH Chemicals, Poole, UK
^{99m}Tc-DTPA	Radiopharmacy, Western Infirmary, Glasgow, UK.

2.1.2 Chemicals

Deionised water	Produced in-house
Hydrochloric acid	Sigma-Aldrich, Dorset, UK.
Methylene Blue	Sigma Aldrich, Dorset, UK
Potassium phosphate dibasic	Sigma Aldrich, Dorset, UK

2.1.3 Drugs

Caffeine	Sigma-Aldrich, Dorset UK.
Riboflavin	Sigma-Aldrich Chemie GmbH, Germany.
Theobromine	Sigma-Aldrich, Dorset, UK.
Theophylline	Fluka Chemie GmbH, Buchs, Switzerland.

2.1.4 Consumables

Araldite® rapid epoxy glue	Araldite, Leicester, UK.
Blu Tack®	Bostik Ltd, Leicester, Leicestershire, UK.

Bone cement (Palacos® R-40)	Schering-Plough Ltd, Welwyn Garden City, UK

2.1.5 Manufacturing equipments

Benchpress	Spex CertiPrep, Middlesex, UK.
IR press (30 ton press C-30)	Research and Industrial Instrument Company, England.
IR punch and die set	Pye Unicom, England.
Perspex discs	Strathclyde Institute of Pharmacy and Biomedical Sciences' Workshop, Glasgow UK
Sieve 250µm	Endecotts Ltd, London, UK.
Single Punch Tablet Press	Manesty, Liverpool, UK
Turbula mixer	Glen-Creston Instruments, London, England.

2.1.6 Analytical equipments

Analytical balances	Mettler Toledo, Leicester, UK.

Dissolution apparatus	Erweka GmbH, Heusenstamm, Germany.
Dissolution apparatus	Pharma Test, Hamburg, Germany.
Dissolution apparatus	Caleva GB Ltd, Sturminster Newton, UK.
Dissolution apparatus USP 4 type flow through cell	AstraZeneca, Alderley Park, UK
Dose calibrator	Capintec, Southern Scientific Ltd., Sussex, UK.
Nuclear magnetic resonance spectrometer (NMR) Bruker Avance 400	Bruker, Coventry, UK.
pH meter	Radiometer Copenhagan, Denmark.
Stainless steel probes (pin probe Ø2mm, spherical probe Ø5mm, flat face probe Ø2.5 and 5mm)	Stable Micro Systems, Surrey, UK.
Texture Analyser TA-XT2	Stable Micro Systems, Surrey, UK.
Unicam UV-4 spectrophotometer	Unicam, Cambridge, UK.

2.1.7 PC Software

Gamma image analyser	MIE, Seth, Germany.
HPLC Software (Chromoquest)	Thermo Fisher Scientific, Florida, USA.
Minitab Release 14.1	Minitab Limited, Coventry, UK.
Power Vision 4.0	Bruker, Coventry, UK
Texture expert exceed version 2-0-7-0	Stable Micro System, Surrey, UK.

CHAPTER 3

INITIAL SCREENING EXPERIMENTS AND NOVEL TEXTURE ANALYSER METHOD

3.1 INTRODUCTION

This Chapter deals with the investigation of suitable excipients appropriate for designing a drug delivery formulation intended to release its content in the colon to achieve prolonged therapeutic effect. There are many approaches which have been proposed in the literature to deliver drugs to the colon, including pH sensing release (Khan et al., 1999), microbially controlled release (Basit, 2000), pressure sensitive release (Takaya et al., 1997) and time delayed release (Fukui et al., 2000a). Orally administered time delayed dosage forms have been investigated for a variety of purposes; in chronotherapeutics (Cutler et al., 1995) where verapamil is released after a predefined lag time in accordance with the circadian rhythm of the disease; in colon delivery (Takaya et al., 1997) for 5-ASA; and in avoiding pharmacokinetic drug-drug interaction by separation of release of diltiazem and midazolam (Sawada et al., 2003b). Time delayed release systems have been formulated as pellets (Ueda et al., 1994), capsules (Ross et al., 2000, Stevens et al., 2002) or compression coated tablets (Fukui et al., 2000a, Fukui et al., 2000b, Efentakis et al., 2006, Ghimire et al., 2007, Ghimire et al., 2011) to release the drug after predetermined lag time. Compression coated (also known as press coated) tablets contain an inner active core surrounded by a barrier layer and has been discussed briefly in Chapter 1 as a proposed delivery system in this study.

The lag time of drug release from a press coated tablet system is dependent on the following factors: the process of hydration and/or swelling of the layer, dissolution and/or erosion of the barrier layer, and mechanical strength of the barrier layer during these processes. A key aspect to achieve desirable lag time is reliant on the composition of the barrier layer and its mechanism of production (Ghimire et al., 2011, Ghimire et al., 2007).

In this Chapter, pharmaceutical excipients will be tested through preliminary *in vitro* gravimetric hydration and erosion studies, in order to assess their potential for use in further studies as a barrier layer component in a press coated tablet. The excipients chosen for study have been used safely in humans either for sustained release or colonic drug delivery.

3.1.1 Selection of excipients

Acacia is a complex, loose aggregate of sugars and hemicelluloses with a molecular weight of approximately 240,000–580,000. The aggregate consists essentially of an arabic acid nucleus to which are connected calcium, magnesium, and potassium along with the sugars arabinose, galactose, and rhamnose (Rowe et al., 2009). Acacia is mainly used in oral and topical pharmaceutical formulations as a suspending and emulsifying agent. It has been used in modified release tablets in combination with tragacanth (Bhardwaj et al., 2000). Furthermore, due to its anionic nature, other researchers (Meshali and Gabr, 1993) used it at different ratios as an interpolymer complex (combination of anionic and cationic polymer) with pectin.

The sodium salt of alginic acid is a linear glycuronan polymer consisting of a mixture of D-mannosyluronic acid and L-gulosyluronic acid residues. The molecular weight is typically 20,000–240,000. Sodium alginate is soluble in alkali hydroxides, producing viscous solutions, but is only very slightly soluble in water. The cross-linked form of sodium alginate with Ca^{+2} or gelatine has been characterised for controlled-release applications (Saravanan and Rao, 2010, Remunan-Lopez and Bodmeier, 1997). Researchers have demonstrated the use of calcium alginate beads as a core carrying 5-Aminosalicylic acid (Lin and Ayres, 1992) and chitosan-Ca-alginate micro-particulate drug delivery system for colon-specific delivery (Mladenovska et al., 2007).

Carbomer is a synthetic high-molecular-weight polymer of acrylic acid that is cross linked with either allyl sucrose or allyl ethers of pentaerythritol. The molecular weight of carbomer is theoretically estimated at 7×10^5 to 4×10^9. In tablet formulations, carbomers are used as controlled release agents and/or as binders.

Lightly cross linked carbomers (lower viscosity) are generally more efficient in controlling drug release than highly cross linked carbomers (higher viscosity) (Neau et al., 1996). Carbomers disperse in water to form a colloidal dispersion that after neutralisation with base produce a highly viscous gel. Commonly, carbomers designated with letter 'P' e.g. Carbopol 971P are the pharmaceutical grade polymers for oral and mucosal purposes.

Chitin is a white, hard, inelastic, nitrogenous and naturally abundant mucopolysaccharide, obtainable from crab or shrimp shells and fungal mycelia (Kumar and Majeti, 2000). The N-deacetylated derivative of chitin is called chitosan, although this N-deacetylation is almost never complete. Chitosan is a copolymer of varying amounts of N-acetyl glucosamine and N-glucosamine repeated units (Bansal et al., 2011). Chitin and chitosan are considered as suitable cationic functional materials, due to their excellent properties such as biocompatibility, biodegradability, non-toxicity, adsorption, etc. Chitin is highly hydrophobic and is insoluble in water and most organic solvents, though soluble in hexafluoroisopropanol, hexafluoroacetone, and chloroalcohols (Kumar and Majeti, 2000). Chitosan is degradable by the micro-flora of the colon as a result it has found its place in colon drug delivery systems (Hejazi and Amiji, 2003).

Carboxymethylcellulose sodium (CMC sodium) is described as a sodium salt of polycarboxymethyl ether of cellulose. CMC sodium is extensively used in oral and topical pharmaceutical formulations, mainly for its viscosity-increasing properties. CMC sodium is commercially available in various grades that have differing aqueous viscosities; low, medium, and high. The viscosity of CMC sodium solutions is fairly stable over a pH range of 4–10 (Rowe et al., 2009). Dabbagh et al., (1999) investigated three viscosity grades of CMC sodium for their ability to provide a sustained release of propranolol hydrochloride and found that the order of drug release was viscosity dependent.

Eudragit® E is a cationic polymer based on dimethylaminoethyl methacrylate and other neutral methacrylic acid esters. It is soluble in gastric fluid as well as in weakly acidic buffer solutions (up to pH 5). It is commercially available as a solution or dry powder. The powder form of Eudragit® E contains 98% dried weight content.

Eudragit® L is an anionic copolymerised products of methacrylic acid and methyl methacrylate. The ratio of free carboxyl groups to the ester is approximately 1:1 in Eudragit® L. This polymer is readily soluble in neutral to weakly alkaline conditions (pH 6–7) and form salts with alkalis, and as a result provide film coats that are resistant to gastric fluid but soluble in intestinal fluid. Eudragit® L-100 is a white free-flowing powders with at least 95% of dry polymer. Previous studies illustrate that Eudragit ® has potential in colon delivery system as a pH-dependent system (Khan et al., 1999) or an interpolyelectrolyte complex with sodium alginate (Moustafine et al., 2009).

Hydroxypropylmethyl cellulose (HPMC) is widely used excipients in oral, ophthalmic, ocular, nasal, and topical formulations. HPMC is a cellulose derivative, consisting of methoxy and hydroxypropoxy groups substituted onto a glucose backbone. It is available in different substitution grades and viscosities (Dow Chemical Company, 2011). HPMC is soluble in cold water forming a viscous colloidal solution though practically insoluble in ethanol, hot water, chloroform, and ether but soluble in mixture of alcohol and water. It is stable between pH 3 and pH 11, and considered resistant to enzyme attack (Rowe et al., 2009). In oral formulations, HPMC has been used as a tablet binder (Chowhan, 1980), film former (Rowe, 1980), time delayed colon delivery (Gazzaniga et al., 1994) and as a matrix former in extended-release drug delivery (Velasco et al., 1999).

Lactose anhydrous occurs as white to off-white crystalline particles or powder and commercially available as a mixture of anhydrous α-glucopyranose and β-galactopyranosyl lactose. Lactose is directly compressible and widely used in direct compression tableting applications mainly as a tablet and capsule filler and binder. Anhydrous lactose can be used with moisture-sensitive drugs due to its low moisture content. Lactose is soluble in water but sparingly soluble in ethanol and ether (Rowe et al., 2009).

Low-hydroxypropyl cellulose (L-HPC) is described as a partially low-substituted poly(hydroxypropyl) ether of cellulose with few free hydroxyl groups per glucose subunit converted to a hydroxypropyl ether (Kleinebudde, 1993). There are several types of L-HPC available which differ owing to different degree of substitution and

average particle size. L-HPC is practically insoluble in ethanol and ether but dissolves in sodium hydroxide solution (1 to 10) and produce viscous solution. It remains insoluble in water but swells upon hydration. L-HPC can be used in granulation and tableting as a binder and disintegrant. Ghimire et al (2007) illustrated the use of L-HPC in varying ratios with glyceryl behenate as a barrier layer in press coated tablet for pulsatile delivery.

Magnesium stearate is described as a mixture of solid organic acids consisting of variable proportions of magnesium stearate and magnesium palmitate obtained from vegetable or animal origin. It is practically insoluble in water, ethanol and ether (Rowe et al., 2009). In pharmaceutical formulations magnesium stearate is mainly used as a lubricant in tablets and capsules at a concentration of 0.25% to 5%. It is hydrophobic in nature and may retard the dissolution of oral solid dosage forms, therefore wherever possible it should be used in the lowest possible concentration in these formulations (Hussain et al., 1992, Wang et al., 2010).

3.1.2 Gel layer properties

Many pharmaceutical dosage formulations are designed to rely on polymer hydration and gel formation to achieve desired performance. Controlled drug release through matrix formation and barrier layer functions for colon delivery or pulsatile release are often dependent on maintenance of a cohesive gel layer over many hours. Different hydration layers and fronts may be present within the same formulation in response to gradual water ingress from the surrounding media to the tablet core as shown in Figure 3.1.

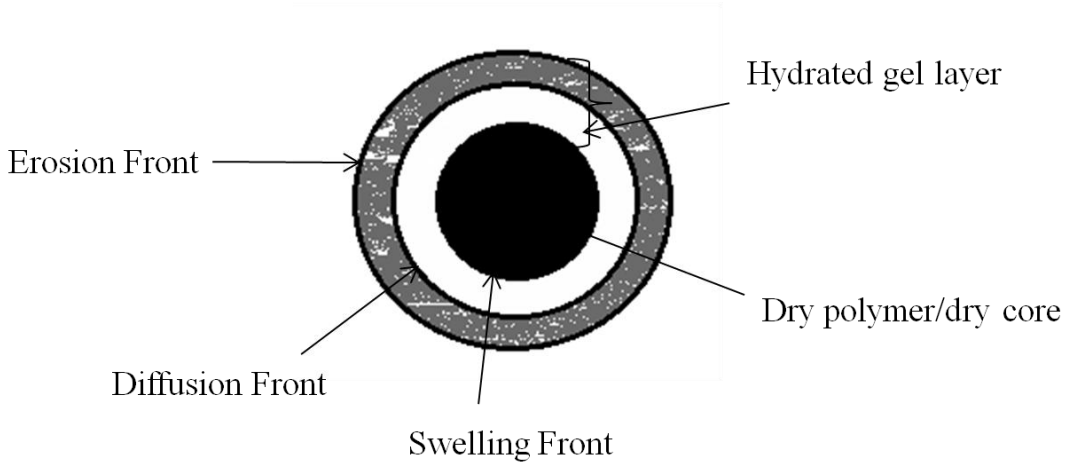

Figure 3.1 Schematic diagram of a hydrophilic matrix during the hydration process, illustrating hydrated gel layer fronts (erosion, diffusion and swelling) and dry core/polymer. Re-drawn from Colombo (1993).

These fronts can be named as erosion front at the periphery, diffusion front in the middle and swelling front at the tablet dry core (Colombo, 1993). When the polymer is soluble enough, the movement of swelling and erosion fronts becomes parallel and is called front synchronisation (Harland et al., 1988).

There are a number of techniques like optical microscopy (Tu and Ouano, 1977, Papadimitriou et al., 1993, Colombo et al., 1995), image analysis (Vlachou et al., 2004), ^{1}H NMR imaging (Rajabi-Siahboomi et al., 1994), ultrasound (Konrad et al., 1998), confocal laser scanning microscopy (Adler et al., 1999, Bajwa et al., 2006), and light scattering imaging (Gao and Meury, 1996) which have been used in the past to characterise swelling properties in a hydrating gel. However, these techniques can be expensive, time consuming and difficult to perform which impose a limitation on their routine application.

The texture analyser (TA) is a widely utilised technique in pharmaceutical research and development (Li and Gu, 2007). Figure 3.2 shows a schematic diagram of the TA, which consists of a compression arm with upward and downward movements, load cell, and compression probe.

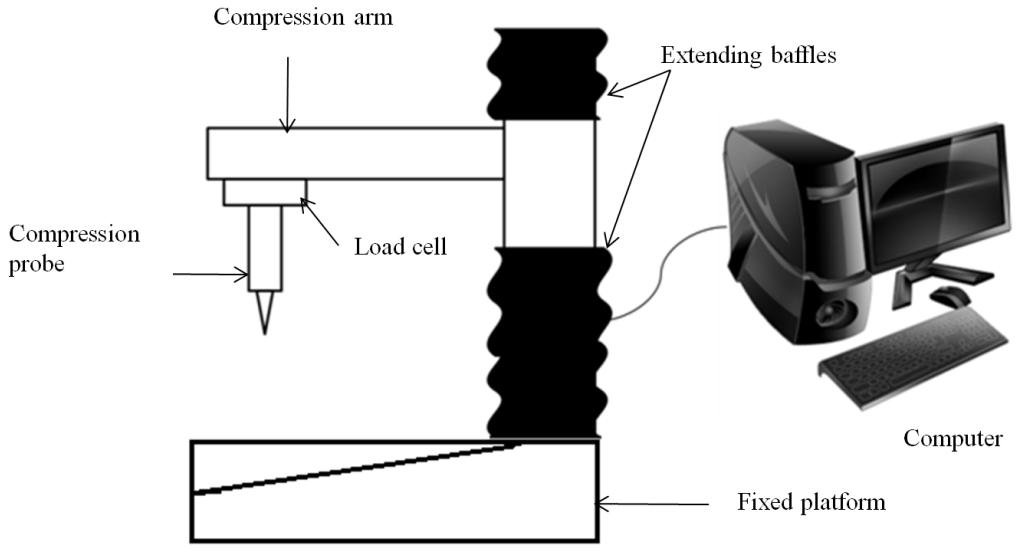

Figure 3.2 A schematic diagram of texture analyser.

The TA components are connected to a computer with built in software for data acquisition and analysis. The TA can be fitted with different probes and programmed to perform different tests. The force of resistance encountered by the probe is measured by the force transducer fitted within the analyser. Additionally, the TA is capable of measuring the complete and accurate stress-strain profile for the material under investigation. The TA has been used in the past to calculate the mechanical strength of polymeric films (Hodges et al., 2004), and adhesive and muco-adhesive properties of hydrophilic polymers (Walewijk et al., 2008, Thirawong et al., 2007). In tablet formulations the TA has been used to calculate the real time measurements of swelling and erosion rate of matrix tablets (Nazzal et al., 2007), and the quantitative correlation of drug dissolution and polymer hydration in modified release tablets of pseudoephedrine hydrochloride (Li and Gu, 2007). Baumgartner et al (2008) used the TA to calculate the gel strength at predefined depth within the tablet (4mm) to evaluate the behaviour of xanthan matrix tablets in the presence or absence of Ca^{+2} ions in the dissolution medium. Yang et al., (1998) used a texture analyser to monitor water advancement, swelling process and gel growth in an

HPMC compact. Although most researchers were able to identify a swelling front and the nature of intermediate region, no detailed description was reported for the interface between glassy core and hydrating gel layer using the TA. Additionally, there have not been any reported data on quantitative measurement of gel strength in different regions of the hydrating gel.

Therefore, this Chapter also deals with the development and use of the texture analyser (TA) to accurately measure the resistance of a sample to penetration by a test probe, as a means of screening proposed formulations in terms of gel layer strength and thickness. The understanding of these physical and mechanical properties of potential excipients would then aid in rationalising the choice of appropriate barrier layer formulation to achieve the desired lag time from the press coated tablet system.

3.2 PRELIMINARY SCREENING STUDIES

3.2.1 Methods

3.2.1.1 Tableting for erosion and hydration studies

All tablets were made with 13mm flat face IR punch and die using compression pressure of 8 and 10 ton and each tablet contained total weight of 200 mg. In order to ensure agglomerate free powder all excipients were passed through the steel mesh number 250 µm. Magnesium stearate was used to improve the inherent tableting problems such as tablet sticking and ejection wherever its use was inevitable and necessary. Otherwise, most formulations were kept simple by having polymer alone or in combination with other polymers as it is known that addition of excipients can change polymer properties (Khan and Jiabi, 1998, Majid Khan and Zhu, 1999). The batch size of 10 tablets equivalent to 2 gram powder weight was prepared for all formulations (1-26) as described in Tables 3.1-3.7. In case of formulations 1-3, 19-21 and 22-23 as detailed in Tables 3.1, 3.5 and 3.6 respectively, the tablet powders were weighed, sieved, mixed in mortar and pestle and compressed as tablet compact. All ingredients in formulations 4-9 (Table 3.2), 10-12 and 16-18 (Table 3.3), and 13-15

(Table 3.4) weighed and sieved, and mixed in mortar and pestle for 5 minutes without magnesium stearate. After 5 minutes of mixing, magnesium stearate was added to the pre-blended powder and again mixed for additional 3 minutes. Table 3.6 describes the formulations 24-26, containing pure polymers compressed as tablets weighing 200mg directly after sieving.

Table 3.1 Formulations 1-3 with their percentage excipients ratios.

Formulations	**Excipients**	
	Acacia	**Sodium Alginate**
1	20	80
2	50	50
3	80	20

Table 3.2 Formulations 4-9 with their percentage excipients ratios.

Formulations	**Excipients**		
	Carbopol	**L-HPC**	**Magnesium stearate**
4	80	20	
5	50	50	
6	20	80	
7	60	38	2
8	58	40	2
9	55	40	5

Table 3.3 Formulations 10-12 and 16-18 with their percentage excipients ratios.

Formulations	Excipients		
	Carbopol	**Chitin**	**Magnesium stearate**
10	69.5	30	0.5
11	69	30	1
12	65	30	5
16	59.5	40	0.5
17	49.5	50	0.5
18	19.5	80	0.5

Table 3.4 Formulations 13-15 with their percentage excipients ratios.

Formulations	Excipients			
	Carbopol	**Chitin**	**Magnesium stearate**	**Lactose**
13	50	34.5	0.5	15
14	35	34.5	0.5	30
15	15	34.5	0.5	50

Table 3.5 Formulations 19-21 with their percentage excipients ratios.

Formulations	Excipients			
	Eudragit E	**Eudragit L**	**Acacia**	**Sodium alginate**
19	50	50		
20	50		50	
21	50			50

Table 3.6 Formulations 22-23 with their percentage excipients ratios.

Formulations	Excipients		
	Eudragit E	**Carbopol**	**Carrageenan**
22	50	50	
23	50		50

Table 3.7 Formulations 24-26 with their percentage excipients ratios.

Formulations	Excipients		
	L-HPC	**HPMC K100M**	**CMC Sodium 20,000**
24	100		
25		100	
26			100

3.2.1.2 *In vitro* gravimetric erosion and hydration studies

Phosphate buffer adjusted to pH 7.4 was prepared by mixing 225ml of 0.2M potassium dihydrogen orthophosphate with 16.75ml of 0.2M sodium hydroxide and diluting it with distilled water to make 900ml. The tablets prepared in Section 3.2.1.2 were placed into a cylindrical polyethylene cap like tablet holder (with Blue tack®) that had an internal diameter (Ø13mm) equal to the diameter of the prepared tablets. Tablet samples prepared in this matter would allow water penetration from only one surface of the tablet matrix and produce gel swelling and erosion in one direction, which also further facilitated the tablet removal from dissolution vessel for easy weighing of hydrated tablet. These tablet samples were then placed in 900mL of phosphate buffer pH 7.4, and subjected to the erosion and hydration in USP dissolution apparatus II, with paddle speed of 100 rpm, and a temperature at 37°C ± 0.5. The hydration time of 3 or 5 hours was employed to collect the hydrated tablets keeping in mind the transit time of 3±1 hours for small intestine (Davis et al., 1986, Yuen, 2010).

The tablets were individually weighed before starting erosion and hydration studies. After 3 hrs and 5 hrs tablets were removed and weighed, dried in an oven for 36 hrs at 80ºC, and re-weighed to calculate percentage erosion and residual hydration. Percentage erosion and residual hydration were calculated using equations (1) and (2) respectively.

$$(M1-M2)/M1\times100 \quad (1)$$

$$(X2-M2)/M2\times100 \quad (2)$$

M1 = Initial tablet weight

M2 = Weight of dry eroded tablet

X2 = Weight of the tablet after dissolution before drying

3.3 RESULTS AND DISCUSSION FOR INITIAL SCREENING STUIDES

The prime requisite for a barrier layer in a press coated tablet designed for colon delivery is not to disintegrate in 3-5 hour time (normal intestinal transit time) during *in vitro* erosion studies. Otherwise, premature drug release from this type of barrier system is likely to happen during *in vivo* studies before it reaches the targeted site. Secondly, if the matrix forming excipients are used as a barrier layer composite they should hydrate, swell and form a durable gel layer before matrix erosion can expose inner core to hydration and disintegration. Due to aforementioned reasons any formulation which did not sustain itself for the period of 3 to 5 hour erosion studies and disintegrated or on visual and morphological inspection showed non-cohesive tablet surface would be disregarded for further studies.

3.3.1 Formulation 1-3

Acacia and Sodium alginate were investigated in ratios of 20:80, 50:50 and 80:20 and showed complete disintegration in 3 hour erosion studies as shown in Figure 3.3.

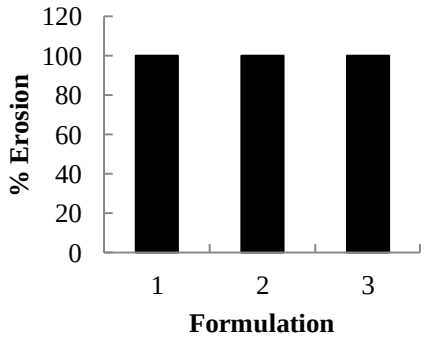

Figure 3.3 The bar charts representing percentage erosion for formulation 1-3 having acacia : sodium alginate at ratio (%) of 20:80 (1), 50:50 (2), and 80:20 (3) respectively (n=1).

Both excipients are water soluble (Rowe et al., 2009) in nature that could be one of the reasons which attributed to complete tablet erosion. Furthermore, erosion characteristics vary for sodium alginate in various pH conditions, according to Siramornsak et al (2007) alginate showed less erosion 30% in acidic medium compared to more than 50% erosion in basic medium during 120 minutes erosion studies. The buffer at basic pH 7.4 was used as dissolution medium during erosion studies for formulation 1-3 which would have further contributed to complete erosion in 3 hour time. Thus, there further use was not considered appropriate as a barrier layer composite as these formulations were unable to maintain their integrity during 3-5 hour hydration and erosion studies.

3.3.2 Formulation 4-9

In formulation 4-6, L-HPC and Carbopol were mixed without magnesium stearate in ratios of 20:80, 50:50, and 80:20, respectively. However, magnesium stearate was added as a lubricant and hydrophobic excipients in formulation 7-9 at 2-5% concentration having L-HPC and Carbopol at a concentration level of 38:60, 40:58 and 40:55, respectively. Figure 3.4 shows the percentage residual hydration and erosion after 5 hours hydration in formulation 4-9.

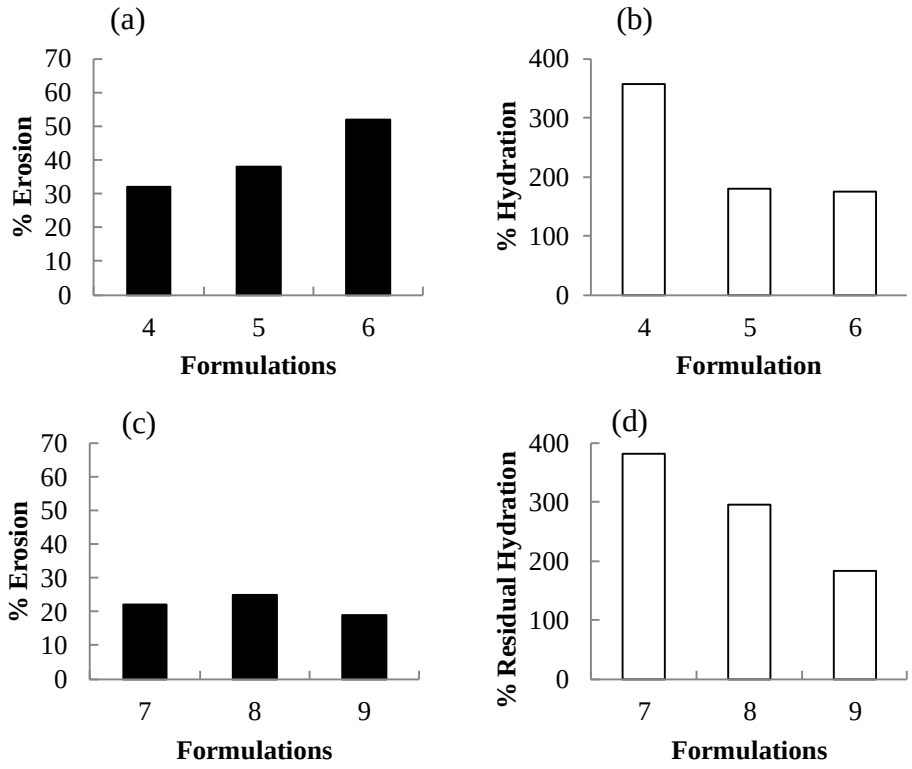

Figure 3.4 The bar charts representing (a) percentage erosion and (b) percentage residual hydration for formulation 4-6 having L-HPC : Carbopol at ratio (%) of 20:80 (4), 50:50 (5), and 80:20 (6) respectively; (c) percentage erosion and (d) percentage residual hydration for formulation 7-9 having L-HPC : Carbopol : magnesium stearate at a concentration level (%) of 38:60:2 (7), 40:58:2 (8) and 40:55:5 (9), respectively after 5 hours hydration (n=1).

The results in Figure 3.4 (a and b) for formulation 4-6 indicate that the increase in L-HPC concentration with reference to Carbopol resulted in increase percentage erosion though decreasing effect was observed for percentage residual hydration. Figure 3.4 (c) depicts the results for formulation 7-9, where increase in L-HPC concentration from 38% to 40% in formulation 7 to 8, respectively resulted in increase in % erosion similar to what observed for formulation 4-6. In case of formulation 9 the concentration of magnesium stearate was increased from 2% to 5%

resulted in less erosion (Figure 3.4, c), compared to formulation 8 having equal L-HPC concentration, this could be directly attributed to magnesium stearate hydrophobic effect being more pronounced at 5% concentration. The trend observed for formulation 7-9 was downward with regards to % residual hydration as shown in Figure 3.3 (d).

As mentioned earlier that Carbopol is an anionic polymer which is negatively charged at pH 7.4, and due to repulsion forces among these negative charges high degree of swelling occurs in Carbopol. Although L-HPC also swells in water, addition of L-HPC in Carbopol seems to control overall swelling and provided stronger and viscous gel (visual inspection) due to the stronger hydrogen bonding between the carboxyl groups of Carbopol (anionic polymer) and hydroxyl groups of cellulose ether L-HPC (non-ionic polymer), leading to stronger cross-linking between two polymers (Madhusudan et al., 2001, Samani et al., 2003). Overall presence of magnesium stearate in formulation 7-9 resulted in less % erosion (22, 25 and 19) compared to formulation 4-6 (32, 38 and 52).

On the basis of morphological characteristics of hydrated tablet through visual observation and evaluation of erosion and hydration data, formulation 9 having erosion 19% could have a potential for future studies as a barrier layer composite.

3.3.3 Formulation 10-18

In these experiments different combinations of Carbopol (anionic polymer) and chitin (cationic polymer) were investigated to exploit their ionic interaction (Rinaudo, 2006) as physical mixture with or without the addition of lactose and magnesium stearate. The formulation 10-12 were made using Carbopol: chitin: magnesium stearate at concentration ratio of 69.5:30:0.5, 69:30:1, and 65:30:5, respectively. While, in formulations 13-15, concentrations of magnesium stearate (0.5%) and chitin (34.5%) were kept constant; however Carbopol: lactose concentrations were changed with respect to each other 50:15, 35:30 and 15:50, respectively. Figure 3.5 shows the results for formulation 10-15 in terms of their erosion and hydration after 5 hrs of hydration.

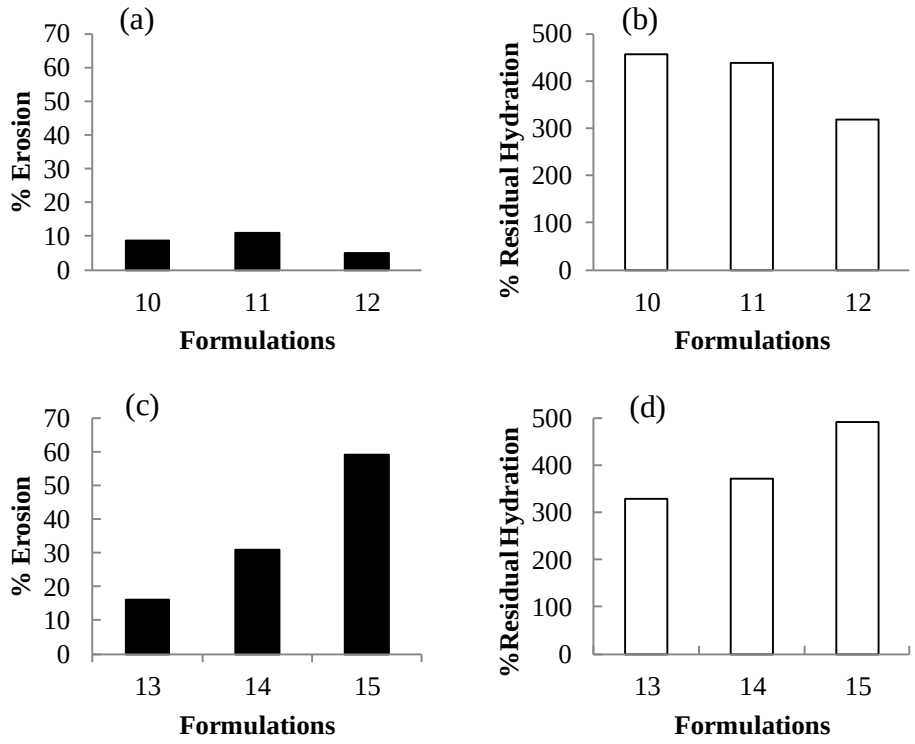

Figure 3.5 The bar charts representing (a) percentage erosion and (b) percentage residual hydration for formulation 10-12 having Carbopol : chitin : magnesium stearate at ratio (%) of 69.5:30:0.5 (10), 69:30:1 (11), and 65:30:5 (12) respectively; (c) percentage erosion and (d) percentage residual hydration for formulation 13-15 having constant concentration of chitin (34%) and magnesium stearate (0.5%) and Carbopol : lactose at a concentration level (%) of 50:15 (13), 35:30 (14) and 15:50 (15), respectively after 5 hours hydration (n=1).

The data indicate that the difference in erosion and hydration between formulation 10 (erosion 8.8% and residual hydration 457%) and formulation 11 (erosion 11% and residual hydration 439%) is relatively small due to small difference in formulation composition. However, erosion (5%) and residual hydration (318%) in formulation 12 are comparatively lower than both formulation 10 and 11.

Again, it can be argued that the presence of magnesium stearate at 5% concentration in formulation 12 depicted its hydrophobic effect and resulted in less erosion (Figure

3.5). Additionally, physical examination of formulation 12 also revealed more stable and cohesive gel structure after 5 hour hydration. The polyelectrolyte complex (PEC) or interpolyelectrolyte complec (IPEC) is usually formed when two aqueous solutions of anionic and cationic polymers are mixed together due to the electrostatic attraction between the oppositely charged groups (Kovacevic et al., 2007). It is highly unlikely that a physical mixture of these two polymers (chitin and Carbopol) would have formed polyelectrolyte complex (PEC) which usually required a set condition and depends on factor like the nature of ionic groups, initial polyelectrolyte concentrations, pH, ionic strength, temperature, and preparation procedure (Dash et al., 2011). However hydrogen bonding between carboxylic group of Carbopol and hydroxyl group of chitin might be the reason for cohesive gel structure observed in these formulations (Rinaudo, 2006). Figure 3.5 also shows the results for formulation 13-15, indicating that as the concentration of lactose was increased from 15% to 50% a simultaneous increase in erosion and residual hydration was observed. The addition of lactose on one hand provided better strength to formulated tablets due to its filler and binder properties however; due to its higher water solubility it might have caused more erosion in formulation 13-15. The effect of increasing quantities of lactose to enhance drug dissolution due to its water soluble nature has also been previously published (Allahham and Stewart, 2007).

In case of formulations 16-18, concentration of chitin was increased while concentration of Carbopol was subsequently decreased 40:59.5, 50:49.5 and 80:19.5, respectively whilst keeping magnesium stearate concentration constant at 0.5% in all three formulations. Figure 3.6 shows the results for formulation 16-18 in terms of their erosion and residual hydration after 5 hrs of hydration.

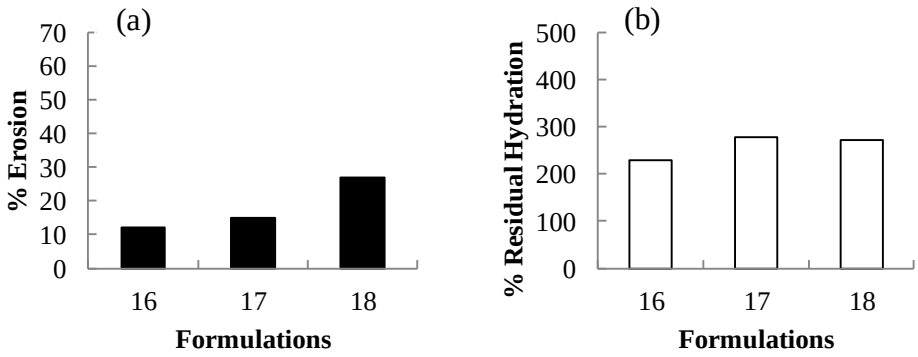

Figure 3.6 The bar charts representing (a) percentage erosion and (b) percentage residual hydration for formulation 16-18 having Carbopol: chitin: magnesium stearate at ratio (%) of 59.5:40:0.5 (16), 49.5:50:0.5 (17), and 19.5:80:0.5 (18) respectively, after 5 hours hydration (n=1).

The data indicate that the increase in chitin concentration resulted in overall higher hydration and erosion. This effect is understandable because chitin has a very low capacity to swell on its own (Synowiecki and Al-Khateeb, 2003) and it was Carbopol which contributed towards gel formation at pH 7.4. Thus, decrease in Carbopol concentration resulted in decrease in gelling and interaction between chitin and Carbopol allowing more water to ingress and caused more erosion to take place.

Through morphological inspection and erosion-hydration data it was concluded that the formulation 12 and 17 have cohesive gel structure and showed less erosion, so can be useful for further studies.

3.3.4 Formulations 19-23

In formulation 19-23, Eudragit® E as a cationic polymer were mixed as a physical mixture with opposite anionic polymers Eudragit® L, acacia, sodium alginate, Carbopol and carrageenan at 50:50 ratios. In recent years researchers (Moustafine and Bobyleva, 2006, Obeidat et al., 2008, Gómez-Burgaz et al., 2008) have investigated the properties of IPEC complex prepared from Eudragit® E with other anionic polymer as a sustain release delivery system or proposed their application

suitable for colon delivery. The hydration and erosion studies revealed that all formulations (19-23) were completely eroded in 3 hours time leaving no mass to calculate erosion and hydration. Therefore, the data cannot be shown for formulation 19-23.

Obeidat et al (2010) demonstrated that the physical mixture of Eudragit® E/Eudragit® L (50:50) showed a slight hydration before they were completely disintegrated in 2.5 hour at pH 6.8 attributing this hydration effect to weak interaction but not significant to form interpolymer interaction between Eudragit® E and L. It can be postulated that interpolymer interactions were either absent or very weak between cationic polymer Eudragit® E and other anionic polymers used in formulation 19-23 that could be the reason they would not have maintained their integrity in 3 hour and completely disintegrated. However, only further investigations with analytical tool such as IR can prove this theory. Figure 3.7 shows the condition of Eudragit® E: sodium alginate ratio 50:50 after 3 hour erosion studies.

Figure 3.7 Hydration state of sodium alginate: Eudragit® E ratio 50:50 after 3 hour of hydration and erosion.

Thus, use of these formulations is evidently not suitable for future studies as they clearly demonstrated lack of formulation integrity during 3-5 hour erosion and

hydration studies. Furthermore, no attempt were made to make IPEC as these new polymer would require a safety data before they could be use safely in animal and human.

3.3.5 Formulations 24-26

In case of formulation 24, 25 and 26, L-HPC, HPMC K100M and sodium CMC 20,000Pa, respectively were used as 100 percent pure polymers without any added excipients. Figure 3.8 shows the residual hydration and erosion data for formulation 24, 25 and 26.

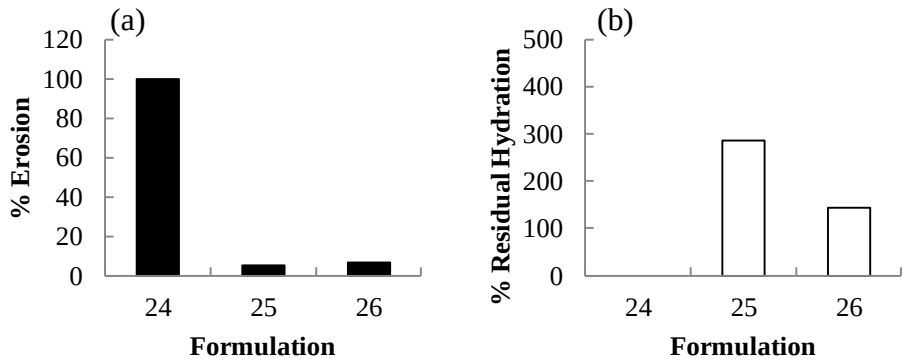

Figure 3.8 The bar charts representing (a) percentage erosion and (b) percentage residual hydration for formulation 24-26 containing L-HPC, HPMC K100M and sodium CMC 20,000 respectively, after 5 hours hydration (n=1).

The data indicate that the L-HPC (formulation 24) was completely disintegrated due to excessive swelling, the property extensively exploited as tablet and capsule disintegrant in oral formulation. In case of HPMC and sodium CMC the erosion was found 5.3% and 6.7% respectively and residual hydration was 286% and 143% respectively, after 5 hour. The hydrophilic polymers like HPMC and sodium CMC

once in contact with intestinal fluid or water, quickly hydrate and form a cohesive gel layer (Siepmann and Peppas, 2001). In general, in hydrophilic polymer erosion was found to be inversely proportional to the polymer molecular weight (Reynolds et al., 1998) which could be the reason for small erosion values observed for high molecular weight HPMC and sodium CMC. Additionally, hydration states of these polymers revealed that morphologically they had more cohesive gel structure and have a potential for future studies as a barrier layer component in press coated tablet.

It can be concluded that the erosion and hydration characteristics of the polymers described above have provided to some extent some information regarding integrity and cohesiveness of the hydrated gel. However, due to lack of quantitative data on the performance of gel layer, it was difficult to compare different formulations for their suitability as a barrier layer composition. Nevertheless, formulation 9, 12, 17, 25 and 26 did indicate their potential application for further studies. It was decided though that to characterise and understand further the barrier layer properties simple system like sodium CMC and HPMC capable of forming a cohesive and strong gel would be taken forward for future studies.

3.4 DEVELOPMENT AND VALIDATION OF NOVEL TEXTURE ANALYSIS METHOD

3.4.1 Methods

3.4.1.1 Tableting for TA studies

A series of control experiments were performed, using the Texture Analyser. The powder containing different grades of either sodium CMC or HPMC were sieved through the mesh number 250 µm and compressed as a single compact tablets weighing 200mg. The texture analyser studies were performed on sodium CMC having viscosity of 100, 1000, 1000/07, 20,000 and 40,000, and HPMC K4M PREM, K100M and E4MCR.

3.4.1.2 Texture analyser studies

The TA probes (Ø5mm (flat and spherical), Ø2.5mm (flat), and Ø2mm (pin)) initially travelled at a rate of 2.0mm/sec until the surface of the hydrated tablet was detected at 0.1N of the force, at which point the probe penetrated the swollen hydrated gel layer at a speed of 0.1mm/sec. Once the probe detected 5N of the force, which was determined as the dry tablet core layer, the probe would withdraw automatically out of the gel layer at a rate of 1.0mm/sec. However, it is worth mentioning here that during early method development different scan speeds and detection forces were tested and optimised method was selected. The data obtained from texture analyser (TA) studies were analysed using textural expert exceed 32 (TEE 32) software.

To prepare samples for texture analysis, three methods were used. During early method development each prepared matrix tablet as detailed in Section 3.4.1.1 was adjusted into tablet holder using Blue tack® and these tablet samples were then placed in 900ml of deionised water, and subjected to the same condition as described in Section 3.2.1.2. Samples were collected at 0.5, 1, 1.5, 2, 2.5 and 3 hours for texture analysis and analysed using the Ø5mm (flat) TA probe.

However, the variability in results due to Blue tack®, hydrodynamics in dissolution vessels and size of TA probe resulted in adaptation of second method where tablets were placed on a square of aluminium foil with the help of double sided sellotape and immersed in beakers of 500ml at 37°C without stirring. Tablet samples prepared in this way would allow water to penetrate from axial and radial side of the tablet matrix and produce gel swelling without constrains from any direction apart from bottom surface. This also resulted in easy removal of the tablets from beaker without disturbing the gel layer. The samples were analysed for TA using probe sizes Ø5mm (flat and spherical), Ø2.5mm (flat), and Ø2mm (pin) after 0.5, 1, 1.5, 2, 2.5 and 3 hours of hydration time.

The second method was able to overcome some of the variations as mentioned above though; aluminium foil was considered another variable to control. In order to further improve TA method, in third method, before starting the TA studies tablet samples were dried in an oven at 60°C and kept for 10 min in desiccators in order to remove any moisture already present in the tablet. Tablets were then affixed on a round Perspex disc with double sided sellotape and subjected for the same conditions as described above in second method.

The calculations were made for distance (mm) (gel thickness) that the probe travelled within the gel layer, force (N) (gel strength) that the probe encountered during probe penetration, time (sec) that the probe taken to travel through the gel layer, area under the curve (AUC) which represents the work done by the probe (force (N) × distance (mm) or time (sec) or Joules) and the gradient or slope in the TA graph represents the stiffness or deformability shown by the sample (force/distance (mm) or time (mm)). In order to calculate gel thickness/distance, area under the curve (AUC), gradient (stiffness) and forces (gel strengths), the typical texture analyser graph was divided into three different regions wherever possible. A typical TA graph for measurement is shown in Figure 3.9.

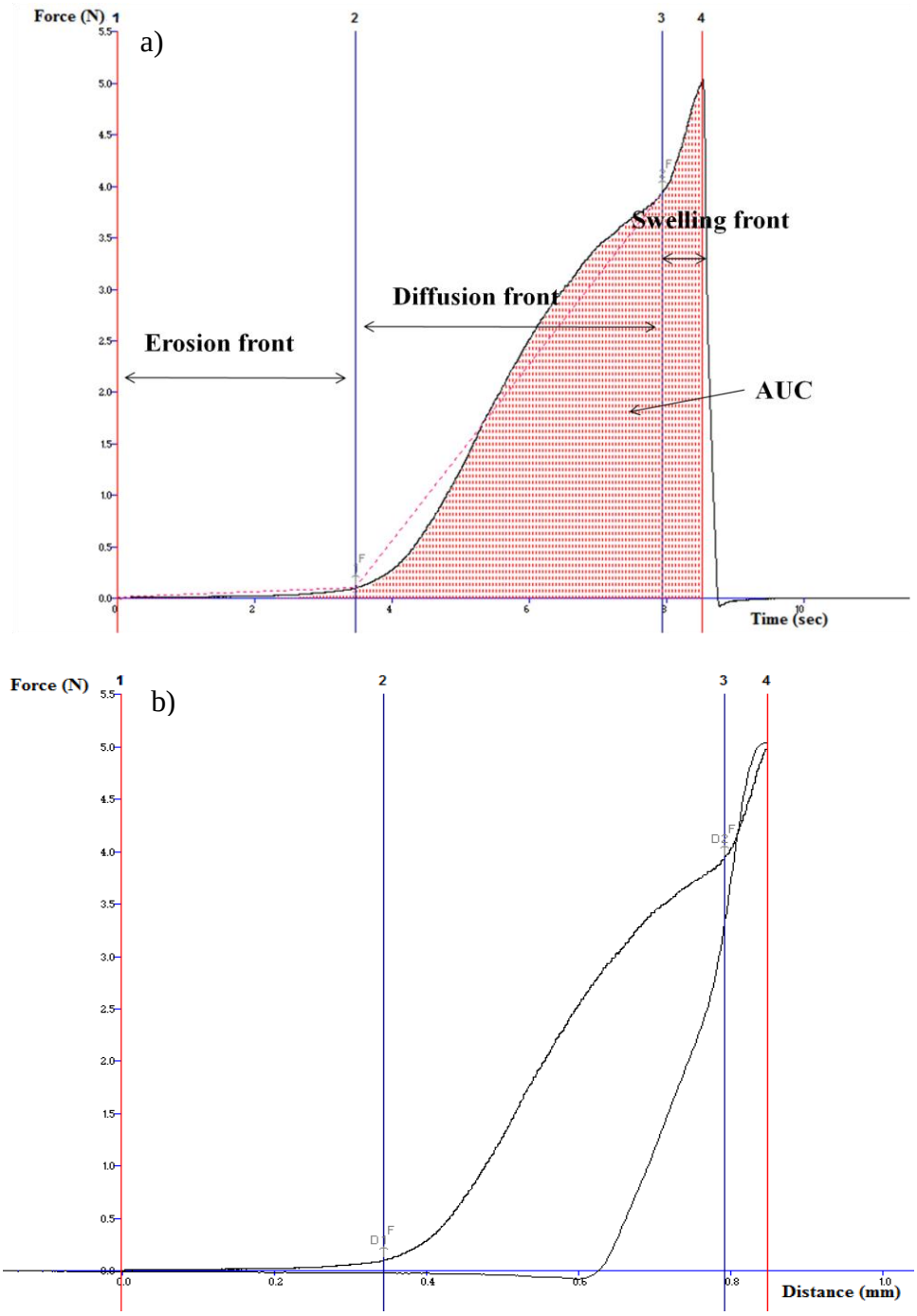

Figure 3.9 The TA graph showing the position of anchors and the values on X-axis in (a) time and (b) distance. The shaded area shown on graph (a) represents AUC. The anchors 1, 2, 3 and 4, were selected as standardized points for a meaningful comparison of all textural profiles.

An anchor is a reference point in time on the TA graph generated by the texture expert software and shown as a vertical line, with a number above (Figure 3.9). Anchors are the key to making measurements from the data. The anchors were placed at the graph whenever a sharp rise was observed during probing into the swollen gel. The first anchor was placed at zero point on X-axis, second anchor at first sharp rise observed in the graph, third anchor at second sharp rise in the graph and last the fourth anchor at the highest force peak value. The value on X-axis can be changed to time or distance to calculate total time of probing and thickness/distance of the gel, respectively. Whenever an anchor was placed on TA profile the values for time, distance and force were automatically generated by the textural expert software.

The three different regions on a typical texture analyser force-time profile, shown in Figure 3.9, were also named as erosion front, diffusion front and swelling front at tablet dry core representing the regions between anchor 1-2, 2-3, and 3-4, respectively. The AUC or work done by the probe on the hydrating gel layer is obtained from the area under the force–distance TA profile between either anchor 1-2, 2-3, 3-4 or 1-4 using the trapezoid rule. Gradient is obtained from the slope of the ascending portion of the TA profile between either anchor 1-2, 2-3, 3-4 or 1-4.

3.4.1.3 Photographic imaging for hydrating matrix tablet

The purpose of this experiment was to visually observe different hydration layer or fronts in hydrating matrix tablet with the help of photographic image. Methylene blue, a water soluble dye was used for imaging purpose. The HPMC K100M tablet weighing 200mg was affixed on Perspex disc and immersed in methylene blue 1%w/v solution (in water) to hydrate. After 60 minutes hydration, tablet was removed from solution and vertically cut into two half using a surgical knife. The photograph of cross-sectional half of the tablet was taken with digital camera (Kodak Easy Share Z1275).

3.5 RESULTS AND DISCUSSION FOR TEXTURE ANALYSIS METHOD

It is essential to develop a relatively simple and rapid test which would differentiate among the potential excipients and provide detailed data on the performance of the gel forming components in the formulation as water gradually hydrates the polymer.

It is known that the thickness of hydrated gel layer and mechanical gel strength can impart a substantial influence on *in vivo* performance of swellable matrices as matrix integrity might change under mechanical forces presented in human stomach (1.89N) (Kamba et al., 2000) and small intestine (1.2N) (Kamba et al., 2002). This information is valuable to formulation scientist in early designing of drug delivery systems. The TA is an instrument capable of accurately measuring the resistance in the sample to penetration by a test probe, and could be useful to screen proposed formulations in terms of gel layer strength.

3.5.1 Comparison between different grades of sodium CMC

In these experiments different grades of sodium CMC were subjected for texture analysis studies using a flat faced probe (Ø5mm). The calculations were made for area under the curve (AUC) and the stiffness or deformability shown by the sample. The different grades used in these experiments were 100 Pa, 1000 Pa, 1000/07 Pa, 20,000 Pa and their results are shown in Figure 3.10.

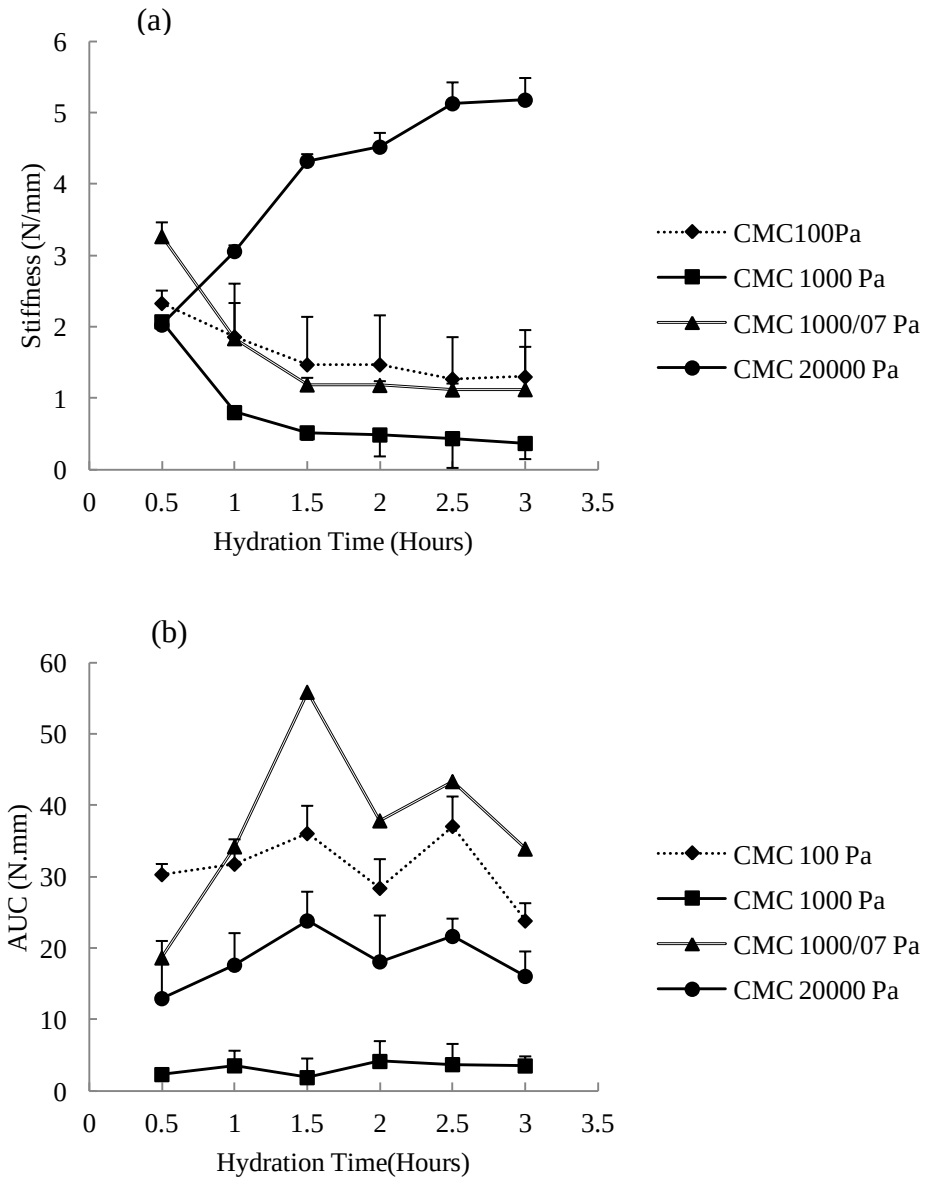

Figure 3.10 The calculations of (a) gel stiffness and (b) area under the curve using TA for different viscosity grades of sodium CMC 100 Pa, 1000 Pa, 1000/07 Pa, 20,000 Pa (n=3).

From Figure 3.10, it can be seen that the results vary quite significantly and it was impossible to conclude any trends from these graphs. For instance, due to high viscosity of sodium CMC 20,000 Pa, it was expected that the work done should be higher than other grades but it was not the case and the work done shown by this grade was even less than the 100 Pa grade. On the other hand, the gel stiffness for

sodium CMC 20,000 Pa was higher as expected however, the trend was upward opposite to anticipated downward trend as observed in other grades. Moreover, one anticipate a stiffer gel from high viscosity grades of sodium CMC (1000Pa and 1000/07Pa) however, there overall gel stiffness was even lower than low viscosity grade (100Pa).

These results raised the question about the suitability of TA for this study. However, when further investigations were carried out it was found that there were some variables which would need to be controlled. Mainly these variables were

- Tablet holder and use of Blue Tack®
- Position of the hydrating tablet in the dissolution apparatus

Additionally, as an alternative to Ø5mm flat face probe which was used initially, other probe types were also studied so that the best probe should be chosen for future studies. Instead of using the tablet holder and Blue Tack®, the aluminium foil and double side sellotape were used for easy handling and immersion of the tablet in hydrating medium.

The effect of hydrodynamics generated by the dissolution apparatus and position of the tablet in the apparatus caused hydrating gel to angle at one side due to that reason it was suggested that hydration should be done without any rotation in simple beaker.

3.5.2 The TA probe comparison

In order to select the suitable probe capable of detecting differences among different polymers on the basis of gel thickness/distance, area under the curve (AUC), gradient (stiffness) and forces (gel strength). In these experiments different probes were used as shown in Figure 3.11.

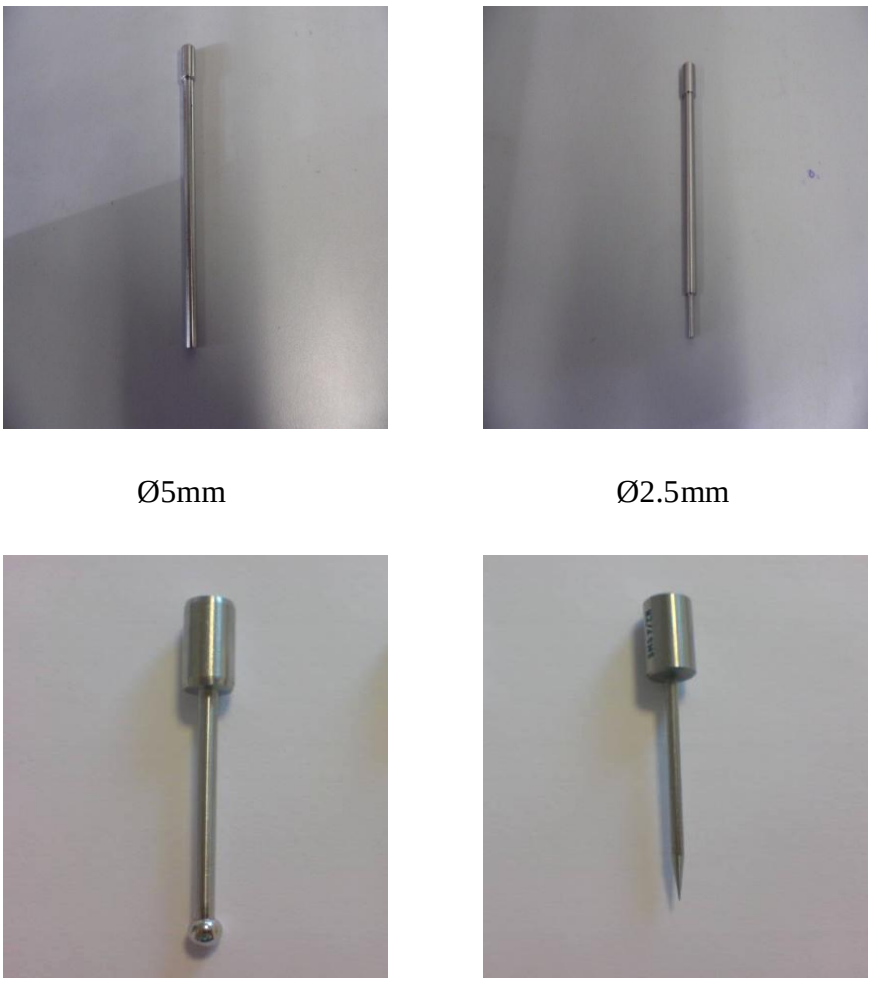

Figure 3.11 The different probes used for T.A studies.

Figures 3.12, 3.13, and 3.14 show the trends observed for gel thickness (mm), gel strength (N), area under the curve (N.mm) and gel stiffness (N/mm) respectively, in response to increasing hydration time and comparison of pin probe Ø2mm, flat face probe Ø2.5mm and flat face probe Ø5mm for these trends.

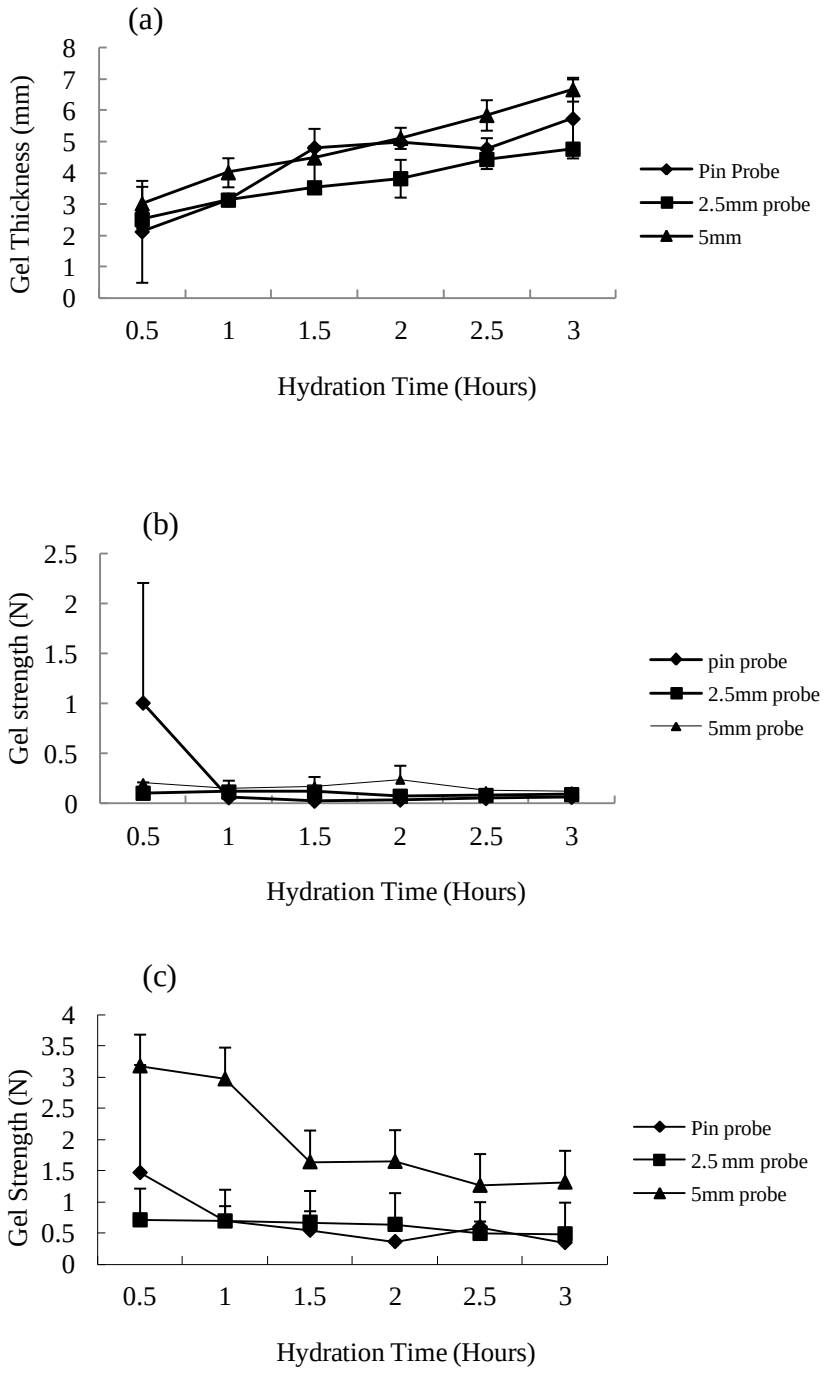

Figure 3.12 Comparison of gel thickness and gel strength and trends observed for sodium CMC 20,000 Pa in three different TA probes (Ø2.5mm, Ø5mm, and Ø2mm), representing (a) total thickness, (b) gel strength at erosion front, (c) gel strength at diffusion front (n=3).

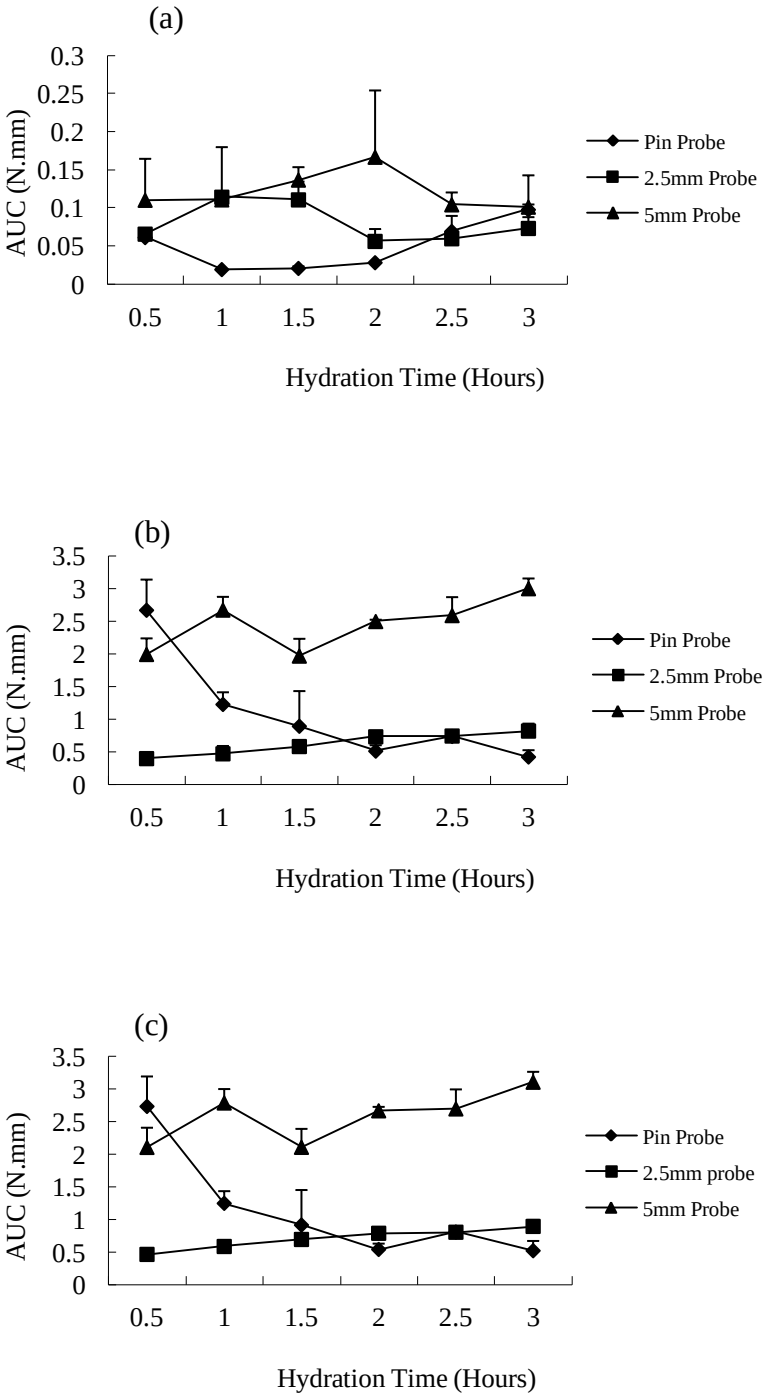

Figure 3.13 Comparison of area under the curve (AUC) at (a) erosion front, (b) diffusion front, (c) collective AUC at erosion and diffusion fronts and trends observed for sodium CMC 20000 Pa in three different TA probes (Ø2.5mm, Ø5mm, and Ø2mm) (n=3).

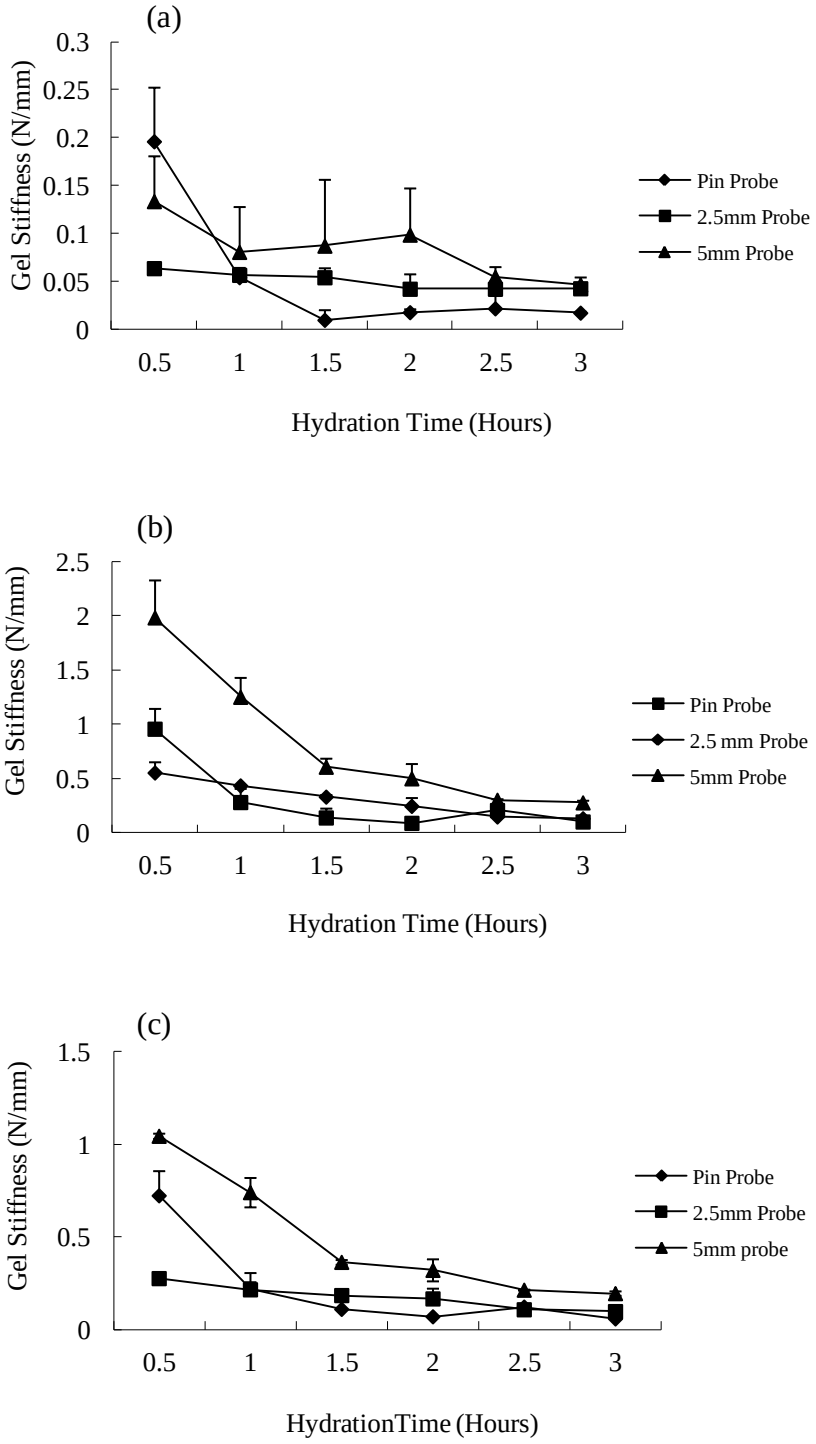

Figure 3.14 Comparison of gel stiffness at (a) erosion front, (b) diffusion front, (c) collective gel stiffness at erosion and diffusion fronts and trends observed for sodium CMC 20000 Pa in three different TA probes (Ø2.5mm, Ø5mm, and Ø2mm) (n=3).

Figure 3.12 shows that the thickness of the gel increased with hydration time however, there was a decline observed in the gel strength which could be due to weakening of the gel layers over a long hydration time.

The area under the curve (AUC) was calculated for three different regions in the graphs. It was found that three probes had provided variable results for area under the curve as shown in Figure 3.13. For instance, in case of flat face probes Ø 2.5mm and Ø 5mm the trend was upward, while in case of pin probe the trend was downward. These trends could be directly related to probes diameters i.e. large surface area will experience more resistance and so higher work done is required to penetrate into the surface of the gel and vice versa is true for small diameter probe.

In case of gradient which represents gel stiffness from the sample, it was observed that over all trends in all three probes were descending which means that gel layers became weaken over hydration time as shown in Figure 3.14.

It was observed that the pin probe performed as a more sensitive tool to detect changes in gel layer bringing micro disturbances in local environment during TA profiling and considered more appropriate than the flat face probe for use in further studies.

In order to observe the effect of different compaction forces with respect to their hydration and to evaluate the suitability of TA to differentiate any trends by comparing the results from spherical (Ø5mm) and pin (Ø2mm) probes, HPMC tablets were compressed with 8 ton and 10 ton compression pressure.

Figure 3.15 shows the comparison of pin probe with spherical probe in sodium CMC 20000 Pa at diffusion front for thickness and gel strength. As expected, the detected gel layer in sodium CMC 20000 Pa increased in thickness over time, while maximum gel strength detected decreased.

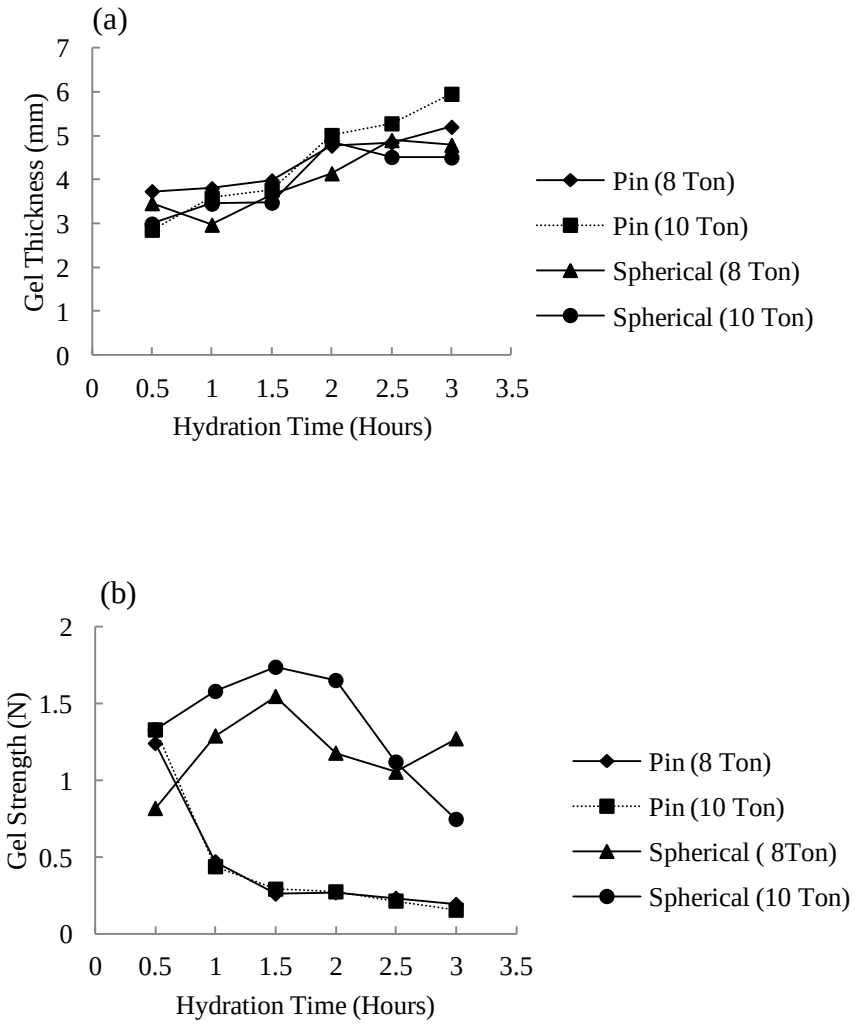

Figure 3.15 Comparison of TA probes (pin probe (♦ and ■) and spherical probe (● and ▲)) using sodium CMC 20000 Pa at diffusion front to calculate (a) thickness and (b) gel strength (n=1).

Figure 3.16 shows the comparison of pin probe with spherical probe in sodium CMC 20000 Pa for area under the curve at erosion front, diffusion front and collective AUC for erosion and diffusion front.

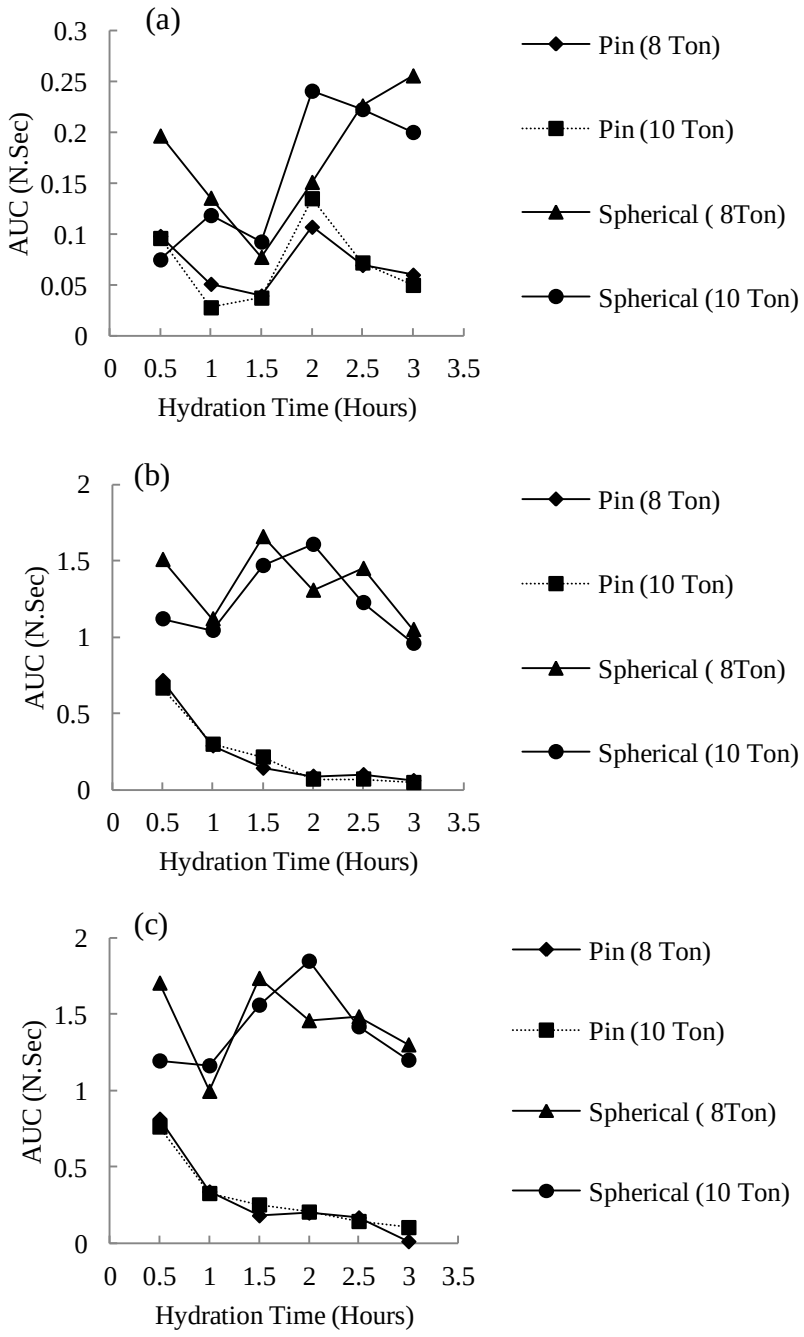

Figure 3.16 Comparison of TA probes (pin probe (♦ and ■) and spherical probe (● and ▲)) using sodium CMC 20000 Pa to calculate area under the curve at (a) erosion front (b) diffusion front and (c) collective AUC for erosion and diffusion front (n=1).

The area under the curve by pin probe suggested the negative trend similar to the one showed in Figure 3.13, whereas any trend for spherical probe was difficult to conclude.

Figure 3.17 shows the comparison of pin probe with spherical probe in sodium CMC 20000 Pa for gel stiffness/gradient at erosion front, diffusion front and collective gel stiffness for erosion and diffusion front.

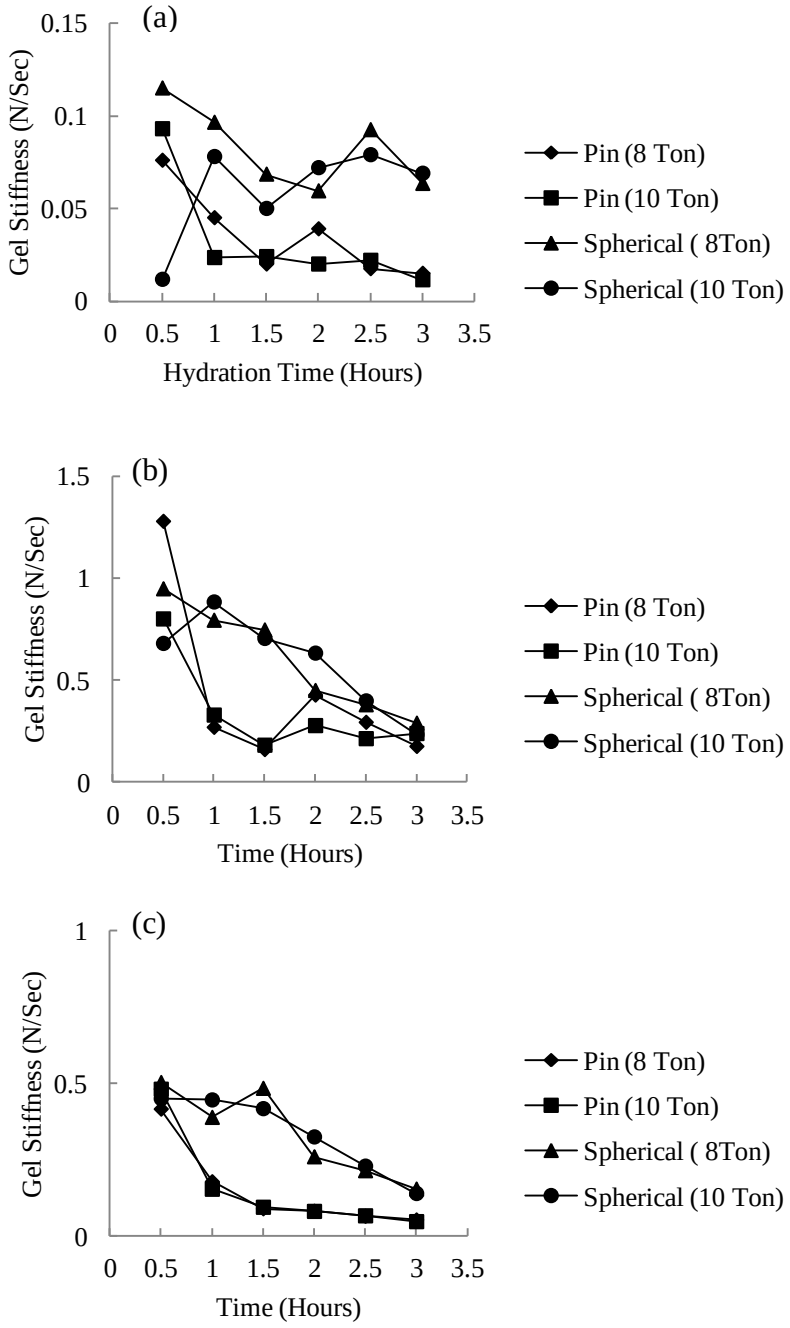

Figure 3.17 Comparison of TA probes (pin probe (♦ and ■) and spherical probe (● and ▲) using sodium CMC 20000 Pa to calculate gel stiffness/gradient at (a) erosion front (b) diffusion front and (c) collective gel stiffness for erosion and diffusion front (n=1).

The trends in case of gradient/stiffness were downwards for both probes; however variability in results were obvious for spherical probe. It is also clear from the data (Figures 3.15, 3.16 and 3.17) that pin probe did not detect any significant difference between the tablets made with 8 ton and 10 ton pressure and their resulted values were more or less overlapped each other. In case of spherical probe there was some difference in the resulted values for tablets compressed with 8 ton and 10 ton compression pressure however, it is difficult to make any conclusion on the basis of these results. As this data values correspond for n=1, this may be another reason for inconclusive results. Though, several researchers (Velasco et al., 1999) stated that the compression force is statistically significant in case of tablet hardness, its effect on drug release from HPMC tablets was minimal. Presumably, the variation in compression forces should be closely related to a change in the porosity of tablets (Nokhodchi et al., 1996). However, as the porosity of the hydrated matrix is independent of the initial porosity (Sarisuta and Mahahpunt, 1994), it can be assumed that the compression force seems to have little influence on hydrating gel layer properties.

Most previous studies mentioned the use of flat face probe (diameter Ø2.0 mm) for textural analysis profiling (Yang et al., 1998, Pillay and Fassihi, 1999, Pillay and Fassihi, 2000, Jamzad et al., 2005, Li and Gu, 2007, Körner et al., 2010) however, according to these results it can be concluded that the pin probe has provided more consistent results and is more sensitive tool than other probes. So for future studies pin probe will be chosen as a suitable probe for texture analyser studies.

3.5.3 Detection of three distinctive regions in hydrophilic polymer

It was constantly observed that the gel layers from these hydrophilic polymers can be dividable into three distinctive layers or fronts, and were called erosion front (hydrated layer), diffusion front (partially hydrated layer) and swelling front at the dry core. Figure 3.18 explains these three fronts using texture analyser profile and with photographic image of vertically sliced hydrated tablet of HPMC K100M.

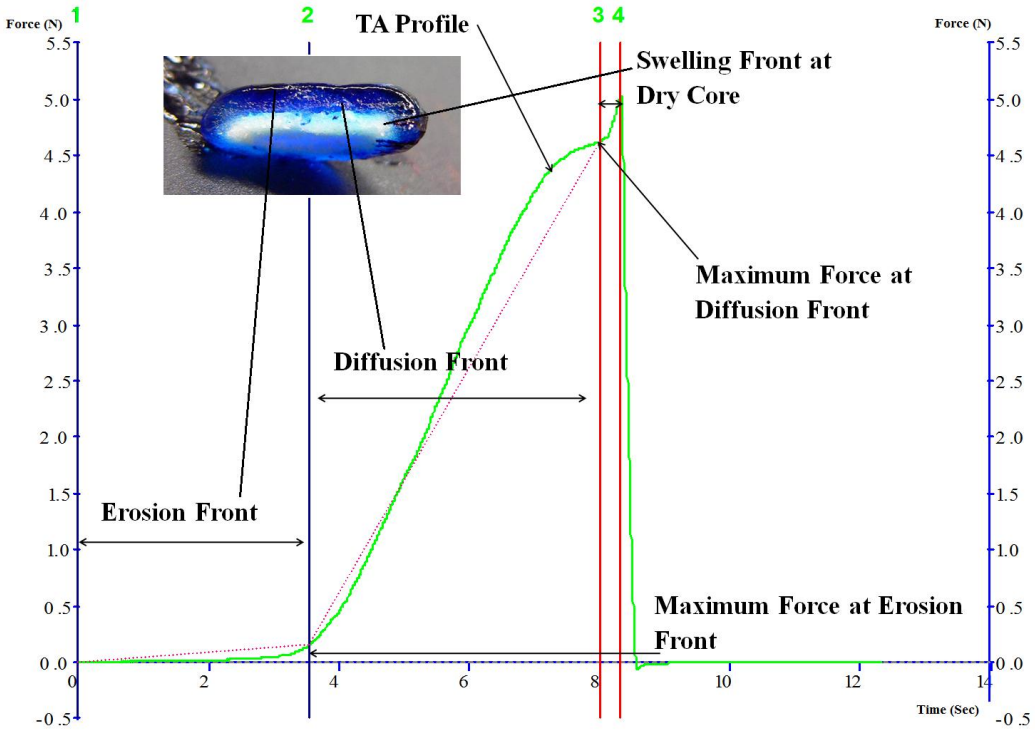

Figure 3.18 Texture analyser force-time profile and photographic image of HPMC K100M after 60 minutes hydration explaining three different region of hydration namely; erosion front, diffusion front and swelling front at dry core.

The visual observation of front movements/positions in hydrophilic matrix have previously been reported using confocal and NMR imaging after clamping the matrix compact in two Plexiglas plate (Bettini et al., 2001, Colombo et al., 1995, Colombo et al., 2000). However, in these experiments constrain on axial direction resulted in observation of front movements only in radial direction. The method developed here using a TA presented an opportunity for polymer to swell in all directions (radial and axial) however; front movements were calculated in axial direction only. The front movement is important parameter with relation to drug release kinetics in hydrating polymer (Conte et al., 1988, Colombo et al., 2000).

The changes in gel layer thickness usually takes three stages i.e. initial increase due to polymer swelling, continuance of steady gel layer between erosion and diffusion

front and disappearance of gel layer once the dry core is fully hydrated (Sako et al., 2002). As the time increased, the depth of probe penetration (before maximum force was reached) increased as shown in Figure 3.19.

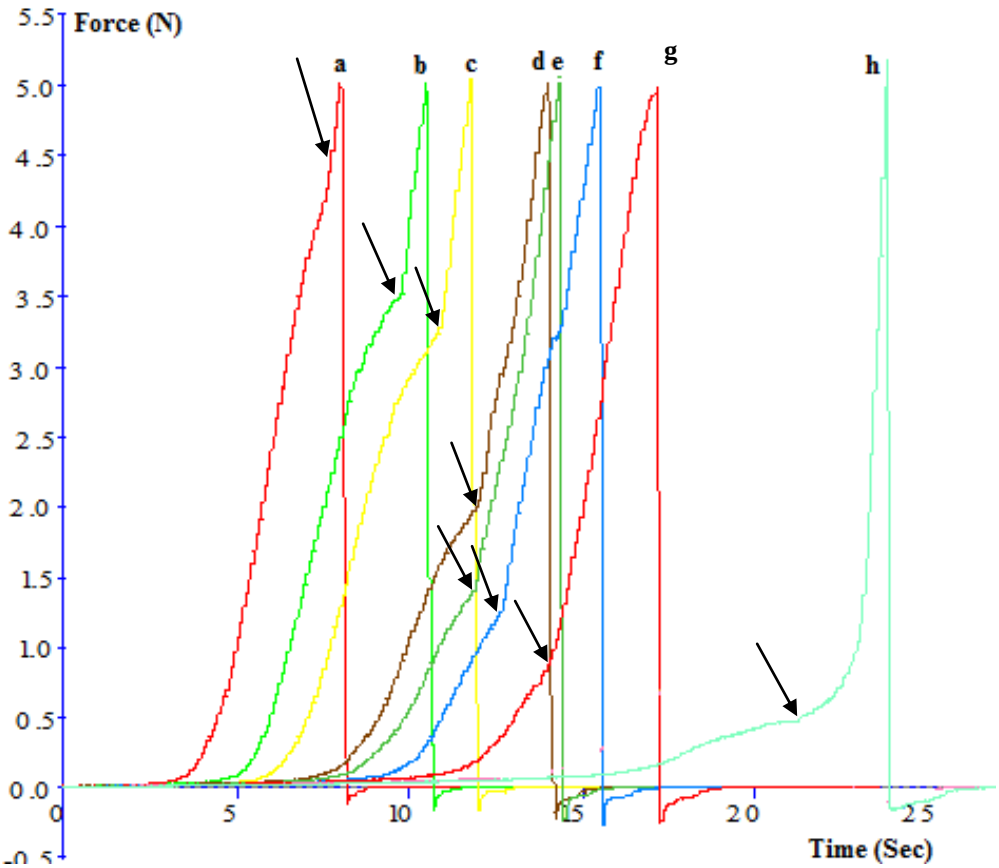

Figure 3.19 Typical TA profiles of HPMC K100M obtained following a) 30, b) 50, c) 70, d) 90, e) 110, f) 130, g) 150, and h) 300 minutes hydration time, the arrows emphasise the changes observed at diffusion front.

This indicated that as expected, the thickness of the overall gel layer increased with hydration time. Maintenance of constant gel layer is considered a crucial phenomenon to achieve drug release in zero order kinetics from modified release dosage form (Colombo et al., 2000).

It can also be observed that as the probe progressed through the sample, a sharp change in resistance was detected (Figure 3.19). A gradual decline in the slope indicated by black arrows in Figure 3.19 at diffusion front indicates that more and more dry core is being hydrated along with a decrease in the stiffness and strength of the cohesive gel layer.

In literature, the total area under the curve (AUC), which is indicative of resistance or work done encountered by the probe during textural profiling, is used as a mean to characterise the gel strength of the hydrophilic polymer (Yang et al., 1998, Jamzad et al., 2005, Li and Gu, 2007) however, AUC might not present the actual gel strength values at different hydrating fronts during polymer hydration. Therefore, the maximum force obtain at diffusion front in this study is used in Section 3.5.5 as an alternative to AUC to present the trueness of gel strength for hydrating polymer. It is worth remembering here that the thickness of hydrated gel layer and mechanical gel strength can impart a substantial influence on in vivo performance of swellable matrices as matrix integrity might change under mechanical forces presented in human stomach (1.89N) (Kamba et al., 2000) and small intestine (1.2N) (Kamba et al., 2002).

3.5.4 Comparison between two grades of sodium CMC (1000 and 40,000) using pin probe (Ø2mm)

In this comparison two grades of sodium CMC one was from low viscosity grade (1000Pa) and other from high viscosity grade (40,000Pa) were selected.

The objective was to demonstrate the suitability of the chosen pin probe to differentiate between these two different viscosity grades. As expected the value for stiffness and gel strength at partially hydrated layer/diffusion front are higher for sodium CMC 40,000 as compared to sodium CMC 1000 due to its high molecular weight and viscosity (Figure 3.20).

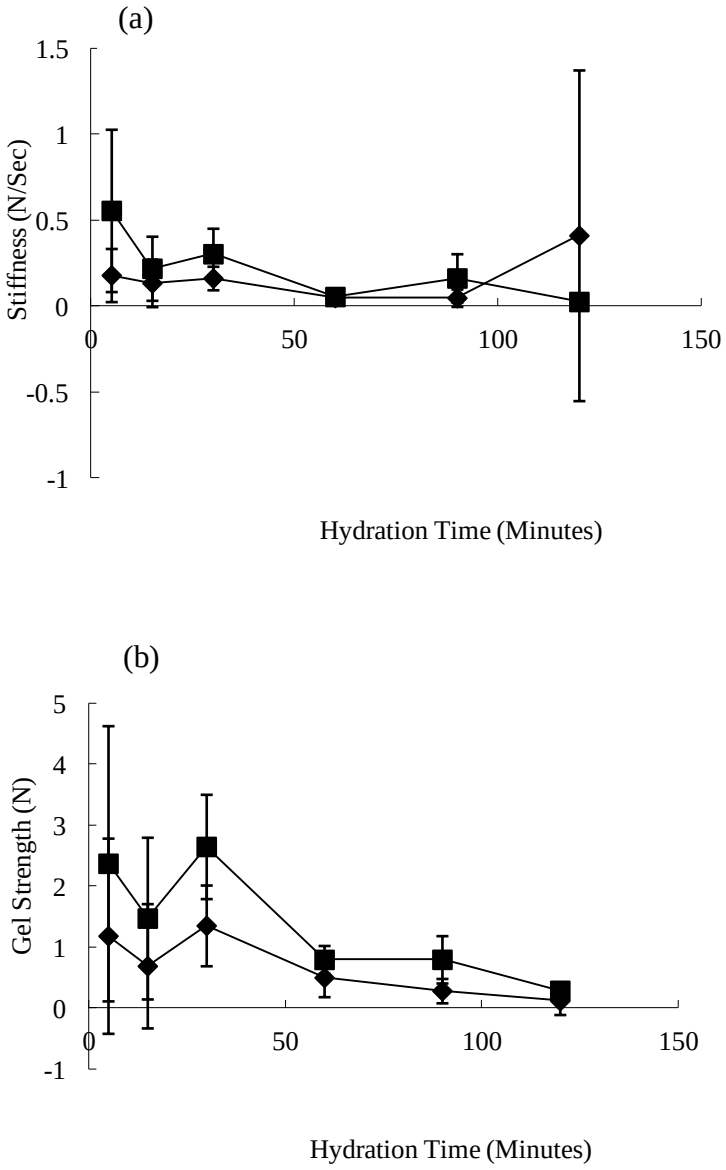

Figure 3.20 The values of gel stiffness (a) and strength (b) measured by texture analyser using a pin probe (Ø2mm) method at diffusion front for sodium CMC 40,000 (■) and 1000 (♦) (n=6).

The pin probe was able to comprehend this difference and proved to be suitable for further studies. The gel strength value for sodium CMC 40,000 at 120 minute was about 0.285N indicating that the gel was not very strong and might not be able to withstand the crushing force present in the human small intestine (1.2N) (Kamba et

al., 2002). This leads to the conclusion that other polymers should be tested for their suitability in this regard.

3.5.5 Validation of novel TA method by comparison between HPMC K100M, K4M, and E4MCR

Aim of this study was to validate the suitability of the developed texture analyser method for other polymers like hydroxypropylmethyl cellulose (HPMC). Previously, aluminium foil was used to affix the tablets and for their removal from the hydration medium however, even that had introduced variability in TA results. So a round Perspex discs (diameter 25mm) with double sided sellotape were made and used in these and other studies (Figure 3.21).

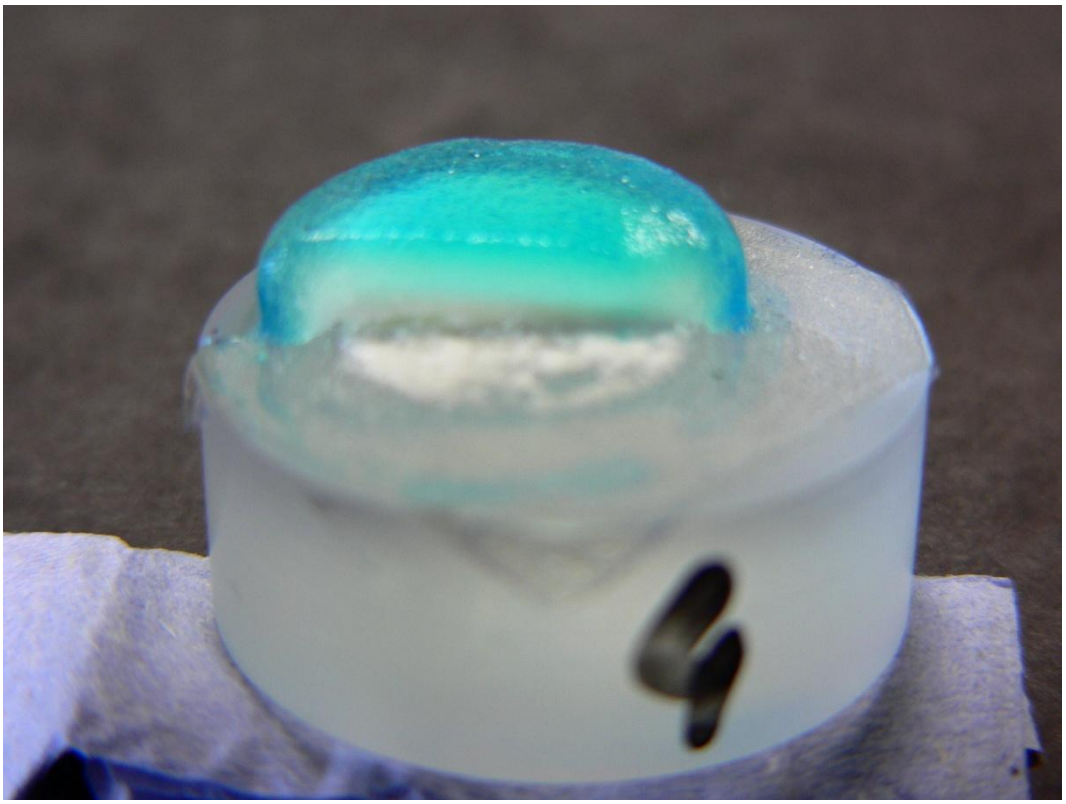

Figure 3.21 Hydrated tablets with double sided sellotape attached to round Perspex disc (25mm).

Three grades of HPMC (K100M, K4M and E4MCR) were selected. They differ from each other due to their substitution, viscosities and molecular weight. Figures 3.22 shows the trends observed in gel thickness in response to increasing hydration time in three different grades of HPMC.

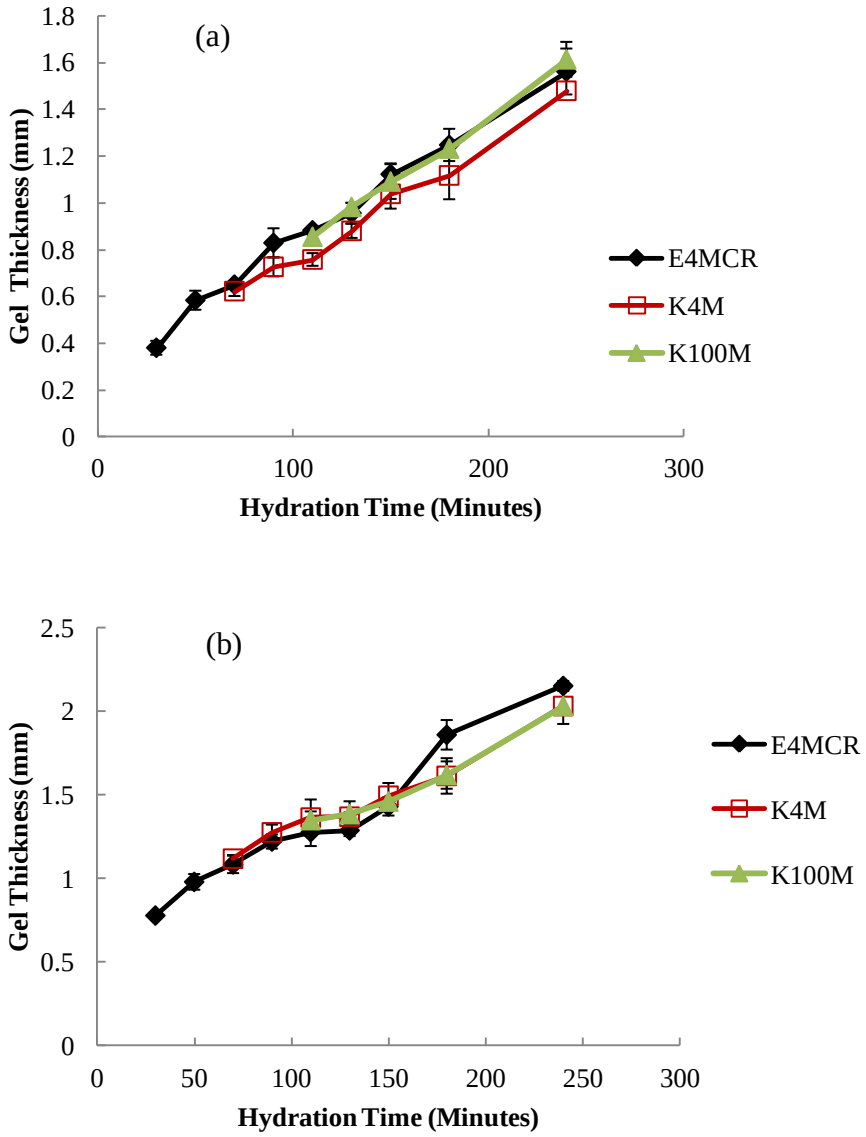

Figure 3.22 Gel layer thickness for (a) erosion front and (b) diffusion front with time (n=6).

As expected, the detected gel layer increased in thickness over hydration time. Unexpectedly, no difference between different grades of HPMC was observed in terms of gel layer thickness which could be due to their high molecular weights (Yang et al., 1998) or because of similar gel growth kinetics in all types of HPMC (Rajabi-Siahboomi et al., 1994).

Figure 3.23 shows the gel strength of different HPMC grades at diffusion front with time.

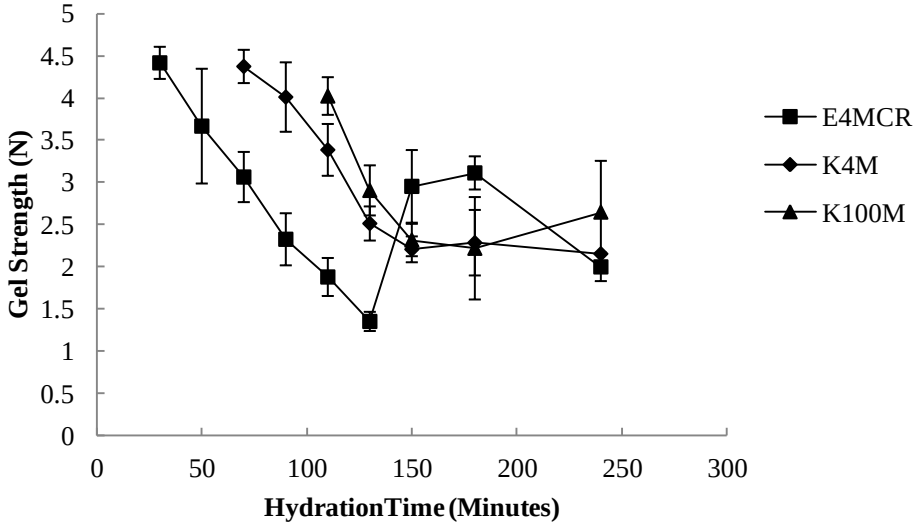

Figure 3.23 Gel strength of different HPMC grades at diffusion front with time (n=6).

The data show the declining trend for gel strength at diffusion front in response to increasing hydration time in three different grades of HPMC. The HPMC grades K100M, K4M and E4MCR are easily distinguishable in terms of their gel strength according to their high, medium and low viscosity grades respectively, and crucially it was possible to identify formulations with gel strength around the level of the destructive forces suggested for the GI tract (Kamba et al., 2000, Kamba et al., 2002).

As can be seen in Figures 3.22 and 3.23, the initial data points are missing for HPMC K4M and HPMC K100M. This could be directly attributed to their viscosities which caused slow hydration of the polymers, resulting in the late appearance of different regions/layers for these polymers. In the case of HPMC E4M CR, an increased was observed in gel strength at diffusion front at 150 min, which may be another more defined / undetectable small border or an area of phase transition present between swollen glassy core and diffusion front as described by Chen et al (2010)

3.6 CONCLUSION

On the basis of above results it can be concluded that water capacity of the drug delivery system can be manipulated with suitable polymers, moreover the hydrophilic and hydrophobic mixture of different excipients like Carbopol, chitin, L-HPC and magnesium stearate can also have future applications for these systems. Interactions between cationic and anionic polymers have not given any significant improvement in mixed polymer properties.

Hydrating gel layers of polymer tablets were probed using a texture analyser, and changes in gel layer properties with time could successfully be detected using this technique. The effect of the type of probes helped to choose pin probe as a candidate probe in TA method development. A novel texture analysis method was developed to identify and quantify different regions of hydration in polymer matrices, namely hydrating erodible layer, partially hydrated/ diffusion/ rubbery layer and glassy core layer. Additionally, this method enables quantification of the thickness and strength changes during hydrating in different regions of the gel over a range of hydration times.

By the use of this novel texture analyser (TA) method it is possible to screen proposed formulations in terms of gel layer strength and thickness. In future studies, different viscosity grades of HPMC will be evaluated further as a selected polymer to be used as a barrier layer composite in press coated tablet.

CHAPTER 4

HYDRATION AND EROSION STUDIES

4.1 INTRODUCTION

A number of researchers have reported the process of gel hydration, gel formation and dissolution of a polymer with respect to controlled release drug delivery systems (Langer and Peppas, 1981). Once the polymer is in contact with an aqueous liquid i.e., dissolution medium or gastrointestinal fluid, it swells and forms a protective gel layer to control the drug release from the matrix (Korsmeyer et al., 1983, Michailova et al., 2000). In addition to that higher viscosity of the gel is more resistant to erosion and dissolution. Therefore, the viscosity of the gel is also a rate controlling factor in drug dissolution.

A polymer exists in either the glassy or the rubbery state depending on the temperature. The glassy state of the polymer results when the temperature is below glassy transition (T_g), and above, in the rubbery state (Vergnaud, 1993). The penetration or diffusion of the liquid differs considerably when it passes through a glassy or rubbery polymer. Vergnaud (1993) described the process of liquid transport in polymeric matrices via three processes namely case 1, 2 and 3. Case 1; in rubbery state the polymer chains quickly adjust themselves to the presence of the liquid. The rate at which the liquid diffuses is much less than that of the segments relaxation of the polymer resulting in Fickian diffusion (Vergnaud, 1993) and given by the equation 4.1

$$M_t = kt^{0.5} \qquad \text{(equation 4.1)}$$

where k is constant depending on the amount of liquid transferred after an infinite time, the shape of the polymer and the diffusivity.

Case 2; in the glassy state in a polymer, the process of relaxation is very slow compared with the rate of diffusion. This means that the liquid diffuses with a constant velocity indicating an advancing front separating the glassy state to rubbery

state behind and ahead of this advancing front, respectively (Vergnaud, 1993). The amount of liquid at time *t*, M_t, is then given by equation 4.2

$M_t = kt$ (equation 4.2)

Case 3; in this case the rate of diffusion of the liquid becomes equal in magnitude to the rate of polymer relaxation and thus anomalous or non-Fickian diffusion is observed (Vergnaud, 1993). These types of systems are in between case 1 and 2. The amount of the liquid absorbed at time *t*, M_t, is given by equation 4.3

$M_t = kt^n$ (equation 4.3)

where *n* is between 0.5 (case 1) and 1 (case 2).

The equation 4.3 encompasses all three cases in one equation and has been used in past by other researchers (Sinha Roy and Rohera, 2002, Ebube et al., 1997) to describe the water uptake phenomenon, therefore this equation was used in this Chapter to describe the process of hydration.

The cellulose ether derivatives like hydroxypropylmethyl cellulose (HPMC) are the most common polymers used in controlled release formulation (Colombo, 1993) mainly due to their rapid and consistent gel formation, avoiding matrix disintegration, and forming a strong and viscous gel layer (Asare-Addo et al., 2010). Additionally, HPMC has been used widely in marketed products and is generally considered safe by the regulatory authorities for human consumption. The rate of hydration of these polymers depends upon the nature of their substitution and the degree of substitution. The gel growth kinetics is very similar for all types of HPMC, however the differences in swelling behaviour are due to differential expansion of the glassy core (Rajabi-Siahboomi et al., 1993, Adler et al., 1999).

Matrix erosion occurs once chain disentanglement begins after complete hydration of polymer at the outer surface (Chaibva et al., 2010). A new inner layer must replace the outer fully hydrated and dissolved layer and must be cohesive and strong enough to hold up the ingress of water and control drug diffusion. Once these polymer

hydrate and form a gelatinous layer, a rate of erosion will be directly changed by the polymer viscosity and its molecular weight.

The HPMC polymer is made up of cellulose, a natural carbohydrate that contains a basic repeating structure of anhydroglucose unit as shown in Figure 4.1.

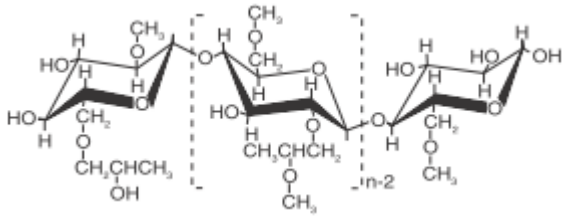

Figure 4.1 Typical structure of hydroxypropylmethyl cellulose (Dow Chemical Company, 2011).

During their manufacturing, cellulose fibres are heated with caustic solution which is in turn treated with methyl chloride to obtain methyl ($-CH_3$) substitution and propylene oxide to obtain hydroxylpropyl substitution ($-CH_2CH(OH)CH_3$) on the anhydroglucose units. The degree of substitution (DS) (Table 4.1) is the amount of substitution groups on the anhydroglucose units of cellulose and can be designated by weight percent or the average number of substitution groups attached to the ring.

Table 4.1 Degree of substitution for HPMC products

Product	**Methoxyl Degree of substitution**	**Methoxyl %**	**Hydroxypropyl Molar Substitution**	**Hydroxypropyl %**
HPMC E	1.9	29	0.23	8.5
HPMC F	1.8	28	0.13	5.0
HPMC J	1.3	18	0.82	27
HPMC K	1.4	22	0.21	8.1

The HPMC polymer with varying substitution types and levels possess different degrees of hydrophilic and hydrophobic substituent. HPMC E and HPMC F both have a higher percentage of hydrophobic methoxyl substituent (about 29%) compared to HPMC K (22%) (McCrystal et al., 1999). HPMC E has a similar percentage of hydrophilic hydroxypropoxyl substituent to HPMC K (about 8%), unlike HPMC F which has a lower hydroxypropoxyl percentage content (5%) (McCrystal et al., 1999).

If all three positions on each unit are substituted, the DS is designated as 3, if an average of two on each ring is treated; the DS is 2, etc. The molar substitution (MS) is the number of moles of hydroxypropyl groups per mole of anhydroglucose (Dow Chemical Company, 2011). Thus the letters (E, F, J and K) identifies the chemistry of the HPMC as shown in Table 4.1 and the number that follows the chemistry (e.g. 100 in case of HPMC K100) identifies the viscosity of that product in millipascal-second (mPa.s) at 2% concentration in water at 20℃. The letter "C and M" implies the multiplier of 100 and 1000, respectively. Different suffixes are used to identify special products. "LV" refers to special low-viscosity products, "CR" denotes a controlled-release grade having a smaller particle size (Dow Chemical Company, 2011).

It was mentioned in Chapter 3 that different viscosity grades of HPMC will be evaluated further as a selected polymer to assess their performance as a barrier layer composite in a press coated tablet designed to release its content in the colon. Thus the purpose of this chapter was to investigate the hydration and erosion rates in selected grades of HPMC polymer. A Texture Analyser (TA) method has already been developed (Section 3.4) and will be used to quantify the gel strength at 240 minute hydration time. Another objective of this work was to gravimetrically quantify erosion rates of candidate polymers defined through this novel TA screening method, and quantify any correlation between rate of erosion and gel strength.

4.2 METHODS

4.2.1 Tableting for hydration, erosion and TA studies

All tablets contained total weight of 200 mg and were manufactured manually on a single punch tablet press with a 8.0 mm flat faced punch and die at a compression force of 4-6kP. In order to ensure agglomerate free powder all polymers equivalent to 100 tablets (20 grams) were passed through a steel mesh number 250 µm. Different grades of HPMC E5LV, E6LV, E15LV, E50LV, E4MCR, E10MCR and K4M alone or mixed in combination E10MCR:E5LV 75:25, 50:50, 25:75 and K4M:E4MCR 75:25, 50:50, 25:75 were used. In the case of single pure HPMC grades the tablet powders were sieved and compressed as tablet compacts. For mixed HPMC grades, tablet powders were weighed, sieved and mixed in a Turbula mixer for 5 minutes and compressed as tablet compacts.

4.2.2 *In vitro* gravimetric erosion and hydration studies

The tablets prepared in Section 4.2.1 were individually weighed, dried in an oven at 60°C and kept for 10 min in desiccator in order remove any moisture already present in the tablet, and then fixed on a round Perspex disc with double sided sellotape. These tablet samples were then placed in 900ml of distilled water, and subjected to erosion and hydration in a USP dissolution apparatus II, with paddle speed of 100 rpm, and a temperature at 37°C ± 0.5. The tablets were affixed on the Perspex disc to allow easy removal of the tablets from the dissolution vessel without disturbing the gel layer. A hydration time of 30, 60, 90, 120, 150, 180, 240 and 300 minutes was employed to collect the hydrated tablets and afterwards tablets were weighed, dried in an oven for 36 hours at 80ºC, and re-weighed to calculate percentage erosion and percentage residual hydration using the method described in Section 3.2.1.2. The slope of the individual erosion profile was used as rate of erosion (% erosion/min) of the polymer. Percentage erosion data were subjected to similarity factor analysis (f_2) in order to determine the erosion profile similarity and concomitant dissimilarity where applicable.

It was noticed during the hydration and erosion studies as described in Section 3.2.1.2 that the process of gravimetric erosion is very tedious and time consuming. For example, it can take almost 20 hours to complete 8 time points for percentage erosion-time profile of one formulation with at least 6 repetitions when tablets are individually subjected for erosion studies. In order to expedite the process of obtaining erosion data for all formulations, a Perspex disc (diameter 70-75mm, thickness 10-12mm with a hole in the middle for easy handling of the disc from the dissolution vessel) was developed and used to facilitate gravimetric erosion studies, allowing up to five tablets of varying sizes to be attached with the help of double sided sellotape as illustrated in Figure 4.2.

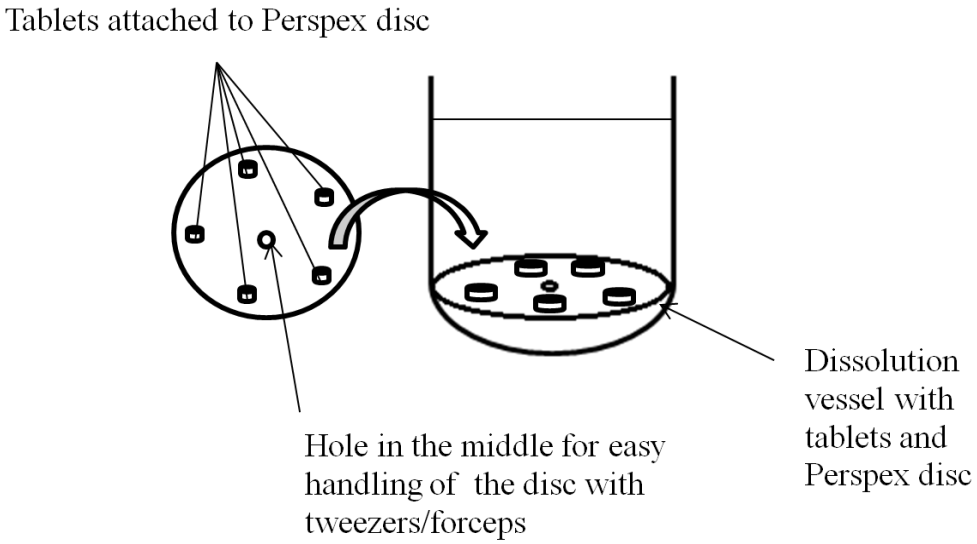

Figure 4.2 A schematic diagram of new disc method for gravimetric erosion studies illustrating the tablets affixed on the Perspex disc and their set up in the dissolution vessel during erosion studies.

This procedure shortened the erosion process to complete in 5 hours instead of 20 hours. Additionally, it allowed multi-polymer erosion studies to complete in only a

few days' time. It is also believed that this method would have caused minimum variability in results because all tablets were subjected to the same hydrodynamics or fluctuation in temperature. Although meaning that less trust can be placed in an individual data point, as all the data at a given time point was subject to the same deviation.

However, this method did not allow introducing standard error bars in erosion profile data due to erosion and hydration of five tablets on the disc being measured simultaneously rather than individually. Furthermore, as the bottom of the tablet was firmly attached with the Perspex disc with double sided sellotape which would have prevented the hydration from the bottom of the tablet but not from the top and sides.

4.2.3 Texture analyser studies

In order to perform TA studies, the tablets prepared in Section 4.2.1 were individually affixed on Perspex discs (25mm) and subjected to the same erosion and hydration conditions as described above. The hydrated tablets were removed after 240 minutes hydration time and used for TA characterisation. Due to the destructive nature of the TA, each time new tablet was used for obtaining a new reading. The description of TA setting is given in Section 3.4.1.2. In the case of TA data analysis, the maximum force at the diffusion front quantified by the TA was taken as the maximum strength of the hydrated gel layer as described in detail in Chapter 3, Sections 3.5.3 and 3.5.5. All reported values for texture analyser are at 240 min, the expected time of colon arrival post stomach though variability do exist depending on timing in relation to food intake or between individual (Varum et al., 2010).

The data obtained from the texture analyser (TA) studies were analysed using textural expert exceed 32 (TEE 32) software.

4.3 RESULTS AND DISCUSSION

4.3.1 Matrix erosion or percentage erosion

In order to investigate the process of erosion, tablets were manufactured comprising of different grades of HPMC polymers. Figure 4.3 shows the percentage erosion of tablets composed of selected HPMC grades (E5LV, E6LV, E15LV, E50LV, E4MCR, E10MCR and K4M) in the dissolution apparatus with time.

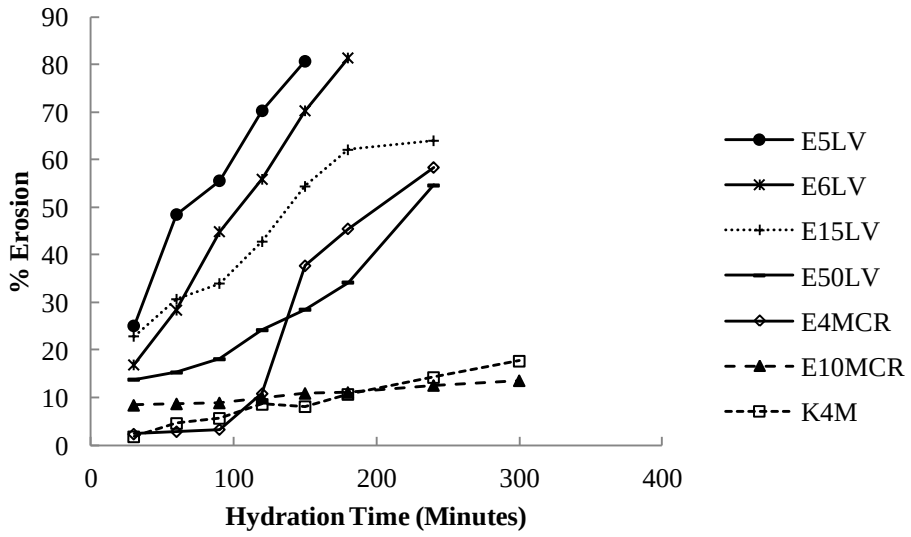

Figure 4.3 Percentage erosion versus hydration time of tablet composed of selected HPMC grades using distilled water (900ml) in a USP dissolution apparatus II, with paddle speed of 100 rpm and a temperature at 37℃ ± 0.5 (n=5).

The data indicate that in general, the percentage erosion increased progressively with the erosion time. It can be observed that the higher molecular weight/viscosity HPMC grades (K4M and E10MCR) eroded to lesser extend when compared to lower viscosity grades (E5LV, E6LV and E15LV). The erosion of E50LV stands in the middle of higher and lower molecular weight HPMC grades which was expected due

to its intermediate viscosity/molecular weight. The erosion behaviour of E4MCR was slightly different; its erosion was similar to K4M and E10MCR until 120 minutes, after that there was an abrupt increase in its erosion. This will be further discussed in conjunction with hydration data in Section 4.3.3.

Figure 4.4 shows the erosion profiles of tablets composed from mixed E10MCR and E5LV grades at ratio of 75:25, 50:50 and 25:75 respectively, compared to tablets manufactured from the individual polymers alone.

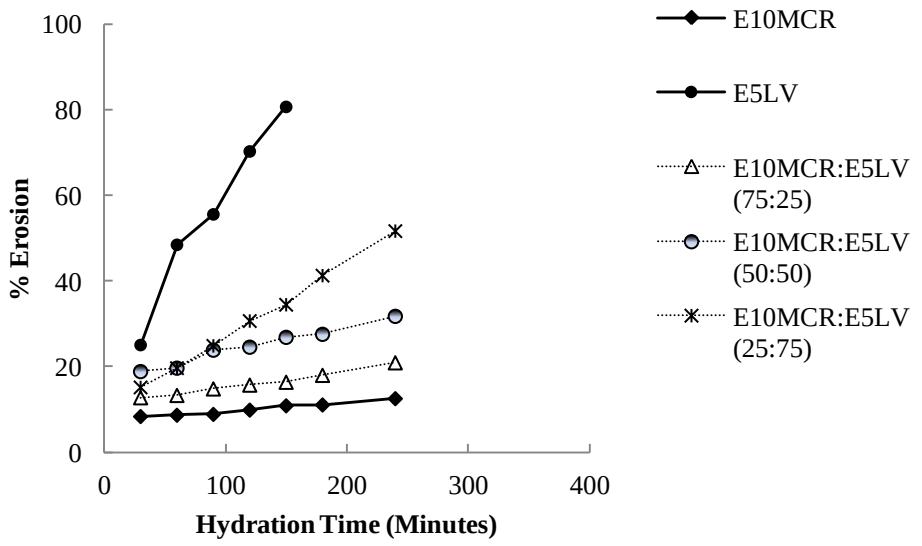

Figure 4.4 Percentage erosion of tablets composed from mixed HPMC polymer grades (E10MCR:E5LV 75:25, 50:50, 25:75) compared to tablets manufactured from the individual polymers alone versus time. Erosion was performed using distilled water (900ml) in a USP dissolution apparatus II, with paddle speed of 100 rpm and a temperature at 37°C ± 0.5 (n=5).

In general, the amount of the erosion increased gradually with time of exposure. As expected, increasing the amount of the E5LV (low viscosity/molecular weight and

fast eroding polymer) in the mixed grades with respect to E10MCR (high viscosity/molecular weight and slow eroding polymer) resulted in higher rate of erosion and vice versa. It can also be observed that both pure grades E5LV and E10MCR represent higher and lower rate of erosion corresponds to their respective lower and higher viscosity, while their mixed grades stand in the middle of these two grades. This suggests that overall erosion was governed by the molecular weight and viscosity of the polymers.

Figure 4.5 compares the percentage erosions versus hydration time of tablets composed of mixed HPMC K4M:E4MCR grades at ratios of 75:25, 50:50 and 25:75 with tablets composed of the pure grades alone.

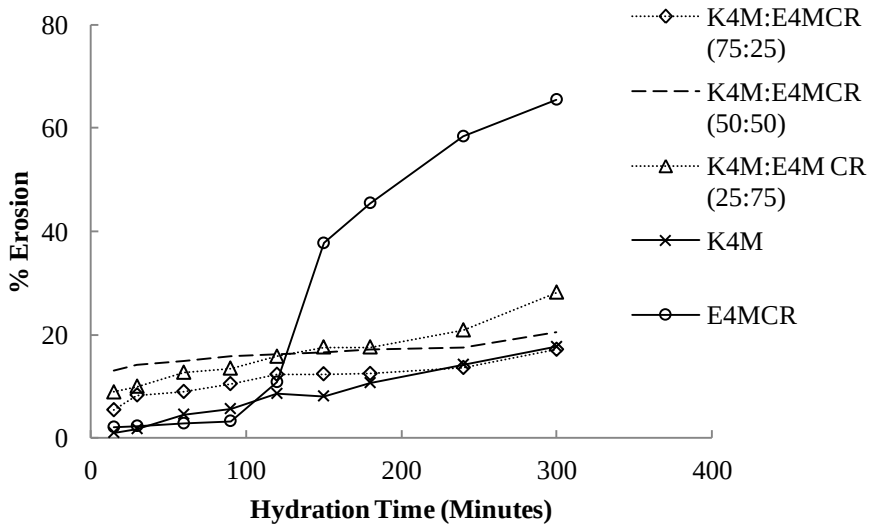

Figure 4.5 Percentage erosion versus time of tablets composed of mixed HPMC grades (K4M:E4MCR 75:25, 50:50, 25:75) compared with their pure grades alone. Erosion was performed using distilled water (900ml) in a USP dissolution apparatus II, with paddle speed of 100 rpm and a temperature at 37℃ ± 0.5 (n=5).

The data indicate that the overall rate of erosion increased with hydration time. The individual erosion profiles for K4M and E4MCR suggested that their behaviour is different from each other. The erosion profile of K4M was relatively slow and steady in comparison with E4MCR, which displayed two distinctive phases. Initially, the erosion rate of E4MCR was low up to 100 minutes, following which there was sharp rise in the erosion rate. As the viscosity of E4MCR is equivalent to K4M, it might be proposed that there should not be a much difference in their erosion profiles, however while both polymers have the same viscosity they are chemically different (Table 4.1). HPMC E4MCR has a higher percentage of the hydrophobic methoxyl substituent (about 29%) compared to HPMC K4M (22%). In general, HPMC polymers with K chemistry are more resistant to erosion than polymers with E chemistry (Dow Chemical Company, 2011). The measurement of self-diffusion coefficient (the measure of transport due to the thermal energy (also known as Brownian motion) of molecules in the absence of a chemical concentration gradient and strongly depends on the mobility of the water) of water in pure gels of K4M is found significantly and consistently lower than E4MCR. This implies that the mobility of water within the gel layer of K4M is lower, leading to greater diffusional resistance to water.

Despite varying the ratios of the two different HPMC chemistries in the mixed grade formulations, it can be observed that the erosion profiles of the mixed K4M:E4MCR tablets are reasonably similar. For instance, the erosion profile of mixed grade K4M:E4MCR 50:50 and 25:75 tablets were found similar to each other (similarity factor (f_2) 71.24). Equally, the erosion profile of mixed grade K4M:E4MCR 75:25 was of a similar magnitude and rate to both 50:50 (f_2, 63.97) and 25:75 (f_2, 62.37) mixes. Tiwari and Rajabi-Siahboomi (2009) discussed that mixing polymers of different chemistries (HPMC K15M Premium CR and E15 Premium LV) produced matrices with improved physical characteristics over the individual polymers, which exhibited similar dissolution profiles at agitation speeds of both 100 and 150 rpm. It was suggested that the combination of two HPMC polymers with different chemistry produced a robust matrix system which was evidenced by the lack of effect of hydrodynamics on performance. In the case of the current work, it appears the formation of this robust matrix meant that despite using different ratios of two

different polymer chemistries, overall erosion behaviour between the mixed grade formulations was similar.

Table 4.2 shows the rate of erosion of the tablet formulations studied with their r^2 values.

Table 4.2 Rate of erosion for different HPMC polymer with their r^2 values

Name of the HPMC Polymer	**Rate of erosion (%/min)**	**r^2**
E5LV	0.4433	0.9688
E6LV	0.4373	0.9974
E15LV	0.2162	0.9411
E50LV	0.1896	0.9287
E4MCR	0.3091	0.8965
E10MCR	0.0204	0.9828
E10MCR:E5LV (75:25)	0.0398	0.9899
E10MCR:E5LV (50:50)	0.0627	0.9475
E10MCR:E5LV (25:75)	0.1768	0.9987
K4M	0.0565	0.9840
HPMC K4M & E4MCR (75:25)	0.0337	0.9908
HPMC K4M & E4MCR (50:50)	0.0216	0.9465
HPMC K4M & E4MCR (25:75)	0.0607	0.9644

The data indicates that in most cases, the profiles are almost linear (r^2= 0.8965-0.9974) with their rates of erosion in the range of 0.0204-0.4433%/min. A lower value for rate of erosion indicates slower erosion and vice versa. In tablets composed of pure polymer, the rate of polymer erosion increases with a decrease in polymer molecular weight, except in the case of E4MCR which as discussed previously unexpectedly exhibited a two phase erosion profile. Other researchers (Tahara et al., 1995, Kavanagh and Corrigan, 2004) also observed a faster erosion rate for tablets prepared with lower viscosity and molecular weight grades of HPMC.

The same principle is followed by the combination of E10MCR:E5LV. A higher content of high molecular weight polymer resulted in less erosion and vice versa.

4.3.2 Correlation between percentage erosion and HPMC E-grades

In order to observe any trend in erosion behaviour of tablets prepared using the HPMC E-series, the % erosion values at 240 min, the expected time of colon arrival post stomach, was plotted against the different viscosity grades. Figure 4.6 shows the percentage erosion of different HPMC E grade formulations at 240 minutes.

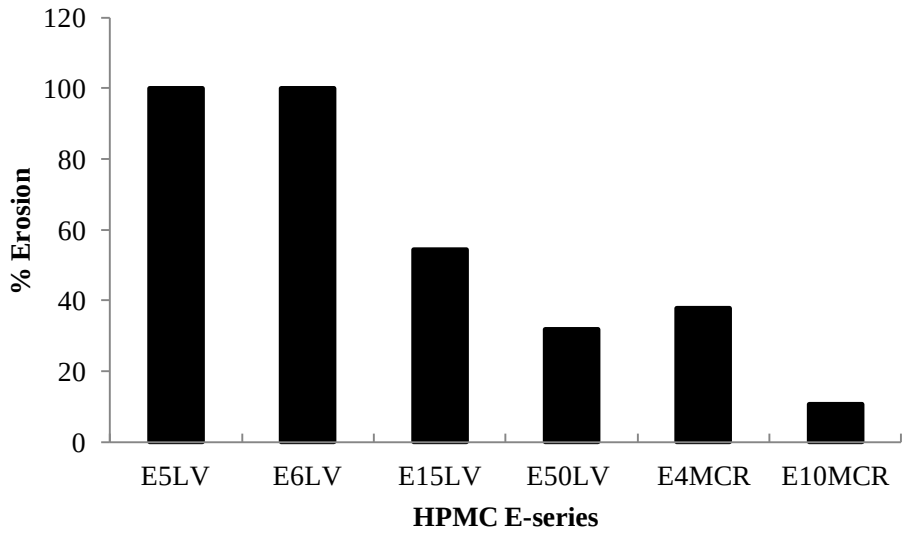

Figure 4.6 Percentage erosion of tablet composites containing different HPMC E grades. Erosion was performed using distilled water (900ml) in a USP dissolution apparatus II, with paddle speed of 100 rpm and a temperature at 37°C ± 0.5 (n=5).

As expected, higher molecular weight polymers showed less erosion and vice versa, similar to the results reported by Reynolds et al (1998) for different HPMC K-grades. The exception to this was the E4MCR grade, whose erosion profile displayed two different rates of erosion (Figure 4.3), and did not fit into the general trend. It is also noticeable that at 240 minutes, E5LV and E6LV were completely disintegrated which correspond to their 100% erosion in the graph.

4.3.3 Hydration studies

In these experiments, tablets composed of different HPMC grades were manufactured in order to investigate their hydration behaviour. The water uptake measurements were calculated as described in Section 3.2.1.2 using the disc method as detailed in Section 4.2.2. The values for percentage residual hydration were calculated using the same tablets which were used to calculate the % erosion, therefore the hydration data in this section will be discussed with reference to the corresponding erosion data. Figure 4.7 shows the residual hydration profiles of tablets composed of HPMC E5LV, E6LV, E15LV, E50LV, E4MCR and E10MCR with their erosion profiles over hydration time.

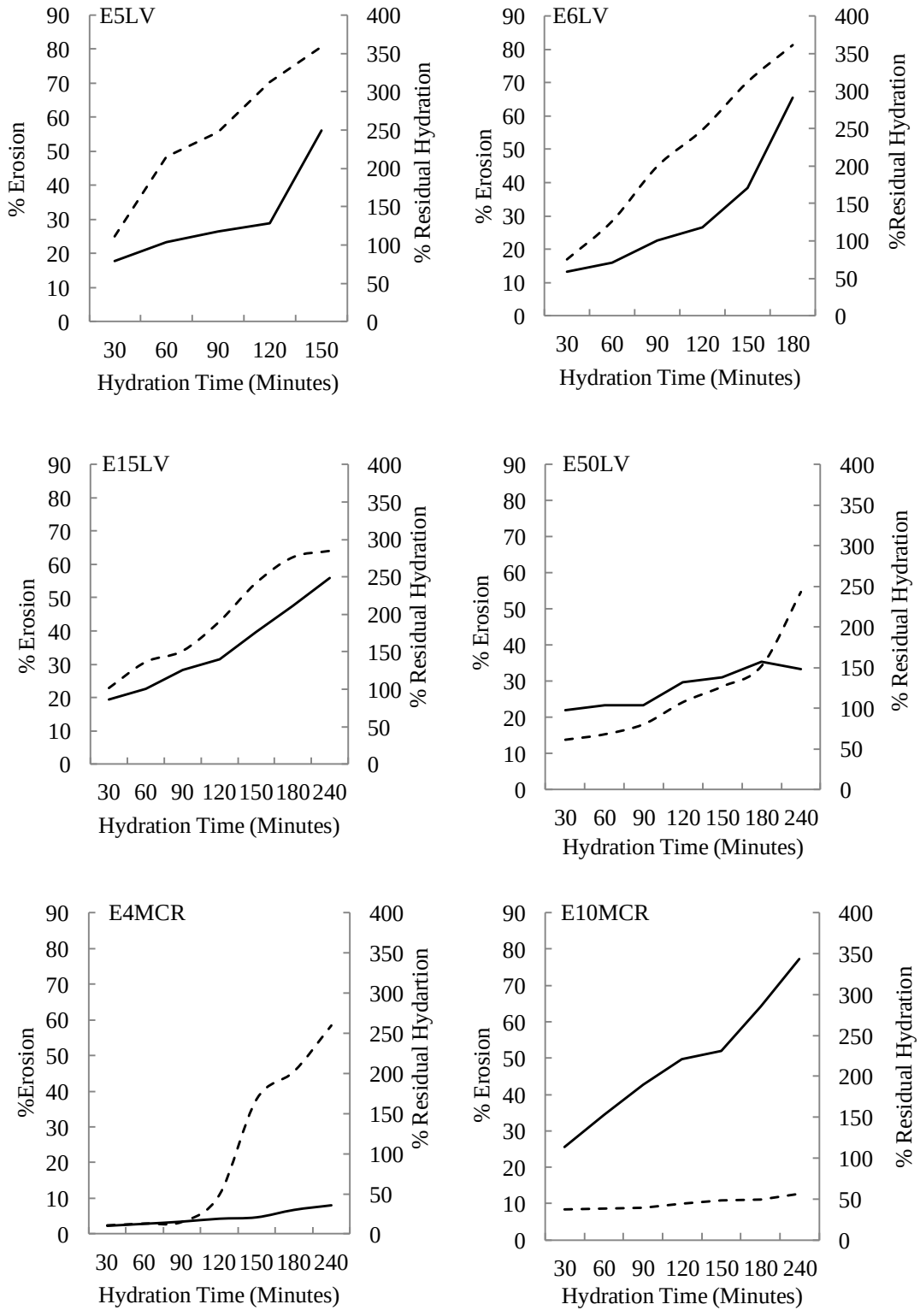

Figure 4.7 Percentage residual hydration and erosion profiles with time of different HPMC E grades (n=5). Dotted line (…) indicates % erosion and solid line (—) indicates % residual hydration.

The hydration behaviour observed for these polymers indicates the rate at which they absorb water and swell, and in most cases the rate of increase in % residual hydration appeared relatively linear except for E5LV and E6LV. In the case of these two polymers, hydration was almost linear up to 120 minutes, following which the rate of increase in residual hydration became non-linear due to the rapid matrix erosion observed. Furthermore, it was difficult to calculate any hydration data after 150 min and 180 min in HPMC E5LV and E6LV, respectively due to complete erosion of the polymers.

The data also shows that in the case of the lower molecular weight polymers E5LV, E6LV and E15LV, rate of erosion was higher than rate of hydration due to which their hydration profiles were comparatively low. On the other hand as the viscosity of the polymer increased, for example from grades E50LV to E10MCR, the rate of erosion decreased and rate of hydration increased resulting in less erosion and more hydration. The reason for higher hydration values in higher molecular weight E grade (e.g. E10MCR) could be attributed to a rapid and cohesive gel formation behaviour which is usually observed in high viscosity HPMC grades (Colombo et al., 2000), diminishing the extent of matrix erosion. However, the observed behaviour of E4MCR did not fit this pattern. It was found that the rate of hydration and erosion was almost equivalent up to 120 minutes in E4MCR, following which a slight increase in hydration was observed while erosion was relatively fast. This phenomenon is difficult to explain.

Figure 4.8 shows the residual hydration profiles of mixed HPMC E10MCR:E5LV (75:25, 50:50, and 25:75) with their erosion profiles at different hydration times.

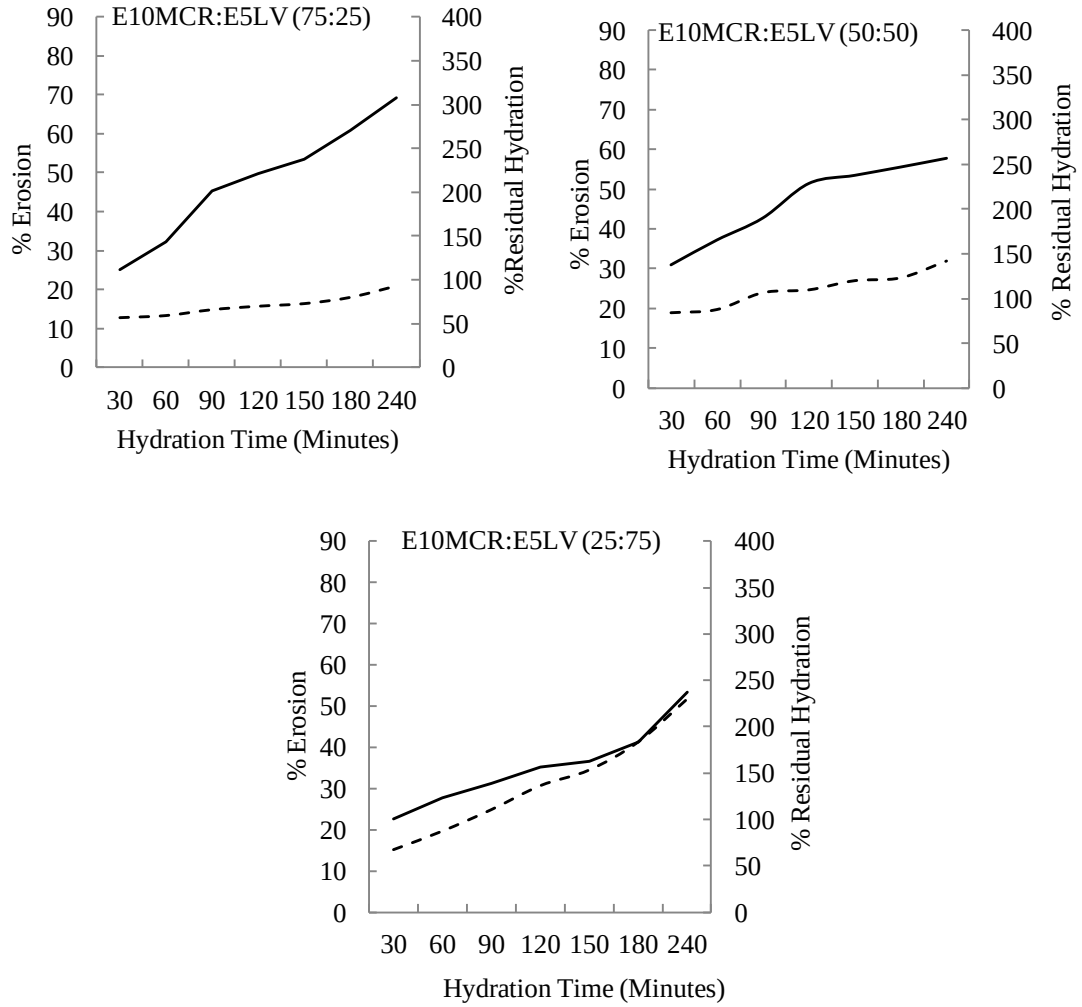

Figure 4.8 Percentage residual hydration with time of mixed HPMC E10MCR:E5LV (75:25, 50:50, and 25:75) with their erosion profiles (n=5). Dotted line (…) indicates % erosion and solid line (—) indicates % residual hydration.

The data indicates that generally, there is a gradual increase in percentage residual hydration over the hydration period. From the data presented previously in Figure 4.7, it was clear that the formulation composed of E10MCR displayed a much greater capacity for residual hydration in comparison with the lower viscosity grades such as E5LV. Expectedly, increasing the ratio of high viscosity E10MCR grade with respect to E5LV resulted in a higher extent of hydration. The percentage residual hydration

in these three mixed grades can be ranked in the following order E10MCR:E5LV 75:25>50:50>25:75. As discussed in Section 4.3.1, the reverse was true for erosion behaviour in these formulations, as E5LV erodes rapidly in comparison with E10MCR (Table 4.2). This demonstrates the complex interplay between polymer erosion and hydration, where one of these properties may dominate over the other, depending on the polymer molecular weights and their relative ratios within the system.

Figure 4.9 shows the hydration profiles of tablets composed of HPMC K4M and mixed grade K4M:E4MCR at a ratio of 75:25, 50:50 and 25:75 versus time with their erosion profiles.

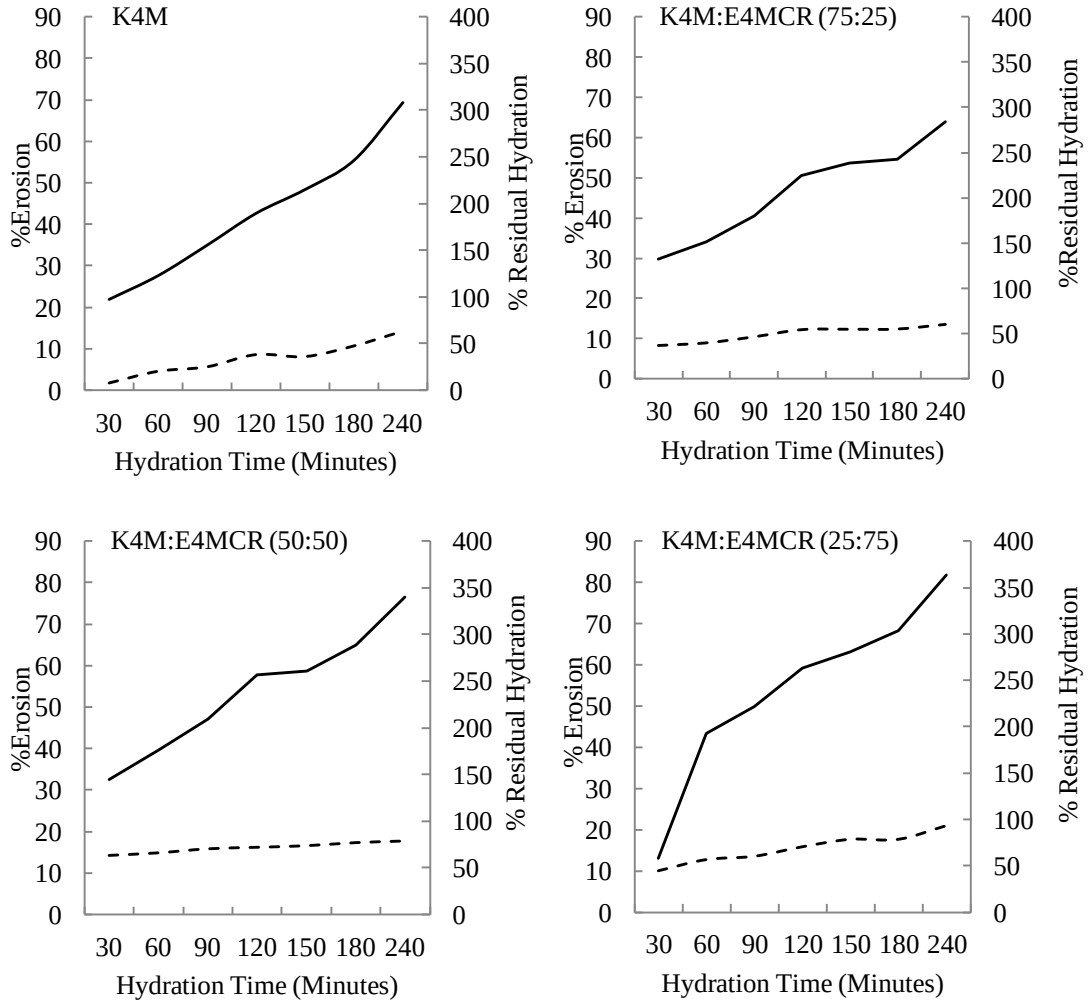

Figure 4.9 Percentage residual hydration with time of K4M and mixed HPMC K4M:E4MCR 75:25, 50:50, and 25:75 with their erosion profiles (n=5). Dotted line (…) indicates % erosion and solid line (—) % residual hydration.

The data shows that K4M displayed high rate of hydration in combination with low erosion as expected from its high molecular weight and rapid and cohesive gel formation (Colombo et al., 2000). Therefore, a higher rate of hydration was expected in the formulation composed of mixed grade K4M:E4MCR 75:25, compared to the formulations which contained a lower quantity of this grade. Surprisingly, the high content of HPMC K4M with respect to E4MCR in mixed grade formulation did not

yield a higher rate of residual hydration, rather the rate of hydration for these mixed polymer ratios followed the reverse order, being highest for HPMC K4M:E4MCR 25:75 followed by 50:50 and lowest for 75:25.

It has already been discussed in Section 4.3.1 that mixing K4M and E4MCR formed a robust matrix system, and as a result varying relative ratio of the two grades produced no effect on the erosion. So it was expected that the hydration profiles of the mixed grades would present a similar behaviour. However, this was not the case and therefore erosion alone cannot explain these unexpected hydration profiles in the mixed grades. It was clear from the data presented previously in Figure 4.7, that the tablets composed of E4MCR displayed a lower rate of residual hydration in comparison to K4M (Figure 4.9). As discussed, E4MCR contains a higher percentage of hydrophobic methoxyl substitution (29%) compared to K4M (22%). This would suggest that the presence of a higher content of E4MCR in comparison to K4M in the mixed grade formulations would result in a slower rate of hydration. However, data revealed the opposite behaviour in the mixed grade formulation hydration profiles. So neither mixed grade erosion nor individual polymer hydration profiles alone were able to explain the hydration profiles of the mixed grades. However, this behaviour could be understood with reference to the stronger gel forming behaviour of the K4M grade upon hydration which creates a diffusion barrier to further water ingress. Thus, decreasing the K4M content in the mixed grades resulted in a decrease in this barrier layer to diffusion which increased the capability to hydrate further, while mixing of the two grades prevented erosion from counteracting the hydration capacity.

Previous studies (Sinha Roy and Rohera, 2002, Ebube and Jones, 2004, Chaibva et al., 2010) describe the use of the Vergnaud model or the Schott second order model to determine the rate and mechanism of hydration/water uptake in polymeric matrices. However, water uptake data did not show a good fit in terms of r^2 values (r^2 <0.5) for the Schott second order model (Schott, 1992), so the results are not discussed further in the context of that model.

Thus, the water uptake/percentage residual hydration data was then subjected to the Vergnaud model (Vergnaud, 1993) to determine the mechanism of water uptake. The generalised form of Vergnaud model is taken from equation 4.3 (Section 4.1)

$M_t = kt^n$ (equation 4.3)

Where M_t represents the amount of liquid absorbed at time t, and k is constant depending on the amount of liquid transferred after infinite time (Vergnaud, 1993). Therefore, in the current study k is considered to represent a hydration constant. The exponent, n, indicates the mechanism of water ingress.

To obtain the values for the Vergnaud model, the percentage residual hydration versus time was plotted on a logarithmic scale. As an example % residual hydration data of HPMC E10MCR on logarithmic scale is shown in Figure 4.10.

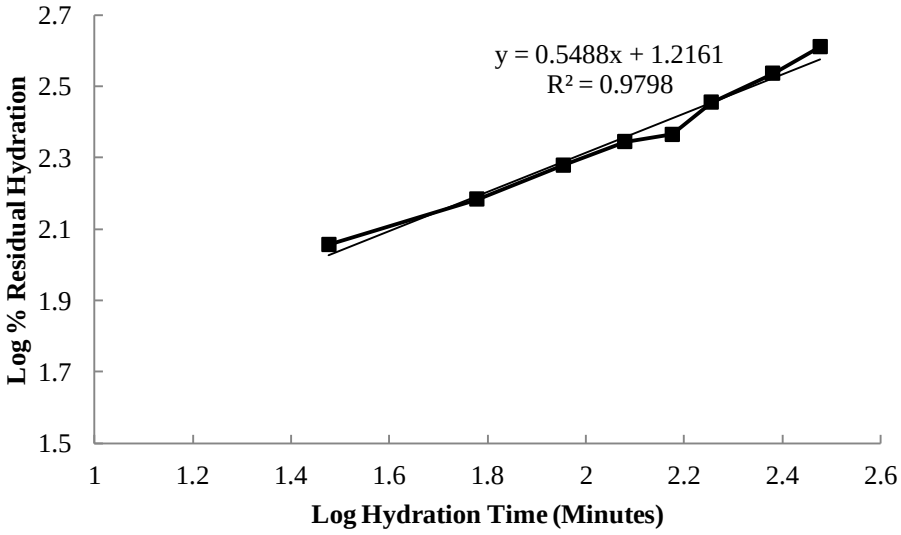

Figure 4.10 Plot of log % residual hydration by HPMC E10MCR as a function of log time according to Vergnaud model with its regression equation.

The values of *k* were obtained by taking the anti-log of the intercept in the regression equations and the slope represents the exponent, *n*. The results for kinetic values (*k*, *n*, r^2 and regression equations) for different HPMC grades and mixed grades are presented in Table 4.3.

Table 4.3 Kinetic parameters and regression equations according to the Vergnaud model computed using equation (4.3) for different HPMC polymers, where *n* denotes exponent and *k* represents swelling kinetics.

Name of the HPMC Polymer	**Regression equation**	***n***	***k***	$\mathbf{r^2}$
E5LV	0.7236x+0.3508	0.72	2.24	0.9771
E6LV	0.8942x-0.107	0.89	0.78	0.9961
E15LV	0.6032x+0.9637	0.6	9.2	0.9169
E50LV	0.5096x+1.1862	0.51	15.3	0.9775
E4MCR	0.5127x+0.2531	0.51	1.77	0.9303
E10MCR	0.5488x+1.2161	0.54	16.4	0.9798
E10MCR:E5LV (75:25)	0.4443x+1.2998	0.44	18.8	0.9879
E10MCR:E5LV (50:50)	0.3474x+1.6142	0.34	41.1	0.9789
E10MCR:E5LV (25:75)	0.5134x+1.2752	0.51	19.9	0.9086
K4M	0.5243x+1.2103	0.52	16.22	0.9683
K4M & E4MCR (75:25)	0.3787x+1.5454	0.38	35.1	0.9830
K4M & E4MCR (50:50)	0.387x+1.5881	0.39	38.7	0.9873
K4M & E4MCR (25:75)	0.7497x+0.8137	0.75	6.5	0.9365

In most cases, the water uptake data revealed a good fit in the model with r^2 = 0.9086-0.9961. Ebube et al. (Ebube et al., 1997) further defined the Vergnaud model with reference to the exponent, *n*. A value of 0.5 or less for *n* indicates a diffusion controlled mechanism in which the rate of diffusion of the liquid is much less compared to the rate of relaxation of the polymer segment, which Vergnaud (1993) referred to as case 1 as explained in Section 4.1. A value of 1 for *n* suggests that the stress relaxation process is very slow compared to the rate of diffusion. Vergnaud (1993) explained this with equation 4.2 (case 2, Section 4.1). This means that the

liquid diffuses through the polymer matrix at a constant velocity, showing an advancing front marking the limit of liquid penetration. Behind this front is a swollen gel, and ahead of it is the polymer in the glassy state. Ebube et al (1997) further states that a value of *n* between 0.45 and 1 indicates an anomalous or complex behaviour in which the rate of diffusion of the liquid and that of relaxation are of the same magnitude, which is the same as case 3 in Vergnaud model (1993).

The exponent, *n*, for HPMC E5LV (0.72), E6LV (0.89), E15LV (0.6), E50LV (0.51), E4MCR (0.51), E10MCR (0.54), K4M (0.52), suggests an anomalous or complex diffusion behaviour i.e., the rate of diffusion of the liquid and that of molecular relaxation are almost of the same magnitude (Vergnaud, 1993, Ebube et al., 1997). The data also show that the value of the exponent, *n*, in the case of E-grade is in the range of 0.45-1.0, suggesting that the same substitution series have a similar diffusion mechanism.

Joshi et al., (2009) expressed hydration kinetics using a power law (Ritger and Peppas, 1987), without consideration of dissolution during hydration and swelling, and reported a diffusion controlled mechanism for HPMC polymers with a viscosity of 4000 mPa.s as being opposite to the anomalous or complex diffusion behaviour observed in these experiments for E4M and K4M. The difference could be attributed to the different methods chosen for calculation and sources of polymers.

In the case of mixed HPMC E10MCR and E5LV grades, the value of the exponent, *n* for E10MCR:E5LV 25:75 (n=0.44) and 50:50 (n=0.34) was less than 0.5, while for E10MCR:E5LV 75:25 (n=0.51) was slightly greater than 0.5, indicating that an increase in the amount of E10MCR in mixed grade resulted in shift in mechanism of liquid diffusion from Fickian to anomalous. However, it is worth mentioning that E10MCR and E5LV both exhibited anomalous diffusion (n=0.5-1, Table 4.3) when used alone as a pure grade.

As mentioned earlier, K4M and E4MCR both displayed anomalous diffusion with the value of the exponent n=0.52 and n=0.51, respectively. However, in their mixed grades (K4M:E4MCR (25:75, n=0.75), K4M:E4MCR (50:50, n=0.39) K4M:E4MCR (75:25, n=0.38)) increasing the concentration of K4M resulted in a change in

diffusion mechanism from diffusion controlled or Fickian to anomalous. It could be postulated that the presence of different diffusion mechanisms in these mixed grades at different concentration levels could be the reason for the unexpected behaviour observed earlier during hydration in Figure 4.9 for these mixed grades.

The hydration constant (*k*) derived from the Vergnaud model depends on the amount of the liquid transferred plus porosity of the matrix and diffusivity of water in the matrix (Vergnaud, 1993), and can be used as an indicator of the rate of polymer hydration (Sinha Roy and Rohera, 2002, Chaibva et al., 2010). The smaller values of hydration constant k = 0.78, 2.24, 1.77, 6.5 and 9.2 for HPMC E6LV, E5LV, E4MCR, K4M:E4MCR (25:75) and HPMC E15LV respectively, indicated an absence of burst effect in polymer hydration or water uptake. However, the higher values of hydration constant (k = 16.22, 16.4, 15.3, 18.8, 19.9, 35.1, 38.7, and 41.1) for K4M, E10MCR, E50LV, E10MCR:E5LV (75:25), E10MCR:E5LV (25:75), K4M:E4MCR (75:25) and (50:50), and E10MCR:E5LV (50:50) respectively (Table 4.3), imply that the rate of water penetration is considerably higher and suggest burst water uptake (Chaibva et al., 2010) for these HPMC polymers. The value of higher hydration constant (*k*) also suggests that the process of gel formation is rapid (Chaibva et al., 2010) due to the formation of a barrier to the penetrant entry thereby slowing the process of polymer erosion and vice versa. Surprisingly, the values of hydration constant (*k*) at 50:50 ratios for both mixed grades (E10MCR:E5LV and K4M:E4MCR) have shown higher values than their combine hydration constant values. In the case of HPMC E10MCR:E5LV (50:50), due to the low viscosity of E5LV, a more extensive ingress of water might had taken place providing an opportunity for E10MCR to further hydrate and swell. With regards to K4M:E4MCR (50:50), both polymers (K4M and E4MCR) have almost the same viscosity, however they have different molecular weights and substitution. A possibility exist that there is a synergistic effect produced by the presence of equal amount of hydrophilic hydroxypropyl content (about 8%, Table 4.1) in both grades which could have caused more hydration. Alternatively, it is possible to postulate a physical explanation for these anomalies, based on particulate properties and packaging / porosity within the compacts.

In summary, as these combinations had provided a sustained rate of hydration over a time period of 300 min, this made them promising candidates for future investigation in this work. As detailed in Section 4.2.2, in order to perform gravimetric erosion and residual hydration studies, a new disc method was employed which allowed multiple data replicates to be obtained in a relatively short time, which could otherwise have restricted the extent of the experimental work. Therefore the method developed in this work has potential as a rapid screening method in future erosion studies.

4.3.4 Correlation between percentage erosion and strength of hydrating gel layer

According to Kamba et al, (2002, 2000) the destructive forces in the human stomach under fed and fasting conditions are 1.89N and 1.5N respectively, and in the human small intestine it is potentially around 1.2N. It is also known that the mechanical stress existing in the human gastrointestinal tract could be the reason for dose dumping where a larger than anticipated amount of drug is released as a bolus, resulting in dangerously high blood levels in the patient (Shameem et al., 1995). Mechanical gel strength of the polymer can impart a substantial influence on *in vivo* performance of swellable matrices as matrix integrity might change under the mechanical forces presented in human stomach and small intestine (Jamzad et al., 2005).

The maximum force at the diffusion front quantified by the TA (method detailed in Section 3.4.1.2) was taken as the maximum strength of the hydrated gel layer, and was correlated with percentage erosion at 240 minutes (Figure 4.11).

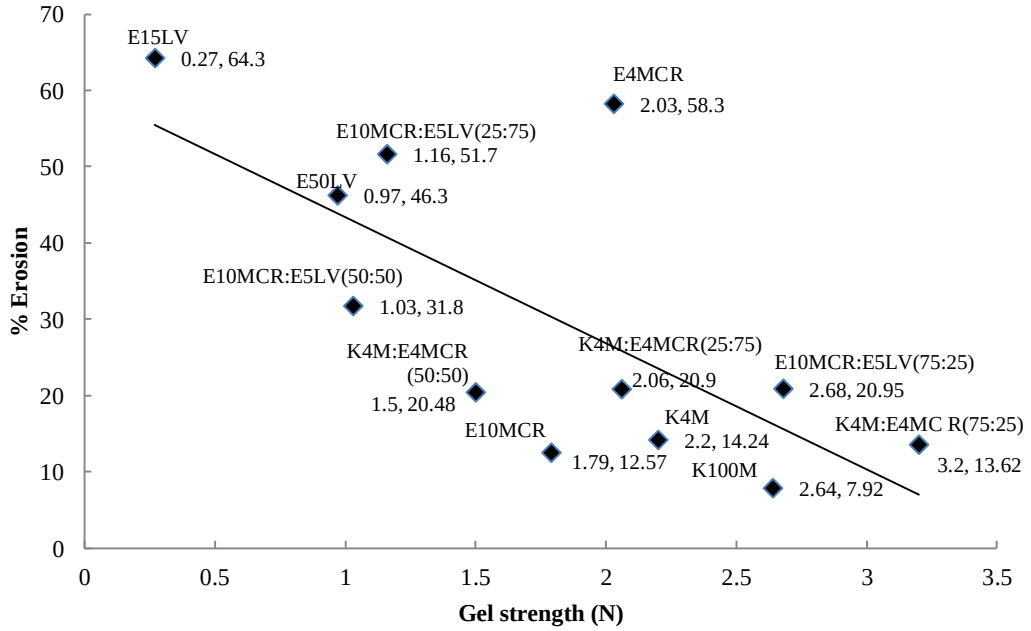

Figure 4.11 Correlation between gel strength and % erosion at the diffusion front (n=6) after 240 min hydration.

The values for HPMC E5LV, E6LV and E10LV are not presented due to their excessive erosion at 240 min. In all cases the error bars for gel strength were smaller than their symbols. It is noticeable that low viscosity grade polymers (E15LV and E50LV) showed more erosion and have weaker gel strength compared to high viscosity grade polymers (E4MCR, E10MCR, K4M and K100M). This indicates that low viscosity grades are more prone to erosion and form weak polymer gels compared to high viscosity grades. However, a combination of low and high viscosity grades provided values in the middle region for both % erosion and gel strength. Although, unexpectedly the mix polymer grade K4M:E4MCR at a ratio of 75:25 demonstrated gel strength of 3.2N, higher than the gel strength (2.64N) of the highest HPMC viscosity grade K100M. There is possibility of development of strong hydrogen bonding between the two HPMC grades, which differ from each other in terms of their degree and ratio of methoxyl (Section 4.1, Figure 4.1), resulting in formation of a stronger gel. However, TA and gravimetric erosion are incapable to

prove this theory which needs further evaluation through more sophisticated analytical tools (e.g. IR or NMR).

One of the main aims of this Chapter was to select suitable candidate polymer/polymers as a barrier layer composite in press coated tablets, and in order to achieve this aim several parameters presented in this chapter were critically analysed. A higher value of hydration constant (*k*) indicates a burst swelling and rapid hydration (Chaibva et al., 2010). Rapid hydration of a polymer indicates the formation of cohesive gel layer, which act as a barrier to penetrant entry, and without this protection polymer disintegration is likely to be fast. Therefore, the polymers with a higher hydration constant should be selected. One of the aims of the proposed colon delivery design (Chapter 1, Section 1.6) was to form a barrier layer with gradual erosion, therefore the polymers with very small or very high values for rate of erosion indicating slower and faster erosion, respectively would not be ideal candidates. For example, the polymers with higher erosion rate constant such as HPMC E5LV or E6LV (0.4433%/min and 0.4373%/min, respectively, Table 4.3) would erode almost completely in 3-4 hours small intestine transit time and be of no use for colon delivery system. Thus, the polymers with a rate of erosion and overall % erosion in the medium to higher range should be selected. The last most important criteria adopted for the selection of the barrier layer composite was the polymer gel strength (N). Although Kamba et al.,(2002) reported average crushing force in human small intestine 1.2N however, more closer analysis of their data revealed that the value ranged between 0.8-1.2N. Therefore, polymers which have shown gel strength values around 1.2 N indicating the crushing force in human small intestine would be considered appropriate tool for candidate selection, assuming that the tablet is enteric coated and would not crush in stomach.

After analysing the data presented in this Chapter, with respect to the swelling constant (*k*), rate of erosion (%/min), % erosion, and gel strength (N), it was decided to choose six polymers/polymer combinations on the basis of these parameters for future studies (Table 4.4).

Table 4.4 Selected HPMC polymers with their swelling constant (*k*), rate of erosion (%/min), % erosion, and gel strength (N) values.

Name of the HPMC polymer	**Swelling Constant *k***	**Rate of Erosion (%/min)**	**% Erosion at 240 min**	**Gel Strength (N) at 240 min**
E50LV	18.7	0.1896	46.3	0.97
E10MCR:E5LV (75:25)	18.8	0.0398	20.95	2.68
E10MCR:E5LV (25:75)	19.9	0.1768	51.7	1.16
K4M:E4MCR (75:25)	35.1	0.0337	13.62	3.2
K4M:E4MCR (50:50)	38.7	0.0216	20.48	1.5
E10MCR:E5LV (50:50)	41.1	0.0627	31.8	1.03

4.4 CONCLUSIONS

A new gravimetric erosion method was developed and used which helped to reduce laborious and time consuming erosion studies in short time. The polymer erosion profiles were found generally linear over a 4 to 5 hour hydration time. It was found that polymer erosion is directly dependent on its molecular weight. It was demonstrated that the Vergnaud model/equation is a useful tool to understand and explain some of the complex behaviour shown by the HPMC polymers especially in a mixed grade. Hydrating gel layers of polymer tablets were probed using a texture analyser, and changes in the gel strength properties were compared with their erosion values. A good correlation between erosion and gel strength was demonstrated, showing that this simple methodology can be used to quantify polymer performance as a rate controlling barrier layer. It was also found that polymer erosion and its gel strength were highly dependent on molecular weight.

A suitable polymer or a combination of polymers were selected from this study, which will hopefully provide a progressively weakening cohesive gel layer with affordability to erode in 3 to 4 hours time in small intestine.

CHAPTER 5

DEVELOPMENT OF NOVEL METHOD OF CALCULATION AND PREDICTION OF LAG TIME

5.1 INTRODUCTION

In the last two Chapters (3 and 4), some important characteristics regarding the barrier layer composite such as polymer gel strength, thickness, hydration, swelling and erosion were discussed for an oral press coated tablet. The aim of this chapter was to accurately predict the quantity of hydroxypropylmethyl cellulose (HPMC) required forming an eroding barrier layer. It was understood through literature review that the quantity of barrier layer composite required to attain a particular behaviour in press coated tablets, had never been calculated, rather researchers tend to use experimentation to achieve the desired result. Mostly tablets are coated with an increasing polymer quantity or by changing barrier layer composition, and a correlation is then established with lag times thus selecting the best lag time formulation for desired purpose (Conte et al., 1993, Sirkiä et al., 1994a, Sirkiä et al., 1994b, Moussa and Cartilier, 1997, Fukui et al., 2000a, Fukui et al., 2001a, Fukui et al., 2001b, Sawada et al., 2003a, Abdul and Poddar, 2004, Sundy and Paul Danckwerts, 2004, Ugurlu et al., 2007, Rujivipat and Bodmeier, 2010b, Liu and Cetinkaya, 2010, Rujivipat and Bodmeier, 2010a, Ghimire et al., 2007). In order to achieve such a correlation the number of required experimental studies to develop a new and/or optimise an existing tablet formulation can be significant. Thus, one of the major driving forces for the use of mathematical modelling in this type of drug delivery system is to save time and to cut down costs by reducing the number of experimental formulations to be developed. Mathematical predictive calculations may therefore provide a good estimate of the required composition, geometry, dimensions and preparation procedure of the respective dosage forms (Siepmann and Siepmann, 2008). Therefore, an attempt has been made through this work to establish a quantitative predictive method on the basis of polymer erosion to achieve required lag times for pulsatile delivery system.

5.2 METHODS

5.2.1 Approaches for calculation of barrier layer polymer quantity

In order to predict the quantity of the polymer required in the barrier layer to achieve a predictable lag time before drug release, two different approaches were developed based on surface area to volume ratio (SA/VOL), and using true density and inverse of true density.

5.2.1.1 Calculations based on surface area to volume ratio (SA/VOL)

Reynolds (2002) examined the release of highly water soluble drugs (promethazine HCl, propanolol HCl and diphenhydramine HCl) from HPMC matrices and demonstrated that when the surface area to volume ratio (SA/VOL) is kept constant, similar drug release profiles are achievable for the same and for different tablet shapes (round or oval). Another researcher (Patel et al., 2009) also concluded parallel findings with round, caplet, dumbbell and pentagon shape tablets using metformin HCl, as a freely soluble drug and indapamide, as a practically insoluble drug. The mechanism of drug release is supposed to be primarily diffusion-controlled for water soluble drugs and erosion-controlled for water insoluble drugs from HPMC matrices.

It has been already established in the Chapter 4 that the rates of erosion of selected polymers in most cases were almost linear. According to Reynolds et al., (2002) if constant SA/VOL ratio yielded similar drug release profile for both water soluble and water insoluble drugs then it was hypothesised that maintaining a constant SA/VOL ratio for different tablet sizes might also result in similar erosion profiles. In order to test this theory, compacts containing HPMC [E10MCR:E5LV] (50:50) mix polymer or E50LV alone, with a tablet weight of 100mg (SA/VOL 1.54/mm or 1.51/mm), 150mg (SA/VOL 1.20/mm and 1.18/mm), 200mg (SA/VOL 1.03/mm and 1.03/mm), 238mg (SA/VOL 1.54), 250mg (SA/VOL 1.51/mm), 350mg (SA/VOL 1.19/mm and 1.18/mm), and 410mg (SA/VOL 1.03/mm) were manufactured for evaluation in erosion studies. Flat face punches were used so that the shape of the

tablet was cylindrical (Figure 5.1) to make the calculation of surface area and volume simple.

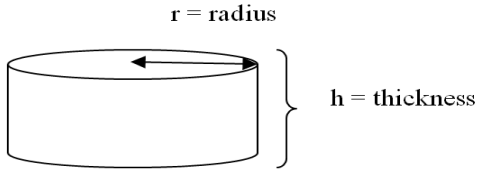

Figure 5.1 Cylindrical tablet made of HPMC.

Tablet physical properties were conducted on 10 tablets for tablet hardness (crushing strength) and thickness. Tablet surface area (equation 5.1), volume (equation 5.2), and SA/VOL (equation 5.3), were calculated as follows:

$$\textit{Surface area of cylindrical tablet} = 2\pi r^2 + 2\pi rh \qquad \textit{(equation 5.1)}$$

$$\textit{Volume of cylindrical tablet} = \pi r^2 h \qquad \textit{(equation 5.2)}$$

$$SA/VOL = 2\pi r(r+h)/\pi r^2 h = 2(r+h)/r \times h \qquad \textit{(equation 5.3)}$$

Where 'r' represents the radius of the tablet and 'h' indicates the thickness of the tablet.

The direct compression of tablets was achieved with a relatively constant compression pressure. The compression pressure can be calculated by the following equation

Compression pressure = compression force/ surface area = (Newton or ton/πr^2) = (ton/mm^2)

For example, if a compression force of 3 ton was used for 8mm flat faced round (FFR) tablet then according to above equation the compression pressure would be 0.0596 ton/mm^2; in order to keep the same compression pressure on 13mm FFR tablet the required compression force would be 8 ton. Tablet weights varied depending on the desired tablet SA/VOL values. The tablets prepared above were

subjected to the same erosion condition using disc method as detailed in the Section 4.2.2 at 60, 90, 120, 150, 180 and 240 minutes hydration time and their percentage erosion was calculated as detailed in Section 3.2.1.2. The % erosion values can be converted into eroded weight (mg) by multiplying % erosion values at different time points to its average tablet weight and dividing by 100. The values of eroded weight (mg) divided by surface area (mm^2) of the tablet used for erosion would provide the values of eroded weight / tablet surface area (mg/mm^2). The erosion constant (K_E) was calculated from the slope of the linear regression equations.

Taking the values obtained using equations 5.1-5.3, and the experimentally derived mg polymer eroded/ tablet surface area, a method of calculating the quantity of polymer required to form the barrier layer for press coated tablets of predictable pulse time was developed.

If a press coated tablet is required to be designed with a 90 minute lag time, then the first step is to know how much barrier layer polymer would erode by 90 minutes (presume it was *a* (mg/mm^2)). Also assume that the SA/VOL value is *b* (mm^2/mm^3) for the tablet which was used to obtain eroded weight/ surface area (mg/mm^2) value during erosion studies. If the surface area of the outer tablet is known (in mm^2), then using a simple multiplication the total weight of polymer required for coating can be calculated.

For example, if we need to press coat equally *x* (mm) of barrier layer polymer on top and bottom on the inner core tablet (presume the thickness is *h* (mm) and radius is *r* (mm) aiming to achieve the outer tablet radius *R* (mm) (Figure 5.2) then following steps can be followed;

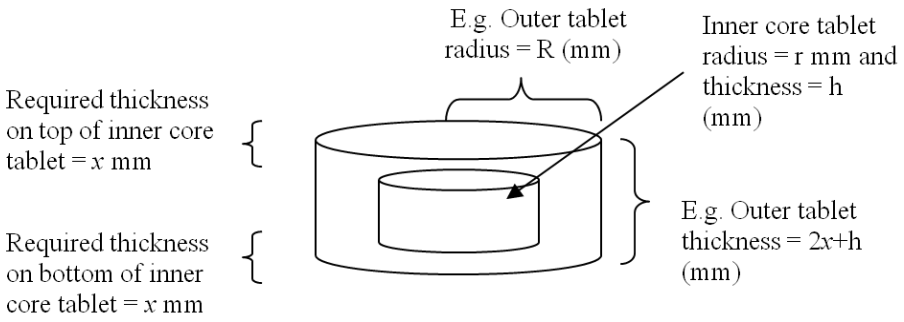

Figure 5.2 The schematic diagram of press coated tablet including inner core tablet with hypothetical dimensions.

Volume of the hypothetical outer press coated tablet = $\pi R^2 H$ *(equation 2)* = $3.14 \times R^2 \times (2x+h)$

Where *H* is total tablet thickness equal to $2x+h$, R is radius of press coated tablet.

The surface area of the outer tablet can be calculated by two ways. One is by simple mathematics using equation 1. However, in order to obtain the similar amount of polymer eroded weight per surface area, *a*, from outer barrier layers as well as discussed earlier, it was thought reasonable to keep the outer press coated tablet's SA/VOL ratio constant at *b* (mm^2/mm^3). So to calculate the surface area for outer tablet the SA/VOL ratio *b* was multiplied with outer hypothesised press coated tablet volume $3.14 \times R^2 \times (2x+h)$

Total surface area of new hypothesised press coated tablet = $SA/VOL \times VOL = b\ (1/mm) \times 3.14 \times R^2 \times (2x+h)\ (mm)^3 = b \times 3.14 \times R^2 \times (2x+h)\ (mm)^2$

By this means theoretically a constant SA/VOL ratio should be achieved for outer tablet

$SA/VOL = b \times 3.14 \times R^2 \times (2x+h)\ (mm)^2 / 3.14 \times R^2 \times (2x+h)\ (mm)^3 = b\ (mm^2/mm^3)$

Thus the required polymer to be coated on the inner core to achieve a lag time of 90 minutes can be calculated by multiplying the eroded weight *a* (mg/mm^2) with new hypothesised tablet surface area

Required polymer for outer barrier layer at 90 minutes = Eroded weight in mg/mm^2 × surface area (mm^2) = a (mg/mm^2) × [b × 3.14×R^2× (2x+h)] (mm)^2 = a × b × 3.14×R^2× (2x+h) (mg)

To understand these calculations an example is done with arbitrary values. In order to design a press coated tablet for a 90 minute lag time, presume the barrier layer polymer erode by 90 minutes would be *a*= 0.24mg/mm^2. Also assume that the SA/VOL value of *b*= 1.02/mm for the tablet which was used to obtain eroded weight/ surface area (mg/mm^2) value during erosion studies. If we need to press coat equally 1mm of barrier layer polymer on top and bottom on the inner core tablet (presume that the inner core thickness was *h*= 4mm and radius was *r*= 4mm) aiming to achieve the outer tablet radius *R*= 6.5mm.

Then

Volume of the hypothetical outer press coated tablet = $\pi R^2 H$ (equation 2) = 3.14×6.5^2×6 = 796.39mm^3

So to calculate the surface area for outer tablet the SA/VOL ratio 1.02/mm was multiplied with outer hypothesised press coated tablet volume 796.39 mm^3

Total surface area of new hypothesised press coated tablet = SA/VOL×VOL= 1.02/mm×796.39mm^3= 812.32mm^2

By this means theoretically a constant SA/VOL ratio would be achievable for outer tablet

SA/VOL = 812.32mm^2/796.39mm^3 = 1.02 mm^2/mm^3

Thus the required polymer to be coated on the inner core to achieve a lag time of 90 minutes can be calculated by multiplying the eroded weight 0.24 mg/mm^2 with new hypothesised tablet surface area

Required polymer for outer barrier layer at 90 minutes = Eroded weight in mg/mm^2 × surface area (mm^2) = 0.24×812.32 = 194.95mg

Similarly the required amount of the barrier layer polymer to achieve different lag times can be calculated using this methodology.

It is noteworthy that these calculations were based on the erosion data which was acquired using the disc method described in Section 4.2.2. During erosion studies the erosion was restricted from the bottom surface while tablet was free to hydrate and erode from top and side surfaces. However, in order to develop these calculations the mg eroded/surface area was knowingly calculated using the initial total surface area (top, bottom and sides) rather sum of the surface areas from top and sides. There are two reasons for this. Firstly, once hydrophilic polymers such as HPMC are in contact with water they undergo hydration, resulting in swelling and formation of gel. As a result there would be an increase in surface area of the tablet compare to its initial surface area; this means all calculations become futile regardless of its origin whether based on initial surface area or surface areas from top and sides. Secondly, a further complicating factor arises due to the process of erosion which is happening at the periphery of the matrix and effectively forcing the tablet surface area to reduce. These two processes occur at the same time though one process may be more dominant than the other at any given time. This means that the dimension of the tablet does not remain constant and subject to micro and macro-changes during hydration and erosion. However, the introduction of these changes in these mathematical models is beyond the scope of this study. Therefore, the mathematical models proposed here adopted the simple approach in both calculations (Section 5.2.1.1 and 5.2.1.2) and used the initial total surface area of the tablet as a constant value.

5.2.1.2 Calculation based on polymer true density, inverse of true density, surface area and volume

A second method of calculation based on polymer true density, surface area, volume and eroded weight per surface area was developed to predict the amount of barrier layer required in press coated tablet. The true density defined as mass of solid material divided by its exact volume without porosity (Cao et al., 2008). Helium pycnometer is widely used instrument to calculate the value of true density however, Sun (2005) suggests that a maximum tablet density, equal to the true density, can be achievable at higher pressure (> 100 megapascal (MPa)). Therefore, in these calculations the tablet density (mg/mm^3) calculated at 8 tonnes (≅ 123.5 MPa) would be used to represent the true density. In order to keep the barrier layer system simple a pure HPMC E50LV grade was used instead of mix grade HPMC E5LV:E10MCR (50:50). Due to supplier change a batch of 100 tablets weighing 40 gram was prepared for HPMC E50LV using IR press with 13 mm flat faced round punch and die at a compression force of 8 ton to obtain percentage erosion data. The tablets were subjected for erosion using disc method (Section 4.2.2) and their percentage erosion was calculated as detailed in Section 3.2.1.2 at 60, 120, 180, 240 and 300 minutes. The percentage polymer erosion values were then converted to obtain weight eroded per surface area of the tablet (mg/mm^2) as discussed above in Section 5.2.1.1.

The quantity of polymer required to form a delay/barrier layer around an inner core tablet to achieve desired lag time was calculated as described below;

Mg required for barrier layer (A) = *(a)* × *(b)*

(*a*) Weight of the HPMC tablet eroded in mg at different time points/surface area of the HPMC tablet

(*b*) Surface Area of the inner core tablet to be covered [top and bottom only] (mm^2)

Volume required (B) = *(c)* × *(A)*

(*c*) Volume of the HPMC tablet (mm^3)/weight of the HPMC tablet (mg) [inverse of true density]

Thickness required (C) $= (B) / (\pi \times (r)^2)$

r = radius of the final required tablet

Total Thickness (D) $= (C) + (d)$

(*d*) Thickness of inner core tablet (mm)

Total volume (E) $= (D) \times (\pi \times (r)^2)$

Required remaining volume [F] $= (E) – (e)$

(*e*) Inner core volume (mm^3)

Required mg needed to be coated (G) $= (F) \times (f)$

(*f*) Weight of HPMC tablet (mg)/volume of HPMC tablet (mm^3) [true density]

If one merge all these equations together it is possible to write a single final equation as described below

Required mg needed to be coated (H) $= [\{(a \times b \times c) + \{(d) \times (\pi \times r^2)\} - (e)\} \times (f)]$

To illustrate this series of calculations, suppose a press coated tablet is required to be designed with 180 minute lag time using HPMC as an outer barrier layer coating. The quantitative data on following variables is required before commencing the calculation, all values given here are arbitrary in order to illustrate the calculations: weight of the HPMC tablet eroded in mg at 180 minutes /surface area (*a* = 0.5mg/mm^2), volume of HPMC tablet (mm^3)/weight of HPMC E50LV tablet (mg) [inverse of true density] (*c* = 0.8mm^3/mg), weight of HPMC tablet (mg)/volume of HPMC tablet (mm^3) [polymer true density] (*f* = 1.5mg/mm^3), surface area of the

inner core tablet to be covered [top and bottom only] (b = 100mm^2), r = radius of the final required tablet (6.5mm), height of the inner core tablet (d = 3mm) and inner core tablet volume (e = 140mm^3). The calculations were performed as follow;

Mg required for barrier layer (A) $= 0.5mg/mm^2 \times 100mm^2 = 50mg$

Volume required (B) $= 50mg \times 0.8mg/mm^3 = 40mm^3$

Thickness required (C) $= 40mm^3/(\pi \times (6.5mm)^2) = 0.301mm$

Total Thickness (D) $= 0.301mm + 3mm = 3.301mm$

Total volume (E) $= 3.301mm \times (\pi \times (6.5mm)^2) = 438.2mm^3$

Required remaining volume (F) $= 438.2mm^3 - 140mm^3 = 298.2\ mm^3$

Required mg needed to be coated (G) $= 298.2\ mm^3 \times 1.5mg/mm^3 = 447.3mg$

Or

Required mg needed to be coated (H) $= [\{(a \times b \times c) + \{(d) \times (\pi \times r^2)\} - (e)\} \times (f)]$

Required mg needed to be coated $= [\{(0.5 \times 100 \times 0.8) + \{(3) \times (\pi \times 6.5^2)\} - (140)\} \times (1.5)]$

Required mg needed to be coated= 447.3mg

Therefore, to achieve different lag times, the required amount of barrier layer polymer can be calculable using this methodology.

5.2.2 Manufacture of inner core tablets

Formulation composition for the two inner core tablets is given in Table 5.1. The batch size for inner core powder mixture was 80g.

Table 5.1 Formulation composition of inner core tablets

Formulation composition	Core Tablet	
	Theophylline (%)	Riboflavin (%)
Theophylline	50	-
Riboflavin	-	5.5
Avicel	29	92.25
Lactose	20	-
Potato starch	0.5	1.5
Aerosil	-	0.25
Magnesium stearate	0.5	0.5

Theophylline, Avicel and lactose were sieved through a steel mesh # 250 µm and mixed in Turbula ® mixer for 15 minutes followed by additional 5 minutes mixing after the addition of magnesium stearate and potato starch. Riboflavin inner core powder mixture was processed in similar manner as described above for theophylline with added Aerosol in the last step to improve flow properties. Due to riboflavin's yellow colour, the inner core tablets made with riboflavin were also used for photographic purposes. Inner core riboflavin and theophylline tablets weighing 200mg were made manually using an IR press with an 8 mm flat face round punch and die at a compression force of 3 ton.

5.2.3 Manufacture of press coated tablet based on SA/VOL calculation

The required amount of HPMC E5LV:E10MCR (50:50) as a barrier layer composite in press coated tablets for predictive lag times at 90, 120, 150, 180 and 240 minutes were calculated as 152.27, 158.61, 171.30, 177.64, and 203.03mg, respectively according to the method described in Section 5.2.1.1. The one half of the required polymer powder (as calculated above) 76.1, 79.30, 85.65, 88.82 and 101.51mg was coated on the bottom and the other half on top of the centrally aligned inner core tablet (Section 5.2.2) using IR press with a compression force of 8 ton.

5.2.4 Manufacture of press coated tablet based on true density, inverse of true density, surface area and volume method

As described above in Section 5.2.1.2, due to supplier change HPMC E50LV from two manufacturers was used. The one will be called HMPC E50LV-S which was obtained from Shin-Etsu Chemicals and other HPMC E50LV-D from Dow Chemicals. The quantity of E50LV-S required forming a barrier layer for 60, 120, 180, and 240 minutes lag time was calculated as 294mg, 308mg, 321mg and 335mg respectively, using the method described in Section 5.2.1.2. The quantity of E50LV-D required to produce a barrier layer for 180, 240 and 300 minutes lag time was calculated as 295mg, 317mg and 339mg respectively, using the same method described in Section 5.2.1.2. Two manufacturing procedure were followed to prepare the press coated tablets for these predicted calculation. In first procedure, half of the E50LV-S powder was placed first then an inner core riboflavin tablet was placed centrally. The tablet was lightly pressed manually in powder bed and then remaining half was placed on top before finally compressed at 8 ton.

Through this method unequal barrier layer coating was obtained on top and bottom sides of the inner core tablet. Thus it was thought that improved method was needed to achieve equal polymer coating on top and bottom of the inner core tablet. This was accomplished by skilfully removing the coated polymer from top and bottom of the inner core tablet and measuring their thickness and weighing them to quantify the amount acquired. In order to achieve this the sides of the press coated tablets were removed in such a way that the amount of the barrier layer coating covering the top and bottom of the inner core tablet could be exactly calculated. By changing the amount of the powder layer at bottom with respect to top layer, it was possible to achieve the equal amounts on both sides of the tablets.

Therefore, in this second procedure, to get equal amounts of barrier layer, almost one third (33%) of the required powder (HPMC E50LV-D) was placed in 13mm die an immediate release 8mm flat faced theophylline inner core tablet (200mg) was then placed centrally on the powder bed. The remaining two third (66%) was distributed on top of the core tablet and compressed at 8 ton to form pulsatile release tablets.

5.2.5 *In vitro* dissolution studies

The press coated tablets prepared in Sections 5.2.3 and 5.2.4 containing riboflavin or theophylline as an inner core tablets (disintegration time less than 5 minutes) were tested in dissolution studies. Dissolution studies were performed at 37±0.5°C in 900 ml of dissolution medium (distilled water) in USP apparatus II with the paddle speed of 100 rpm. Samples were automatically withdrawn every 5 seconds for riboflavin and theophylline, filtered in-line, and assayed in 1cm quartz cell on an ultraviolet (UV) spectrophotometer (absorption maximum (λ_{max}) 267nm for riboflavin; λ_{max} 273nm for theophylline) for absorption values. The dissolution was terminated after observing the pulse or up to maximum of 720 minutes. In order to obtain calibration curves for riboflavin and theophylline, stock solutions containing 50mg riboflavin or theophylline in 100ml of distilled water were prepared. Riboflavin stock solution was further diluted by 1.6, 2, 2.5, 3.3, 5, 10 and 200 times to obtain 30, 25, 20, 15, 10, 5 and 0.25mg/100ml of calibrators, respectively while theophylline stock solution was diluted by 20, 25, 33.33, 50, 100, 250 and 500 times to get 2.5, 2, 1.5, 1.0, 0.5, 0.2 and 0.1mg/100ml of calibrators, respectively using the distilled water to make up the final volumes. After preparation, the absorbance was immediately measured for these calibrators using the UV spectrometer with distilled water as blank. In order to obtain the regression equations for riboflavin and theophylline the absorbance values were plotted against their concentrations. The percentage of riboflavin and theophylline release from the inner core tablet was calculated from the absorbance values using the linear equation derived from the calibration curves shown in Appendixes I and II.

As described above in Section 5.2.4 that uneven coating was observed in press coated tablets when equal quantity of the powder layers were used on top and bottom of the inner core tablet. To explore further the impact of this unequal coating during dissolution, press coated tablets (prepared with E50LV-S having predicted pulse times at 60, 120, 180 and 240 minutes using the method described in Section 5.2.1.2) were individually marked as bottom and top. These individual tablets were then affixed on 25cm Perspex disc and then selectively placed in the dissolution apparatus such that either bottom or top was facing the stirring.

5.3 RESULTS AND DISCUSSION

5.3.1 Effect of increasing SA/VOL ratio on erosion profile of HPMC E10MCR:E5LV (50:50) tablets

It was hypothesised in Section 5.2.1.1 that maintaining a constant SA/VOL ratio for different tablet sizes might result in similar erosion profiles. In order to evaluate this hypothesis as a first step a set of experiments containing HPMC E10MCR:E5LV (50:50) tablets with increasing SA/VOL ratio were manufactured as detailed in Section 5.2.1.1 and evaluated for erosion. Table 5.2 shows tablet dimensions, SA, hardness and erosion constant values for 8mm FFR E10MCR:E5LV (50:50) tablets with increasing SA/VOL values. The data indicates that decreasing tablet weight and height resulted in increasing SA/VOL ratios and decreasing SA, hardness and erosion constant values for HPMC E10MCR:E5LV (50:50) tablets having the same tablet diameter (8mm).

Table 5.2 Tablet dimensions, SA, hardness and erosion constant values for 8mm FFR E10MCR:E5LV (50:50) tablets with increasing SA/VOL values

Tablet weight (mg)	**Tablet thickness (mm)**	**SA (mm^2)**	**SA/VOL (1/mm)**	**Hardness (Kpa)**	**Erosion constant (K_E, % erosion/min)**
100	1.92±0.09	148.7±2.3	1.54±0.52	6.90±0.27	0.1797
150	2.58±0.04	172.1±1.1	1.20±0.11	10.8±0.29	0.1505
200	3.77±0.03	195.3±0.9	1.03±0.005	15.2±0.45	0.1106

Previous studies (Siepmann et al., 1999, Reynolds et al., 2002) indicated that the increase in SA/VOL resulted in increase in drug release from HPMC matrixes. Figure 5.3 shows similar behaviour in terms of polymer erosion indicating that the increasing SA/VOL values (1.03, 1.21 and 1.54) with time resulted in increasing percentage erosion profiles.

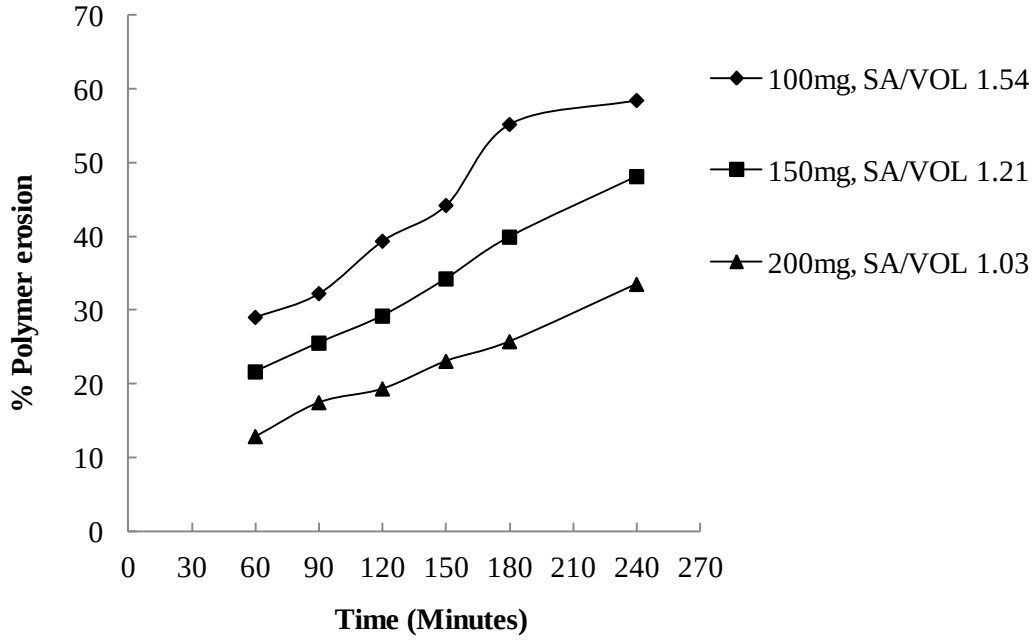

Figure 5.3 Percentage erosion of HPMC E10MCR:E5LV (50:50) tablets versus hydration time exhibiting the effect of increasing SA/VOL 1.54 (♦), 1.21 (■), 1.03 (▲) using 8mm FFR tablets (n=5).

This is also obvious from their rate of erosions or erosion constant (K_E) given in Table 5.2. The increasing SA/VOL values 1.03, 1.20 and 1.54mm^2/mm^3 resulted in increasing K_E values 0.1106, 0.1505 and 0.1797 %erosion/min, respectively as shown in Figure 5.4.

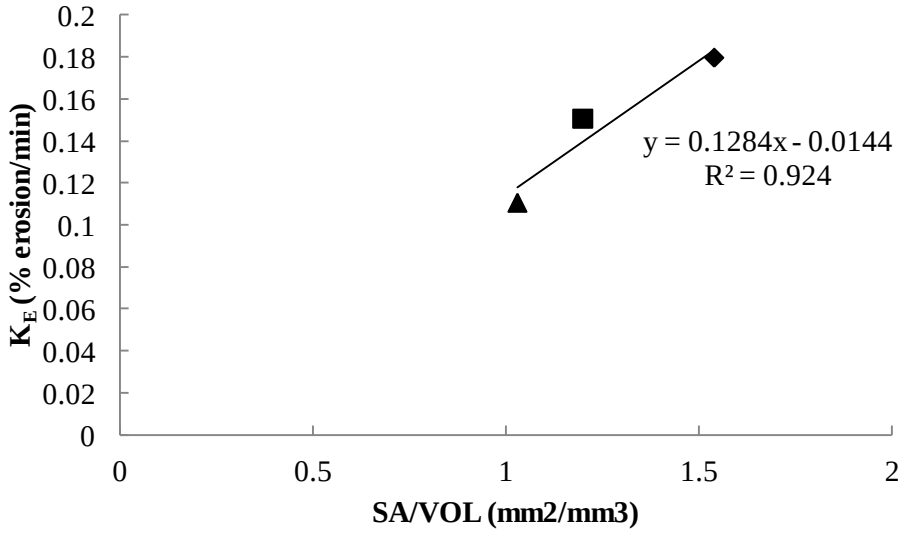

Figure 5.4 Correlation between the SA/VOL 1.54 (♦), 1.21 (■), 1.03 (▲) versus their respective erosion constant (K_E) 0.1797, 0.1505 and 0.1106 %erosion/min obtained using 8mm FFR HPMC E10MCR:E5LV (50:50) tablets (n=5).

The value of increased erosion constant indicates more polymer erosion. Thus it can be concluded that the tablet percentage erosion profiles are directly proportional to their surface area to volume ratios.

5.3.2 Effect of constant SA/VOL ratio on erosion profiles of HPMC E10MCR:E5LV (50:50) and E50LV tablets

It was established in Section 5.3.1 that increasing SA/VOL value resulted in increase percentage erosion. In these experiments the surface area to volume ratio was held constant by adjusting the tablet weight for the same FFR shape tablets, and by varying tablet diameter i.e. 8 and 13 mm. Table 5.3 shows the change in tablet dimensions, SA, hardness and erosion constant by keeping the constant SA/VOL ratio for HPMC E10MCR:E5LV (50:50) tablets.

Table 5.3 Tablet dimensions, SA, hardness and K_E values for HPMC E10MCR:E5LV (50:50) tablets used for % erosion profiles with constant SA/VOL values having different tablet diameters, 8 and 13 mm

Tablet diameter (mm)	Tablet weight (mg)	Tablet thickness (mm)	SA (mm^2)	SA/VOL (1/mm)	Hardness (KPa)	Erosion constant (%/min)
8	100	1.92±0.094	148.7±2.36	1.54±0.520	6.90±0.27	0.1797
13	238	1.61±0.018	331.1±0.76	1.54±0.014	7.18±0.28	0.1221
8	150	2.58±0.047	172.1±1.19	1.20±0.116	10.8±0.29	0.1505
13	350	2.30±0.013	359.32±0.5	1.19±0.005	11.9±0.25	0.0956

Expectedly, tablets with constant SA/VOL ratios (using 8mm and 13mm tablets) yielded almost constant hardness values (Table 5.3) due to the use of constant compression pressure as described in Section 5.2.1.1. The percentage erosion profiles versus time for the HPMC E10MCR:E5LV (50:50) tablets are shown in Figure 5.5.

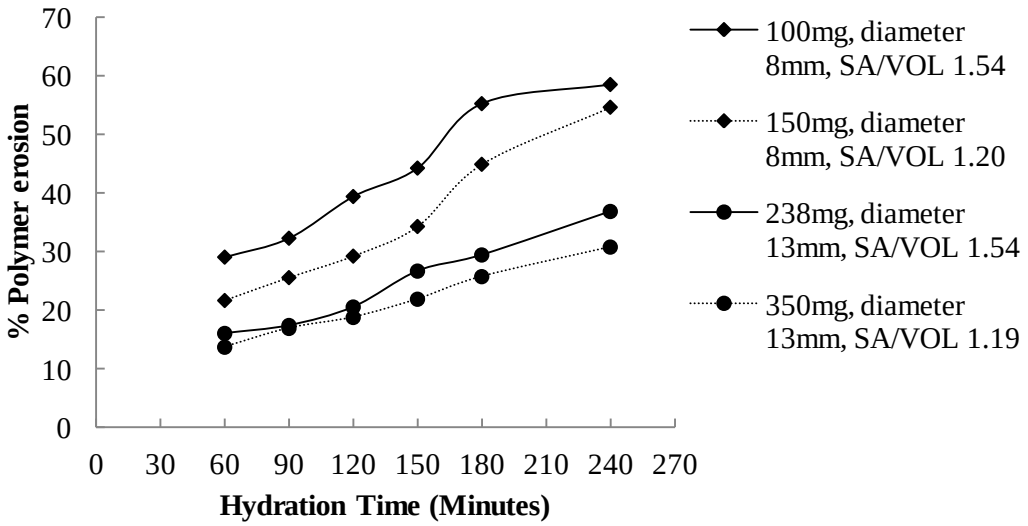

Figure 5.5 Comparison of percentage erosion profiles versus time representing the effect of constant SA/VOL ratio for HPMC E10MCR:E5LV (50:50) FFR tablets with different tablet diameters, 8mm (♦) and 13mm (●) (n=5).

The data indicates that the percentage erosion increases with time. In general, tablets with high SA/VOL values resulted in higher overall % erosion at any time point and vice versa (Figure 5.5). As a consequence of maintaining the constant SA/VOL ratio (1.54 and 1.20 or 1.19) in different tablet sizes (diameter 8 and 13 mm), the percentage erosion profiles versus time were found dissimilar i.e. the erosion profiles do not overlap over each other (Figure 5.5). This is also obvious from their erosion constant or rate of erosion values (Table 5.3) where constant SA/VOL ratios 1.54 and 1.20 or 1.19 yielded different K_E values 0.1797 and 0.1221%/min or 0.1505 and 0.0956%/min, respectively.

Reynolds (2002) and Patel (2009) illustrated that a constant SA/VOL for different tablet shapes (dimensions and geometries) resulted in relatively constant diffusional drug release rates and drug release profiles from HPMC matrixes using water soluble and insoluble drugs, respectively. However, similar behaviour with regards to erosion was not observed when SA/VOL ratio was kept constant (Figure 5.5).

It is known that drug release from matrix forming polymer could be attributed to either process of diffusion or combination of erosion and diffusion depending on the properties of polymer and drug both in use. In contrast, the process of polymer erosion is purely surface phenomenon depending on the disentanglement of the individual molecules from the matrix surface and their disappearance into the bulk solution. Thus it can be concluded that the process of erosion differs from drug release in HPMC matrices due to which keeping the SA/VOL ratio constant did not offer the similar erosion profiles as was previously anticipated in Section 5.2.1.1 based on Reynolds (2002) and Patel (2009) observation.

There is a possibility that these dissimilar percentage erosion profiles keeping SA/VOL ratio constant might be polymer grade specific. In order to investigate this possibility, another HPMC polymer grade E50LV was tested and its physical dimensions, SA, hardness and erosion constant values are given in Table 5.4.

Table 5.4 Tablet dimensions, SA and hardness for HPMC E50LV-S tablets used in % erosion profiling having decreasing and constant SA/VOL values using tablet diameters, 8 and 13 mm with their erosion constant.

Tablet diameter (mm)	**Tablet weight (mg)**	**Tablet thickness (mm)**	**SA (mm^2)**	**SA/VOL (1/mm)**	**Erosion constant (K_E)**	**Tablet hardness (Kpa)**
8	100	1.99±0.02	151.3±0.48	1.51±0.009	0.2638	6.90±0.27
8	150	2.96±0.04	173.5±1.73	1.18±0.010	0.2429	10.8±0.29
8	200	3.78±0.03	195.43±0.88	1.03±0.005	0.0528	15.2±0.45
13	240	1.65±0.041	332.68±0.56	1.51±0.034	0.2069	9.45±1.25
13	350	2.34±0.018	360.8±0.745	1.18±0.006	0.1971	12.9±0.27
13	410	2.76±0.016	378.4±0.678	1.03±0.004	0.1511	17.46±0.38

Again it was observed that decreasing tablet weight and thickness would result increase in SA/VOL ratio and erosion constant with decreasing SA and tablet hardness values.

The percentage erosion profiles versus time for the HPMC E50LV-S tablets having SA/VOL ratio 1.51, 1.18 and 1.03 from different tablet sizes (diameter 8 and 13mm) are shown in Figure 5.6.

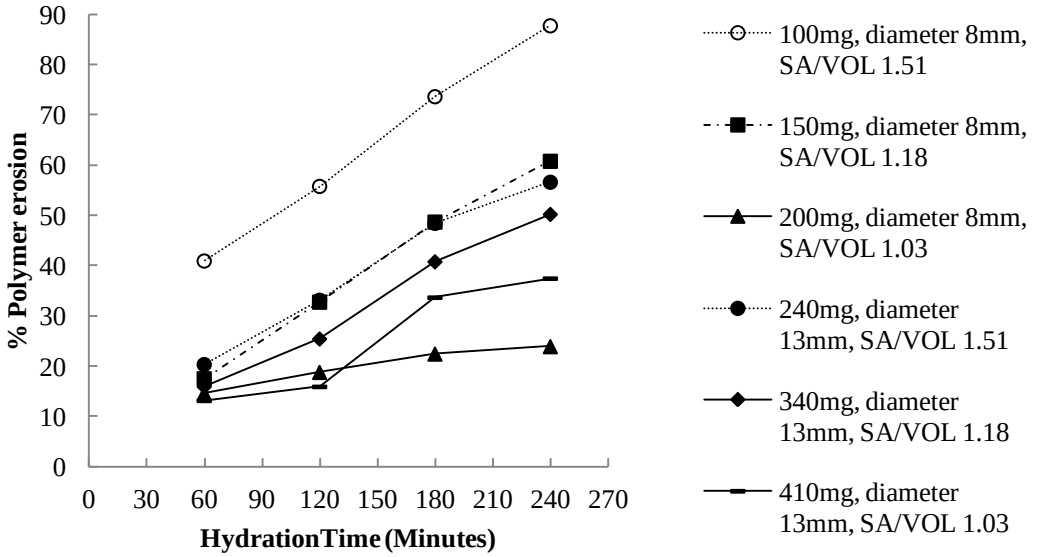

Figure 5.6 Comparison of percentage erosion profiles versus time representing the effect of constant SA/VOL ratio for HPMC E50LV-S FFR tablets with different tablet diameters, 8mm and 13mm (n=5).

The data illustrate that the percentage erosion increased with time. As a result of retaining the constant SA/VOL ratio in different tablet sizes (diameter 8 and 13 mm), the percentage erosion profiles versus time were again found dissimilar just like previously resulted for HPMC E5LV:E10MCR (50:50).

However, it is interesting to note that the two erosion profiles for two different tablet size diameter 8 and 13mm were found similar though not having constant SA/VOL values 1.18 and 1.51, respectively (Figure 5.6). The erosion constants (K_E) (Table 5.4) for these two tablets are roughly close to each other 0.2429%/min and 0.2069%/min indicating that erosion constant might be more important variable to consider if similar erosion profiles are required from different tablet sizes. Furthermore, it can also be seen in Table 5.4 that in same tablet size e.g., either 8mm or 13mm, increasing the tablet thickness due to increasing weight resulted in decrease in erosion constant. So it can be inferred that the tablet thickness or tablet weight has an inverse relation with erosion constant.

5.3.3 *In vitro* drug release from predicted press coated tablets using constant SA/VOL ratio method

As discussed briefly in Section 5.2.1, the surface area to volume ratio method had already been developed calculating the amount of HPMC E10MCR:E50LV (50:50) as a barrier layer polymer on each side of riboflavin inner core tablet for pulsatile drug delivery. Figure 5.7 shows the % riboflavin release from 5 individual press coated tablets having predicted lag times at 90, 120, 150 180 and 240 minutes.

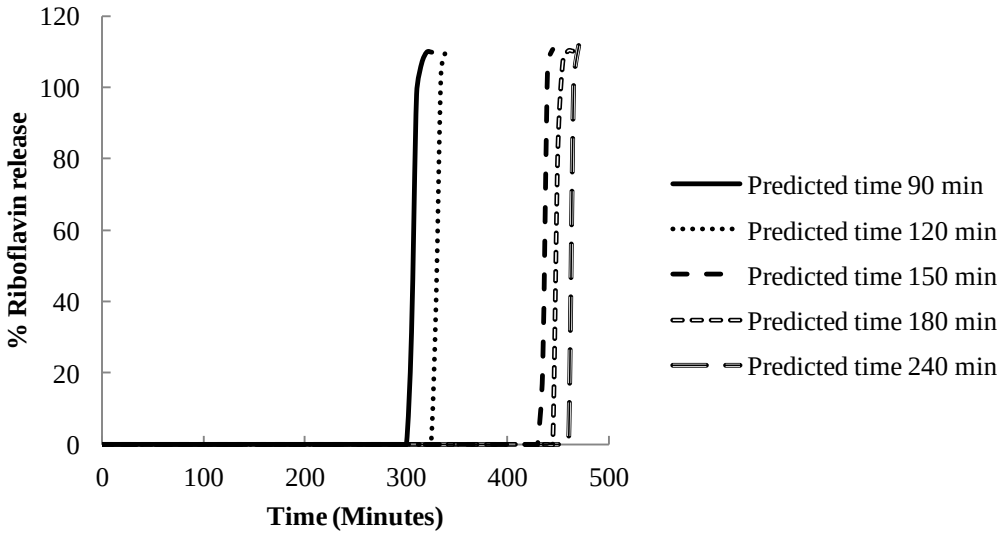

Figure 5.7 Comparison of percentage riboflavin release versus predicted release from press coated tablet (diameter 13mm) having HPMC E10MCR:E5LV (50:50) as a barrier layer polymer calculated on the basis of SA/VOL ratio method (Section 5.2.1.1) (n=1).

The experimental results did not fully comprehend the prediction as obvious from the data. The actual riboflavin released at 305, 330, 435, 450 and 465 minutes for predicted press coated tablets calculated at 90, 120, 150, 180, and 240 minutes, respectively.

It has previously been demonstrated in Section 5.3.2 that a constant SA/VOL ratio did not provide similar erosion profiles which could be one of the main reasons for failed prediction using SA/VOL ratio calculation method. Another reason thought for these inconsistent results could be improper mixing of HPMC E5LV and E10MCR. There is always a chance that the powders are not homogenously mixed due to electrostatic repulsion between particles (Gennaro, 2005) or tend to segregate due to difference in particle size influencing the degree of mixing and density and shape influencing the degree of compaction (Carstensen, 2001). Therefore, instead of using a polymer mix in second method of calculation only single pure HPMC E50LV polymer grade was used. The method evaluated here demonstrated a poor predictability due to this reason its further evaluation in future studies was abandoned.

5.3.4 Calculation based on polymer true density, surface area, volume and milligram eroded/area

In order to develop this last set of calculation it was necessary to overcome some of the variations which have made previous calculations non-workable. It was important to choose the right tablet size (diameter), weight and thickness which was used during erosion studies and then feed them back into this novel calculation method. As described previously in Section 5.3.2 that the erosion studies using HPMC E50LV were conducted on two different tablet sizes 8 and 13mm. In order to choose the right tablet size, it was decided to use the erosion data from the tablet size 13mm because the final press coated tablet was intended to be made in this size. It was also previously discussed in Section 5.3.2 that the erosion constant is inversely proportional to tablet thickness and weight. This means that different tablet thicknesses and weights from the same tablet size (13mm) would have different erosion data. The erosion data is an important requisite which was required to calculate the polymer eroded weight/surface area value as briefly discussed in Section 5.2.1.1. The inner core riboflavin and theophylline tablets having an average tablet thickness (2.78mm) were prepared using method 5.2.2, so that they can be used in press coated tablet. Thus it was decided that the erosion data from tablet

thickness of ≈ 2.78mm (Table 5.4) should be used to calculate the weight eroded/surface area values and then feed them back in this calculation method. In addition to that the compression force was kept constant at 3 ton and 8 ton for inner core tablets (8mm diameter) and tablet used for erosion studies plus press coated tablet (13mm diameter) respectively. By defining these parameters it was possible to control variability in tablet weight, thickness, volume and density.

In order to evaluate the calculation method developed in Section 5.2.1.2, press coated tablets having HPMC E50LV-S as a barrier layer polymer were made according to the manufacturing method described in Section 5.2.4. Figure 5.8 shows the % riboflavin release from 5 individual press coated tablets for predictive 180 minutes lag time.

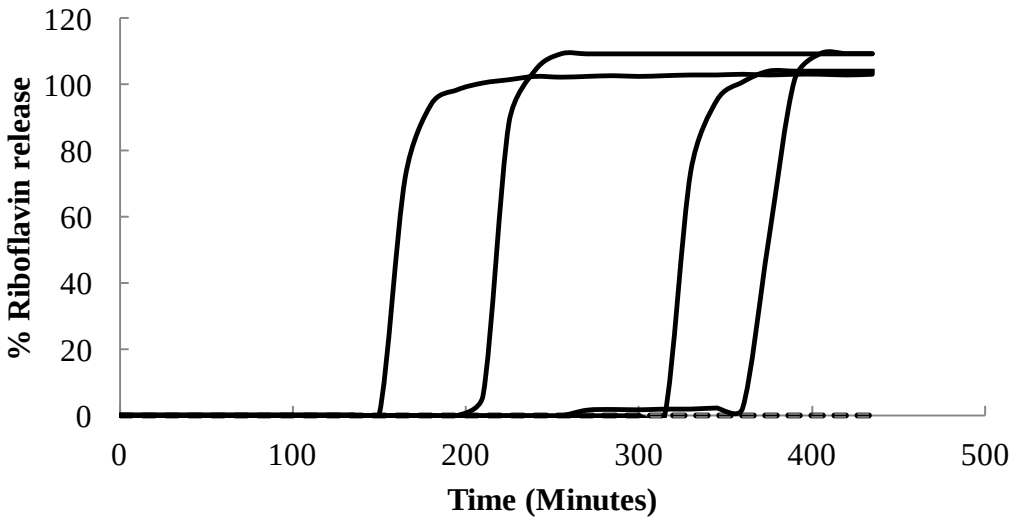

Figure 5.8 Percentage riboflavin release from five individual press coated tablets having HPMC E50LV-S as a barrier layer polymer calculated on the basis of method described in Section 5.2.4, for predictive 180 minutes lag time, the dotted line without pulse representing zero riboflavin release from inner core up to 435 minutes from one of the press coated tablet.

The data shows that the 5 individual tablets pulsed at 150, 195, 315 and 345 minutes while 1 of the press coated tablet did not show any release until 435 minutes dissolution time for the predicted 180 minutes lag time.

In case of predicted 240 minutes lag time the individual % riboflavin release was observed at 315, 395, 405, 510 and 540 minutes, as shown in Figure 5.9.

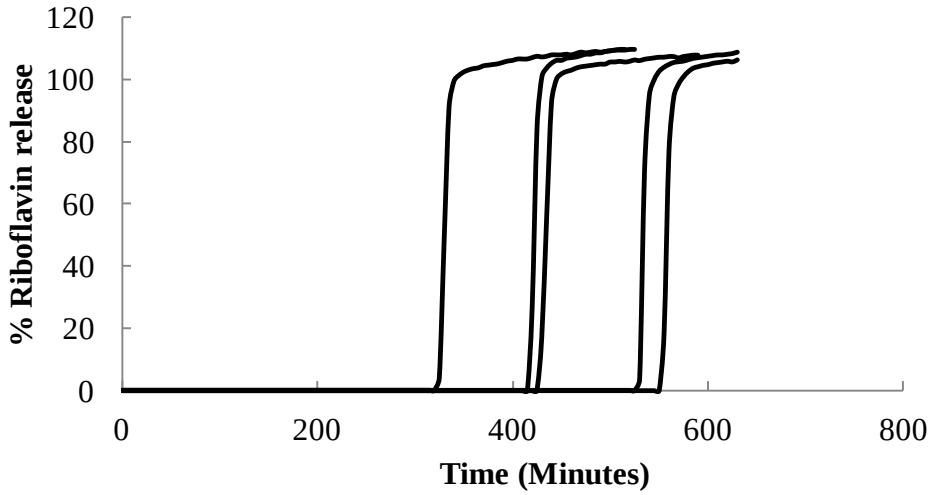

Figure 5.9 Percentage riboflavin release from five individual press coated tablets having HPMC E50LV-S as a barrier layer based on the method described in Section 5.2.4, designed to pulse after theoretical 240 minutes lag time.

These results indicate serious variability in actual release representing a huge deviation from their respected predicted values. It was found through visual inspection (Figure 5.10) that the one side of the tablets was more coated than the other which could have lead to these variations.

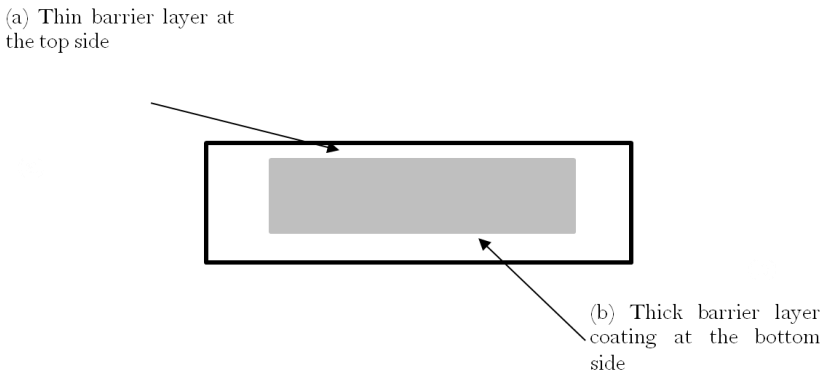

Figure 5.10 The inconsistent HPMC E50LV-S barrier layer coating on riboflavin inner core in press coated tablet showing less quantity of the barrier layer polymer on top (a) compared to bottom (b).

In order to investigate further the reason for this variability the tablets were individually marked as bottom and top and then selectively placed in the dissolution apparatus such that either bottom (3 tablets) or top (3 tablets) was facing the stirring using Perspex disc as discussed in method 5.2.5. Figures 5.11, 5.12, 5.13 and 5.14 show the percentage release of riboflavin from six individual press coated tablets for predicted lag times at 60, 120, 180 and 240 minutes, respectively.

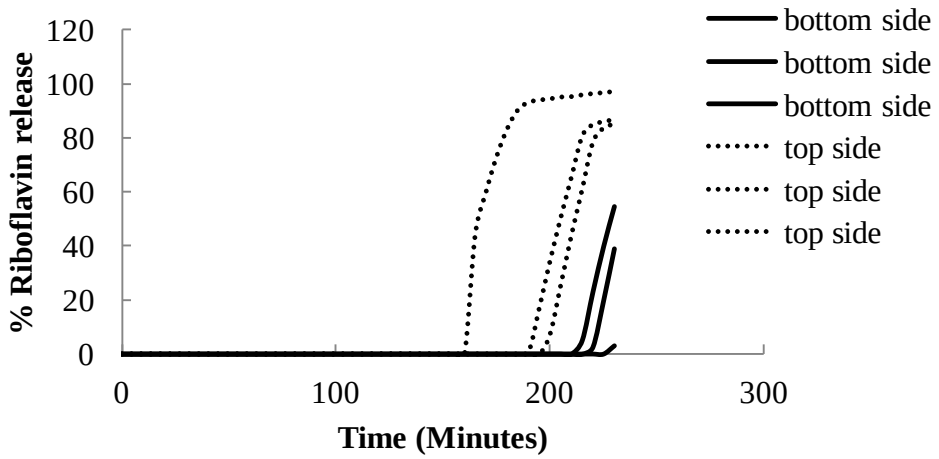

Figure 5.11 Percentage riboflavin release from six individual press coated tablets having HPMC E50LV-S as a barrier layer based on the method described in Section 5.2.4 affixed on Perspex disc such that either bottom (▬) or top (…) of the tablet was exposed to the dissolution medium for predictive 60 minutes lag time.

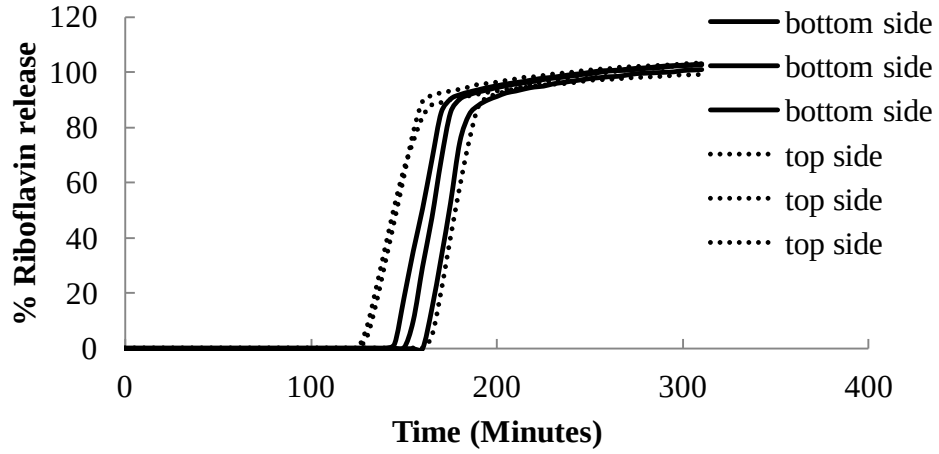

Figure 5.12 Percentage riboflavin release from six individual press coated tablets having HPMC E50LV-S as a barrier layer based on the method described in Section 5.2.4 affixed on Perspex disc such that either bottom (▬) or top (…) of the tablet was exposed to the dissolution medium for predictive 120 minutes lag time.

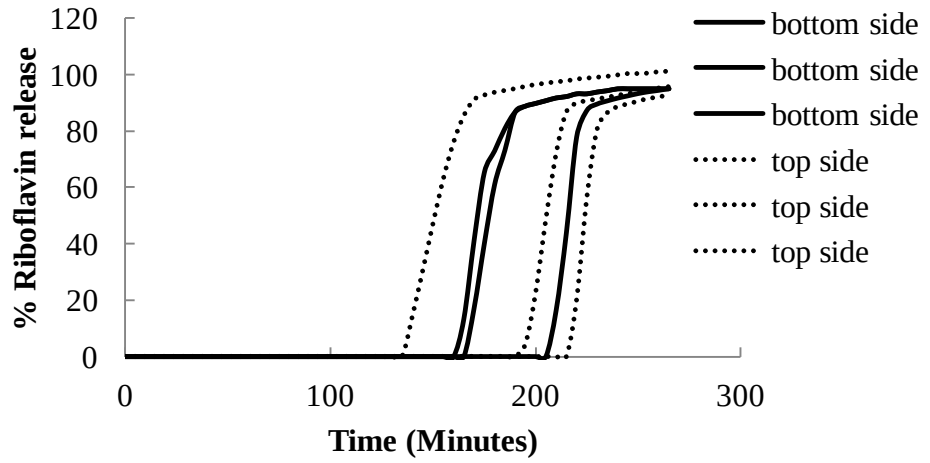

Figure 5.13 Percentage riboflavin release from six individual press coated tablets having HPMC E50LV-S as a barrier layer based on the method described in Section 5.2.4 affixed on Perspex disc such that either bottom (▬) or top (…) of the tablet was exposed to the dissolution medium for predictive 180 minutes lag time.

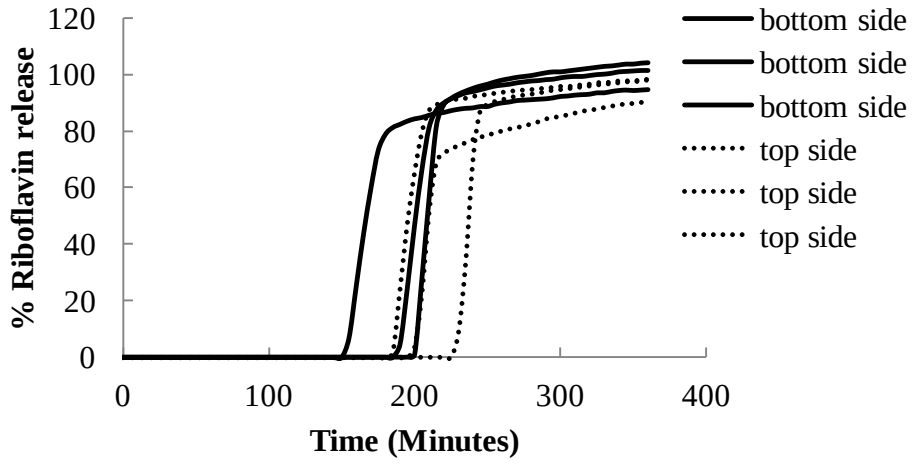

Figure 5.14 Percentage riboflavin release from six individual press coated tablets having HPMC E50LV-S as a barrier layer based on the method described in Section 5.2.4 affixed on Perspex disc such that either bottom (▬) or top (…) of the tablet was exposed to the dissolution medium for predictive 240 minutes lag time.

The collective riboflavin release for all four predicted time points is shown in Figure 5.15.

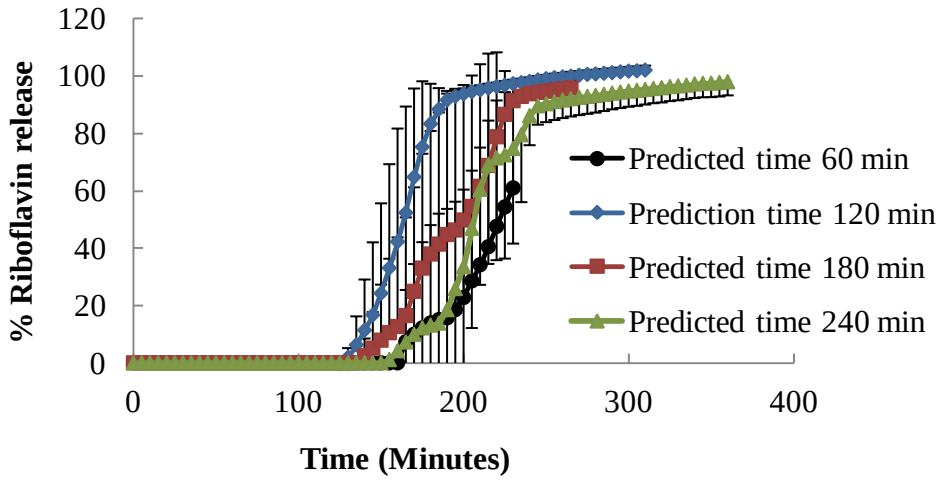

Figure 5.15 Cumulative percentage riboflavin release from press coated tablets having HPMC E50LV-S as a barrier layer manufactured using the method described in Section 5.2.4 for predictive 60, 120, 180 and 240 minutes lag times (n=6).

It was anticipated that by controlling the erosion of press coated tablet from only one side (either bottom or top facing stirring) would improve the reproducibility. For example, in case of press coated tablet with predictive 60 minutes pulse time, it was expected that the actual release should be around 60 minutes however, the actual riboflavin release from individual tablets were observed at 160, 195, 200, 225 and 300 minutes (Figure 5.11). Similarly the actual release from other press coated tablets with predictive time 120 minutes (Figure 5.12), 180 minutes (Figure 5.13) and 240 minutes (Figure 5.14) did not follow the hypothesis and drug release was still variable.

The manufacturing process was identified as a main reason for this inconsistency. During the process of manufacturing, half of the powder was placed first then an inner core tablet was placed centrally. The tablet was lightly pressed manually in

powder bed and then remaining half was placed on top before final compression. This method yielded final tablets with uncontrollably higher or lower thickness on top (35-50%) and bottom (65-50%) surfaces of the tablets thus resulted in variable results.

Figure 5.16 shows the change in inner core tablet due to deformation during press coating compression process.

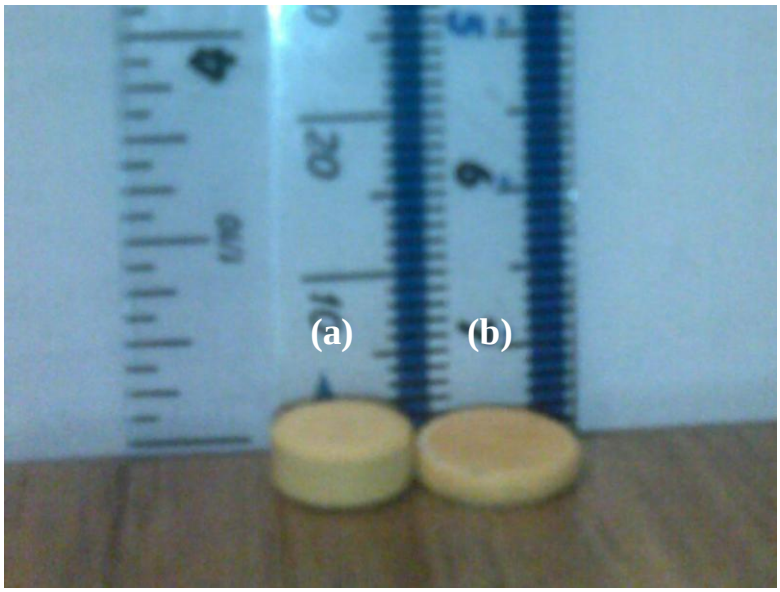

Figure 5.16 The change in the dimension of riboflavin inner core tablet (a) before and (b) after being encased in press coated tablet.

This change could be attributed to the availability of the space in the bigger diameter die for easy expansion around the inner core tablet. This could also be accredited to the compaction properties of the polymer plus the amount of the polymer used. Recently, Liu and Cetinkaya (2010) investigated 25 press coated tablets and observed the variability in the top and bottom layer thicknesses using two different methods of ultrasonic measurement: the pitch-catch and the pulse-echo. Additionally, they compared their results within different parts of the press coated tablet after slicing the tablet into two halves and measuring the thicknesses with callipers. Their

results indicated similar variability in upper and lower layers in 25 press coated tablets using a similar method of manufacture as the current work. Fukui et al (2000b) reported a change in the inner core tablet thickness with respect to increasing compression pressure. The core thickness (2.6mm before compression coating) in press coated tablet decreased to 2.52, 2.48, and 2.43mm using a 550, 910 and 1570Kg/cm^2 compression load, respectively. Their data also revealed that the change in the thickness of the inner core tablet at different compression loads did not alter the thickness of the outer shell (1.11mm). However, it was not indicated whether the top and bottom surfaces had different or equal thicknesses. On the other hand, it can be deduced from their investigation that deformation in the inner core tablet does occur during press coating.

To address the issue of unequal polymer coating on top and bottom of the inner core tablet, it was thought that improved method was needed to achieve equal polymer coating. This was accomplished by skilfully removing the coated polymer from top and bottom of the inner core tablet and measuring their thickness and weighing them to quantify the amount acquired. Figure 5.17 shows that it was possible to remove just top and bottom coatings without sides from press coated tablet containing riboflavin inner core tablet in the middle.

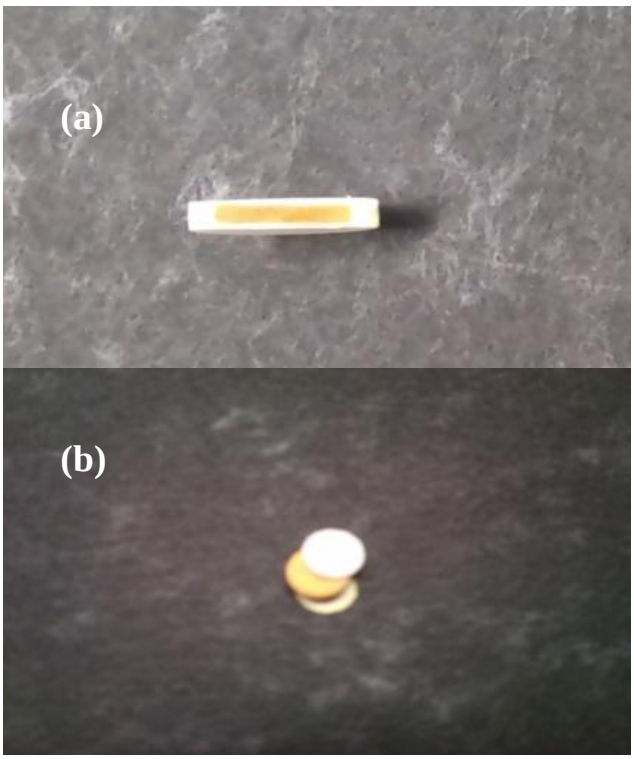

Figure 5.17 The cross-sectional area of the press coated tablet showing yellow inner core tablet in the middle containing riboflavin as an active surrounded by white outer barrier layer of HPMC E50LV (a), the sides of the press coated tablet were removed in such a way that only precise amount of top and bottom coatings covering inner core tablet could be isolated (b).

Through this procedure a ratio between top and bottom barrier layers was calculated. By changing the amount of the powder layer at bottom with respect to top layer, it was possible to achieve the equal amounts on both sides of the tablets. To form 50:50 ratios, it was found that around almost one third (33%) of the powder needed for bottom layer while the rest of two third (66%) would require for top.

Due to some technical reasons hydroxypropylmethyl cellulose E50LV (HPMC E50LV) from Shin-Etsu Chemicals was not availability, therefore an equivalent grade polymer was used from Dow Chemicals. The possibility existed that due to supplier change, the erosion profiles might change as well. Thus, the erosion was

again performed and % erosion was calculated as described in Section 5.2.1.1. Figure 5.18 shows the % erosion versus time for both E50LV-S (tablet weight 402mg±0.08, SA 375.3mm^2±0.12, VOL 357.4mm^3 and K_E 0.2097) and E50LV-D (tablet weight 405mg±0.007, SA 373.5mm^2±0.13, VOL 355.3mm^3±0.18 and K_E=0.1557).

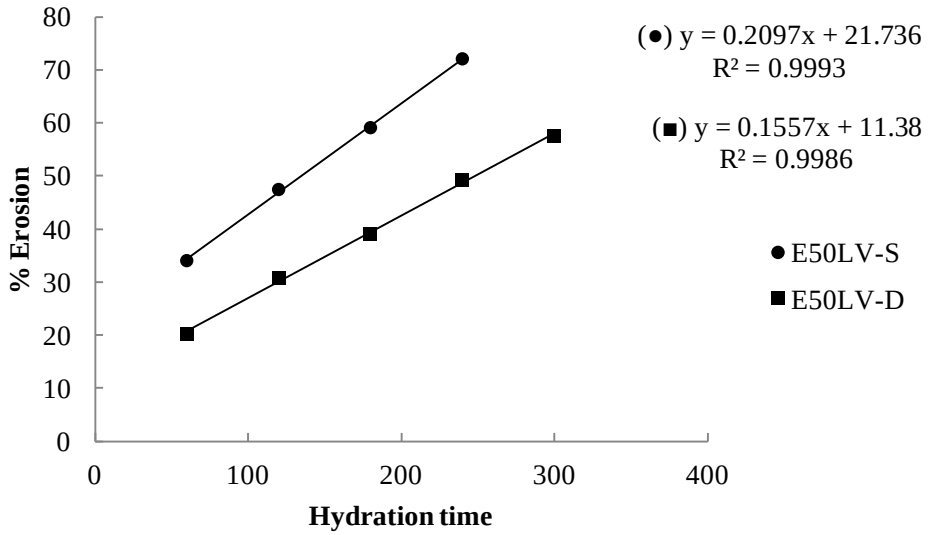

Figure 5.18 Comparison of % erosion versus time of HPMC E50LV from Shin-Etsu (●) and Dow Chemicals (■) with their linear regression equations.

The data indicate that the rate of erosion increased gradually with time; however E50LV-D eroded more slowly when compared to E50LV-S. As a result, the calculations for three lag times 180, 240 and 300 minutes were redone as explained in Section 5.2.1.2. As discussed above, it was always found that the original dimension of the inner core tablet was changed when it was compressed into a press coated tablet. The first step in the calculation method as described in Section 5.2.1.2 was to calculate the amount of the polymer located on the top and bottom surfaces of the inner core tablet. At the time when these calculations were developed it was not known that this phenomenon of expansion could occur in the inner core tablet, so the

calculations were based on the original diameter of the inner core tablet. Therefore, in the light of these new observations, the amount of HPMC E50LV-D barrier layer required for the top and bottom surfaces in the first step of the calculations method (Section 5.2.1.2) was recalculated taking into account the expanded diameter of the inner core tablet. However, the recalculated theoretical quantities of polymer required to achieve predicted lag times of 180, 240, and 300 minutes did not experimentally yield the required results due to presence of inadequate amount on the bottom and top surfaces. The reason for this is that at the time of press coating, inner core tablet do not have an expansion therefore the calculations on the basis of expanded inner core did not provide adequate amount, while calculations considering the non-expanded inner core tablet could not work because inner core tablet expanded during the process of compression coating. It is worth mentioning here that the amount of the polymer calculated for the top and bottom surfaces was experimentally found more crucial in controlling the lag time which was practically not possible without adjusting the total barrier layer amount. Therefore, following adjustment in total barrier layer amount was made using the old recalculated quantity as a reference value in order to achieve required predicted lag times: 295mg ((predicted lag time 180 minutes), 317mg (predicted lag time 240 minutes), 339mg (predicted lag time 300 minutes). Table 5.5 shows the dimensions (thickness and diameter) and the amount of the barrier layer used during compression coating for three press coated tablets at 180, 240 and 300 minutes predicted lag time.

Table 5.5 Physical dimensions of the three press coated tablets having three different predicted lag times and the amount of barrier layer (HPMC E50LV-D) used during compression coating (n=6).

Predicted press coated tablet lag time (minutes)	**180**	**240**	**300**
Diameter (press coated tablet (mm))	13	13	13
Total amount of barrier layer (mg)	295	317	339
Amount of bottom barrier layer (mg)	98	115	134
Amount of top barrier layer (mg)	197	202	205
Inner core diameter (before press coating (mm))	8	8	8
Thickness (press coated tablet (mm))	2.83±0.015	3.12±0.008	3.42±0.03

It was found that to achieve equal barrier layer coating for the top and bottom layers during press coating following ratios 34%:66%, 36%:64% and 40%:60% of HPMC E50LV-D were used to achieve 180, 240 and 300 minutes lag time, respectively.

Table 5.6 provides information regarding the dimensional changes in the inner core tablet before and after compression in three press coated tablets, with additional data on the amount of the polymer which was experimentally removed from the top and bottom surfaces of the inner core tablet after press coating and then weighed along their respective thicknesses and densities.

Table 5.6 Dimensional changes in the inner core tablet before and after press coating plus the amount of the polymer which was experimentally removed from the top and bottom surfaces of the inner core tablet after press coating and then weighed along their respective thicknesses and densities (n=10).

Predicted press coated tablet lag time (minutes)	**180**	**240**	**300**
Inner core thickness (before press coating (mm))	2.79±0.027	2.79±0.027	2.79±0.027
Inner core thickness (after press coating (mm))	1.98±0.85	2.12±0.02	2.20±0.02
Inner core diameter (after press coating (mm))	9.79±0.07	9.21±0.01	9.01±0.12
Weight acquired of bottom surface (mg)	30.51±1.09	38.95±0.43	45.81±0.48
Bottom surface thickness (mm)	0.42±0.02	0.51±0.01	0.59±0.01
Weight acquired of top surface (mg)	30.53±0.85	38.84±0.49	45.83±0.44
Top surface thickness (mm)	0.43±0.03	0.51±0.01	0.60±0.01
Total thickness of both surfaces (mm)	0.85±0.04	1.02±0.01	1.19±0.02
Density of both (top and bottom) surfaces (mg/mm^3)	0.95±0.03	1.14±0.02	1.20±0.04

The data indicate that the diameter and thickness of the inner core tablet changed before and after press coated compression. The diameter of the original inner core tablet was 8mm before compression which was changed to 9.79, 9.21, 9.01mm after compression in predictive press coated tablet having 180, 240 and 300 minutes lag time, respectively. The thickness of the inner core tablet was also reduced from 2.79mm to 1.98, 2.12 and 2.20mm in predictive 180, 240 and 300 minutes lag time tablets, respectively. This indicated that increasing the amount of the barrier layer decreased the deformation in the inner core tablet during press coating.

Table 5.6 also shows the amount of polymer acquired from bottom and top surfaces of the inner core tablet with their respective thicknesses at three predicted lag times 180, 240, and 300 minutes as 30.51/30.53mg (thickness 0.42/0.43mm),

38.95/38.84mg (thickness 0.51/0.51mm) and 45.81/45.83mg (thickness 0.59/0.60mm), respectively. The density of these top and bottom surfaces were found as 0.95, 1.14 and 1.20mg/mm^3 in three press coated tablets having predictive lag times 180, 240 and 300 minutes, respectively.

Figures 5.19, 5.20 and 5.21 show the percentage release of theophylline from six individual press coated tablets having predicted lag times at 180, 240 and 300 minutes, respectively.

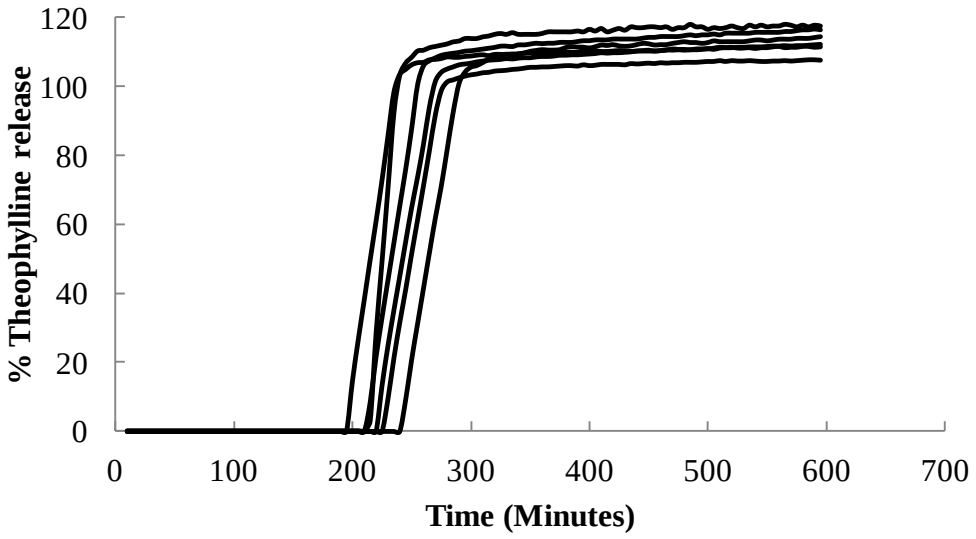

Figure 5.19 Percentage theophylline release from six individual press coated tablets (thickness 2.83mm±0.015, size 13mm) for predictive 180 minutes lag time using HPMC E50LV-D as a barrier layer coating.

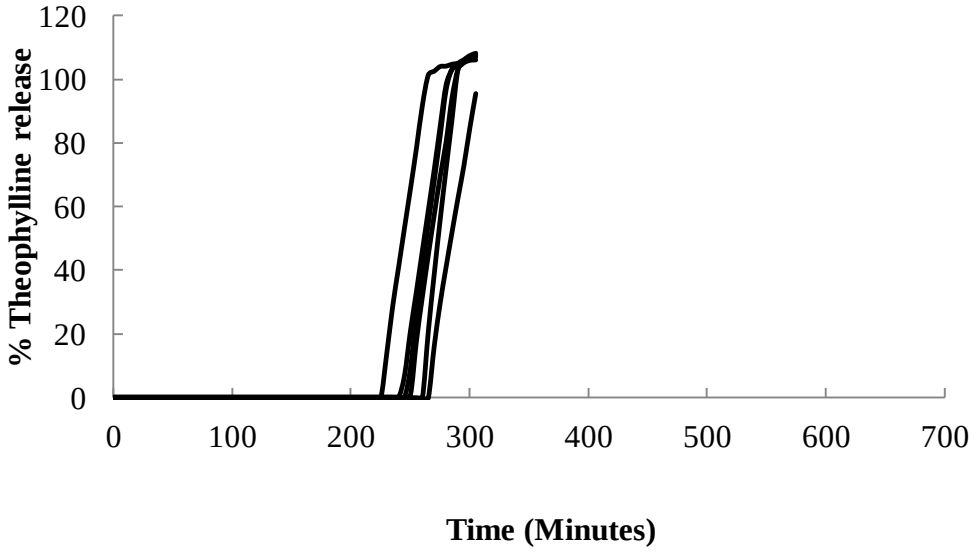

Figure 5.20 Percentage theophylline release from six individual press coated tablets (thickness 3.12±0.008mm±0.015, size 13mm) for predictive 240 minutes lag time using 317 mg of HPMC E50LV-D as a barrier layer coating.

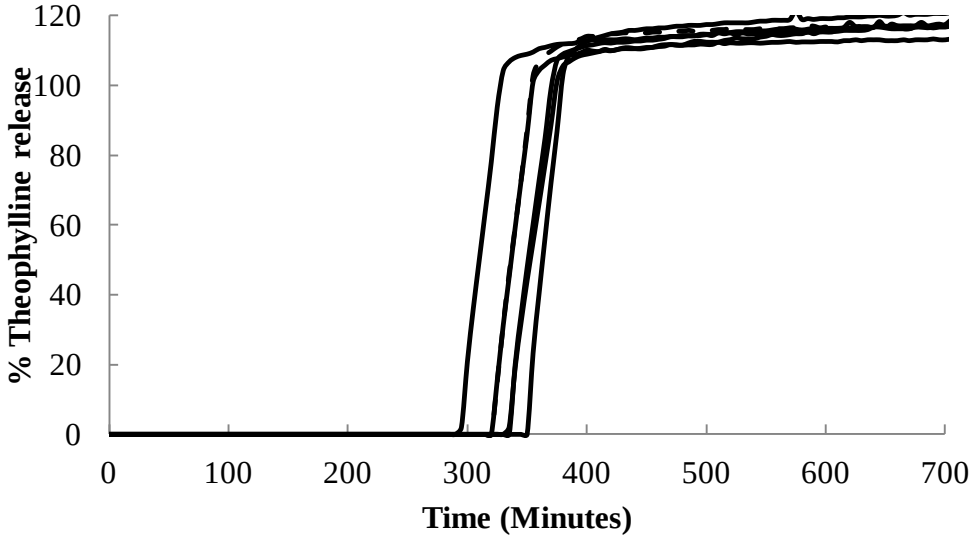

Figure 5.21 Percentage theophylline release from six individual press coated tablets (thickness 3.42±0.03mm±0.015, size 13mm) for predictive 300 minutes lag time using 339 mg of HPMC E50LV-D as a barrier layer coating.

The data in Figures 5.19, 5.20 and 5.21 indicate that the individual tablets did pulse at predicted lag times. Figure 5.22 shows the overall percentage release for these three selected time points.

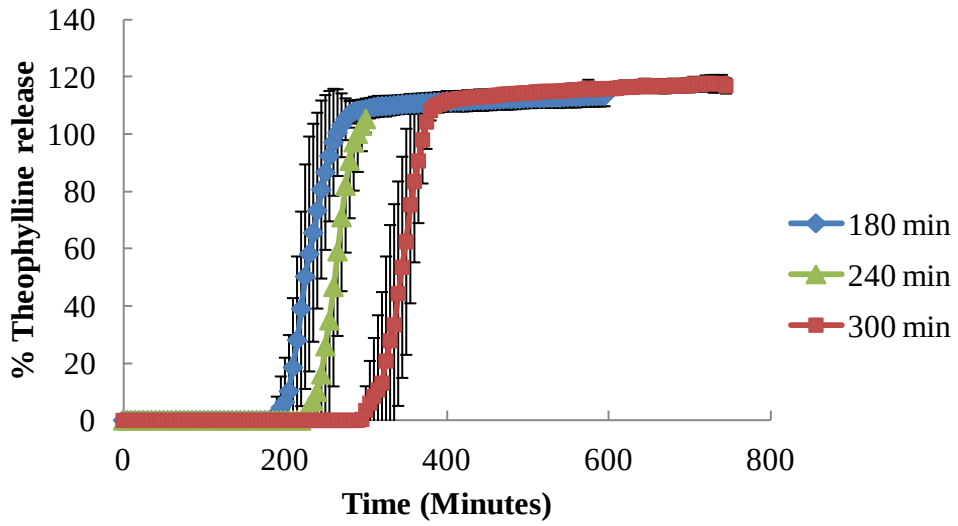

Figure 5.22 Cumulative percentage theophylline release from press coated tablets having HPMC E50LV-D as a barrier layer manufactured using the method described in Section 5.2.4 for predictive 180, 240 and 300 minutes lag time (n=6).

It is obvious from Figure 5.22 that actual release did follow the prediction pattern and tablets with a predicted lag time of 180mins, 240mins and 300mins displayed actual average release at 185mins, 230mins and 295mins respectively. The error bars in drug release profile shows the standard deviation.

Figure 5.23 shows that a reasonably good correlation existed between *in vitro* lag times and predicted values validating the method of calculation proposed in Section

5.2.1.2 based on erosion data, polymer true density, inverse of true density, surface area and volume.

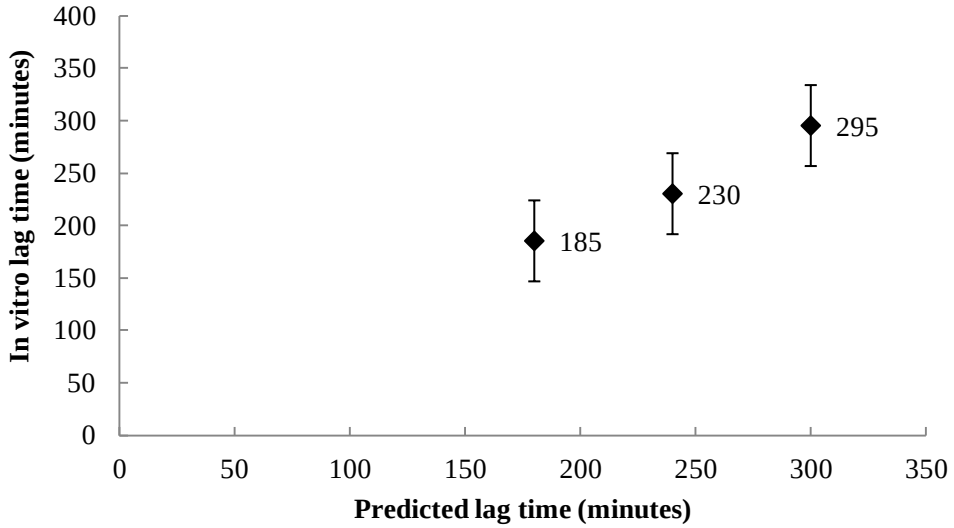

Figure 5.23 Correlation between lag times from *in vitro* theophylline release obtained during dissolution from three press coated tablets (n=6) with their corresponding predictive values.

It was discussed above that the density of polymer acquired from top and bottom surfaces increased as the predicted lag times (180, 240 and 300 minutes (Table 5.6)) increased in three press coated tablet. This means that the as the total amount of the barrier layer increased the polymer was more densely packed on top and bottom surfaces. It is known that the more densely the polymer is packed the more resistant it would be to hydration and erosion (Ozeki et al., 2004). This suggests that the lag time could be affected by both the amount and the density of the coated polymer.

Previous studies (Fukui et al., 2000b, Conte et al., 1993, Rujivipat and Bodmeier, 2010a, Ghimire et al., 2007) used 50:50 ratios for bottom and top layer as a standard to manufacture press coated tablets and the duration of the lag time was later controlled by amount or composition of the barrier layer. For instance, Fukui et al

(2000b) achieved different lag times either by changing different viscosities of hydroxypropyl cellulose (HPC) having constant amount (200mg) in the outer shell or by increasing the amount (160, 180, 200 and 220mg) of the Low-HPC (viscosity 8.5mPa.s) in the outer shell. In another study Conte et al (Conte et al., 1993) used different grades of HPMC erodible (E3, E5 and E50) and swellable (K4M and K100M) having fixed quantity in barrier layer (200mg for bottom and 200mg on top of inner core tablet) concluding that the increasing lag times from press coated tablets are achievable by increasing polymer viscosity. Ozeki et al., (2003), on the other hand mentioned the use of suitable amount of polymer coating for upper and lower layers so that the equal thicknesses in press coated tablets could be achieved using the newly developed one-step dry-coated tablet machine. However, there was no detail given on the actual amounts used during compression or the actual measured thicknesses which were achieved for top and bottom surfaces.

These examples illustrate that the required lag times can be accomplished by controlling either the amount or composition of the barrier layer. However, the work in this Chapter clearly indicated that the process of tablet press coating is quite intricate and complex. It requires more in depth understanding of the changes which occur to the inner core tablet during manufacturing. Additionally, the knowledge of the quantity and thickness of the coated polymer on the top and bottom of the inner core tablet was also found to be crucial, as small increase or decrease in coated polymer quantity can modify the lag time of the press coated tablet. An inner core tablet can be off set with respect to axial and radial direction in a press coated tablet. Other researchers (Liu and Cetinkaya, 2010, Ozeki et al., 2004, Ozeki et al., 2003) also emphasised the importance of concentricity of inner core in press coated tablet for reproducible results.

The predictive method developed here evidently is more simple, easy and reasonably accurate to predict the required lag time. The only laborious part was during manufacturing where the amount of the barrier layer covering the top and bottom of the inner core had to be removed skilfully in order to establish a 1:1 ratio to achieve equal barrier layer amount (thickness) which was achieved by varying the quantity

used for bottom and top layers. This step was essential so that the eccentricity of the inner core tablet could be minimised during the process of press coatings.

5.4 CONCLUSION

A direct relationship was found between SA/VOL ratio and erosion profiles of HPMC grades. The constant SA/VOL ratio was achieved using different tablet sizes (8mm and 13mm) which did not provide similar erosion profiles for HPMC E10MCR:E5LV (50:50) and E50LV. Due to this reason the first predictive method based on constant SA/VOL ratio was failed to predict accurately different lag times.

The second predictive method was developed using polymer erosion, true density, inverse of true density, volume and surface area values. In order to develop and successfully implement this type of calculation method it was necessary to characterise the factors like choice of barrier forming polymer, tablet size of the eroding polymer, selection of final tablet size, control over applied compression force, and ratio of the quantity of barrier layers. When half of the barrier layer quantity was used as bottom layer and remaining half on top of the centrally aligned inner core tablet, the thickness variations were observed for top and bottom surfaces. However, after achieving an equal ratio between top and bottom layers the *in vitro* dissolution revealed a good correlation between actual and predictive lag times. Additionally, it was noticed that the erosion data differ for same HPMC polymer grade from different manufacturer, therefore only one supplier should always be used for the entire experimental work.

It can be concluded that a predictable model with reasonable accuracy was developed using the erosion of polymer as a main predictor which could be used in future for pulsatile or colon delivery in press coated tablets.

CHAPTER 6

MAGNETIC RESONANCE IMAGING OF PULSATILE TABLETS

6.1 INTRODUCTION

Magnetic resonance imaging (MRI) is a widely used technique in the field of clinical diagnosis due to its ability to differentiate soft tissues. However, the application of MRI in non-medical fields has been growing due to the availability of micro-imaging accessories which can be attached with conventional nuclear magnetic resonance (NMR) spectrometer. An example of this is in the pharmaceutical sector, where formulations have been studied by imaging tablet hydration and subsequently its effect on dissolution and drug release (Melia et al., 1998, Richardson et al., 2005). It has also been used to investigate the underlying mechanisms controlling release from a pulsatile formulation (Sutch et al., 2003), and characterisation of push-pull osmotic controlled release system (Malaterre et al., 2009).

MRI is a complex technique based on the phenomenon and properties nuclear magnetic resonance (NMR), therefore the principle of NMR will be discussed first in detail. The nuclei of certain atoms such as ^{1}H, ^{13}C and ^{19}F, have a property of spinning or rotating around their axes (Robinson et al., 2005). The spinning of these charge particles or the circulation of charge creates magnetic moment along the axes of spin, or generates a nuclear dipole, thus these nuclei act like a tiny bar magnets. As a result, when an external magnetic field ($\mathbf{B_0}$) is applied to these nuclei, according to quantum mechanics, these nuclei must align themselves either with the external magnetic field (low energy level, more stable, ground state) or against it (high energy level, less stable, excited state) (Gennaro, 2005). Each direction of alignment is associated with an energy level. Only certain well-defined energy levels are permitted; that is, the energy levels are quantized. Hence the nucleus can become aligned only in well-defined directions relative to the magnetic field ($\mathbf{B_0}$) (Robinson et al., 2005). The transition among different energy level is only possible if an electromagnetic radiation having frequency equivalent to the frequency difference of

two energy levels (that is higher or lower state) is absorbed flipping the tiny bar magnet to the less stable excited state (alignment against the field) (Watson, 2005).

In general, the NMR can apply to any of several atoms, unless otherwise stated it is usually referred to proton (or ^{1}H) NMR. The charge nuclei due to its spin possesses angular momentum which is expressed by spin quantum number, *I*. The, *I*, value of an isotopes may vary by integral values 1, 2, 3 ... or half integral values 1/2, 3/2 ...9/2. An integral value of zero indicates no spin. Nuclei with an even number of proton and neutron exhibit zero spin number or no spin (e.g. ^{12}C, ^{16}O). Nuclei with an odd number of neutrons and protons have an integral value 1, 2, 3.... (e.g. ^{2}H, ^{10}B, ^{14}N) and nuclei with an odd mass number has spin quantum number of 1/2, 3/2.....9/2 (e.g. ^{1}H, ^{13}C, ^{19}F, ^{31}P). The nuclei having integral value greater than zero ($I > 0$) when placed in magnetic field will acquire number of orientations or number of energy levels equal to ($2I + 1$). The value of *I* for proton (^{1}H) is 1/2, so there will be two orientations or spin states as shown in Figure 6.1: (1) where the nuclei are in alignment with the external magnetic field (parallel orientation (α), low energy state), (2) where the nuclei are in alignment against the external magnetic field (anti-parallel orientation (β), high energy state).

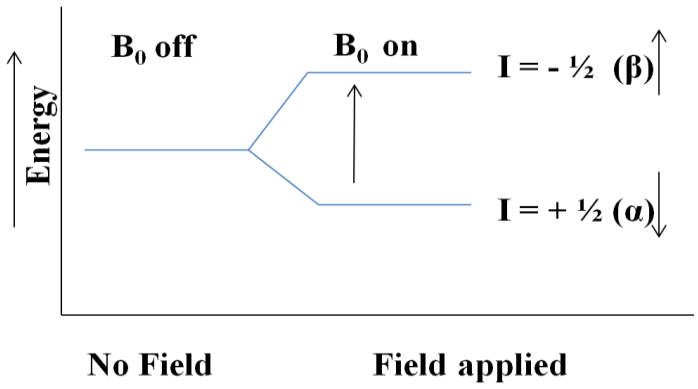

Figure 6.1 Orientation of nuclear magnets in an external magnetic field showing the ground (α) and excited states (β) in nuclear magnetic resonance (Gennaro, 2005).

It is worth noting that the energy value of these two states (low energy state and high energy state) can be calculated using the Larmor equation. An external source of electromagnetic radiation frequency (ν_1) causes the transition of the nuclear spins between the two energy states (or flipping). When the ν_1 frequency is tuned to the exact frequency value of the nucleus (ν_o) under study, a transition from the more stable α to the less stable β state can occur. These two states can be thought of as being in resonance and this, in part, represents the origin of the term nuclear magnetic resonance (Fifield, 2000). The energy difference between these spin states aligned with the field and against the field depends on the strength of the magnetic field applied. The greater the field strength the greater the energy difference

$$\Delta E = h\gamma \mathbf{B_o}/2\pi$$

Where

h = Planck's constant, γ is the magnetogyric ratio of a particular nucleus and $\mathbf{B_o}$ = applied magnetic field.

The excited nuclei return from the higher energy state to lower energy ground state via the process of relaxation. This process of relaxation is divided into two further processes and both processes contribute simultaneously: the spin-lattice (longitudinal) relaxation, T_1, and spin-spin (transverse) relaxation, T_2 (Melia et al., 1998).

The spin-lattice relaxation involves a transfer of nuclear energy to the energy of the lattice component as a result of transition to lower energy state. In any physical form the framework of molecules is referred as lattice. The components of lattice include transitional, vibrational and rotational energies of the molecules. There are varieties of magnetic fields present due to the presence of these various types of energies whose proper alignment with a precessing nucleus can cause transition to a lower energy state. The energy which releases due to transition to a lower energy state thus causes an increase in transitional, vibrational and rotational energies. The overall change of energy in the system is zero. This process is responsible for maintaining the nuclei in the lower energy state.

Spin-spin (transverse) relaxation involves the mutual exchange of energy between two proximal precessing nuclei. This type of relaxation helps to decrease the lifetime of the excited state nucleus (Rajabi-Siahboomi et al., 1994).

Figure 6.2 shows a basic NMR instrument with major component including sample, radio frequency (RF) transmitter, detector (RF receiver) and recorder or display device.

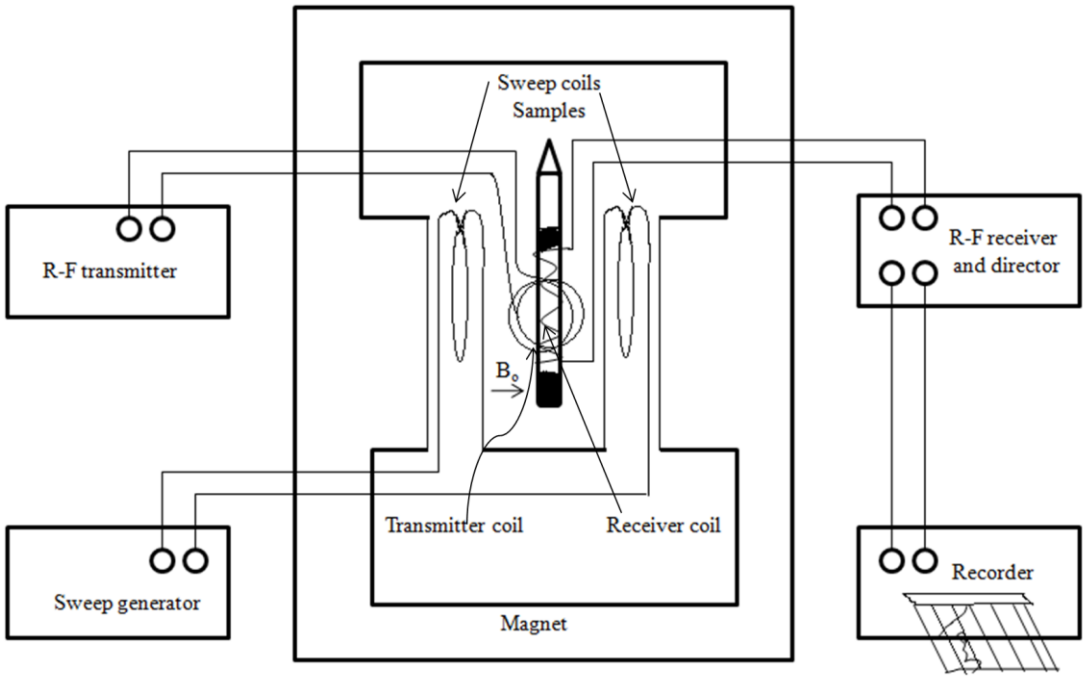

Figure 6.2 A schematic diagram of NMR spectrometer.

Either a permanent magnet or electromagnet can be employed in the NMR to supply $\mathbf{B_o}$. The RF transmitter is used to provide RF field from transmitter coil whose magnetic vector component moves in a plane perpendicular to the direction of $\mathbf{B_o}$. The RF field induces the transition from lower energy to the higher energy state. The flipping of the nuclei due to RF insertion induces a voltage in the RF receiving coil, whose axis is at the right angle to the axis of the transmitter coil and $\mathbf{B_o}$. This voltage

from the receiving coil is then amplified and observed in a recorder as a signal (Robinson et al., 2005).

If during the NMR acquisition another magnetic field is applied across the static magnetic field, it is possible to spatially encode the NMR signals to obtain magnetic resonance (MR) images. Unfortunately, NMR signals are inherently weak but can be increased in strength with increasing γ or $\mathbf{B_0}$. MRI is therefore applied to the sample containing high concentration of ^{1}H nuclei. In most applications, MRI is used to measure the distribution of water and at commonly used magnetic field strengths (0.05–18T) the frequency of the NMR signal is in the range 2–750MHz (Richardson et al., 2005).

In general, the intensity of the MRI image is dependent on the ^{1}H density which is related to water concentration, and also on T_1 and T_2 values, which are related to water mobility. The relaxations are dependent on the local molecular environment and provide extra information about the sample. Generally, T_2 relaxation is shorter for the sample with lower molecular mobility such as solid or viscous liquid therefore, the signals from the water bound in viscous gel decays faster (1-100msec) compared to the free water (seconds) (Rajabi-Siahboomi et al., 1994) as shown in Figure 6.3.

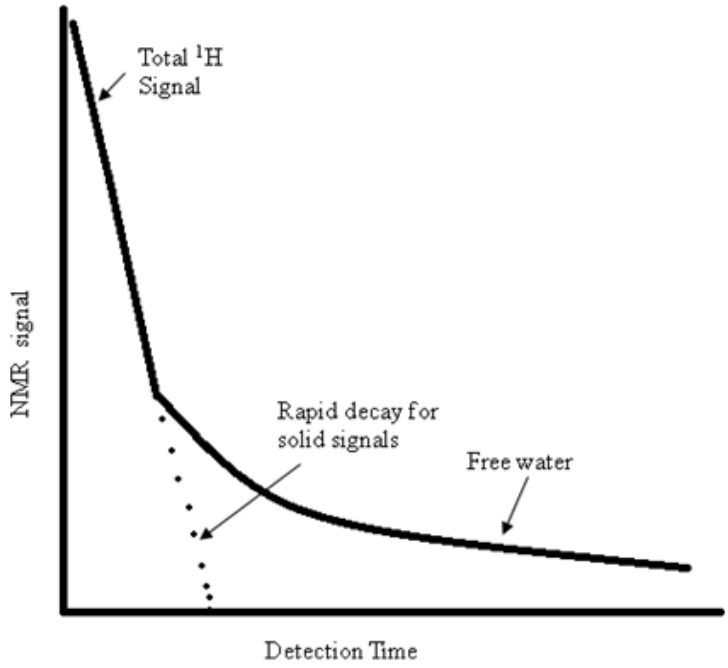

Figure 6.3 Schematic representation of NMR signal decay in liquid and solid.

In solids it is few tens of microseconds which are not enough for spatial encoding. As a result, most MRI studies have used T_1/T_2 'weighted' or contrast images to understand different features pertaining to water concentration and its mobility (Nott, 2010).

Baumgartner et al (2002) used T_1 and T_2 times to study the water distribution in hydrophilic gel made from cellulose ether having different substitution and molecular weights (hydroxypropyl cellulose (HPC), hydroxyethyl cellulose (HEC) and hydroxypropylmethyl cellulose K4M and K100M (HPMC)). They found that the polymer substitution is sensitive to relaxation rate 1/ T_1 but not to the molecular mass, while the rate $1/T_2$ was less sensitive to polymer distribution. By using these values they were able to calculate the number of water molecules bound to polymer repeating unit, which correlated well with polymer hydrophilic substitution. As an

example, MRI image for hydrating hydrophilic HPMC matrix tablet is shown in Figure 6.4.

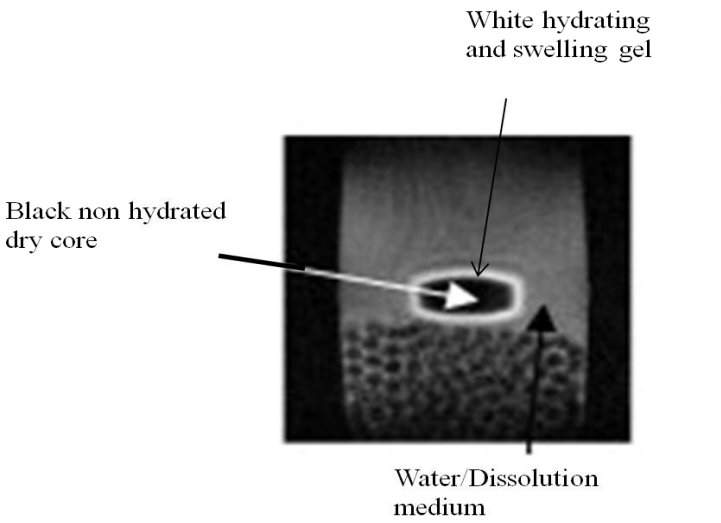

Figure 6.4 A typical cross section of magnetic resonance image of hydrated hydrophilic HPMC tablet indicating clear differentiation between hydrated gel and non-hydrated core during dissolution (Nott, 2010).

Dark or black area in the MRI image refer to low spin densities or short T_1 relaxation times, which are related to dry parts of the tablet. Bright white area of the tablet compared to the distilled water surrounding the matrix tablet may lead to the conclusion that the spin density (T_1) in this area is higher than the black area, but was much shorter than the T_1 of the free water. As the magnetisation of the free water in the medium, in contrast to the water in the tablet, was not able to return to equilibrium, the signal intensity for water inside the tablet increased although its spin density was lower. Thus it is possible to follow hydration characteristics and gel formation in hydrophilic matrix system more easily. In some other studies quantification of water ingress into the tablet and subsequent physical changes such as swelling and erosion were defined by a sharp gradient in signal intensity. For instance, a series of MRI studies were used to measure the swelling and water uptake

of tablets with cross-linked high amylase starch in order to investigate the effect of tablet sizes, initial diffusion and temperature (Baille et al., 2002, Malveau et al., 2002, Therien-Aubin et al., 2005). They observed that the water uptake and swelling depend on tablet size. Additionally, the swelling was found to be anisotropic (not identical in all direction), whereas water diffusion was almost isotropic (identical in all directions). They also found that the diffusion behaviour changed from Fickian to Case II diffusion with increasing temperature and attributed this effect to the gelatinization of starch and the pseudo-cross-linking effect of double helix formation.

The MRI signal intensity can be based on a number of sample and experimental parameters, some studies utilised the T_2 relaxation time and self-diffusion coefficients to obtain better distinction between the gel layer and the dissolution medium. Masazumi et al. (1998) used T_2 and self diffusion coefficient to characterise the diffusivity and mobility of the absorbed water on variety of water soluble, swellable cellulose derivative (HPC, HPMC and HPC 41) and they also observed different expansion in different directions due to compression of the original tablet.

The hydration and swelling mechanism of floating tablet formulation has also been studied by using MRI (Strübing et al., 2008). They monitored different phases regarding swelling and carbon dioxide which develop during hydration inside the floating tablet. Swelling processes started with an initially hydrated polymer film, followed by carbon dioxide development on the top side of the tablet directly on the surface of the tablet core leading to the observation of a dome shaped floating tablet. Continuing diffusion of hydrochloric acid inside the tablet led to a biconvex and swollen tablet with gas development on the top side as well as on the bottom side of the tablet core. The carbon dioxide inside the floating device expanded the tablet coat intensively, leading to the formation of a balloon shaped floating tablet. They observed that the process of formation of these above phases of swelling and gas development was much faster for samples with a lower Kollicoat® SR/Kollicoat® IR ratio and a lower coating level compared to higher Kollicoat® SR/Kollicoat® IR ratio.

MRI has been used to investigate hydration in a range of other dosage forms. The hydration processes within fast and slow release osmotic pump tablets have been qualitatively distinguished (Shapiro et al., 1996). Fahie et al. (1998) used MRI to

study the drug release processes by following the movement of water in and out of a complex matrix dosage form in which internal barriers were used to create zero order drug release characteristics. MRI images provided clear evidence that the porosity of these internal barriers affected release control, and this was crucial in optimising the dosage form for successful development. MRI has provided detailed understanding into the mechanisms of release from preliminary pulsatile capsules (Sutch et al., 2003). The basic designs consist of an insoluble capsule body coated with ethyl cellulose, sealed with a plug and containing an expulsion system together with the drug or dosage form to be released. Erosion, dissolution or expansion of the plug controls the lag time before release. The intention was that the tablet plug would slowly erode, providing a delay before water entered the capsule, triggering the swelling of the expulsion agent, and initiating release of the capsule contents. Through MRI it was found that the capsule coated with aqueous-dispersion ethyl cellulose released erratically and prematurely whereas the organic-solvent coated capsules provided a reliable timed pulse. MRI showed that in case of the aqueous coated capsule, the plug forms a particularly inefficient seal with the capsule body, and water is able to rapidly penetrate through this gap which did not allow the plug to sufficiently erode and subsequently build up a pressure inside the capsule wall causing the rupturing and premature drug release. In contrast, water penetrates the plug of the organically coated capsule in a controlled manner and the plug is slowly eroded allowing expulsion of the capsule contents in timely mannered.

Recent developments have enabled the integration of USP apparatus 4 with MRI instrument consists of a flow-through cell, inside the bore of the magnet for dissolution studies to measure the hydration rate and to visualise the release mechanism of commonly available tablets, as well as to provide a dedicated system for reproducible dissolution measurements. Fyfe et al., (2000) was first to incorporated a modified USP apparatus 4 flow-through cell design to study the hydration of HPMC and elementary osmotic pump tablets. UV spectroscopy was employed to measure the total drug released during the dissolution. Abrahmsen-Alami et.al (2007) constructed a small release cell with rotating disc aiming to be able to make quantitative measurements of polyethylene oxide tablet concentration during hydration, swelling and erosion processes under conditions that simulate

stirring. Nott (Nott, 2010) recently published the results describing the dissolution of a chloropheniramine drug loaded gel matrix tablet using a bench-top MRI system incorporating a standard USP 4 dissolution apparatus. Additionally, the dissolution medium was passed to a UV analyser for online drug content analysis thereby enabling a direct comparison of quantitative drug release from the UV results with the swelling behaviour of the tablet from the MRI images.

In this Chapter, MRI is used to follow the routes and timescale of hydration within press coated tablets which were made according to the novel predictive model presented in Section 5.2.1.2 and 5.2.4. The aim is to understand the internal processes and sequence of events that underlie the process of hydration, swelling, gelling and eventually a pulse release from these pulsatile release tablets.

6.2 METHODS

6.2.1 Manufacture of inner core theophylline tablets

Inner core theophylline tablets weighing 200mg and containing theophylline, Avicel, lactose, magnesium stearate and potato starch were manufactured using an IR press with an 8 mm flat face round punch and die at a compression force of 3 ton as described in Section 5.2.2.

6.2.2 Manufacture of press coated tablets

The press coated tablets having predicted lag time of 3 hour (PLT-3) and 5 hour (PLT-5) were manufactured according to the method detailed in Section 5.2.4. Briefly, almost one third (33%) of the required powder (HPMC E50LV) was placed in 13mm die an immediate release 8mm flat faced theophylline inner core tablet (200mg) was then placed centrally on the powder bed. The remaining two third (66%) was distributed on top of the core tablet and compressed at 8 ton.

6.2.3 Sample preparation and set-up for MRI studies during tablet dissolution

Each tablet (PLT-3 or PLT-5) prepared above in Section 6.2.2 was individually mounted radially on flat plastic platform accessory as a part of USP 4 type flow through cell using epoxy glue (Figure 6.5a). The platform including mounted tablet was inserted in USP 4 type flow through cell (Figure 6.5b) which was later introduced into micro imaging probe (Figure 6.5c). The RF connector was attached with micro imaging probe (Figure 6.5d) and the whole assembly was carefully inserted in NMR spectrometer (Figure 6.5e) to acquire MR images.

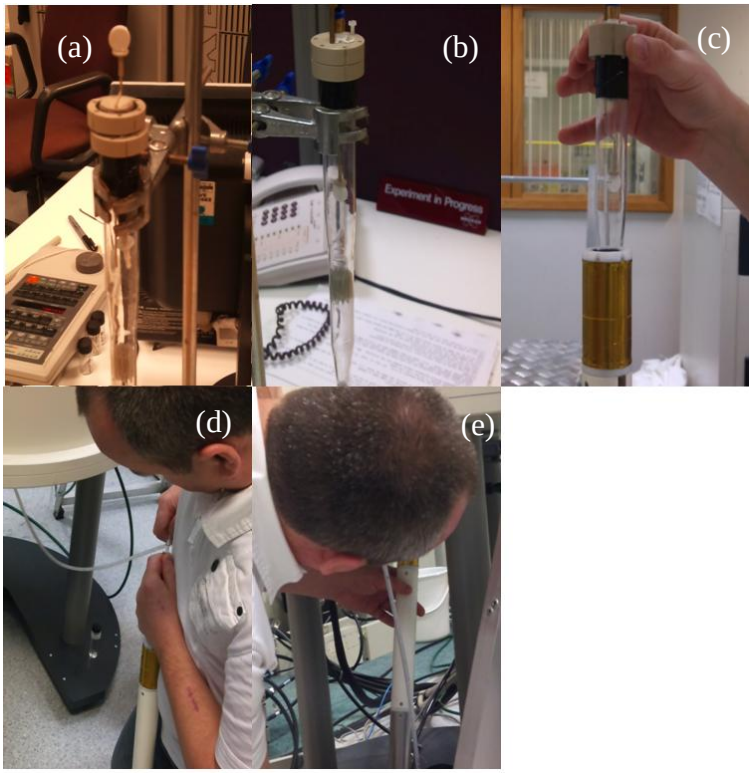

Figure 6.5 Different steps before the start of MRI data acquisition (a) mounting of press coated tablet on flat plastic platform, (b) assembled USP 4 type flow through cell with press coated tablet, (c) insertion of USP 4 apparatus in micro imaging probe, (d) attachment of RF connector with probe and (e) introduction of probe along USP 4 apparatus in NMR spectrometer.

The MRI data was acquired using NMR spectrometer (Figure 6.6) fitted with micro imaging probe (the Micro 2.5 probe having modular components: gradient system, probe body (with variable temperature fittings), and exchangeable RF-inserts). The software used for data acquisition was Power Vision 4.0.

Figure 6.6 Bruker Avance 400 NMR spectrometer along with micro imaging probe for MRI experiments

Theophylline release was continuously monitored every 30 seconds in deionised water used as a dissolution medium using an automated Unicom UV-4 spectrophotometer attached to a USP 4 type dissolution flow through cell assembly (Figure 6.7).

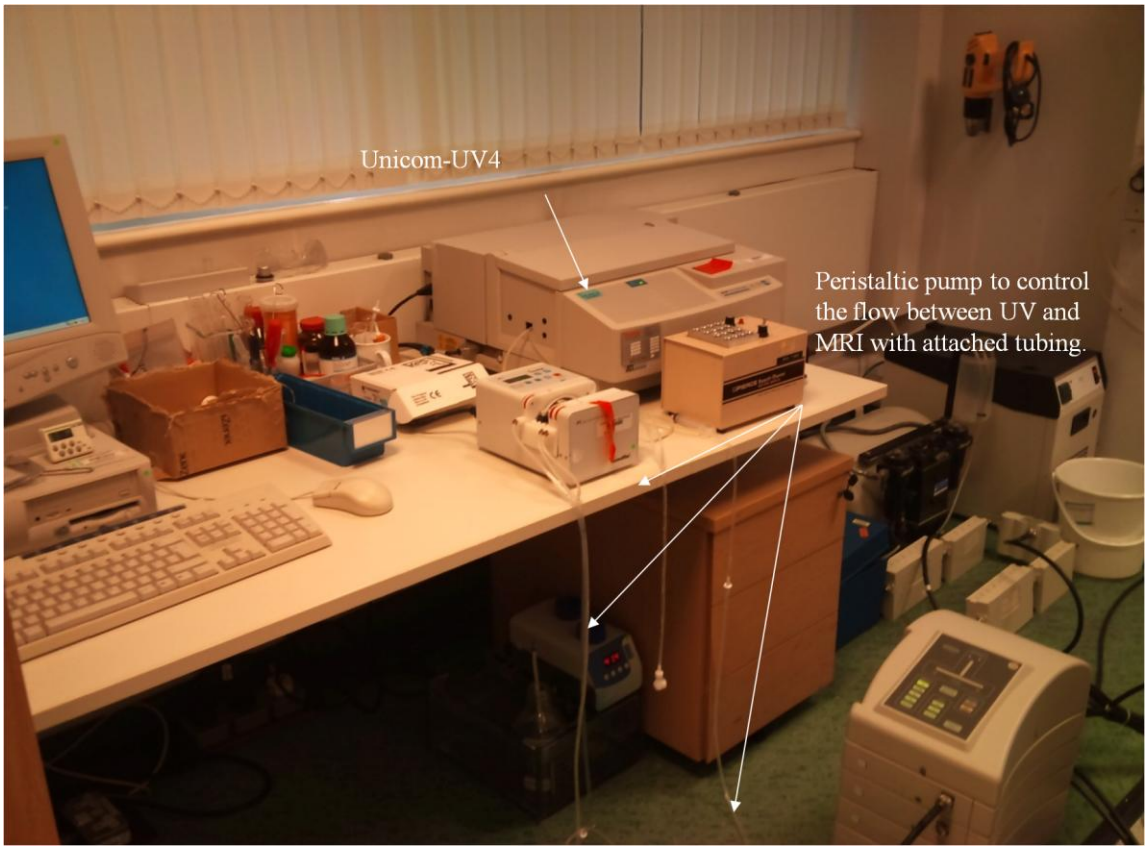

Figure 6.7 The Unicom-UV4 spectrometer attached to peristaltic pump and USP 4 type dissolution apparatus through connected plastic tubing for UV data acquisition.

A flow rate of 15ml/min through the MRI and 7.5ml/min through a UV cell of 1cm path length was used at 272 nm wavelength. Dissolution was terminated after observing the pulse or up to maximum of 900 minutes dissolution time.

To perform MRI experiments a single echo multi-sliced protocol was used with an echo time of 8 millisecond and recycle delay of 1 second. The images were acquired with a field of view of 2.5cm. The images were taken in 16 consecutive slices horizontally and vertically with no space between them and a slice thickness of 1mm with a matrix size of 256 × 256 pixel resulting in total image time of 4 minutes and 16 second.

Figure 6.8 shows the MR images taken at 0 minute and 130 minutes hydration time illustrating that the NMR spectrometer acquires the images from the bottom and the top of the tablet in 16 consecutive slices. In order to calculate the changes in tablet diameter, gel thickness and non-hydrated core thickness, the horizontal image slice number 11 was used as a representative image for each time point.

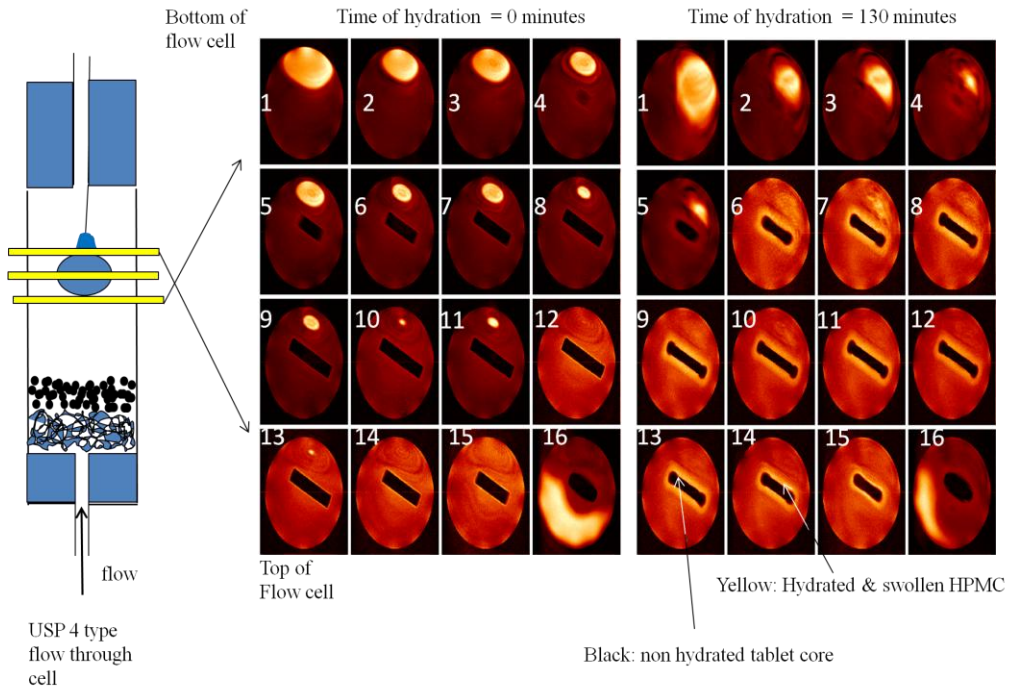

Figure 6.8 The 16 consecutive horizontal slices of the press coated tablet obtained during single MRI acquisition showing the images taken at top and bottom of the USP 4 type cell and also illustrating visibly demarcated yellow hydrated outer swollen layer and non hydrated black inner core in images acquired at 130 minutes hydration time which is absent in images acquired at 0 minute hydration time.

The boundary between the gel layer and the dissolution media was defined by varying the image intensity to highlight the tablet for a series of images until the gel layer becomes so diffuse that it becomes difficult to define; in practice, this was a narrow window. The boundary between hydrated and non-hydrated regions was chosen by using the image intensity that was half way between the highest (gel) and the lowest (non-hydrated core) intensities for the first image, which was used throughout the series. Gel thickness was calculated by measuring the distance between the gel layer and dissolution medium boundary and the gel layer and non hydrated core boundary (Figure 6.9).

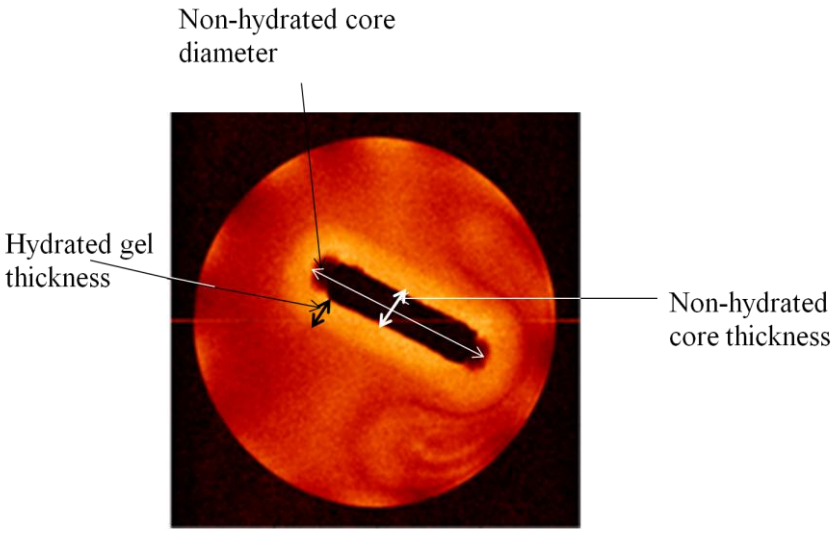

Figure 6.9 An MRI image illustrating the measurements for thickness and diameter in non-hydrated core plus the thickness measurements in hydrated gel.

The measurements for apparent non-hydrated core in MRI image were used to calculate the inner core and diametric thicknesses as shown in Figure 6.9. As discussed earlier in Section 6.1 that MRI signal (or ^{1}H signals) decay faster in solids compare to liquids and gels. Unless, the whole barrier layer coating is fully hydrated it would be very hard to differentiate between non-hydrated inner core tablet and non-hydrated barrier layer as they both appear as a black rectangle (Figure 6.9). Therefore, the term "apparent non-hydrated core" was used as a collective term throughout this Chapter which encompass the non-hydrated state of the barrier layer plus inner core tablet. The time taken by the tablet to indicate the disintegration which corresponds to the collapsing of the gel layer during MRI imaging was considered as MRI lag time. Physical dimensions of PLT-3 and PLT-5 press coated tablets were also calculated on six separate tablets using the digital calliper.

6.3 RESULTS AND DISCUSSION

6.3.1 PLT-3 press coated tablet

PLT-3 press coated tablet having HPMC E50LV as an outer barrier layer coating and an inner core tablet containing theophylline as an active ingredient with an expected lag time of 3 hours (according to the *in vitro* dissolution studies as described in Section 5.3.4) were imaged during hydration using MRI. Table 6.1 details the size and dimensions of PLT-3 press coated tablet and physical changes in immediate release inner core tablet dimensions before and after press coating.

Table 6.1 Physical dimensions (mean ± standard deviation) of PLT-3 press coated tablet and theophylline inner core tablet before and after press coating.

Diameter (press coated tablet (mm))	**13**
Thickness (press coated tablet (mm))	2.85±0.015
Inner core diameter (before press coating (mm))	8
Inner core thickness (before press coating (mm))	2.79±0.027
Inner core thickness (after press coating (mm))	1.98±0.85
Inner core diameter (after press coating (mm))	9.79±0.07
Total thickness of barrier layer (mm)	0.87±0.04

Figure 6.10 shows a series of MRI images illustrating that at 0 minute the tablet was present as a black rectangle showing no sign of water ingress around it however, a clear discrimination was observed between swollen hydrated gel layer and non-hydrated core as the hydration process progressed to the later stages.

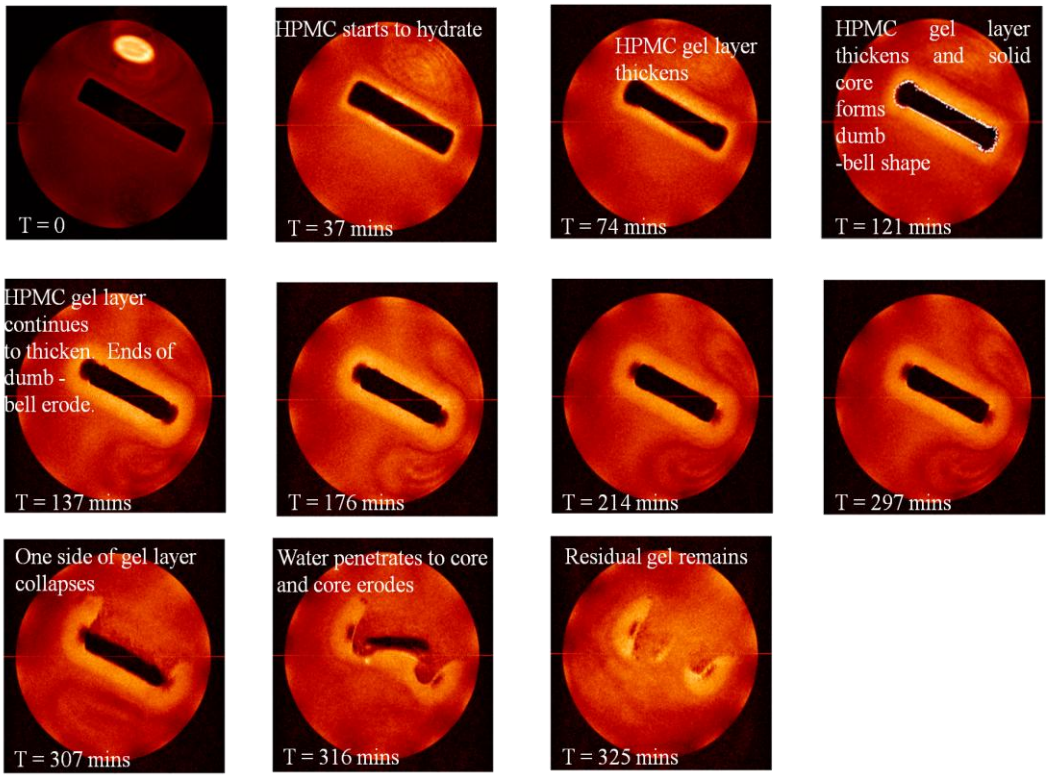

Figure 6.10 Series of MRI images acquired during 325 minutes dissolution time performed in USP 4 type flow through cell for press coated tablet with expected predicted lag time 3 hours containing HPMC E50LV as an outer barrier layer and theophylline as an active ingredient in the inner core tablet (PLT-3 tablet diameter: 13mm, thickness 2.85mm).

Initially the HPMC present in the barrier layer started to hydrate and developed a thick gel layer which continued to grow progressively over a period of 297 minutes hydration time. It was observed that after 300 minutes hydration time (Figure 6.10) the gel layer from one side of the tablet started to collapse which eventually allowed the dissolution medium to penetrate and completely dissolve the inner core tablet.

The appearance of dumb-bell shape, which could be observed in MR images (Figure 6.10) and also illustrated in Figure 6.11 as an enlarged image, indicating that the dry core of the press coated tablet expanded predominantly in axial direction. This effect was also observed by other researchers (Rajabi-Siahboomi et al., 1994, Melia, 1998) and will be discussed later in more detail with reference to gel thickness.

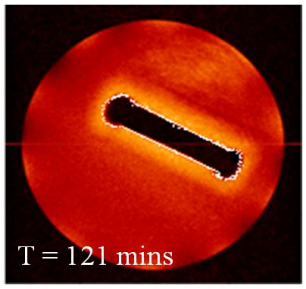

Figure 6.11 An enlarge MR image at 121 minutes dissolution time from Figure 6.10 illustrating the appearance of dumb-bell shape as a white dotted line around non-hydrated core.

MRI images can also be used as a quantitative tool to quantify the changes in gel thickness and inner core/non-hydrated core in formulation during the process of the hydration (Rajabi-Siahboomi et al., 1994, Tajarobi et al., 2009, Nott, 2010, Mikac et al., 2010). The change in diameter and thickness of apparent non-hydrated tablet core was quantified using the method described in Section 6.2.3 and calculated values are given in Table 6.2.

Table 6.2 The calculated values of the diameter and thickness of the apparent non-hydrated core tablet and hydrated gel layer for PLT-3 press coated during MRI hydration study.

Time (minutes)	Non-hydrated core diameter (mm)	Non-hydrated core thickness (mm)	Gel thickness (mm)
0	13.1	2.86	0
30	12.8	2.71	0.66
60	12.7	2.49	0.87
90	12.6	2.23	1.14
120	12.6	2.19	1.36
150	12.5	2.14	1.57
180	12.3	2.12	1.68
210	12.1	2.1	1.79
240	12	2.1	1.85
270	11.8	2.05	1.9
297	11.5	2.01	1.76
307	11.1	1.96	1.71

It is noticeable that the diameter and thickness of the non-hydrated core were reduced from 13mm to 11.1mm and 2.86 to 1.96mm, respectively while the thickness of the hydrated gel was increased from 0 to 1.76mm over a 307 minutes hydration time. Figure 6.12 shows the relationship between apparent non-hydrated tablet core diameter for PLT-3 press coated tablet with time.

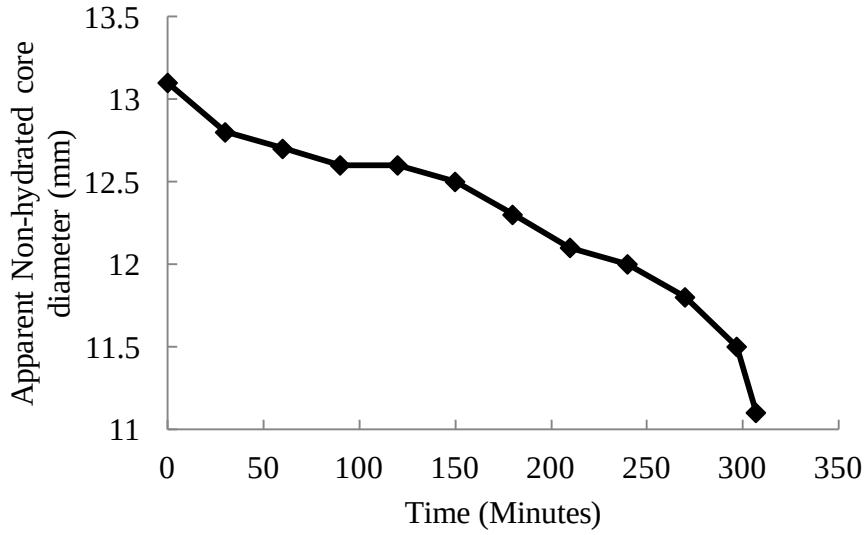

Figure 6.12 Changes in diameter of the apparent non-hydrated core during MRI hydration study for PLT-3 press coated tablet.

The diameter of the apparent non-hydrated tablet core was steadily reduced from 13mm to the point where no further reduction was observed (11.1mm) due to the pulse as observed at 307 minutes in MRI images as previously shown in Figure 6.10. The diameter of the non-hydrated core was 11.1mm at 307 minutes hydration time slightly higher than the diameter of the deformed inner core tablet (9.79mm, Table 6.1) for PLT-3 press coated tablet. MRI image (Figure 6.10) at 307 minutes also indicate that the PLT-3 press coated tablet was not fully hydrated in radial direction when pulse was observed which could be the reason for the slightly higher value for inner core diameter during MRI imaging.

Figure 6.13 shows the thickness of the apparent non-hydrated core over the period of hydration time.

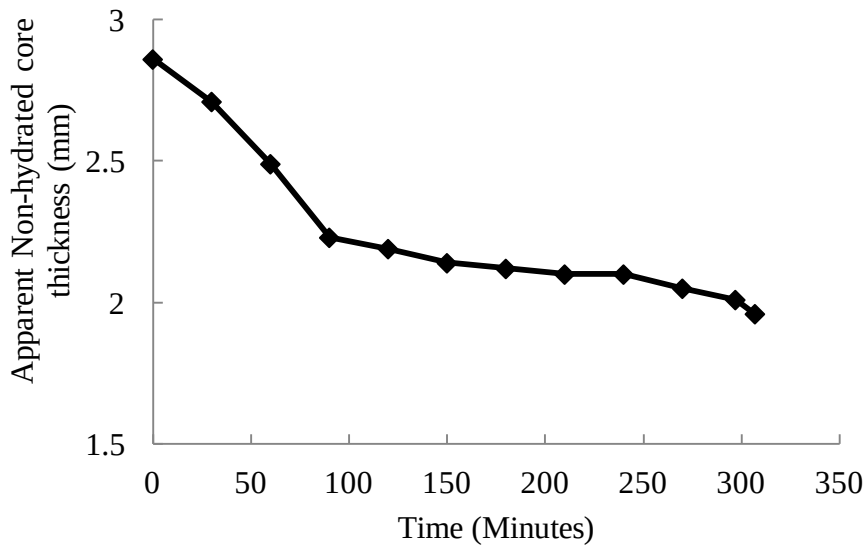

Figure 6.13 Changes in the thickness of apparent non-hydrated tablet core over hydration period in PLT-3 press coated tablet.

The apparent non-hydrated core thickness (2.86mm) was initially declined gradually (visually this effect can also be observed in MRI images in Figure 6.10) which then attained a plateau without further reduction (1.96mm) until a pulsatile release was achieved. The value of non-hydrated core tablet thickness at the time of pulse was around 1.96mm which is in close agreement with the mean reported value of inner core tablet thickness 1.98mm±0.85 (Table 6.1) in PLT-3 press coated tablet. This indicates that the outer barrier layer made of HPMC E50LV was fully hydrated (mostly in axial direction) at the time of pulse. The reduction in the size of the non-hydrated core thickness could be attributed to the hydration of the outer barrier layer in inward direction. These results are in concordance with previously published results where the dry core of the polyethylene oxide (PEO) tablet during hydration using MRI was found depleting in size with time (Abrahmsén-Alami et al., 2007).

Figure 6.14 shows the thickness of the outer barrier gel layer with time for PLT-3 press coated tablet.

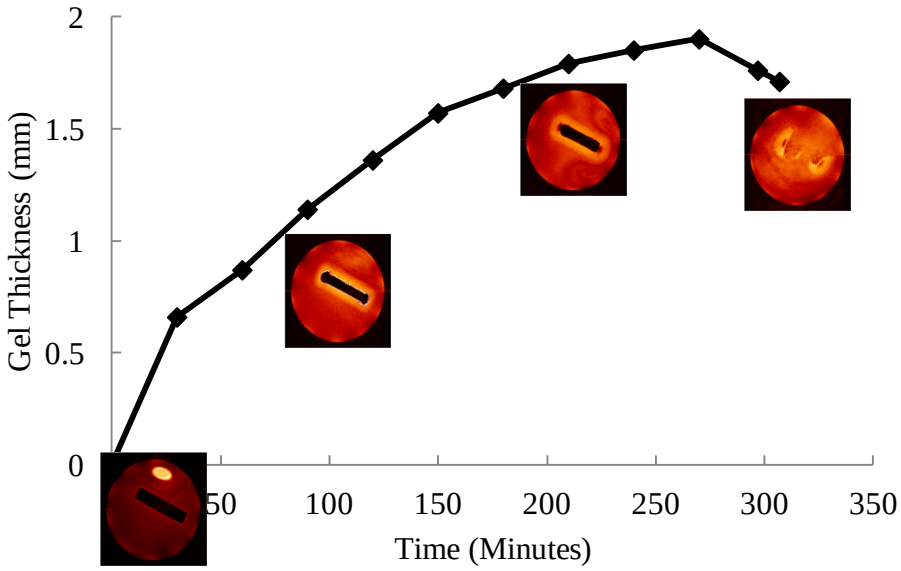

Figure 6.14 The change in outer barrier gel layer thickness over the hydration period in PLT-3 press coated tablet. (MRI images are presented for further clarification).

The thickness of the hydrating gel layer increased steadily until it achieved a constant level, following which it started to reduce until the burst was observed. As water started to ingress in PLT-3 press coated tablet more and more barrier layer made of HPMC E50LV become hydrated and formed a swollen gel layer due to inward water movement. However, decline in swelling process could be attributed to the unavailability of further barrier layer which marked the start of the inner core tablet plus the process of erosion. Other researchers also reported that with increase hydration time the gel thickness increases to point where no additional increase in thickness is possible indicating that the matrix system is fully hydrated followed by decrease in gel thickness due to gel erosion (Rajabi-Siahboomi et al., 1994, Abrahmsén-Alami et al., 2007, Tajarobi et al., 2009).

As discussed in Section 3.5.3 that the changes in gel layer thickness usually takes three stages i.e. initial increase due to polymer swelling, continuance of steady gel layer between erosion and diffusion front and disappearance of gel layer once the dry core is fully hydrated. Colombo et al., (2000) described that the maintenance of

constant gel layer is a crucial phenomenon to achieve drug release in zero order kinetics from modified release dosage forms. Results presented here also suggest that the gel formation and its steady maintenance is an important requisite to achieve desired benefits in pulsatile delayed release formulations of this type.

The dimensional changes of the whole tablet matrix, PLT-3 press coated tablet are shown in Figure 6.15.

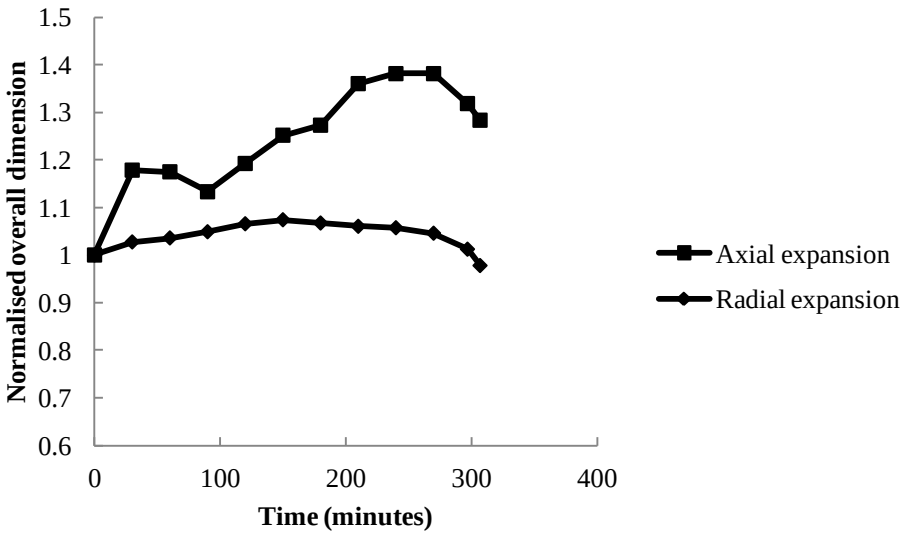

Figure 6.15 Normalised overall dimensional changes (overall dimension at time (t) divided by dimension of the dry tablet) in PLT-3 press coated tablet during hydration.

PLT-3 showed slightly higher axial swelling compared to radial swelling. An expansion of over 128% in axial direction was recorded over a hydration period of 307 minutes (Figure 6.15). Radial swelling occurred to a less extent, approximately 97% over a hydration period of 307 minutes (Figure 6.15).

Anisotropic swelling of HPMC tablets in axial and radial direction has also been discussed by other researchers (Rajabi-Siahboomi et al., 1994, Gao et al., 1996). For

example, Rajabi-Siahboomi et al., (1994) demonstrated that in HPMC tablet an expansion of 300% was observed in axial direction over a 2 hour hydration time compared to only 150% expansion in radial direction over a same period. During tablet compression stresses may induce in HPMC tablets in various directions and this may appear prominent during swelling/erosion behaviour (Abrahmsén-Alami et al., 2007). The release of these compression stresses in axial direction might have caused the large increase in tablet size in axial direction (Rajabi-Siahboomi et al., 1994) due to which normalised tablet dimension with respect to dry tablet showed more expansion in axial direction (Figure 6.15). These results are consistent with previously reported studies on anisotropic expansion in axial direction (Rajabi-Siahboomi et al., 1994, Gao et al., 1996, Abrahmsén-Alami et al., 2007, Tajarobi et al., 2009). The reduction in apparent non-hydrated tablet core size (Figure 6.13) and higher expansion in axial direction (Figure 6.15) in PLT-3 press coated tablet might have led to the formation of dumbbell shape in MRI images (Figures 6.10 and 6.11).

Some researcher (Abrahmsén-Alami et al., 2007, Tajarobi et al., 2009) despite observing axial expansion did not detect dumbbell or concave shape from hydrophilic tablet matrixes rather what they observed was more or less the shape of a tear or drop. Abrahamsen-Alami el al., (2007) and Tajarobi et al., (2009) both used rotating disc method (where a disc was attached on one side with plastic tube and on the other side hydrophilic tablet (HPMC or PEO) was attached with the help of impermeable water glue) capable of rotation at different speed mimicking the stirring condition. They attributed their tear/drop shape to three factors; uni-axial stress relaxation in axial direction, higher shear forces exerted on the tablet surface from the radial direction during stirring (100 and 200rpm) and higher impact of the gravity in the axial direction due to higher water content in the gel. However, no such effect was observed in current study as the flow of the dissolution medium was very slow (16 ml/min through USP 4 cell) compared to their 100 or 200 rpm rotation speed used in previous studies.

As described in Section 6.2.3 that the theophylline release from inner core tablet was continuously monitored through an automated UV-spectrophotometer attached to a

USP 4 type dissolution flow through cell assembly. Figure 6.16 shows the UV data acquired during MR imaging.

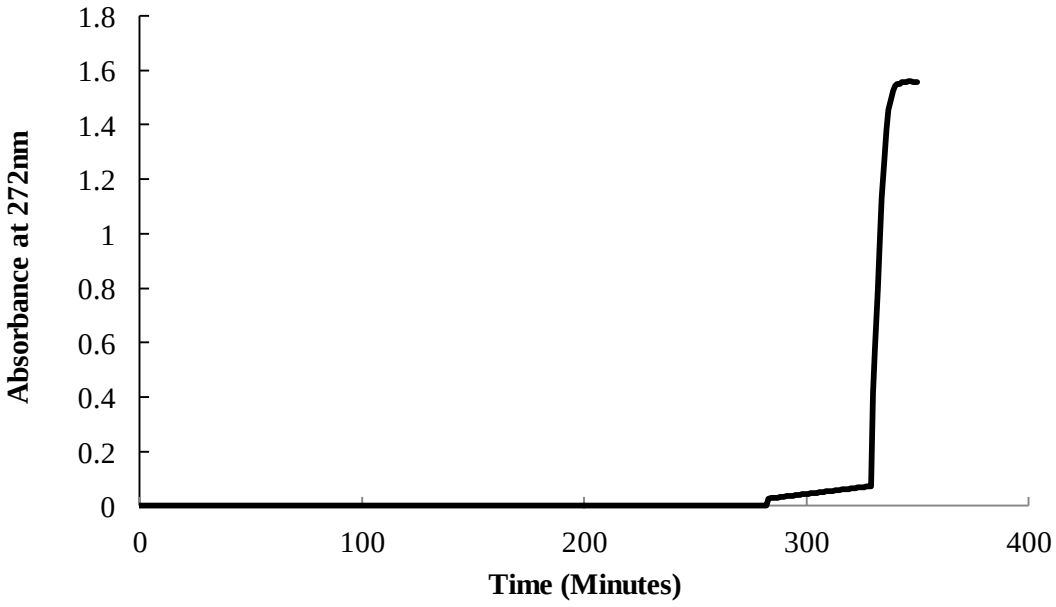

Figure 6.16 The UV absorbance obtained during MRI using deionised water as dissolution medium for PLT-3 press coated tablet showing a pulse release at 307 minutes having theophylline as an active in the middle core and HPMC E50LV in the barrier layer.

There was substantial lag time of 307 minutes before the actual pulse was observed in PLT-3 press coated tablet. Theophylline inner core was manufactured as an immediate release tablet so it was anticipated that the core would release its content immediately after the collapse of the outer barrier layer. Figure 6.16 also shows that the inner core was rapidly disintegrated thereby yielding a pulse indicating that the release profile of the theophylline inner core tablet was not influenced by the coating property of the HPMC E50LV. Conte et al., (1993) also reported the pulse release of the diltiazem from immediate release inner core once the E50 barrier coating was

cleared by the dissolution medium. The lag time (307 minutes) obtained with UV data was almost in concordance with the gel collapse time (307 minutes) observed during MR imaging (Figure 6.10).

It was expected that the lag time during MRI experiments would correspond to the *in vitro* dissolution data (Section 5.3.4) however; the PLT-3 press coated tablet pulse time was found longer during MRI in contrast to the predicted 3 hours lag time which could be attributed to the slow flow rate (15ml/min) of dissolution media (deionised water) through the MRI, which was necessary in order to obtain good quality images. Marcela et al., (2003) found slower dissolution rates for albendazole generic tablets in USP 4 apparatus at 16ml/min compared to their dissolution rates in USP 2 apparatus at 50 rpm paddle speed. They explained this slow release with reference to the differences in hydrodynamics conditions presented in two different apparatuses. In USP 4 apparatus, no stirring mechanism is involved this means the dosage form plus drug particles are continuously expose to homogeneous and non-turbulent laminar flow causing a slow dissolution rate. In contrast, in USP 2 method the turbulent solvent flow in the vessel associated with stirring mechanisms imparts variable degrees of physical abrasion of the solids, due to non-homogeneous shear rate of transfer over the surface of the particles, thus enhancing the dissolution rate (Abdou, 1989). Gao (2009) found that with the paddle method using 50 and 100 rpm paddle speed, the dissolution rates in non-disintegrating salicylic acid tablets were 0.20% and 0.28%/min, respectively, and with the flow-through method (USP 4), the dissolution rates were 0.08% and 0.11%/min at flow rates of 4 and 8 ml/min.

These examples clearly illustrate that the shear forces present in these two dissolution apparatuses were significantly different (higher in USP 2 and lower in USP 4) due to this reason the PLT-3 press coated tablet did not pulse at expected 3 hours dissolution time.

6.3.2 PLT-5 press coated tablet

The general behaviour shown by the PLT-5 press coated tablet was similar to that of PLT-3. The size and dimensions of PLT-5 press coated tablet and physical changes in immediate release inner core tablet dimensions before and after press coating are given Table 6.3.

Table 6.3 Physical dimensions (mean ± standard deviation) of PLT-5 press coated tablet and changes in theophylline inner core tablet before and after press coating.

Physical dimension	**PLT-5 press coated tablet**
Diameter (press coated tablet (mm))	13
Thickness (press coated tablet (mm))	3.42±0.03
Inner core diameter (before press coating (mm))	8
Inner core thickness (before press coating (mm))	2.79±0.027
Inner core thickness (after press coating (mm))	2.20±0.02
Inner core diameter (after press coating (mm))	9.01±0.12
Total thickness of both sides (mm)	1.19±0.02

Figure 6.17 shows a series of MRI images for PLT-5 press coated tablet acquired during 409 minutes dissolution time performed in USP 4 type flow through cell with expected predicted lag time 5 hours containing HPMC E50LV as an outer barrier layer and theophylline as an active ingredient in inner core tablet.

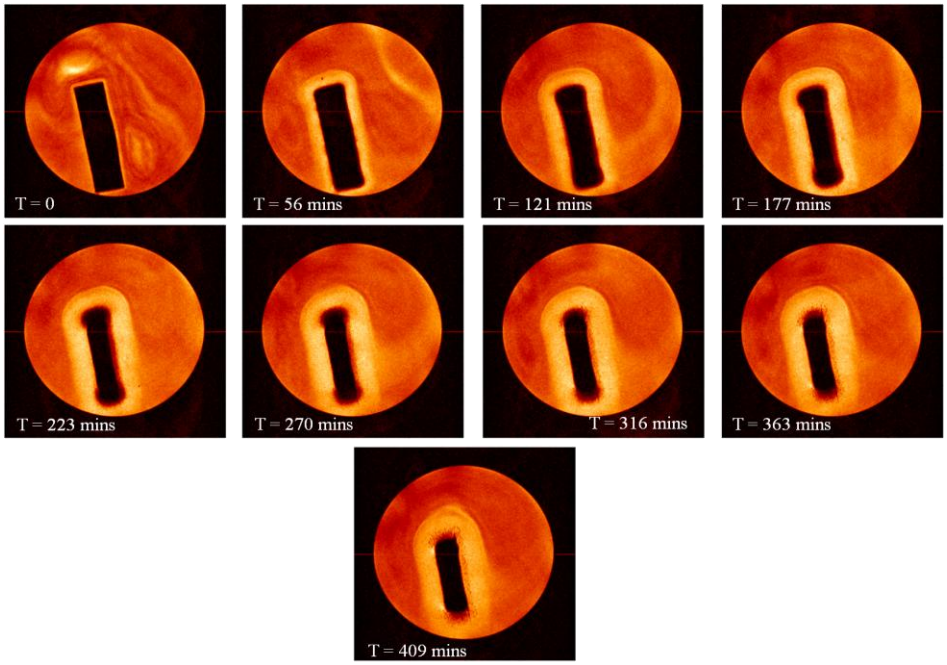

Figure 6.17 Series of magnetic resonance images acquired during 409 minutes dissolution time performed in USP 4 type flow through cell for press coated tablet with expected predicted lag time 5 hours containing HPMC E50LV as an outer barrier layer and theophylline as an active ingredient in inner core tablet (PLT-5 press coated tablet: diameter 13mm and thickness 3.42mm)

The data illustrates an initial hydration of the outer barrier layer followed by the formation of swollen gel layer which continue to grow until the pulse was observed in approximately 660 minutes not shown in MRI images but obvious in UV data in Figure 6.18.

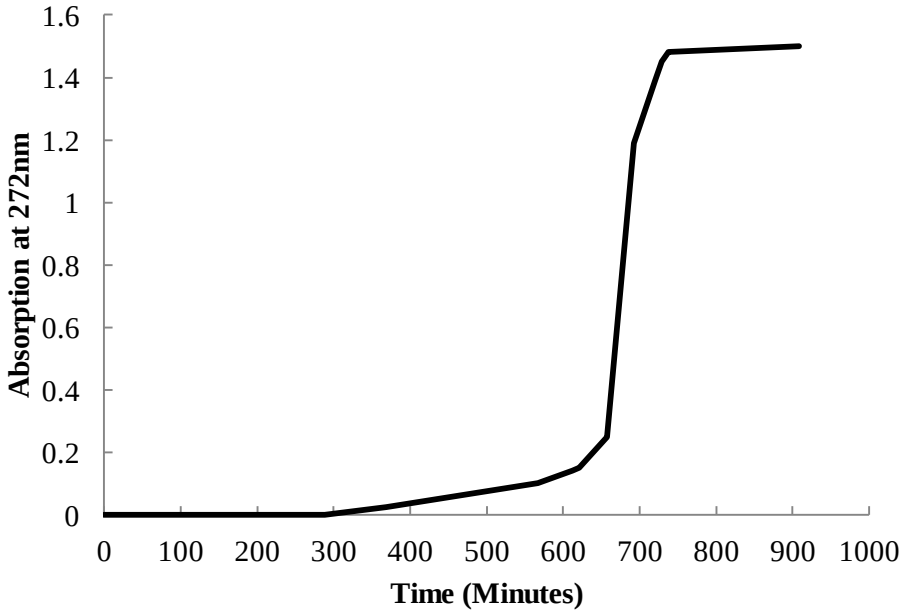

Figure 6.18 The UV absorbance obtained during MRI using deionised water as dissolution medium for PLT-5 press coated tablet showing a pulse release at 660 minutes having theophylline as an active in the middle core and HPMC E50LV in the barrier layer.

The delayed release is again most likely a result of the slow flow rate through MRI instrument. The axial expansion is again considered the reason for dumbbell shape in MRI images (Figure 6.17, image at 177 minutes) as discussed above in Section 6.3.1.

The UV data in Figure 6.18 also shows that there was a small gradual drug release between 300 minutes and 660 minutes before the actual burst. It is known that the soluble drugs such as theophylline, release through the process of diffusion from HPMC matrix tablets (Lapidus and Lordi, 1968, Viridén et al., 2010). Therefore it could be assumed that some of theophylline might have diffused out of the inner core tablet between 300 and 660 minutes through the HPMC E50LV outer barrier layer. It is also possible that similar release of theophylline might have happened in case of PLT-3 (Section 6.3.1) before the actual burst. However, due to technical reasons

some early data was lost during UV data acquisition, which renders it difficult to observe this leaching effect in PLT-3 tablet.

In case of PLT-5 MRI data was acquired only for 409 minutes and therefore the changes in gel thickness and inner core/non-hydrated core were only calculated up to this time. The change in diameter and thickness of the apparent non-hydrated tablet core was quantified using the method described in Section 6.2.3 and calculated values are listed in Table 6.4 for PLT-5 press coated tablet.

Table 6.4 The calculated values of the diameter and thickness of the apparent non-hydrated core tablet and hydrated gel layer for PLT-5 press coated during MRI hydration study.

Time (minutes)	Non-hydrated core diameter (mm)	Non-hydrated core thickness (mm)	Gel thickness (mm)
0	12.9	3.51	0
20	12.6	3.47	1.02
30	12.6	3.45	1.08
60	12.3	3.43	1.59
90	12.4	3.26	1.8
120	12.1	3.15	1.9
150	12	2.96	1.97
180	11.8	2.96	2.18
210	11.7	2.75	2.35
240	11.4	2.47	2.47
270	11	2.45	2.57
300	10.7	2.38	2.64
330	10.4	2.36	2.75
360	10	2.32	2.75
390	9.33	2.3	2.8
409	9.02	2.3	2.83

It can be observed that the diameter and thickness of the non-hydrated core were reduced from 13mm to 9.02mm and from 3.51 to 2.3mm, respectively while the thickness of the hydrated gel was increased from 0 to 2.83mm over a 409 minutes hydration time.

Figure 6.19 shows changes in the diameter of the apparent non-hydrated tablet core with hydration period.

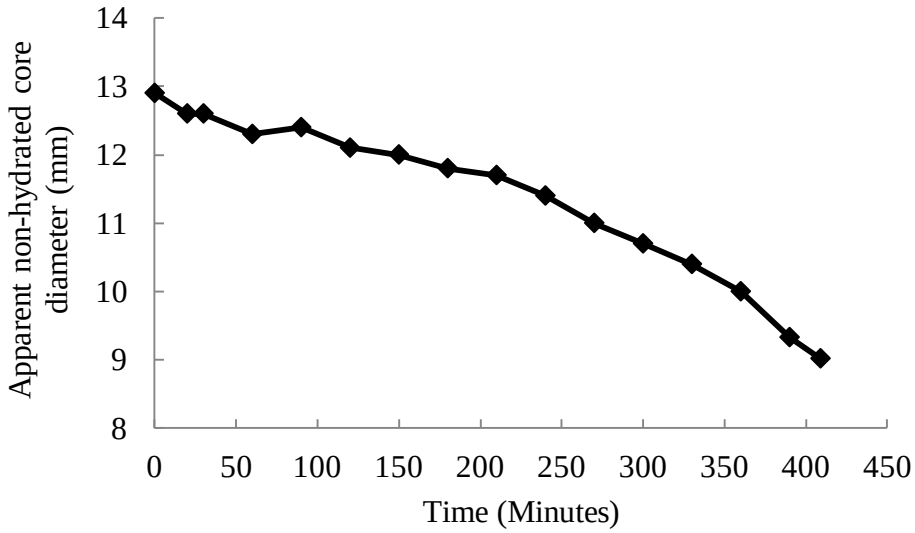

Figure 6.19 Changes in diameter of the apparent non-hydrated core over hydration period in PLT-5 press coated tablet.

The diameter gradually reduced during 409 minutes hydration time, similar to the PLT-3 press coated tablet (Section 6.3.1).

The diameter of the non-hydrated core was 9.02mm at 409 minutes hydration time equivalent to the diameter of the deformed inner core tablet (9.02mm, Table 6.3) for PLT-5 press coated tablet. MRI image (Figure 6.17) also indicates that the PLT-5 press coated tablet was fully hydrated in radial direction at 409 minutes hydration time.

Figure 6.20 shows a relationship between apparent non-hydrated core thickness versus hydration period during MRI study.

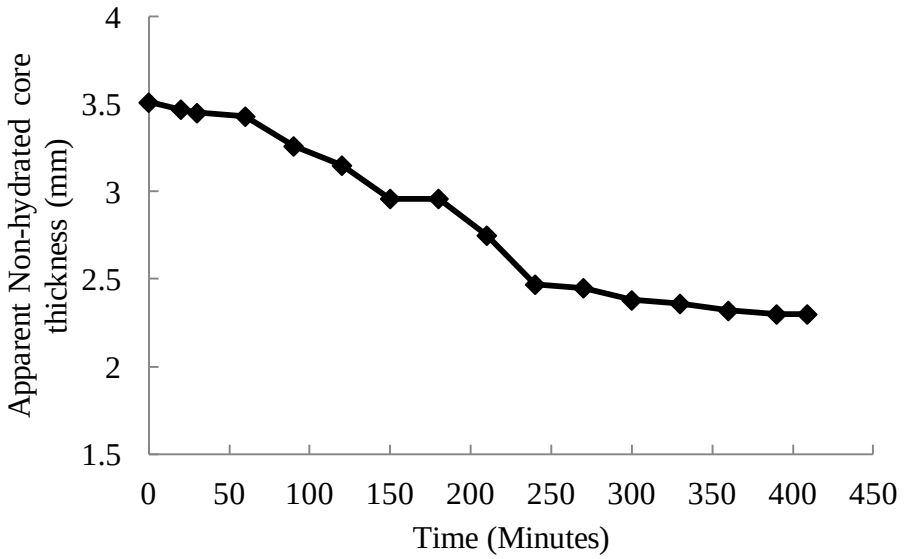

Figure 6.20 Changes in the thickness of apparent non-hydrated core over hydration period in PLT-5 press coated tablet during MRI study.

Initially, a gradual decline in the apparent non-hydrated core thickness was noticed over hydration time which then attained a plateau, without further reduction. The thickness of the apparent non-hydrated core was 9.02mm at 409 minutes (Figure 6.20 and Table 6.4) which corresponded well with the thickness of the inner core tablet 9.01±0.12 (Table 6.3). This indicates that the inner core was fully covered with hydrated outer barrier layer and inner core was still dry at this time.

A change in the thickness of the outer barrier layer in PLT-5 is shown in Figure 6.21.

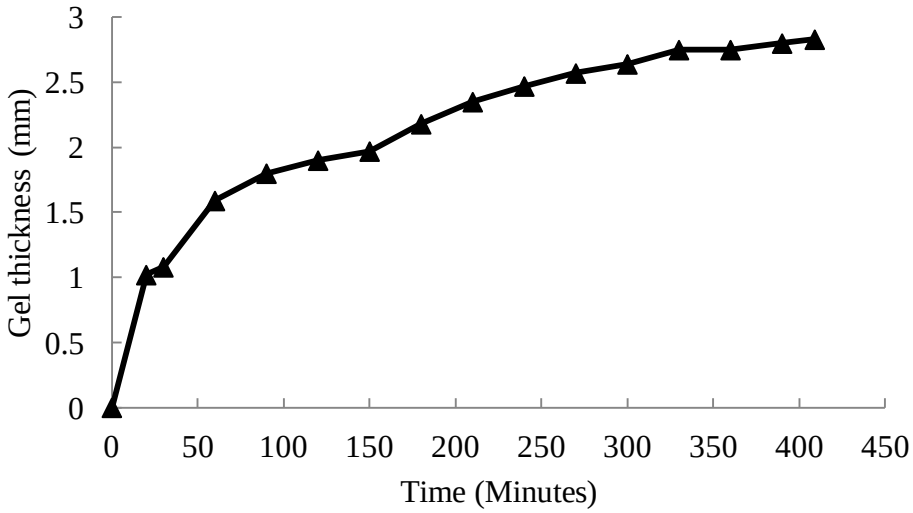

Figure 6.21 The changes in outer core gel thickness over the hydration period for PLT-5 press coated tablet.

The thickness of the outer barrier gel layer in PLT-5 press coated tablet increased progressively with time and almost achieved a constant level similar to the one observed in Figure 6.15. This again indicates that the steadily maintained gel layer was fundamental in avoiding any premature pulse release.

In Chapter 3, it was previously demonstrated that the calculated gel thickness using the texture analyser for two different substituted HPMC grades (K4M, K100M and E4MCR) was found almost similar and their gel thickness values at 240 minutes were between 2.02-2.14mm. The average gel thickness 2.16±0.44 (mean±S.D, n=2) at 240 minutes calculated here for E50LV (used as a barrier layer in PLT-3 and PLT-5) using the MRI falls within the close range of the gel thicknesses calculated by the TA method for other HPMC grades. This further validates the method of texture analysis developed in Chapter 4 and proves that right analytical tool was selected for screening purposes. However, it can also be inferred that the TA method is somewhat superior to MRI, in the sense that TA not only can provide values for gel thickness in HPMC matrices, it can also calculate the gel strength which is not achievable from MRI.

6.4 CONCLUSION

In conclusion, the MRI images provided a real insight into the process of hydration, swelling and drug release in PLT-3 and PLT-5 press coated tablets. The use of USP 4 connected to UV along with MRI provided a powerful tool to understand hydration and dissolution and to track water ingress in these two pulsatile release tablets. The expected lag times, which was hoped to correspond to the *in vitro* lag time (Section 5.3.4), was not achieved due to slow flow rate of the dissolution medium through the MRI and USP 4 cell. The MRI images were used to observe the process of gel formation and its steady maintenance before the pulse and also to calculate the gel thickness and changes which occurred to the non-hydrated core tablet as a result of process of hydration and dissolution.

CHAPTER 7

IN VIVO GAMMA SCINTIGRAPHIC EVALUATION OF HPMC MATRIX TABLETS AND PREDICTIVE PULSATILE TABLETS

7.1 INTRODUCTION

Gamma scintigraphy is non-invasive technique which could be used to observe the transit of a dosage form to its intended site of delivery *in vivo* by means of addition of an appropriate short lived gamma emitting radioisotope to the formulation, which is then detected using the gamma camera (Digenis et al., 1998). The observed transit of the dosage form can then be correlated with rate and extent of drug absorption from plasma drug concentration-time profile. Gamma scintigraphy is also useful to gather information regarding site of disintegration or dispersion. Figure 7.1 shows the schematic diagram of the gamma scintigraphic camera.

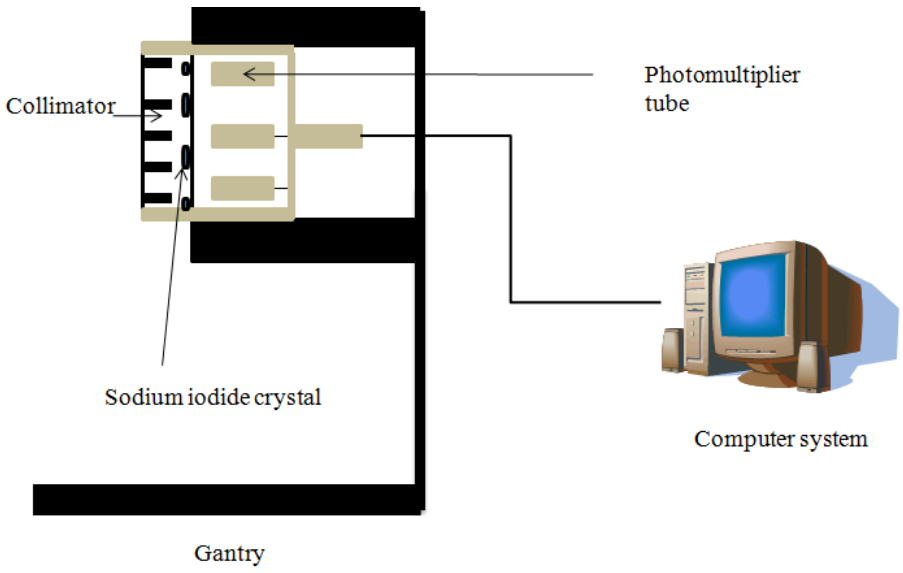

Figure 7.1 Schematic diagram of gamma camera system

The instrument consists of camera head mounted on to mechanical gantry and connected to a computer. The gamma camera head consists of a removable lead plate called a collimator. The collimator has parallel holes and accepts only those gamma rays aligned with the holes thus allowing them to strike sodium iodide crystal detector. The collimators are available in different types, low energy (less than 140 KeV), medium energy (150-300 KeV), and high energy (300-400 KeV), depending upon the thickness of the lead septa between the holes (Prekeges, 2009). In order to achieve different magnifications, the pin hole, parallel hole, diverging hole and converging hole, collimators are available for each energy range.

The gamma photon from the radioisotope is passed through the collimator and strikes a sodium iodide crystals resulting in a release of visible light. The light is then subsequently converted to current pulse by the photomultiplier tube. The outputs of photomultiplier are fed to a system of electronics which display a visual isotopic distribution pattern on computer (Constable, 1969, Pani et al., 2003).

The dosage form for scintigraphic evaluation needs to be radio-labelled so that it can be visualised by the gamma camera. The most commonly used isotopes are described in Table 7.1.

Table 7.1 Some of the commonly used gamma scintigraphic radionuclide and their half life

Radionuclide	**Abbreviation**	**Half life**
Chromium-51	^{51}Cr	28 days
Erbium 171	^{171}Er	7.5 h
Indium-111	^{111}In	2.8 days
Samarium-153	^{153}Sm	47 h
Technetium-99m	^{99m}Tc	6 h

The incorporation of radioisotopes can be achieved by neutron activation technique or by the standard labelling technique (Digenis et al., 1998). The neutron activation

technique procedure includes the incorporation of a small amount of a stable non-radioactive isotope (e.g. Samarium-152, Erbium-170) in the dosage form by mixing it with the other excipients. The stable isotopes are converted to radioactive isotopes (e.g. Samarium-153 (^{153}Sm), Erbium-171 (^{171}Er)) by subjecting the dosage form to neutron radiation (Parr et al., 1985, Digenis and Sandefer, 1991). This method reduces the exposure to the operator to radioactivity during manufacturing. However, this process is expensive and may cause the polymer cross linking and drug degradation (Marvola et al., 2004, Maggi et al., 2004). The other procedure is by standard radiolabelling method in which the radio isotope (e.g. Indium-111 (^{111}In), Technetium-99m (^{99m}Tc)) is incorporated directly in to the dosage form. The choice of radioactive material depends on the factors like half life, radiation energy, extent of particulate radiation, cost and availability (Wilding et al., 2001). The most popular of these radio nuclei is ^{99m}Tc with its versatile chemistry, good quality images, low radiation dose and short half-life (6 h) (Wilding et al., 2001) and easily available through the use of portable generators. In addition to that it can easily be chelated with chelating agent such as diethylenetriaminepentaacetic acid (DTPA) which had shown the systemic absorption less than 1 % after oral administration (Chaudhuri, 1974). For these reasons gamma scintigraphy using ^{99m}Tc-DTPA was used in current *in vivo* scintigraphic studies.

It is very common in pharmaceutical industry to use dog as an animal model to determine the bioavailability and performance of the oral dosage forms (Polentarutti et al., 2010). Dogs provide some close similarity with humans in terms of their ability to ingest large dosage forms such as tablet and capsule. Moreover, dogs are easy to handle and care during clinical trials and husbandry. However, the gastrointestinal physiology of dog is not similar to human in certain aspects. In fed conditions, the reported value for dog's stomach pH was found 0.5 to 3.5 with average pH 2.1, by Youngberg et.al., (1985) calculated through Heidelberg radiotelemetry capsule. Sagawa et al (Sagawa et al., 2009) reported gastric pH values 1.08 after 10g food, and 1.28 after 200g food in dogs under non fasting condition using Bravo® capsule. In human the gastric pH increases up to 7 due to the buffering effect after food intake (absent in dogs) for an initial 30 to 90 minutes before returning back to fasted average acidic pH 1.3 (Dressman, 1986). The

postprandial gastric emptying time in humans and dogs is variable depending on the amount and type of food being ingested nevertheless most studies reported longer gastric emptying time for dogs than humans. Sagawa et.al (Sagawa et al., 2009) demonstrated that the gastric emptying time (GET) increases with the amount of food given to the dog using Bravo® capsule (200g food, GET>20 hours and 10g food, GET 4-24 hours). The human mean GET±SEM is around 4.8±0.61 (lower than dogs) calculated using Heidelberg radiotelemetry capsule after eating standard 500Kcal breakfast (Mojaverian et al., 1985). Dogs also have shorter intestinal transit time (111±17, range 15-206 minutes) compared to humans (234±14, range 180-300 minutes) due to short small intestine about one half of the human's intestine (Dressman, 1986). On the other hand, during fasting condition the stomach pH (1.5 in dogs and 1.1 in humans) and gastric myo-electric migration cycle (MMC), approximately 2hrs in humans and dogs, are in similar range (Dressman, 1986). Due to aforementioned physiological and anatomical differences one has to take extra care not to wrongly extrapolate a data from dog to human. Nevertheless, researchers have successfully used a dog as an animal model to evaluate the performance of the press coated tablet (PCT) (Ghimire et al., 2007), colon-targeted delivery capsule (CTDC) (Ishibashi et al., 1999), and pressure-controlled colon delivery capsules (Hu et al., 1998).

Biopharmaceutical Classification System (BCS) classifies drug substances in four groups according to their solubility and permeability properties (Amidon et al., 1995), i.e., Class 1; high solubility and high permeability, Class 2; low solubility and high permeability, Class 3; high solubility and low permeability and Class 4; low solubility and low permeability. According to this classification system theophylline which is highly soluble and highly permeable drug falls under Class 1 of Biopharmaceutical Classification System. Theophylline has been shown to have pharmacokinetic parameters in dogs comparable to humans in terms of extent and rate of absorption owing to similar half life in both species. Furthermore, theophylline absorbs throughout the gastrointestinal tract in dogs and humans and its absorption is not pH dependent (Hussein et al., 1987).

The combination of scintigraphic data with conventional pharmacokinetic method is termed pharmacoscintigraphy. This coupling provides useful information regarding extent, rate, site and mode of drug release, and physical changes which occur during release from drug delivery devices and formulations (Wilding et al., 2001). The pharmacokinetic measurements alone may not present a true picture of fate of dosage forms as they are only indicative of results of drug release and not the responsible mechanism (Wilding, 2002). Many researchers have used the combination of scintigraphic technique with pharmacokinetic studies (pharmacoscintigraphy) in oral drug delivery to obtain crucial information about the transit and release behaviour of the dosage forms and subsequently correlated with plasma absorption parameters (Wilding et al., 1991). In oral drug delivery its use is thoroughly demonstrated in gastro-retentive (Sato et al., 2004, Goole et al., 2008), colon targeting (Steed et al., 1997, Krishnaiah et al., 1998, Cole, 2002, Basit et al., 2004, Hodges et al., 2009) and pulsatile drug delivery (Ghimire et al., 2007, Stevens et al., 2002). The use of pharmacoscintigraphic studies also include but not restricted to pulmonary (Cass et al., 1999, Newhouse et al., 2003) and ocular drug delivery system (Greaves et al., 1990, Wei et al., 2002). In recent years pharmacoscintigraphy has emerged as an indispensable tool to evaluate the performance of formulation behaviour in drug delivery systems especially for site targeting studies.

In case of *in vivo* quantitative gamma scintigraphic study, solubility of the radioisotope plays an important role to define the release mechanism from tablet formulation. Gamma scintigraphy has previously been used as a non-invasive method to quantify the *in vivo* dissolution or erosion of a matrix tablets (Ghimire et al., 2011, Ghimire et al., 2010). Most water soluble drugs including compound like ^{99m}Tc-DTPA are released from hydrophilic matrix tablets by diffusion (Alderman, 1984). Therefore, a non-diffusible or water insoluble radioactive isotope is required to be incorporated in tablet matrix ensuring the radioactivity is only released in response to the erosion process. The reported literature revealed the use of water insoluble chromium-51 (Abrahamsson et al., 1998a) or a water-soluble radioisotope (indium chloride) complexed with amberlite resin (Wilson et al., 1989, Wilson et al., 1991). Recently, use of ^{99m}Tc-DTPA dried onto activated charcoal was reported for quantification of erosion of a wax matrix formulation and *in vivo* erosion behaviour

of hydroxypropylmethyl cellulose (HPMC) matrix tablets (Ghimire et al., 2010, Ghimire et al., 2011). The use of radiolabelled activated charcoal as a marker in gastrointestinal transit studies is also well documented (Mullan et al., 1998). Therefore, radiolabelled (^{99m}Tc-DTPA) activated charcoal was used in this study allowing easy incorporation and distribution throughout the solid phase; as a result the tablet erosion was monitored via measuring radioactivity of the isotope remaining in the tablet at different times.

In Chapter 5, a successful predictive method (Section 5.4.1.2) based on polymer erosion was developed to calculate the amount of the barrier layer in pulsatile press coated tablets. The polymer used as a barrier layer composite was HPMC E50LV and its *in vitro* gravimetric erosion has been detailed in Section 5.5.4. Based on the predictive method, three pulsatile press coated tablet having predictive lag times 180, 240 and 300 minutes were proposed. *In vitro* release of these three tablets demonstrated a good correlation with predicted release time (Chapter 5).

The first aim of this Chapter was to quantify the *in vivo* erosion of HPMC E50LV barrier layer as a tablet composite and compare this with *in vitro* erosion data. The second objective of the current Chapter was to evaluate the *in vivo* performance of the pulsatile release press coated tablet with predictive pulse times at 180 and 300 minutes in beagle dogs using pharmacoscintigraphy and to establish a correlation with their *in vitro* dissolution data.

7.2 METHODS

7.2.1 Manufacturing of radiolabelled charcoal HPMC matrix for in vivo scintigraphic erosion studies

It has previously been validated that 3 mg of radiolabelled charcoal can be used for gamma scintigraphic studies without affecting the erosion profiles from HPMC matrix tablets (Ghimire et al., 2010). In the present study ^{99m}Tc-DTPA was added to charcoal (3 mg) and evaporated to dryness with hot air. HPMC E50LV powder (400 mg) was thoroughly mixed with 3 mg radio-labelled charcoal and compressed into a

tablet using 13 mm flat faced round IR punch and die provided radioactivedose of approximately 7-13 MBq at the time of dosing. Compression was achieved with 8 tons using a Benchpress.

7.2.2 *In vivo* scintigraphic erosion studies of HPMC matrix tablets in dog

Animal studies were performed under a UK Home Office Animals (Scientific Procedures) Project License with a wash out period of 1 week between two consecutive studies. *In vivo* scintigraphic studies were carried out on two different days for radio-labelled HPMC matrix tablets in 2 male beagle dogs (n=4) weighing 14-17.5 kg.

The dogs were fasted overnight before the study day without any restriction to water. On the day of study, two external markers of ^{99m}Tc-DTPA were placed on the flanks of the animal for reference and each radio-labelled HPMC matrix tablet was administered to the dogs without water on each separate occasion in fasted state however, when required, about 5 ml to 10 ml of water was given after dose administration to ease the tablet movement from oesophagus to stomach. The dogs were given free access to water and provided a break on the floor at appropriate intervals. A standard dog's meal was fed after the formulation was observed to reach the colon or alternatively at the end of the study.

A gamma scintigraphic camera equipped with low energy high resolution collimator (MIE, Germany) was use to acquire posterior static images of 60 seconds at 10 minutes interval for 2 hours followed by 20 minutes imaging interval for another 4 hours.

The scintigraphic images were analysed using Scintron analysis software (MIE Systems, Germany) for site and transit time, gastric emptying time (GE), small intestine transit time (SITT), and the colon arrival (CA) time. The first appearance of the radio-labelled HPMC E50LV tablet in the small intestine and the colon were defined as gastric emptying and colon arrival time, respectively. The difference between GE and CA was calculated as small intestinal transit time.

The quantification of amount of remaining radionuclide was carried out by selecting the region of interest (ROI) around the formulation and quantification of number of counts in this region at different time points after correction from background radiation.

7.2.3 Manufacture of radiolabelled press coated tablets for pharmacoscintigraphic studies

Theophylline was used in an inner core immediate release tablet as a marker drug for *in vivo* pharmacokinetic studies. Radiolabelled lactose was prepared by mixing lactose (50 mg) with ^{99m}Tc-DTPA evaporating to dryness with hot air.

The press coated pulsatile predictive 3 hrs and 5 hrs tablets were prepared as described in Section 5.2.4. The hole of 2.1 mm deep and 1 mm wide was drilled centrally in tablets. The ^{99m}Tc-DTPA radiolabelled lactose containing approximately 7-13 MBq activity was carefully filled in the drilled hole and subsequently sealed with bone cement. The bone cement was prepared by mixing the liquid monomer with powder in a beaker until a dough-like mass was formed and used immediately within 7 minutes of its manufacturing. However, it was found that the radio-labelled lactose became attached to the bone cement and did not form the part of the inner core tablet which resulted in misleading information regarding pulse during scintigraphic studies. Due to this reason a second technique was introduced as detailed below.

The theophylline inner core tablet were manufactured as detailed in Section 5.2.2, however, 5mg of lactose was replaced with 5mg technetium-99m-DTPA labelled lactose giving approximately 7-13 MBq of activity at the time of the dosing and was carefully mixed with all other ingredients with spatula in the end. The core tablets were prepared manually on Benchpress with 8.0 mm flat face punch and die at a compression force of 3 ton. The press coated pulsatile predictive 3 hour and 5 hour tablets were then prepared as described in detail in method 5.2.4. However, the

compression was performed on Benchpress instead of IR press using 13mm flat faced round punch and die at a compression force of 8 ton.

7.2.4 *In vivo* pharmacoscintigraphic dog studies

Animal studies were performed under a UK Home Office Animals (Scientific Procedures) Project License with a wash out period of 1 week between two consecutive studies. *In vivo* pharmacoscintigraphic studies were carried out for 3 hours and 5 hours predicted lag time formulation in 2 male beagle dogs weighing 14-17.5 kg.

The dogs were fasted overnight before the study day without any restriction to water. On the day of study, two external markers of ^{99m}Tc-DTPA were placed on the flanks of the animal for reference and a cannula was passed into the dog's saphenous vein to withdraw blood samples during the study. Each pulsatile predictive 3 hour or 5 hour formulation were administered to the dogs without water on each separate occasion in fasted state however, when required, about 5 ml to 10 ml of water was given after dose administration to ease the tablet movement from oesophagus to stomach. The blood samples of 2.6 ml were collected in heparinised tubes from each dog at an hourly interval, until core disintegration in two consecutive scintigraphic images was observed. Afterwards the blood samples of 2.6 ml were taken at 0, 15, 30, 45, 60, 90 and 120 minutes in heparinised tubes. The cannula was flushed with heparinised saline after each blood sample. The blood samples were immediately centrifuged while still in heparinised tubes at 2000 rpm for 20 minutes, the upper plasma layer was collected and subsequently stored at -20°C for future analysis. The dogs were given free access to water and provided a break on the floor at appropriate intervals. A standard dog's meal was fed after the formulation was observed to reach the colon or alternatively at the end of the study.

A gamma scintigraphic camera equipped with low energy high resolution collimator was used to acquire posterior static images of 60 seconds at 10 minutes intervals until core tablet disintegration was observed. Then following this, images were taken

at approximately 30 minutes intervals for up to 2 further hours. The tablet disintegration was defined as the time mid-way between the last image of an intact core tablet and disintegrated core in the consecutive image. The time taken by the tablet to indicate the disintegration was considered an *in vivo* lag time. The scintigraphic images were analysed for site and transit time, gastric emptying time (GE), small intestine transit time (SITT), and the colon arrival (CA) time. The first appearance of core coated tablet with HPMC E50LV in the small intestine and the colon were defined as gastric emptying and colon arrival time respectively which was the time mid-way between last image and the consecutive image. The difference between GE and CA was calculated as small intestinal transit time.

7.2.5 Plasma theophylline assay procedure

The HPLC method was adopted from Ghimire et.al (2007) however, adjustments were made to improve the retention time and selectivity of the method. During method development, theobromine was initially selected as an internal standard however, due to its low solubility and percentage recovery it was replaced with caffeine. The method was validated for accuracy, precision, selectivity, linearity and sensitivity as per FDA guidelines for bioanalytical method validation (Food and Drug Administration., 2001).

The chromatographic analysis of plasma theophylline was performed on Hewlett Packard Agilent Series 1100 High Performance Liquid Chromatography (HPLC) module connected to a HP Agilent 1100 photodiode array (PDA) ultraviolet (UV) detector (Agilent Technologies, UK, Ltd). Chromatographic data was analysed using the Chem-Station software version 10.02 and separation achieved on ACE 5 C_{18} (S/N A20843) column (150 × 4.6 mm I.D, 5 µm particle size, from ACE ®) using guard column C_{18} (4.0 L mm × 3.01 D mm) maintained at room temperature (22 °C). The HPLC analysis was achieved under isocratic condition using phosphate buffer (50mM, pH 4.3) and methanol (82:18, v/v) at a flow rate of 1ml/min having injection volume 10µl and the detection wavelength of 272nm. However, the percentage of

organic modifier methanol was changed from 5 parts per volume to 50 parts per volume during method optimization to achieve optimum chromatographic separation.

7.2.5.1 Preparation of calibration curve

Caffeine at a concentration of 5µg/ml in methanol was used as an internal standard. A sample solution of theophylline at a concentration of 5µg/ml in methanol was used to prepare the calibration series (Table 7.2) by spiking the defrosted blank plasma sample with different concentration of theophylline solution along with acetonitrile used to precipitate the plasma protein and water.

Table 7.2 A series for calibration curve of theophylline HPLC analysis.

Calibration series	**Internal standard**	**Acetonitrile**	**Theophylline solution (5µg/ml)**	**Blank plasma**	**Water**	**Plasma theophylline concentration**
1	200 µl	400 µl	0 µl	200 µl	200 µl	0.0 µg/ml
2	200 µl	400 µl	20 µl	200 µl	180 µl	0.5 µg/ml
3	200 µl	400 µl	40 µl	200 µl	160 µl	1 µg/ml
4	200 µl	400 µl	80 µl	200 µl	120 µl	2 µg/ml
5	200 µl	400 µl	120 µl	200 µl	80 µl	3 µg/ml
6	200 µl	400 µl	200 µl	200 µl	0 µl	5 µg/ml

The calibration series 1 to 6 were manually shaken and then centrifuged at 5000rpm for 10 minutes. The supernatant was mixed with 0.3 ml of water and filtered through the 0.22 µm Millex $^{(R)}$ GP (Millipore, Cork, Ireland) filter dried under nitrogen and reconstituted with 0.9 ml of water and 0.3 ml of methanol, centrifuged at 10,000 rpm for 10 minutes and filtered once more through Millex $^{(R)}$ GP filter into 1.5 ml HPLC vial.

7.2.5.2 Analysis of the theophylline in canine plasma

The blank plasma was replaced with thawed sample plasma in calibration series 1 (Table 7.2) and rest of the procedure for plasma extraction and chromatographic conditions were kept the same as described in Section 7.2.5.1.

7.2.5.3 Data analysis and statistics

According to FDA guidelines (Food and Drug Administration., 2001) for bio-analytical method validation the following criterion for accuracy, precision, recovery and lower limit of quantification (LLOQ) and limit of detection (LOD) was fulfilled.

The pharmacokinetic parameters were analysed assuming non compartmental model for drug with first order absorption and elimination. The maximum plasma concentration (C_{max}), time to reach C_{max} (T_{max}) was directly calculated from the plasma concentration time graphs for both 3 hrs and 5 hrs pulsatile formulations. The area under the curve from time of dosing to 2 hours post disintegration ($AUC_{0\text{-}2dis}$) was calculated using the trapezoidal rule. The elimination rate constant (K_{el}) was determined using the following equation from two points on the best-fit line (Joseph, 2010)

$$K_{el} = \ln (Cp_{\text{from left on line}}) - \ln (Cp_{\text{from right on line}}) / t_{\text{from left on line}} - t_{\text{from right on line}}$$

ln = natural log, **Cp** = plasma concentration

The lag time to drug appearance in plasma (T_{lag}) was defined as the time corresponding to the first appearance of theophylline in the plasma. The comparison between in vitro and in vivo disintegration times was performed using a two sample t-test with a 95% confidence interval using Minitab ^{TM} version 15.0-XP.

7.3 RESULTS AND DISCUSSION

7.3.1 *In vivo* erosion studies of HPMC E50LV

The *in vivo* erosion (% radioactivity remaining in the core of HPMC E50LV tablet) study was performed using the four radio-labelled HPMC E50LV tablets (diameter 13mm, (n=4)) in two dogs on two different dosing days. Gamma scintigraphy is considered suitable technique to locate the position of the unit dose in gastro intestinal tract. The GI transit results are described in Table 7.3.

Table 7.3 Gastric emptying (GE), small intestinal transit time (SITT), and the colon arrival (CA) time calculated using scintigraphic images in two beagle dogs by radio-labelled charcoal HPMC tablets

	GE (min)	**CA (min)**	**SITT (min)**
Dog 1	80	220	140
	70	240	170
Dog 2	34	244	210
	70	260	190
Mean	63.5	241	177.5
S.D	20.22	16.45	29.86

The gastric emptying (GE) time in dog 1 was 80 and 70 minutes whilst colon arrival (CA) was 220 and 240 minutes, similarly in dog 2 GE was 34 and 70 minutes whereas CA was 244 and 260 minutes. The mean gastric emptying time (63.5±20, n=4) in this study is in agreement with reported literature value of 35 to 315 minutes in fasted dogs (Lui et al., 1986, Sagawa et al., 2009). The transit time through the small intestine in this study found to be 177±29 (n=4) minutes corresponded with the published range of 15 to 206 minutes (Dressman, 1986). The mean colon arrival time

of 241±16 (n=4) was also in concordance with published literature values of 247.8±79.7 minutes (McInnes et al., 2005b).

Figures 7.2 and 7.3 show the *in vivo* erosion profiles of HPMC E50LV tablets in dog one and two on study day one and two respectively, in comparison to in vitro gravimetric erosion data.

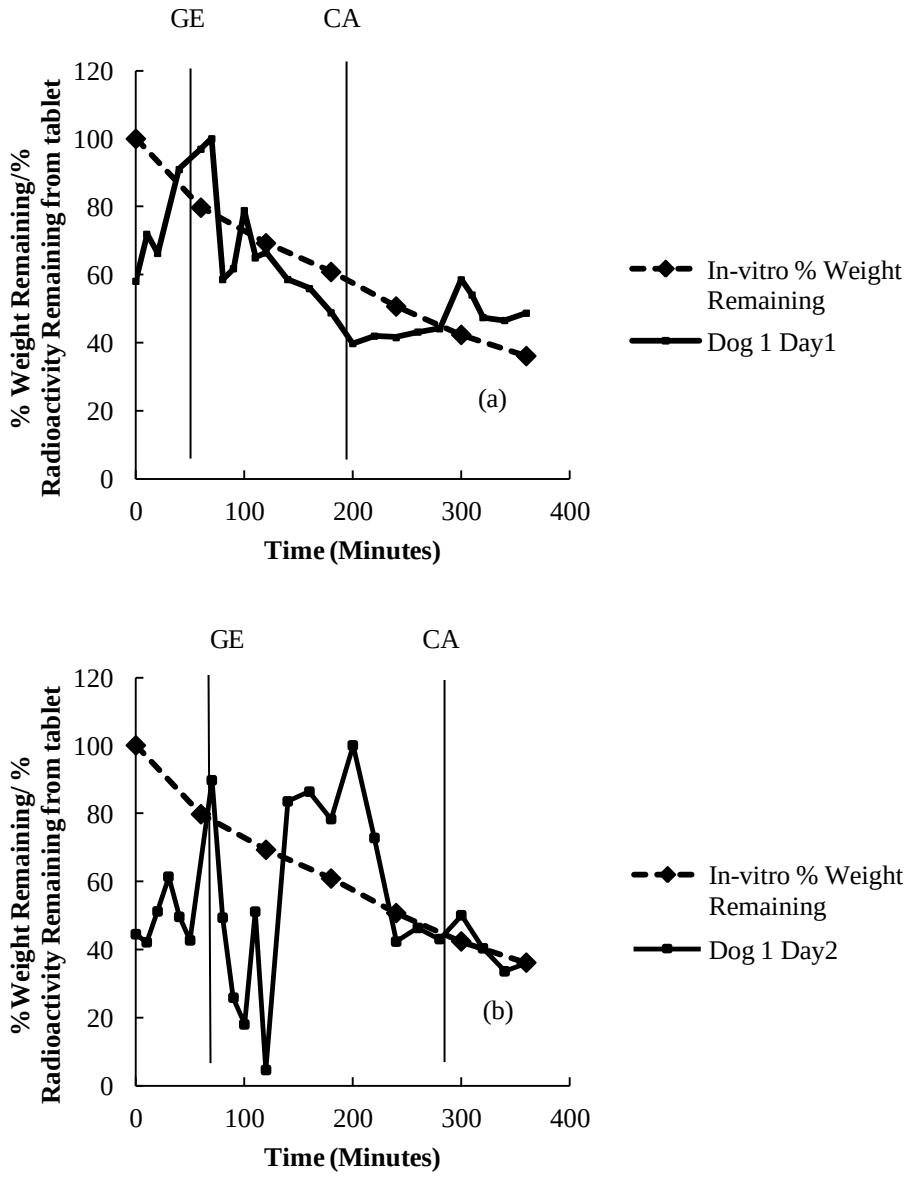

Figure 7.2 Comparison of percentage in-vitro weight remaining (♦) with percentage gamma radioactivity remaining (■) from HPMC E50LV tablets in dog 1 on (a) study day one and (b) study day two. Vertical lines (|) depict the virtual time for gastric emptying and colon arrival respectively.

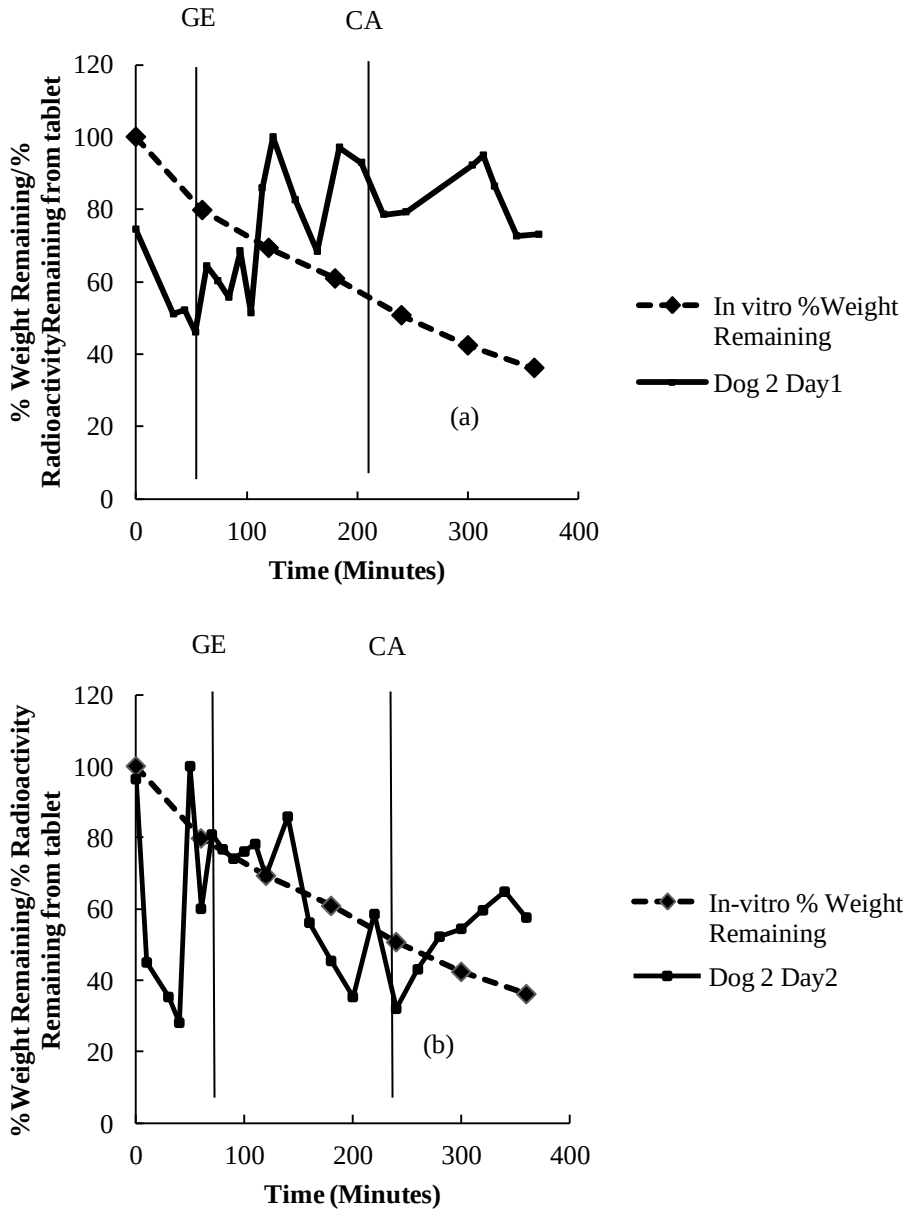

Figure 7.3 Comparison of percentage in-vitro weight remaining (♦) with percentage gamma radioactivity remaining (■) from HPMC E50LV tablets in dog 2 on study day one (a) and study day two (b). Vertical lines (|) depict the virtual time for gastric emptying and colon arrival respectively.

As can be seen from Figure 7.2 (a, b) in dog 1, in general the *in vivo* erosion profiles displayed gradual decline in radioactivity from HPMC matrix tablets however, overall the *in vivo* erosion data is almost erratic ranging from 4.95% to 100%. For instance, the % radioactivity at the start of the study in dog one (Figure 7.2 a, b) on both day 1 and 2 was between 40-60% which increased to around 90-100% at the time of GE (80 and 70 minutes, Table 7.3, also shown in Figure 7.2 as vertical line). The percentage radioactivity was even more unpredictable for HPMC matrix tablets during their small intestinal transit (140 and 170 minutes, Table 7.3) fluctuating between almost 100 to 40% on day 1 (Figure 7.2), and between 90 to 5% and 5 to 38% on day 2 (Figure 7.2). At the time of colon arrival (220 and 240 minutes, Table 7.3) both HPMC tablets displayed % radioactivity of about 40% which rose up to 50% on day 1 and dropped down to around 35% on day 2.

Similar to dog 1, in case of dog 2, the *in vivo* erosion profile (Figure 7.3b representing the second day of the study) again indicates overall down ward trend though with some irregularities in erosion profile. The % radioactivity was 100% (Figure 7.3b) at the start of the study which dropped down to 80% by the time tablet was emptied into the stomach (GE 70 minutes, Table 7.3) though % radioactivity remaining in the core did float between 30-100% during gastric stay. By the time tablet arrived in the colon (CA 260 minutes, Table 7.3) the % radioactivity was around 30%, the value of which again increased to 50% at the end of study day 2. On contrary, in the same dog on the first day of study (Figure 7.3 (a)); the *in vivo* erosion profile indicates an overall upward trend with scattered radioactivity in the range of 50% to 100%. The % radioactivity started off around 75% which dipped down to around 50% at the time of gastric emptying (GE 34 minutes, Table 7.3). However, during small intestinal transit (SITT 190 minutes, Table 7.3), the HPMC matrix tablet demonstrated wide variation in % radioactivity ranging from 50-100%, which was about 85% when tablet arrived in the colon (CA 260 minutes, Table 7.3).

Furthermore, Figures 7.2 and 7.3 also show the comparison of *in vivo* erosion data with *in vitro* percentage weight remaining of HPMC E50LV tablets (Section 5.3.4). However, as discussed earlier that data obtained during *in vivo* erosion study was highly inconsistent due to this reason it is difficult to predict any conclusive trend by

comparing it with *in vitro* percentage weight remaining in HPMC E50LV tablet cores.

A single gamma camera was used from the posterior position to collect the scintigraphic images. As tablet moved through different parts of the gastrointestinal tract, the position and distance of the eroding tablet changed with respect to camera. The gamma radiations emitted from the tablet has to pass through different internal organs like muscular walls of the gastrointestinal tract encountering variable tissue densities before striking the camera. Since formulation has moved to different positions at different depths in dogs GI tract at different time points resulted in variability in number of counts obtained (Maurer et al., 1991, Bailey et al., 1989). This attenuation was more pronounced in case of gastric residence and small intestinal transit as seen in Figures 7.2 (a, b) and 7.3 (a, b). The position of stomach was further away from the camera detector in dogs, which could be the reason for low number of counts and ultimately low percentage radioactivity during gastric residence in these dogs. Only on one occasion in dog 2 on second day of study (Figure 7.3 (b)), the observed radioactivity started at 100% as expected. The small intestine is not a straight long tube rather it is coiled and turned between the stomach and the large intestine (Kararli, 1995) which explains the variability in number of counts obtained and irregularities observed in radioactivity data during small intestinal transit. This effect has clearly been seen in case of Figure 7.2 (b) where the radioactivity dropped to almost zero which was practically impossible. The only way it could happened was that the tablet might have moved to such a depth in small intestine that there was very little radiation which could have reached to camera resulted in apparent low levels of radioactivity. The large intestine is less convoluted compared to small intestine and present close towards the posterior of the dog. Due to this reason less erratic data (Figure 7.2 (a, b) and 7.3 (a, b)) was observed in both dogs after the colon arrival.

The use of two cameras from posterior and anterior positions as published by Abrahamsson et al., (1998a) instead of single camera from the posterior position only has been proven better alternative to avoid influence of the position-dependent attenuation of gamma radiation. The geometric mean value of number of counts from

the cameras is usually used for the quantification of radioactivity avoiding any artefacts introduced due to tablet movement in different parts of the gastrointestinal tract (Bailey et al., 1989). It is worth noting that Abrahamsson et al., (1998a) study was performed on human volunteers where the subject was easily accommodated by the two cameras. However, due to the morphology of the dog and difficulty in positioning a dog under both cameras, it has been reported that the posterior imaging provides optimal animal comfort, image quality and anatomical definition (as was the case in current dog study with single camera) although quantitative variability would be unavoidable as simultaneous anterior imaging is not possible (McInnes et al., 2005a). Due to above mentioned artefacts a conclusive correlation between *in vivo* and *in vitro* erosion data had not been fully comprehended during this study.

7.3.2 Pharmacoscintigraphic evaluation of pulsatile 3 hour and 5 hour tablets

Gamma scintigraphic images were used to locate the site and time of disintegration from the core of pulsatile tablets (3 hours and 5 hours) in the gastro intestinal tract of the beagle dogs as shown in Figures 7.4, 7.5, 7.6 and 7.7. Table 7.4 describes the *in vivo* performance and transit of pulsatile tablet formulations. The comparison of transit time obtained from in vivo erosion studies (Section 7.3.1) and pulsatile tablet formulation from this section for gastric emptying, small intestinal transit and colon arrival were found not significantly different ($P>0.05$) and understood to be due to their similar sizes (tablet diameter 13 mm). Both formulations, predictive pulsatile 3 hours and 5 hours, were of the same size and shape (flat face, 13mm diameter) and expected to behave in terms of transit in a similar way during *in vivo* studies. So for this reason transit data described in Table 7.4 is a collective mean data from both predictive 3 hours and 5 hours tablet formulation.

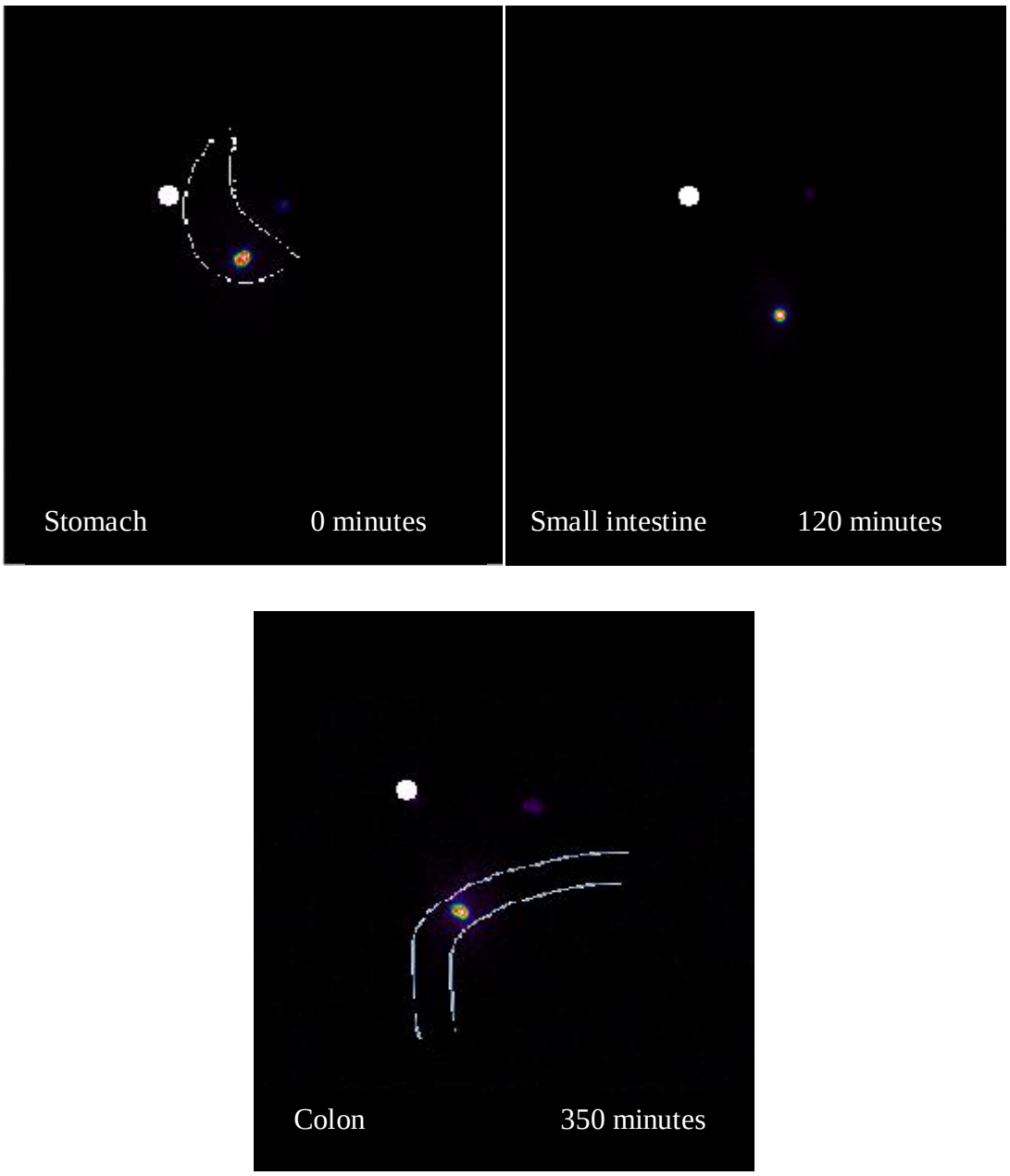

Figure 7.4 Representative posterior scintigraphic images for predictive 3 hour pulsatile tablets showing intact tablet in stomach, small intestine and partial disintegration in colon from dog 1. A small white circle represents the external marker. Representative stomach and colon outlines are provided for visualisation of the tablet location.

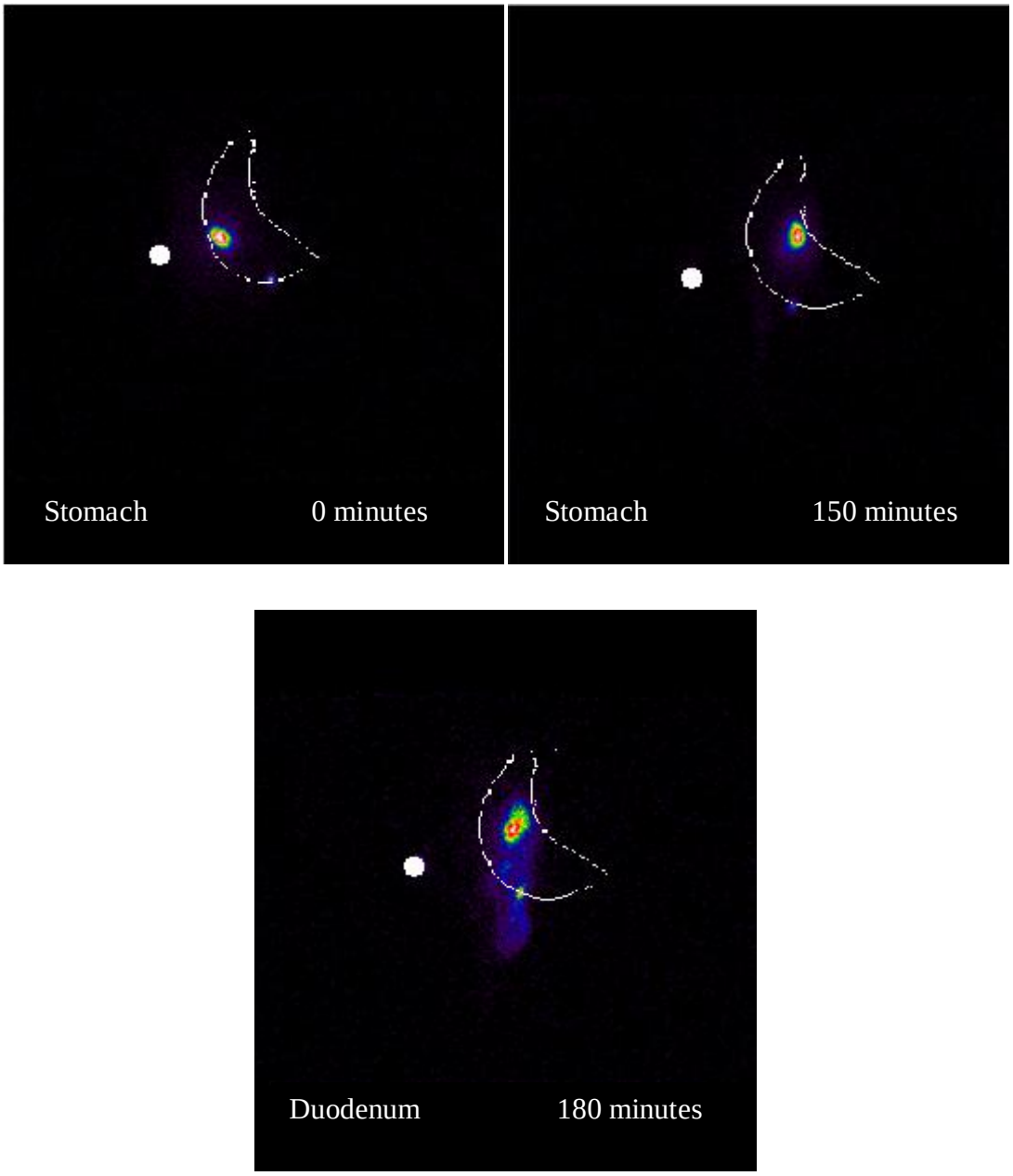

Figure 7.5 Representative posterior scintigraphic images for predictive 3 hour pulsatile tablet showing intact, disintegration and emptying of tablet from stomach in dog 2. A small white circle represents the external marker. Representative stomach and duodenum outlines are provided for visualisation of the tablet location.

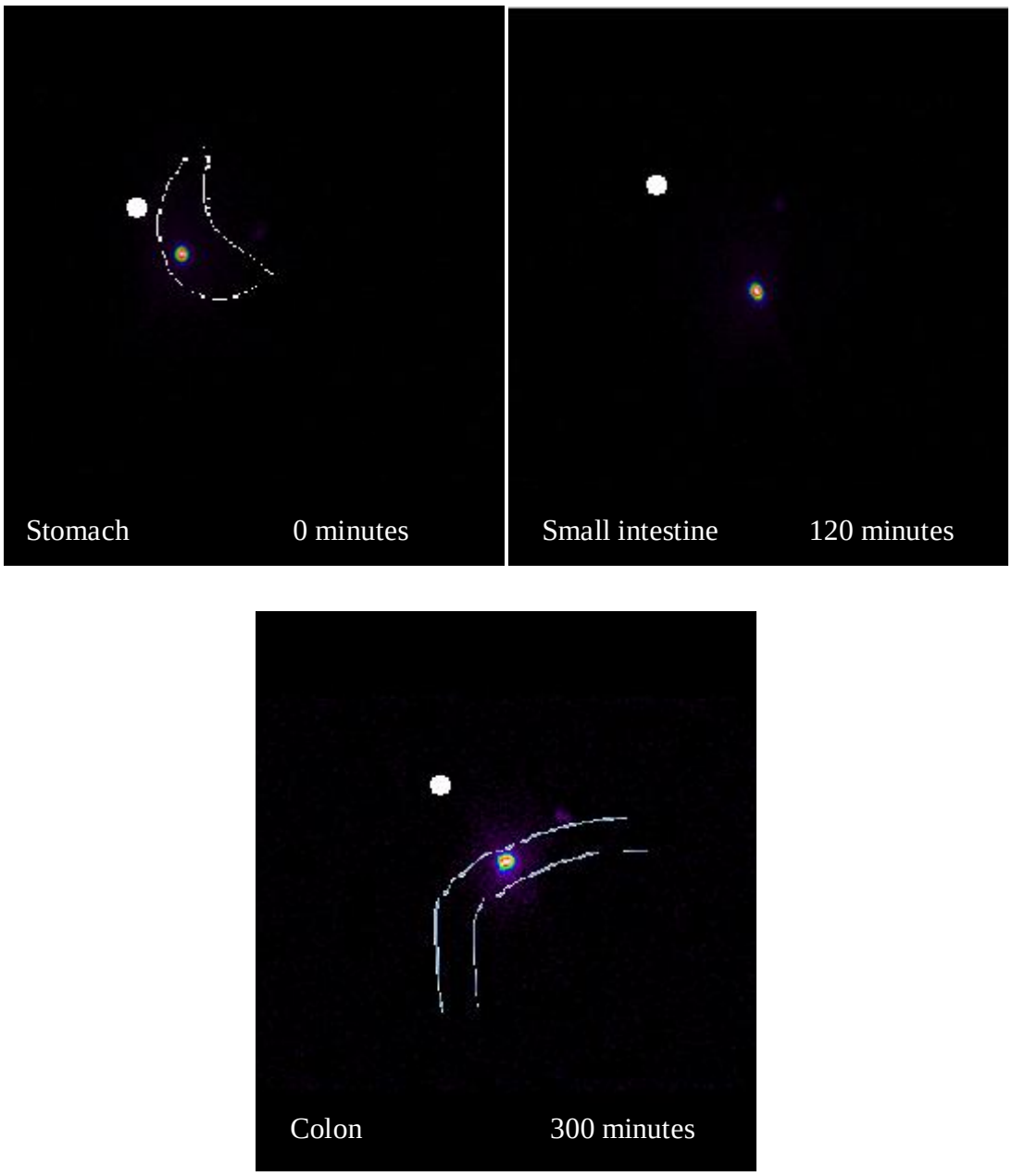

Figure 7.6 Representative posterior scintigraphic images for predictive 5 hour pulsatile tablet showing intact tablet in stomach and small intestine, and disintegration in colon in dog 1. A small white circle represents the external marker. Representative stomach and colon outlines are provided for visualisation of the tablet location.

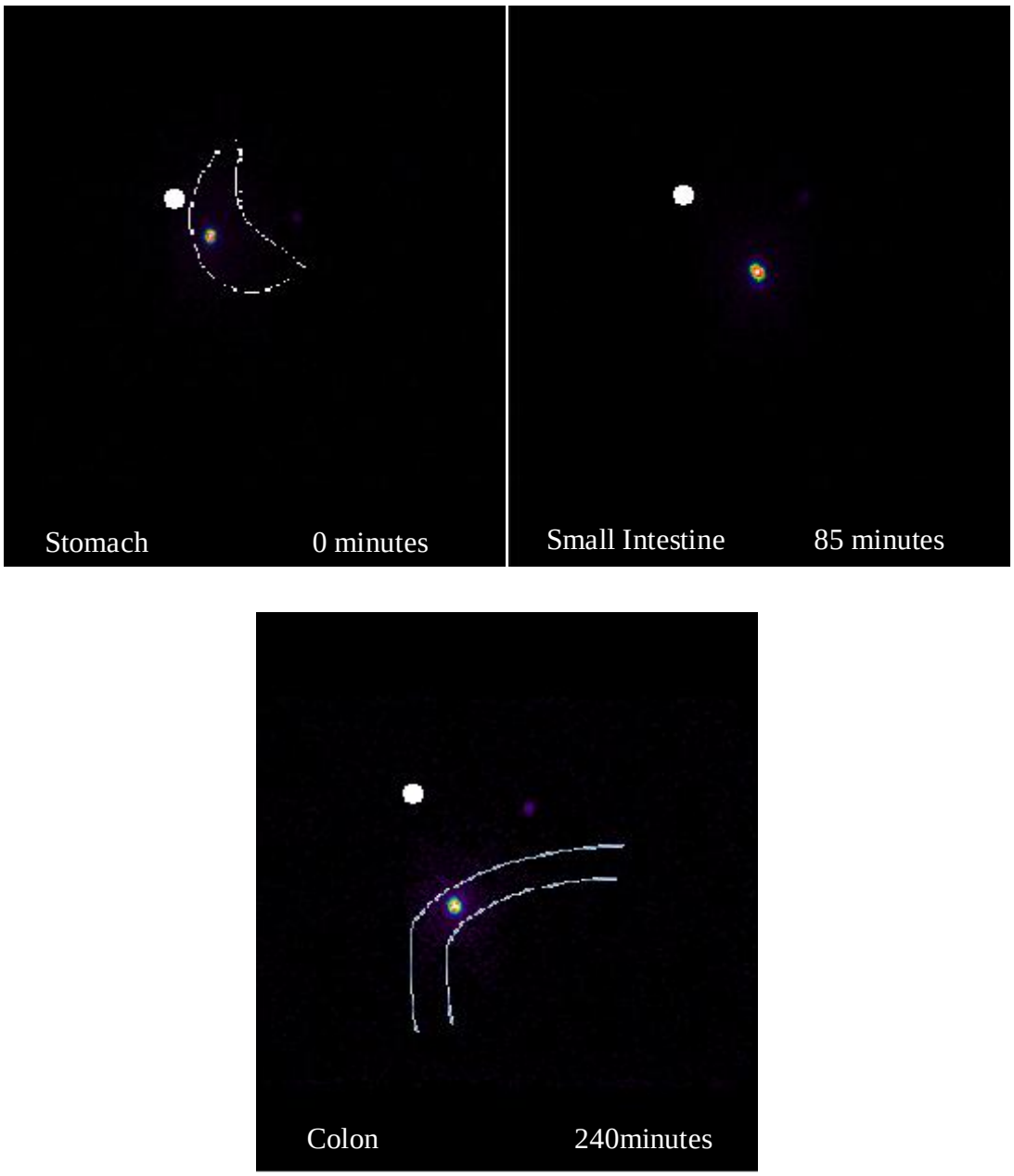

Figure 7.7 Representative posterior scintigraphic images for predictive 5 hour pulsatile tablet showing intact tablet in stomach and small intestine, and disintegration in colon in dog 2. A small white circle represents the external marker. Representative stomach and colon outlines are provided for visualisation of the tablet location.

Table 7.4 *In vivo* disintegration of inner core tablet from predictive 3 hours and 5 hours formulation, the transit data represents the collective mean data from both tablet formulation

Tablet Formulation	Dog	Site of Disintegration	Disintegration time (min)	
			Individual	Mean ±SD
Predictive 3 hours	1	Stomach	130	
	2	Colon	200	165±49
Predictive 5 hours	1	Colon	290	
	2	Colon	310	300±14

Parameter	N	Transit (min)
GE	3	83±20 (60, 100, 90)
SITT	3	148±20 (130, 146, 170)
CA	3	232±3.5 (190, 246, 260)

GE: Gastric emptying, SITT: Small intestinal transit time, CA: Colon arrival

The mean gastric emptying was found to be 83±20 minutes (range 60-160 minutes) lie in agreement with previously published values of 35 to 315 minutes (Lui et al., 1986). However, in one of the dogs the predictive 3 hours pulsatile tablet retained in the stomach, pulsed around 150 minutes and started emptying its content in the next 5 to 10 minutes, as seen in scintigraphic images in Figure 7.5. This variability can be explained by the fasting motility pattern in the dog. The mechanism of gastric emptying is controlled by four phases of migrating myo-electric complex (MMC) cycle. In phase three of MMC, which consists of strong contractions, the stomach content or tablets will move into the small intestine through the open pylorus. The periodicity of the MMC is about 2 hours, if not significantly influence by the physiological variation of the animal and physical nature of dosage form (Code and Marlett, 1975, Davis et al., 1993). It has been known that the size of the dosage form more than 5 mm could take longer than expected to empty during phase three of the MMC cycle in fasted and fed dogs (Itoh et al., 1986). The size of the tablet was 13 mm (i.e. greater than 5 mm) in this study which could be the reason for delayed

gastric emptying. Similar results were also observed by Ghimire et al (2007) with the same size of tablets in fasted dogs.

The mean transit time for small intestine and colon arrival does not include a value from one pulsatile 3 hours formulation because of delayed gastric emptying and disintegration of core in the stomach so the values will represent n=3 instead of n=4. The mean small intestinal transit time was 148±20 minutes (range 130-170, n=3) same as narrated by the other researchers 15-206 minutes and tends to be more variable in dogs compared to humans (Davis et al., 1993, Yamada et al., 1995). The colon mean arrival time in this study was found to be 232±3.5 minutes (range 230-236, n=3), corresponded well in concordance with literature (Schulze et al., 2005).

7.3.2.1 Correlation between *in vitro* dissolution and scintigraphic *in vivo* data

The mean disintegration time for predictive 3 hours and 5 hours pulsatile formulation were found (165±49 and 300±14 minutes) not significantly different ($P>0.05$, t-test) from *in vitro* dissolution release time (185±41 and 295±42 minutes) as described in Section 5.3.4. A good correlation between *in vitro* dissolution release time and *in vivo* disintegration lag time from scintigraphic images for predictive pulsatile 3 hours and 5 hours formulation was observed as shown in Figure 7.8.

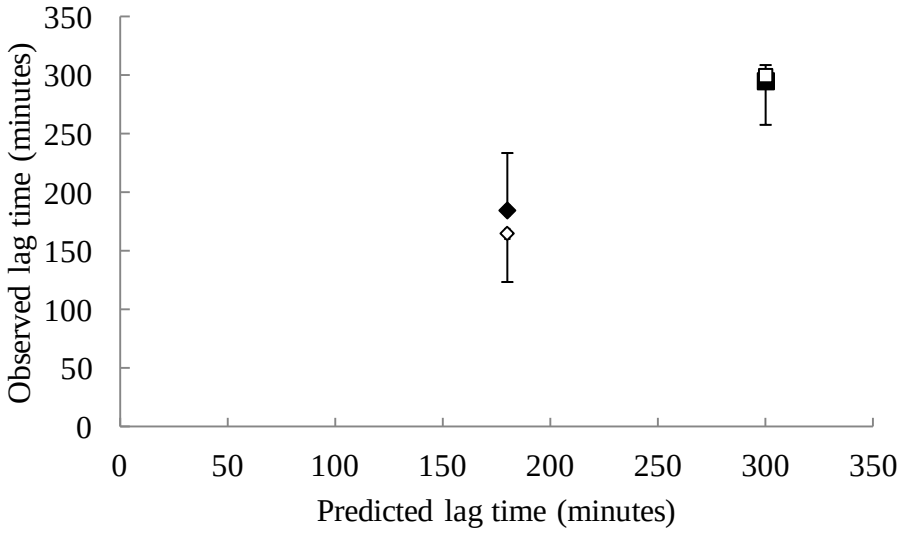

Figure 7.8 Correlation between *in vivo* disintegration time observed in scintigraphic images and *in vitro* dissolution release time for predictive 3 hours (♦ *in vitro* (n=6), ◊ *in vivo*(n=4)), and 5 hours (■ *in vitro*, □ *in vivo*) pulsatile formulation.

It has been previously demonstrated in Section 4.3.4 that the selection of suitably hydrating gel matrix with appropriate gel strength and erosion characteristic might be crucial for the development of pulsatile drug delivery formulation. The hydration and performance of the hydroxypropylmethyl cellulose in modified release dosage form is known to be independent of pH (Segale et al., 2010) which may be one of the reasons that the barrier layer made of HPMC E50LV in pulsatile predictive 3 hrs and 5 hrs formulation behaved similarly in both *in vitro* and *in vivo* environment without being affected by the GI tract variable pH. The reported value for mechanical destructive force in dog's stomach (Kamba et al., 2001, Kamba et al., 2002) did not show any substantial impact on the performance of both pulsatile 3 hrs and 5 hrs tablets. Three out of four pulsatile tablets (one pulsatile 3 hrs and two pulsatile 5 hrs) emptied intact from dog's stomach without showing any sign of premature drug release as shown in Figures 7.4, 7.6 and 7.7. However, the one of the predictive 3 hrs pulsatile tablet, which was retained in the stomach of one of the dogs, depicted disintegration after 130 minutes (Figure 7.5) suggesting that hydrodynamic forces

presented in dog stomach can affect the *in vivo* performance of the eroding HPMC E50LV barrier layer, if a tablet stays in the stomach for unnecessarily prolong period. The decreased availability of water in distal region of the gastrointestinal tract (Schiller et al., 2005, Vertzoni et al., 2010) and an increased colon viscosity (Basit, 2005) might be the reason for apparent concentrated dispersion of the disintegrated core in the colon as seen in Figures 7.4, 7.6, and 7.7. One of the earlier aims of the study was to design and develop a formulation with progressively eroding and weakening barrier layer around the core tablet which would break down during its passage through the ileocecal junction as observed and postulated by some researcher (Muraoka et al., 1998, Wilson, 2010). However, this affect was not witnessed during scintigraphic imaging in dog studies which could be attributed to partial hydration of the barrier layer during its passage through small intestine and ICJ. Although, partial core disintegration was observed once the formulations pulsatile 3 hrs and 5 hrs tablets were in the colon as shown in Figures 7.4, 7.6 and 7.7, after completing hydration and predicted disintegration lag time.

The ability of predictive 3 hours and 5 hours formulation to maintain the performance of the outer barrier layer, formed by the HPMC E50LV, under *in vivo* conditions providing distinctive lag time strengthened the idea of early characterisation of gel strength and process of erosion. In general, a good *in vitro - in vivo* correlation affirms the suitability of the novel predictive model detailed in Section 5.2.1.2 and 5.3.4.

7.3.2.2 HPLC method validation for theophylline

During early method development canine plasma was spiked with internal standard caffeine and marker drug theophylline. Initially, efforts were focused to remove any interference by varying the quantity of organic modifier or altering the pH of the mobile phase. Appendix III shows the chromatogram from blank canine plasma (not spiked) indicating no interfering peak for theophylline or caffeine in the sample and considered suitable to be used in method development.

Appendix IV shows the representative chromatograms of plasma samples spiked with theophylline (0.5µg/ml) and caffeine (0.5µg/ml). The analytes, theophylline and caffeine, were well separated from co-extracted material under the described chromatographic conditions at retention times of 8.5 and 14.8 min, respectively. The peak shapes were good and completely resolved showing no sign of interference from the plasma matrix.

The peak area ratio of theophylline and caffeine in canine plasma was linear with respect to the analyte concentration over the range 0.5–5 µg/ml. The mean linear regression equation of calibration curve shown in Appendix V for theophylline was $y = 0.1394x + 0.028$, where y is the peak area ratio of the analyte to the internal standard and x is the concentration of the analyte. The correlation coefficient (r^2) for theophylline was 0.99 over the concentration range used. The calibration curve was suitable for generation of acceptable data for the concentrations of the analyte in the samples.

The theophylline recovery was determined using canine blank plasma spiked with increasing concentration ranging from 0.5µg/ml to 5µg/ml; the absolute recovery was expressed as the percentage of the directly injected standard solution of theophylline. The data is shown in Table 7.5.

Table 7.5 Precision and recovery data of calculated concentrations of calibration samples for theophylline in canine plasma

Concentration added (µg/ml)	**Concentration found/recovered (mean ± S.D., n = 5; µg/ml)**	**Precision (% CV)**	**Recovery (%)**
0.513	0.508 ± 0.2	15	99
1.026	1.149 ± 0.3	12	112
2.052	2.044 ± 0.2	6	99
3.09	3.366 ± 0.3	5	109
5.13	4.941 ± 0.4	5	96

The recoveries fall between 96 to 112% having percentage coefficient variance (%CV) not more than 15%CV including the lowest concentration used fulfilling the requirements for recoveries as described in FDA guidelines (Food and Drug Administration., 2001).

The lowest concentration (0.5µg/ml) on calibration series was accepted as LLOQ which fulfilled the requirement set out in FDA guidelines (Food and Drug Administration., 2001). The LOD was found 0.1µg/ml.

Inter and intra-day accuracy and precision determinations for the developed HPLC method are shown in Table 7.6.

Table 7.6 Inter and intra-day accuracy and precision determinations for the developed HPLC method for low, medium and high theophylline concentrations in canine sample

Inter-day			
Concentration added (µg/ml)	**Concentration found (mean ± S.D., n = 5; µg/ml)**	**Precision (%CV)**	**Accuracy (%)**
0.508	0.541 ± 0.074	13.19	106.53
2.121	2.179 ± 0.206	9.45	102.75
5.09	4.986 ± 0.221	4.44	97.95
Intra-day			
Concentration added (µg/ml)	**Concentration found (mean ± S.D., n = 5; µg/ml)**	**Precision (%CV)**	**Accuracy (%)**
0.513	0.475 ± 0.023	14.13	93.6
2.052	2.082 ± 0.115	5.55	98.13
5.13	4.951 ± 0.169	3.42	97.26

The data shows that the accuracy and precision values at low, medium and high concentrations of theophylline in plasma on inter-day and intra-day studies were within acceptable limits set out in Section 7.2.5.3 (97-106% inter-day and 93-98% intra-day, n=5 for accuracy and ≤ 15% CV, n=5 for precision) indicating that the assay method is reproducible for replicate analysis of theophylline in canine plasma.

7.3.2.3 Pharmacokinetic analysis of predictive 3 hours and 5 hours pulsatile formulations

The pharmacokinetic data was normalised from the time of disintegration to represent the plasma concentration-time profile after confirming the *in vivo* disintegration from the gamma scintigraphic images. Figure 7.9 shows a normalised plasma concentration time profile of 3 hours predictive pulsatile formulation in dog 1 and dog 2 indicating a distinctive lag phase prior to theophylline release.

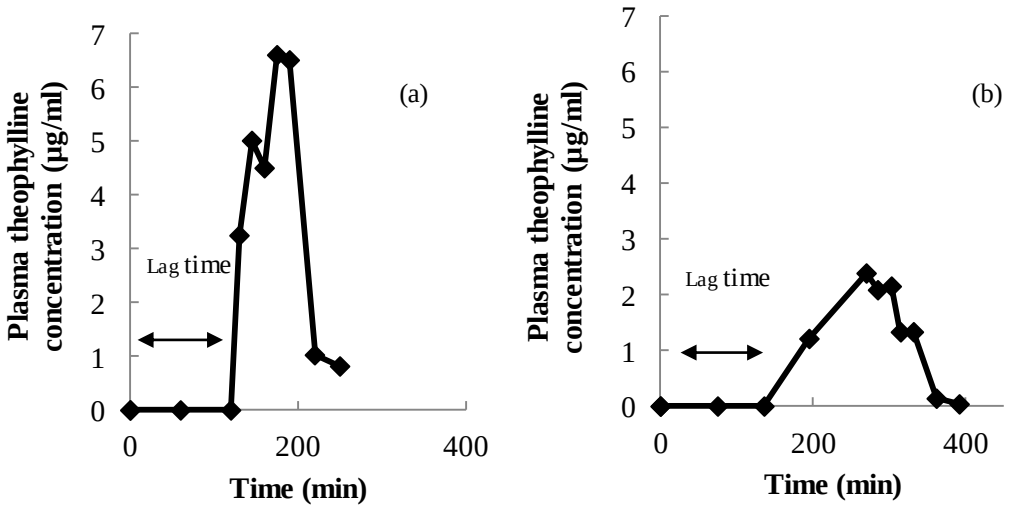

Figure 7.9 Onset normalised plasma concentration-time profile of theophylline after oral administration of predictive 3 hours pulsatile formulation in fasted beagle a) dog 1 and b) dog 2.

Both dogs exhibited the substantial lag time of 190 minutes (Figure 7.9a, dog 1) and 130 minutes (Figure 7.9b, dog 2) prior to drug absorption. In case of dog 2, the tablet was retained in the stomach before the drug started to be absorbed and subjected to the prolonged influence of mechanical forces of the stomach. It is known that the dog's stomach has a mechanical force of 3.2 N (Kamba et al., 2001) however, this mechanical crushing effect did not break the retained predictive 3 hrs formulation in dog 2 for up to 130 minutes though did accelerate its breaking an hour earlier than in dog 1. In addition to that higher AUC (596 µg/ml/min) as described in Table 7.8 for dog 2 represents higher bioavailability due to start of drug absorption in the stomach and subsequently in the small intestine. The presence of higher intestinal juices and the availability of large surface area in form of villi in the small intestine are the main reasons for higher bioavailability. However, *in vivo* drug absorption in dog 1 for pulsatile 3 hrs formulation (Figure 7.9a) started after a lag time of 190 minutes correlated well with observed *in vitro* drug release of 185 minutes (Section 5.3.4).

Figure 7.10 shows a normalised plasma concentration time profile of predictive 5 hours formulation in dog 1 and dog 2 with distinctive pulse phase before theophylline release.

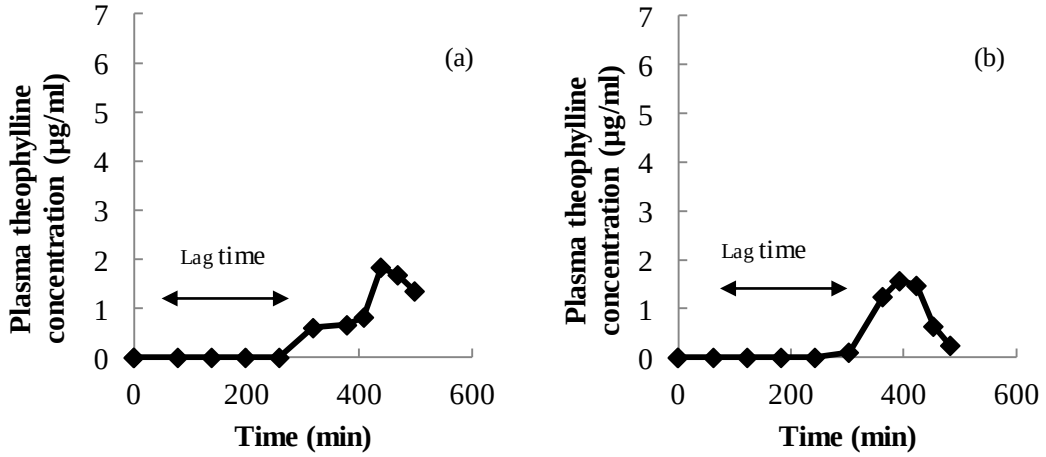

Figure 7.10 Onset normalised plasma concentration-time profile of theophylline after oral administration of predictive 5 hours pulsatile formulation in fasted beagle a) dog 1 and b) dog 2.

As expected this formulation showed longer lag times 313 and 303 minutes in dog 1 and dog 2 respectively, prior to drug absorption. This demonstrates the sustainability and robustness of the barrier layer formed by hydroxypropylmethyl cellulose E50LV in controlling the lag time *in vivo* environment and related well with the experimental *in vitro* lag time of 295 minutes (Section 5.3.4).

The pharmacokinetic parameters are described in Table 7.7 for predictive 3 hours and 5 hours pulsatile formulation.

Table 7.7 Pharmacokinetic parameters for theophylline from orally administered predictive 3 hours and 5 hours pulsatile formulations (n=2 for each formulation) in two dogs at a dose of 100 mg/dog.

Predicted pulse	**Dog fasted**	**T_{lag} (min)**	**C_{max} (µg/ml)**	**T_{max} (min)**	**$AUC_{(0\text{-}2dis)}$ (µg/ml/min)**	**K_{el} (1/min)**
3 hours	1	190	2.4	270	313	0.0174
	2	130	6.6	216	596	0.0115
	Mean	160	4.5	243	454	0.0144
	SD	42	2.9	38	200	0.0041
Predicted pulse	**Dog fasted**	**T_{lag} (min)**	**C_{max} (µg/ml)**	**T_{max} (min)**	**$AUC_{(0\text{-}2dis)}$ (µg/ml/min)**	**K_{el} (1/min)**
5 hours	1	303	1.6	393	229	0.0047
	2	318	1.8	438	519	0.0044
	Mean	310	1.7	415	374	0.0045
	SD	11	0.1	32	205	0.0002

The maximum C_{max} (6.6 µg/ml) and $AUC_{(0\text{-}2dis)}$ (596 µg/ml/min) were observed for pulsatile 3 hrs formulation in dog 2 due to start of core disintegration in stomach as seen in scintigraphic images (Figure 7.5). On three occasions the absorption of theophylline (which is known to be absorbed throughout the GI tract including colon (Hussein et al., 1987)) released from inner core of pulsatile 3 hrs and 5 hrs formulations in the colon have C_{max} (2.4, 1.6 and 1.8µg/ml) and $AUC_{(0\text{-}2dis)}$ (313, 229, 519 µg/ml/min) comparatively low. The incidence of lower absorption from the colon has also been reported for diclofenac sodium (which is also known to be absorbed throughout the GI tract including colon (Tajiri et al., 2010)) in time controlled expulsion system (TES) (Murata et al., 1998) attributing the effect to the slower bowel movement plus lower water content in the colon. The occurrence of low spread due to above mentioned reasons could also be seen in scintigraphic images in Figures 7.4, 7.6 and 7.7.

Tse and Szeto (1982) reported higher theophylline C_{max} 10.3 and 11µg/ml in two dogs for 100mg immediate release capsule compared to the C_{max} (Table 7.8) which was obtained in this study. However, another researcher (Munday et al., 1991) reported theophylline C_{max} 20µg/ml for 300mg immediate release capsule which would roughly equal to C_{max} 6.6µg/ml, if 100mg theophylline would have been used. In this study only one formulation (predicted 3 hour tablet) has given C_{max} 6.6µg/ml (Table 7.7, predictive 3 hour formulation in dog 2) where theophylline started to absorb in the stomach and small intestine. However, in one predicted 3 hour tablet (2.4µg/ml) and in other two 5 hour (1.6 and 1.8µg/ml) tablets C_{max} was lower than the reported values which could be attributed to less absorption of theophylline in distal part of the gut where mostly absorption surface area is smaller compared to upper part of the gut (small intestine). The literature value for T_{max} 120 minutes (Munday et al., 1991) and 72 and 102 minutes (Tse and Szeto, 1982), was found similar in this study in the range of 80-120 minutes for both predicted 3 and 5 hour formulation (Table 7.7) calculated after the pulse time indicating that once the pulse was attained as expected both formulations behaved in terms of T_{max} as an immediate release tablet. Previous reported values for AUC are slightly higher ($AUC_{0\text{-}\infty}$ 9984 µg.min/ml (Munday et al., 1991) and $AUC_{0\text{-}\infty}$ 3186 and 1980 µg.min/ml (Tse and Szeto, 1982)) than this study (predicted 3 hour formulation $AUC_{0\text{-}2dis}$ 313 and 596 µg.min/ml and

predicted 5 hour formulation $AUC_{0\text{-}2dis}$ 229 and 519 µg.min/ml). The reason for lower AUC in this study could be only 2 hour post pulse sampling time compared to 24 hour sampling in literature.

7.3.2.4 Correlation between *in vivo* scintigraphic disintegration and *in vivo* plasma lag time

A good correlation (R^2=0.99) with a slope of 1.08 was achieved between the first appearance of the theophylline in the plasma (T_{lag}) and the disintegration time observed from the scintigraphic studies, as shown in the Figure 7.11.

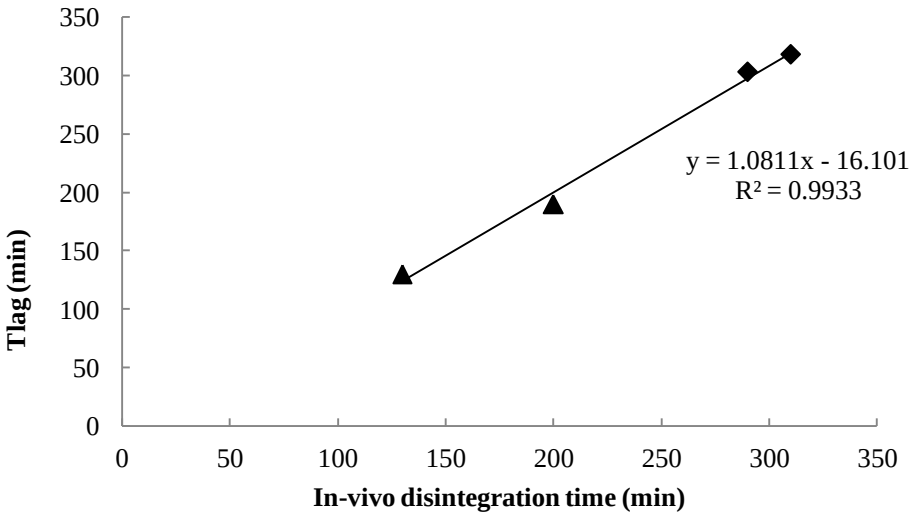

Figure 7.11 Correlation between in vivo drug releases in plasma (T_{lag}) and disintegration observed from scintigraphic images in two beagle dogs for predictive 3 hours (▲), and 5 hours (♦) pulsatile formulation.

7.4 CONCLUSION

Robust and predictive pulsatile formulations were successfully tested in canine model using the gamma scintigraphy as an assisting tool to locate the time and site of pulse in the gastro intestinal tract of the dog. Gamma scintigraphs provided useful information regarding GE, SITT and CA in dogs during this study. The variability in rate and extent of drug absorption observed in pharmacokinetic parameters were better understood with the help of scintigraphic imaging.

Furthermore, a good correlation for both predictive pulsatile 3 hours and 5 hours formulations were observed between *in vitro-in vivo* studies for disintegration and lag time and found independent of pH, site of disintegration and hydrodynamics of GI tract, indicating their vigour and reliability.

However, the scintigraphic study performed in this thesis relied on imaging the dog from posterior aspect leading to highly variable *in vivo* erosion results due to positional factors of the tablet in the GI tract. This resulted in inability to correlate between *in vitro* and *in vivo* erosion profile.

These formulations showed promising results as potential chronopharmaceutical drug delivery systems in the dog as evidence by the observed pulsatile release; however, their suitability in man remains to be determined.

CHAPTER 8

SUMMARY OF CONCLUSIONS AND FUTURE WORK

8.1 CONCLUSIONS

The main aim of the current study was to design a predictable oral controlled release formulation which could be used as a pulsatile or targeted site delivery system to the large intestine.

Time delayed/pulsatile release systems have previously been formulated as pellets, capsules or compression coated tablets. The approach adopted in our studies utilises the methodology of press coating to situate a polymer barrier around an inner core tablet, containing an active pharmaceutical ingredient as an immediate release formulation. It was proposed that the polymer barrier layer, once in contact with the dissolution medium or the intestinal fluid would hydrate and form a cohesive and mechanically strong gel, affording erosion over 3-5 hours, while at the same time keeping the inner core tablet intact. The lag time of drug release from a press coated tablet system is dependent on the following factors: the process of hydration and/or swelling of the layer, dissolution and/or erosion of the barrier layer, and mechanical strength of the barrier layer during these processes.

Therefore, this thesis commences with the investigation of suitable formulation excipients. In Chapter 3, pharmaceutical excipients were tested through preliminary *in vitro* gravimetric hydration and erosion studies, in order to assess their potential for use in further studies as a barrier layer component in a press coated tablet. The prime requisite for a barrier layer in a press coated tablet designed for colon delivery is to remain intact for 3-5 hours (normal intestinal transit time) during *in vitro* erosion studies. Therefore, any formulation which did not sustain itself for the period of 3 to 5 hour erosion studies and disintegrated or on visual and morphological inspection showed non-cohesive tablet surface were considered unsuitable for further studies. *In vitro* gravimetric hydration and erosion studies were initially performed on the following pharmaceutical excipients acacia, sodium alginate, carbopol 971P,

chitin, CMC sodium, Eudragit® E, Eudragit® L, HPMC, lactose, L-HPC and magnesium stearate.

Acacia and sodium alginate were investigated in different ratios and showed complete disintegration in 3 hour erosion studies. Therefore, there further use was not considered appropriate as a barrier layer composite as these formulations were unable to maintain their integrity during 3-5 hour hydration and erosion studies.

L-HPC and Carbopol were mixed with or without magnesium stearate in different ratios. The morphological characteristics of hydrated tablet through visual observation and evaluation of erosion and hydration data revealed that the formulation 9 (L-HPC:Carbopol:magnesium stearate 40:55:5) having erosion 19% could have a potential use for future studies as a barrier layer composite.

Different combinations of Carbopol (anionic polymer) and chitin (cationic polymer) were investigated to exploit their ionic interaction as physical mixture with or without the addition of lactose and magnesium stearate. Through morphological inspection and erosion-hydration data it was concluded that the formulation 12 (Carbopol:chitin:magnesium stearate 65:30:5) and 17 (Carbopol:chitin:magnesium stearate 49.5:50:0.5) have cohesive gel structure and showed less erosion, so can be useful for further studies.

Eudragit® E as a cationic polymer was mixed as a physical mixture with opposite anionic polymers Eudragit® L, acacia, sodium alginate, Carbopol and carrageenan at 50:50 ratios to utilise their ionic interaction as physical mixtures. The hydration and erosion studies revealed that all physical mixtures were completely eroded in 3 hours time leaving no mass to calculate erosion and hydration. Thus, use of these formulations is evidently not suitable for future studies as they clearly demonstrated lack of formulation integrity during 3-5 hour erosion and hydration studies.

L-HPC, HPMC K100M and CMC sodium 20,000Pa were investigated as pure polymers without any added excipients. The data indicates that the L-HPC was completely disintegrated due to its excessive swelling. In case of HPMC and CMC sodium the erosion was found 5.3% and 6.7% respectively and hydration was 286% and 143% respectively, after 5 hour. The hydration states of these polymers revealed

that morphologically they had more cohesive gel structure and have a potential for future studies as a barrier layer component in press coated tablet.

It was concluded that the erosion and hydration characteristics of the polymers have provided to some extent some information regarding integrity and cohesiveness of the hydrated gel. However, due to lack of quantitative data on the performance of gel layer, it was difficult to compare different formulations for their suitability as a barrier layer composition. Therefore, it was decided that to characterise and understand further the barrier layer properties, simple systems like CMC sodium and HPMC capable of forming a cohesive and strong gel would be taken forward for future studies.

It is essential to develop a relatively simple and rapid test which would differentiate among the potential excipients and provide detailed data on the performance of the gel forming components in the formulation as water gradually hydrates the polymer. It is known that the thickness of hydrated gel layer and mechanical gel strength can impart a substantial influence on *in vivo* performance of swellable matrices as matrix integrity might change under mechanical forces presented in human stomach and small intestine. Therefore, the TA instrument, capable of accurately measuring the resistance in the sample to penetration by a test probe was used to screen proposed formulations in terms of gel layer strength. Chapter 3 also discusses the development of a novel texture analysis method, which was capable of identifying and quantifying different regions of hydration in polymer matrices namely hydrating erodible layer, partially hydrated/ diffusion/ rubbery layer and glassy core layer. During TA method development different size and shape of probes (pin Ø2mm, spherical Ø5mm and flat Ø2.5/5mm) were tested. It was observed that the pin probe performed as a more sensitive tool to detect changes in gel layer bringing micro disturbances in local environment during TA profiling and considered appropriate to be used in further studies.

The suitability of the developed texture analyser method was validated using HPMC K100M, K4M and E4MCR as selected polymers. The developed TA method enabled quantification of the thickness and strength changes during hydrating in different regions of the gel over a range of hydration times. By the use of this novel TA

method it was possible to screen proposed formulations in terms of gel layer strength and thickness.

In Chapter 4, different viscosity grades of HPMC were evaluated further as a selected polymer to be used as a barrier layer composite in press coated tablet. The purpose of this chapter was to investigate the hydration and erosion rates in selected grades of HPMC polymer alone or in combination. A new gravimetric hydration and erosion disc method was developed to reduce laborious and time consuming erosion studies. The hydration behaviour observed for these polymers indicated the rate at which they absorbed water and swelled, and in most cases the rate of hydration appeared linear.

The Vergnaud model ($M_t = kt^n$) was used to determine the rate and mechanism of hydration in polymeric matrices. The hydration properties of different HPMC grades (E and K alone or mixture) were best described by using this model. In most cases, the water uptake data revealed a good fit in the model with r^2 = 0.9086-0.987. The exponent, *n*, for HPMC E5LV (0.72), E6LV (0.89), E15LV (0.6), E50LV (0.51), E4MCR (0.51), E10MCR (0.54), K4M (0.52), suggests an anomalous or complex diffusion behaviour i.e., the rate of diffusion of the liquid and that of molecular relaxation are almost of the same magnitude. The value of exponent, *n* is in the range of 0.45-1.0, suggesting that the same substitution series (E-grade) have similar diffusion mechanism. Moreover, it was found that the behaviour of different ratios of mix HPMC K and E grade was complex and difficult to be understood without the help of this model. In case of mixed HPMC E10MCR and E5LV grade, the value of the exponent, *n* for E10MCR:E5LV 25:75 (*n*=0.44) and 50:50 (*n*=0.34) were less than 0.5, while for E10MCR:E5LV 75:25 (*n*=0.51) was greater than 0.5, indicating that an increase in the amount of E10MCR in mixed formulation resulted in a shift in mechanism of liquid diffusion from Fickian to anomalous. Similarly, the K4M and E4MCR mixed grades (K4M:E4MCR (25:75, *n*=0.75), K4M:E4MCR (50:50, *n*=0.39) K4M:E4MCR (75:25, *n*=0.38)) displayed change in diffusion mechanism from diffusion controlled or Fickian to anomalous with increasing concentration of K4M.

The hydration constant (*k*) derived from the Vergnaud model was used as an indicator of the rate of polymer hydration. The smaller values of hydration constant *k* = 0.78, 2.24, 1.77, 6.5 and 9.2 for HPMC E6LV, E5LV, E4MCR, K4M:E4MCR (25:75) and HPMC E15LV respectively, indicated an absence of burst effect in polymer hydration or water uptake. However, the higher values of hydration constant (*k* = 16.22, 16.4, 15.3, 18.8, 19.9, 35.1, 38.7, and 41.1) for K4M, E10MCR, E50LV, E10MCR:E5LV (75:25), E10MCR:E5LV (25:75), K4M:E4MCR (75:25) and (50:50), and E10MCR:E5LV (50:50) respectively, imply that the rate of water penetration is considerably higher and suggest burst water uptake for these HPMC polymers.

The erosion profiles for most HPMC grades were generally found to be linear over a 4 to 5 hour hydration time. The data indicated that in most cases, the profiles were almost linear r^2= 0.8965-0.9987 with their rates of erosion in the range of 0.0204-0.4433%/min. A lower value for rate of erosion indicates slower erosion and vice versa. It can also be observed that the rate of polymer erosion increases with a decrease in polymer molecular weight. It was demonstrated that the rate of erosion for the HPMC shows a decrease in erosion rate with increase in molecular weight. It was also established that the rate of erosion for HPMC E grade has an inverse relationship with its molecular weight that is low molecular weight polymer eroded faster and vice versa.

A texture analyser method developed in Chapter 3 was used to quantify the maximum strength of the hydrated gel layer at the diffusion front at 240 minute hydration time and was correlated with percentage erosion at 240 minutes. A good correlation was demonstrated between erosion and gel strength, showing that this simple methodology can be used to quantify polymer performance as a rate controlling barrier layer. It was also found that polymer erosion and its gel strength were highly dependent on its molecular weight. On the basis of the results obtained for swelling constant (*k*), rate of erosion (%/min), % erosion, and gel strength (N), six polymers/polymer combinations (HPMC E50LV, E10MCR:E5LV 25:75, 50:50, 75:25, K4M:E4MCR 50:50) were chosen as a potential candidates for barrier layer composite in press coated tablets.

In Chapter 5, an attempt was made to predict the quantity of HPMC required to form an eroding barrier layer to achieve required lag times for pulsatile delivery system. Two mathematical methods were developed for the prediction of lag times using the polymer erosion as a main predictor. The first predictive method was based on constant SA/VOL ratio. It was established that increasing SA/VOL value resulted in increase percentage erosion. However, maintaining the constant SA/VOL ratio (1.54 and 1.20 or 1.19) in different tablet sizes (diameter 8 and 13 mm), the percentage erosion profiles versus time were found dissimilar i.e. the erosion profiles did not overlap over each other. It was concluded that the process of erosion differs from that of drug release in HPMC matrices as keeping the SA/VOL ratio constant did not offer similar erosion profiles. Consequently, the SA/VOL ratio method failed to predict accurately different lag times during *in vitro* dissolution studies from press coated tablets.

On the other hand, the second predictive method which was developed using polymer erosion, true and inverse of true density, volume and surface area values provided more promising results. However, in order to develop and successfully implement this type of calculation method it was necessary to characterise the factors like choice of barrier forming polymer, tablet size of the eroding polymer, selection of final tablet size, volume of the inner core tablet, control over applied compression force, and ratio of the quantity of the barrier layers. Initially, during press coated manufacturing, half of the barrier layer quantity was used as bottom layer and remaining half on top of the centrally aligned inner core tablet. This caused the thickness variations for top and bottom surfaces which resulted in variable drug release pattern from press coated tablets. To address the issue of unequal polymer coating on top and bottom of the inner core tablet, the coated polymer was skilfully removed from top and bottom of the inner core tablet and their thickness and weight were measured to quantify the amount acquired. It was found that to maintain a ratio of 1:1 for top and bottom layers almost 34%:66%, 36%:64%, 40%:60% of HPMC E50LV was required to achieve 180, 240 and 300 minutes lag time, respectively. After achieving an equal ratio between top and bottom layers the *in vitro* dissolution revealed a reasonably good correlation between actual and predictive lag times. It

was demonstrated that the new predictable model has a potential in future studies for pulsatile or colon delivery in press coated tablets.

In Chapter 6, the press coated tablets with predicted lag time 3 and 5 hours were imaged using MRI. The routes and timescale of hydration within press coated tablets was followed with the aim of understanding the internal processes and sequence of events that underlie the process of hydration, swelling, gelling and eventually a pulse release from these pulsatile release tablets. MRI setup was attached to USP 4 flow through cell plus UV spectrometer for simultaneous drug release monitoring. The MRI images revealed that the barrier layer made of HPMC E50LV started to hydrate and developed a thick gel layer which continued to grow progressively over the hydration period. It was observed that once the barrier layer was fully hydrated the press coated tablets started to collapse from axial direction which eventually allowed the dissolution medium to penetrate and completely dissolve the inner core tablet.

The expected lag times, which were expected to correspond to the *in vitro* lag time (Chapter 5), were not achieved due to slow flow rate of the dissolution medium through the MRI and USP 4 flow through cell. MRI images were used as a quantitative tool to quantify the changes in gel thickness and inner core/non-hydrated core in formulation during the process of the hydration. It was observed that the tablets expanded more in the axial compared to radial direction which led to the formation of dumbbell shape in MRI images.

In Chapter 7, a scintigraphic dog model was used to compare *in vivo* erosion (*in vivo* percentage radioactivity remaining) with *in vitro* erosion (percentage weight remaining) of HPMC E50LV matrix tablets. The press coated formulations (predictive lag time 3 and 5 hours) performed successfully in the dog using gamma scintigraphy to identify the time and site of pulse in the gastrointestinal tract. The *in vivo* lag time as monitored by scintigraphic images correlated well with the appearance of theophylline in plasma. Scintigraphic imaging was used to explain the observed variability in rate and extent of drug absorption in pharmacokinetic parameters.

In addition to that a good correlation for both predictive pulsatile 3 hours and 5 hours formulations were observed between *in vitro-in vivo* studies and found independent of pH, site of disintegration and hydrodynamics of GI tract, indicating their vigour and reliability.

However, the scintigraphic study performed in this thesis relied on imaging the dog from posterior aspect leading to highly variable *in vivo* erosion results due to positional factors of the tablet in the GI tract. This resulted in an inability to correlate between *in vitro* and *in vivo* erosion profiles.

It was demonstrated through this work that an oral controlled release formulation using press coated technology has been successfully designed which has a potential as a pulsatile or targeted site specific delivery system in the large intestine. The model drug used in this study was theophylline which is hydrophilic and permeable in nature. However, further work is required using the poorly soluble drug as a model compound to access the suitability of this formulation design.

8.2 FUTURE WORK

The current thesis posed some questions which opens some new avenues for future work as suggested below.

- The developed TA method was used to determine the gel strength of a hydrophilic matrix system using distilled water as a dissolution medium however; its usefulness could be further explored with reference to simulated gastric and intestinal media or FDA high fat breakfast.

- A change in diffusion mechanism from diffusion controlled or Fickian to anomalous diffusion was observed during *in vitro* gravimetric hydration-erosion studies when HPMC mix grade (E and K) were used. The applicability of such concepts in the design of controlled release systems could be investigated further.

- A novel mathematical method has been developed to achieve different pulse release times which could be a useful predictive tool in future experiments. Additionally, this method should also be further explored in other eroding polymers such as polyethylene oxide or in other HPMC grades.

- Pulsatile tablets with predicted lag times of 3 and 5 hours were tested in the canine model, however their performance should also be confirmed in human studies.

REFERENCES

Abdou, H. M. (1989). Dissolution, bioavailability & bioequivalence. Mack Pub Co.

Abdul, S. & Poddar, S. S. (2004). A flexible technology for modified release of drugs: multi layered tablets. *Journal of Control Release, 97***,** 393-405.

Abrahamsson, B., Alpsten, M., Bake, B., Jonsson, U. E., Eriksson-Lepkowska, M. & Larsson, A. (1998a). Drug absorption from nifedipine hydrophilic matrix extended-release (ER) tablet-comparison with an osmotic pump tablet and effect of food. *Journal of Controlled Release, 52***,** 301-310.

Abrahamsson, B., Alpsten, M., Bake, B., Larsson, A. & Sjögren, J. (1998b). In vitro and in vivo erosion of two different hydrophilic gel matrix tablets. *European Journal of Pharmaceutics and Biopharmaceutics, 46***,** 69-75.

Abrahamsson, B., Alpsten, M., Jonsson, U. E., Lundberg, P. J., Sandberg, A., Sundgren, M., Svenheden, A. & Tölli, J. (1996). Gastro-intestinal transit of a multiple-unit formulation (metoprolol CR/ZOK) and a non-disintegrating tablet with the emphasis on colon. *International Journal of Pharmaceutics, 140***,** 229-235.

Abrahmsén-Alami, S., Körner, A., Nilsson, I. & Larsson, A. (2007). New release cell for NMR microimaging of tablets: Swelling and erosion of poly(ethylene oxide). *International Journal of Pharmaceutics, 342***,** 105-114.

Adler, J., Jayan, A. & Melia, C. D. (1999). A method for quantifying differential expansion within hydrating hydrophilic matrixes by tracking embedded fluorescent microspheres. *Journal of Pharmaceutical Sciences, 88***,** 371-377.

Alderman, D. A. (1984). A review of cellulose ethers in hydrophilic matrices for oral controlled-release dosage forms. *Internation Journal of Pharmceutical Technology, Production and Manufacturing, 5***,** 1-9.

Allahham, A. & Stewart, P. J. (2007). Enhancement of the dissolution of indomethacin in interactive mixtures using added fine lactose. *European Journal of Pharmaceutics and Biopharmaceutics, 67***,** 732-742.

Amidon, G. L., Lennernäs, H., Shah, V. P. & Crison, J. R. (1995). A Theoretical Basis for a Biopharmaceutic Drug Classification: The Correlation of in Vitro

Drug Product Dissolution and in Vivo Bioavailability. *Pharmaceutical Research, 12***,** 413-420.

Aoyagi, N., Ogata, H., Kaniwa, N., Koibuchi, M., Shibazaki, T., Ejima, A., Tamaki, N., Kamimura, H., Katougi, Y. & Omi, Y. (1982). Bioavailability of griseofulvin from tablets in beagle dogs and correlation with dissolution rate and bioavailability in humans. *Journal of Pharmaceutical Sciences, 71***,** 1169-1172.

Asare-Addo, K., Levina, M., Rajabi-Siahboomi, A. R. & Nokhodchi, A. (2010). Study of dissolution hydrodynamic conditions versus drug release from hypromellose matrices: The influence of agitation sequence. *Colloids and Surfaces B: Biointerfaces, 81***,** 452-460.

Ashford, M., Fell, J., Attwood, D., Sharma, H. & Woodhead, P. (1993a). An evaluation of pectin as a carrier for drug targeting to the colon. *Journal of Controlled Release, 26***,** 213.

Ashford, M., Fell, J. T., Attwood, D., Sharma, H. & Woodhead, P. J. (1993b). An in vivo investigation into the suitability of pH dependent polymers for colonic targeting. *International Journal of Pharmaceutics, 95***,** 193-199.

Aulton, M. E. (2007). Aulton's pharmaceutics.The design and manufacture of medicine. In 3rd (Ed.). Churchill Livingstone.

Awapittaya, B., Pattana-arun, J., Tansatit, T., Kanjanasilpa, P., Sahakijrungruang, C. & Rojanasakul, A. (2007). New concept of ileocecal junction: intussusception of the terminal ileum into the cecum. *World journal of gastroenterology, 13***,** 2855-2857.

Bailey, D. L., Fulton, R. R., Jackson, C. B., Hutton, B. F. & Morris, J. G. (1989). Dynamic Geometric Mean Studies Using a Single Headed Rotating Gamma Camera. *Journal of Nuclear Medicine, 30***,** 1865-1869.

Baille, W. E., Malveau, C., Zhu, X. X. & Marchessault, R. H. (2002). NMR imaging of high-amylose starch tablets. 1. Swelling and water uptake. *Biomacromolecules, 3***,** 214-218.

Bajwa, G. S., Hoebler, K., Sammon, C., Timmins, P. & Melia, C. D. (2006). Microstructural imaging of early gel layer formation in HPMC matrices. *Journal of Pharmaceutical Sciences, 95***,** 2145-2157.

Bansal, V., Sharma, P. K., Sharma, N. & Malviya, O. P. P. a. R. (2011). Applications of Chitosan and Chitosan Derivatives in Drug Delivery. *Advances in Biological Research, 5***,** 28-37.

Bar-Shalom, D., Wilson, C. G. & Washington, N. (2009). Chronotherapy using Egalet™ technology. In B. C. Youan (Ed.) *Chronopharmaceutics.* (pp 165-173.). New Jersey: John Wiley & Sons.

Barberani, F., Corazziari, E., Tosoni, M., Badiali, D., Materia, E., Ribotta, G., Montesani, C., Boschetto, S. & Torsoli, A. (1994). Perendoscopic Manometry of the Distal Ileum and Ileocecal Junction - Technique, Normal Patterns, and Comparison with Transileostomy Manometry. *Gastrointestinal Endoscopy, 40***,** 685-691.

Barrett, K. E., Johnson, L. R., Ghishan, F. K., Merchant, J. L. & Said, H. M. (2006). Physiology of the Gastrointestinal Tract. In 4th (Ed.). Elsevier Science.

Basit, A. W. (2000). Oral colon-specific drug delivery using amylose based film coatings *Pharmaceutical Technology Europe, 12***,** 30-36.

Basit, A. W. (2005). Advances in colonic drug delivery. *Drugs, 65***,** 1991-2007.

Basit, A. W., Newton, J. M., Short, M. D., Waddington, W. A., Ell, P. J. & Lacey, L. F. (2001). The Effect of Polyethylene Glycol 400 on Gastrointestinal Transit: Implications for the Formulation of Poorly-Water Soluble Drugs. *Pharmaceutical Research, 18***,** 1146-1150.

Basit, A. W., Podczeck, F., Michael Newton, J., Waddington, W. A., Ell, P. J. & Lacey, L. F. (2004). The use of formulation technology to assess regional gastrointestinal drug absorption in humans. *European Journal of Pharmaceutical Sciences, 21***,** 179-189.

Basit, A. W., Podczeck, F., Newton, J., Waddington, W., Ell, P. & Lacey, L. (2002). Influence of Polyethylene Glycol 400 on the Gastrointestinal Absorption of Ranitidine. *Pharmaceutical Research, 19***,** 1368-1374.

Basit, A. W., Short, M. D. & McConnell, E. L. (2009). Microbiota-triggered colonic delivery: Robustness of the polysaccharide approach in the fed state in man. *Journal of Drug Targeting, 17***,** 64-71.

Baumgartner, S., Lahajnar, G., Sepe, A. & Kristl, J. (2002). Investigation of the state and dynamics of water in hydrogels of cellulose ethers by 1H NMR spectroscopy. *AAPS Pharmaceutical Science and Technology, 3***,** E36.

Baumgartner, S., Pavli, M. & Kristl, J. (2008). Effect of calcium ions on the gelling and drug release characteristics of xanthan matrix tablets. *European Journal of Pharmaceutics and Biopharmaceutics, 69***,** 698-707.

Bayliss, C. E. & Houston, A. P. (1984). Characterization of plant polysaccharide- and mucin-fermenting anaerobic bacteria from human feces. *Applied and Environmental Microbiology, 48***,** 626-632.

Berliner, D. L. & Nacht, S. (1997). Topical delivery of drugs to the lower gastrointestinal tract. *WO/1997/025980*. USA.

Bettini, R., Catellani, P. L., Santi, P., Massimo, G., Peppas, N. A. & Colombo, P. (2001). Translocation of drug particles in HPMC matrix gel layer: effect of drug solubility and influence on release rate. *Journal of controlled release 70***,** 383-391.

Bhardwaj, T. R., Kanwar, M., Lal, R. & Gupta, A. (2000). Natural Gums and Modified Natural Gums as Sustained-Release Carriers. *Drug Development and Industrial Pharmacy, 26***,** 1025-1038.

Billa, N., Yuen, K.-H., Khader, M. A. A. & Omar, A. (2000). Gamma-scintigraphic study of the gastrointestinal transit and in vivo dissolution of a controlled release diclofenac sodium formulation in xanthan gum matrices. *International Journal of Pharmaceutics, 201***,** 109-120.

Binns, J., Stevens, H. N. E., McEwen, J., Pritchard, G., Brewer, F. M., Clarke, A., Johnson, E. S. & McMillan, I. (1996). The tolerability of multiple oral doses of Pulsincap(TM) capsules in healthy volunteers. *Journal of Controlled Release, 38***,** 151-158.

Bourgeois, S., Harvey, R. & Fattal, E. (2005). Polymer Colon Drug Delivery Systems and their Application to Peptides, Proteins, and Nucleic Acids. *American Journal of Drug Delivery, 3***,** 171-204.

Bruce, L. D., Shah, N. H., Malick, A. W., Infeld, M. H. & McGinity, J. W. (2005). Properties of hot-melt extruded tablet formulations for the colonic delivery of

5-aminosalicylic acid *European Journal of Pharmaceutics and Biopharmaceutics, 59*, 85-97.

Bussemer, T. & Bodmeier, R. (2003). Formulation parameters affecting the performance of coated gelatin capsules with pulsatile release profiles. *International Journal of Pharmaceutics, 267*, 59-68.

Bussemer, T., Dashevsky, A. & Bodmeier, R. (2003). A pulsatile drug delivery system based on rupturable coated hard gelatin capsules. *Journal of Controlled Release, 93*, 331-339.

Cao, X., Leyva, N., Anderson, S. R. & Hancock, B. C. (2008). Use of prediction methods to estimate true density of active pharmaceutical ingredients. *International Journal of Pharmaceutics, 355*, 231-237.

Carstensen, J. T. (2001). Advanced pharmaceutical solids. Marcel Dekker.

Cass, L. M. R., Brown, J., Pickford, M., Fayinka, S., Newman, S. P., Johansson, C. J. & Bye, A. (1999). Pharmacoscintigraphic Evaluation of Lung Deposition of Inhaled Zanamivir in Healthy Volunteers. *Clinical Pharmacokinetics, 36*, 21-31.

Chaibva, F. A., Khamanga, S. M. & Walker, R. B. (2010). Swelling, erosion and drug release characteristics of salbutamol sulfate from hydroxypropyl methylcellulose-based matrix tablets. *Drug Development and Industrial Pharmacy, 36*, 1497-1510.

Chaudhuri, T. (1974). Use of 99mTc. DTPA for measuring gastric emptying time. *Journal of Nuclear Medicine, 15*, 391-395.

Chen , Y. Y., Hughes, L. P., Gladden, L. F. & Mantle, M. D. (2010). Quantitative ultra-fast MRI of HPMC swelling and dissolution. *Journal of Pharmaceutical Sciences, 99*, 3462-3472.

Chowhan, Z. T. (1980). Role of binders in moisture-induced hardness increase in compressed tablets and its effect on in vitro disintegration and dissolution. *Journal of Pharmaceutical Sciences, 69*, 1-4.

Code, C. F. & Marlett, J. A. (1975). The interdigestive myo-electric complex of the stomach and small bowel of dogs. *The Journal of Physiology, 246*, 289-309.

Cohen, S. H. & Levitan, R. (1968). Manometric characteristics of the human ileocecal junctional zone *Gastroenterology, 54*, 72-75.

Cole, S. R. A., Connor A.L, Wilding I.R, Petereit H, Schminke C, Beckert T, Cade D (2002). Enteric coated HPMC capsules designed to achieve intestinal targeting. *International Journal of Pharmaceutics, 231***,** 83-95.

Collins, P. J., Horowitz, M., Cook, D. J., Harding, P. E. & Shearman, D. J. (1983). Gastric emptying in normal subjects--a reproducible technique using a single scintillation camera and computer system. *Gut, 24***,** 1117-1125.

Colombo, P. (1993). Swelling-controlled release in hydrogel matrices for oral route. *Advanced Drug Delivery Reviews, 11***,** 37-57.

Colombo, P., Bettini, R., Massimo, G., Catellani, P. L., Santi, P. & Peppas, N. A. (1995). Drug diffusion front movement is important in drug release control from swellable matrix tablets. *Journal of Pharmaceutical Sciences, 84***,** 991-997.

Colombo, P., Bettini, R., Santi, P. & Peppas, N. A. (2000). Swellable matrices for controlled drug delivery: gel-layer behaviour, mechanisms and optimal performance. *Pharmaceutical Science & Technology Today, 3***,** 198-204.

Constable, A. R. (1969). The gamma camera. *British Journal of Urology, 41***,** 38-45.

Conte, U., Colombo, P., Gazzaniga, A., Sangalli, M. E. & La Manna, A. (1988). Swelling-activated drug delivery systems. *Biomaterials, 9***,** 489-493.

Conte, U., Maggi, L., Torre, M. L., Giunchedi, P. & Manna, A. L. (1993). Press-coated tablets for time-programmed release of drugs. *Biomaterials, 14***,** 1017-1023.

Corá, L. A., Américo, M. F., Romeiro, F. G., Oliveira, R. B. & Miranda, J. R. A. (2010). Pharmaceutical applications of AC Biosusceptometry. *European Journal of Pharmaceutics and Biopharmaceutics, 74***,** 67-77.

Corazziari, E., Barberani, F., Tosoni, M., Boschetto, S. & Torsoli, A. (1991). Perendoscopic Manometry of the Distal Ileum and Ileocecal Junction in Humans. *Gastroenterology, 101***,** 1314-1319.

Coupe, A., Davis, S. & Wilding, I. (1991). Variation in Gastrointestinal Transit of Pharmaceutical Dosage Forms in Healthy Subjects. *Pharmaceutical Research, 8***,** 360-364.

Coupe, A. J., Davis, S. S., Evans, D. F. & Wilding, I. R. (1992a). The effect of sleep on the gastrointestinal transit of pharmaceutical dosage forms. *International Journal of Pharmaceutics, 78*, 69-76.

Coupe, A. J., Davis, S. S., Evans, D. F. & Wilding, I. R. (1992b). Nocturnal scintigraphic imaging to investigate the gastrointestinal transit of dosage forms. *Journal of Controlled Release, 20*, 155-162.

Cutler, N. R., Anders, R. J., Jhee, S. S., Sramek, J. J., Awan, N. A., Bultas, J., Lahiri, A. & Woroszylska, M. (1995). Placebo-controlled evaluation of three doses of a controlled-onset, extended-release formulation of verapamil in the treatment of stable angina pectoris. *The American Journal of Cardiology, 75*, 1102-1106.

Dabbagh, M. A., Ford, J. L., Rubinstein, M. H., Hogan, J. E. & Rajabi-Siahboomi, A. R. (1999). Release of Propranolol Hydrochloride from Matrix Tablets Containing Sodium Carboxymethylcellulose and Hydroxypropylmethylcellulose. *Pharmaceutical Development and Technology, 4*, 313-324.

Dash, M., Chiellini, F., Ottenbrite, R. M. & Chiellini, E. (2011). Chitosan--A versatile semi-synthetic polymer in biomedical applications. *Progress in Polymer Science, 36*, 981-1014.

Davis, S. S. (2005). Formulation strategies for absorption windows. *Drug discovery today, 10*, 249-257.

Davis, S. S., Hardy, J. G. & Fara, J. W. (1986). Transit of pharmaceutical dosage forms through the small intestine. *Gut, 27*, 886-892.

Davis, S. S., Hardy, J. G., Taylor, M. J., Whalley, D. R. & Wilson, C. G. (1984a). A comparative study of the gastrointestinal transit of a pellet and tablet formulation. *International Journal of Pharmaceutics, 21*, 167-177.

Davis, S. S., Hardy, J. G., Taylor, M. J., Whalley, D. R. & Wilson, C. G. (1984b). The effect of food on the gastrointestinal transit of pellets and an osmotic device (Osmet). *International Journal of Pharmaceutics, 21*, 331-340.

Davis, S. S., Khosia, R., Wilson, C. G. & Washington, N. (1987). Gastrointestinal transit of a controlled-release pellet formulation of tiaprofenic acid and the effect of food. *International Journal of Pharmaceutics, 35*, 253-258.

Davis, S. S., Robertson, C. & Wilding, I. R. (1991). Gastrointestinal transit of a multiparticulate tablet formulation in patients with active ulcerative colitis. *International Journal of Pharmaceutics, 68***,** 199-204.

Davis, S. S., Wilding, E. A. & Wilding, I. R. (1993). Gastrointestinal transit of a matrix tablet formulation: comparison of canine and human data. *International Journal of Pharmaceutics, 94***,** 235-238.

Digenis, G. A. & Sandefer, E. (1991). Gamma scintigraphy and neutron activation techniques in the in vivo assessment of orally administered dosage forms. *Critical reviews in therapeutic drug carrier systems, 7***,** 309-345.

Digenis, G. A., Sandefer, E. P., Page, R. C. & Doll, W. J. (1998). Gamma scintigraphy: an evolving technology in pharmaceutical formulation development--Part 1. *Pharmaceutical Science & Technology Today, 1***,** 100-108.

Dinning, P. G., Bampton, P. A., Kennedy, M. L., Kajimoto, T., Lubowski, D. Z., de Carle, D. J. & Cook, I. J. (1999). Basal pressure patterns and reflexive motor responses in the human ileocolonic junction. *American Journal of Physiology - Gastrointestinal and Liver Physiology, 276***,** G331-G340.

Dow Chemical Company (2011). Using Dow Excipients for Controlled Release of Drugs in Hydrophilic Matrix Systems. Retrieved May 8, 2011 from http://msdssearch.dow.com/PublishedLiteratureDOWCOM/dh_0379/0901b803803797ad.pdf?filepath=/198-02075.pdf&fromPage=GetDoc.

Dressman, J. B. (1986). Comparison of Canine and Human Gastrointestinal Physiology. *Pharmaceutical Research, 3***,** 123-131.

Dressman, J. B., Berardi, R. R., Dermentzoglou, L. C., Russell, T. L., Schmaltz, S. P., Barnett, J. L. & Jarvenpaa, K. M. (1990). Upper gastrointestinal (GI) pH in young, healthy men and women. *Pharmaceutical Research, 7***,** 756-761.

Ebube, N. K., Hikal, A. H., Wyandt, C. M., Beer, D. C., Miller, L. G. & Jones, A. B. (1997). Sustained release of acetaminophen from heterogeneous matrix tablets: influence of polymer ratio, polymer loading, and co-active on drug release. *Pharmaceutical Development and Technology, 2***,** 161-170.

Ebube, N. K. & Jones, A. B. (2004). Sustained release of acetaminophen from a heterogeneous mixture of two hydrophilic non-ionic cellulose ether polymers. *International Journal of Pharmaceutics, 272***,** 19-27.

Efentakis, M., Koligliati, S. & Vlachou, M. (2006). Design and evaluation of a dry coated drug delivery system with an impermeable cup, swellable top layer and pulsatile release. *International Journal of Pharmaceutics, 311***,** 147-156.

Evans, D. F., Pye, G., Bramley, R., Clark, A. G., Dyson, T. J. & Hardcastle, J. D. (1988). Measurement of gastrointestinal pH profiles in normal ambulant human subjects. *Gut, 29***,** 1035-1041.

Fadda, H., McConnell, E., Short, M. & Basit, A. W. (2009). Meal-Induced Acceleration of Tablet Transit Through the Human Small Intestine. *Pharmaceutical Research, 26***,** 356-360.

Fahie, B. J., Nangia, A., Chopra, S. K., Fyfe, C. A., Grondey, H. & Blazek, A. (1998). Use of NMR imaging in the optimization of a compression-coated regulated release system. *Journal of Controlled Release, 51***,** 179-184.

Feinle, C., Kunz, P., Boesiger, P., Fried, M. & Schwizer, W. (1999). Scintigraphic validation of a magnetic resonance imaging method to study gastric emptying of a solid meal in humans. *Gut, 44***,** 106-111.

Fifield, F. W. K., D. (2000). Principles and Practice of Analytical Chemistry. In 5th (Ed.). Wiley-Blackwell.

Food and Drug Administration. (2001). Guidance for Industry: Bioanalytical Method Validation. *US Department of Health and Human Services.* Center for Drug Evaluation and Research, Rockville, MD.

Fukui, E., Miyamura, N. & Kobayashi, M. (2001a). An in vitro investigation of the suitability of press-coated tablets with hydroxypropylmethylcellulose acetate succinate (HPMCAS) and hydrophobic additives in the outer shell for colon targeting. *Journal of Controlled Release, 70***,** 97-107.

Fukui, E., Miyamura, N., Uemura, K. & Kobayashi, M. (2000a). Preparation of enteric coated timed-release press-coated tablets and evaluation of their function by in vitro and in vivo tests for colon targeting. *International Journal of Pharmaceutics, 204***,** 7-15.

Fukui, E., Miyamura, N., Yoneyama, T. & Kobayashi, M. (2001b). Drug release from and mechanical properties of press-coated tablets with hydroxypropylmethylcellulose acetate succinate and plasticizers in the outer shell. *International Journal of Pharmaceutics, 217***,** 33-43.

Fukui, E., Uemura, K. & Kobayashi, M. (2000b). Studies on applicability of press-coated tablets using hydroxypropylcellulose (HPC) in the outer shell for timed-release preparations. *Journal of Controlled Release, 68***,** 215-223.

Fyfe, C. A., Grondey, H., Blazek-Welsh, A. I., Chopra, S. K. & Fahie, B. J. (2000). NMR imaging investigations of drug delivery devices using a flow-through USP dissolution apparatus. *Journal of Controlled Release, 68***,** 73-83.

Gao, P. & Meury, R. H. (1996). Swelling of hydroxypropyl methylcellulose matrix tablets. 1. Characterization of swelling using a novel optical imaging method. *Journal of Pharmaceutical Sciences, 85***,** 725-731.

Gao, P., Skoug, J. W., Nixon, P. R., Robert Ju, T., Stemm, N. L. & Sung, K.-C. (1996). Swelling of hydroxypropyl methylcellulose matrix tablets. 2. Mechanistic study of the influence of formulation variables on matrix performance and drug release. *Journal of Pharmaceutical Sciences, 85***,** 732-740.

Gao, Z. (2009). In Vitro Dissolution Testing with Flow-Through Method: A Technical Note. *AAPS Pharmaceutical Science and Technology, 10***,** 1401-1405.

Gazzaniga, A., Iamartino, P., Maffione, G. & Sangalli, M. E. (1994). Oral delayed-release system for colonic specific delivery. *International Journal of Pharmaceutics, 108***,** 77-83.

Gazzaniga, A., Maroni, A., Sangalli, M. E. & Zema, L. (2006). Time-controlled oral delivery systems for colon targeting. *Expert Opinion on Drug Delivery, 3***,** 583-597.

Gazzaniga, A., Palugan, L., Foppoli, A. & Sangalli, M. E. (2008). Oral pulsatile delivery systems based on swellable hydrophilic polymers. *European Journal of Pharmaceutics and Biopharmaceutics, 68***,** 11-18.

Gennaro, A. R. (2005). Remington: the science and practice of pharmacy. In 21st (Ed.). Lippincott Williams & Wilkins.

Ghimire, M., Hodges, L. A., Band, J., Lindsay, B., O'Mahony, B., McInnes, F. J., Mullen, A. B. & Stevens, H. N. E. (2011). Correlation between in vitro and in vivo erosion behaviour of erodible tablets using gamma scintigraphy. *European Journal of Pharmaceutics and Biopharmaceutics, 77***,** 148-157.

Ghimire, M., Hodges, L. A., Band, J., O'Mahony, B., McInnes, F. J., Mullen, A. B. & Stevens, H. N. E. (2010). In-vitro and in-vivo erosion profiles of hydroxypropylmethylcellulose (HPMC) matrix tablets. *Journal of Controlled Release, 147***,** 70-75.

Ghimire, M., McInnes, F. J., Watson, D. G., Mullen, A. B. & Stevens, H. N. E. (2007). In-vitro/in-vivo correlation of pulsatile drug release from press-coated tablet formulations: a pharmacoscintigraphic study in the beagle dog. *European Journal of Pharmaceutics and Biopharmaceutics, 67***,** 515-523.

Gohel, M. C. & Sumitra , M. G. (2002). Modulation of active pharmaceutical material release from a novel tablet in capsule system' containing an effervescent blend. *Journal of Controlled Release, 79***,** 157-164.

Gómez-Burgaz, M., García-Ochoa, B. & Torrado-Santiago, S. (2008). Chitosan-carboxymethylcellulose interpolymer complexes for gastric-specific delivery of clarithromycin. *International Journal of Pharmaceutics, 359***,** 135.

Goole, J., Van Gansbeke, B., Pilcer, G., Deleuze, P., Blocklet, D., Goldman, S., Pandolfo, M., Vanderbist, F. & Amighi, K. (2008). Pharmacoscintigraphic and pharmacokinetic evaluation on healthy human volunteers of sustained-release floating minitablets containing levodopa and carbidopa. *International Journal of Pharmaceutics, 364***,** 54-63.

Greaves, J. L., Wilson, C. G., Rozier, A., Grove, J. & Plazonnet, B. (1990). Scintigraphic assessment of an ophthalmic gelling vehicle in man and rabbit. *Current Eye Research, 9***,** 415-420.

Gupta et al, L. A., F. Theeuwes, P. Wong, P.J. Gilbert and J. Longstreth (1996). Pharmacokinetics of verapamil from an osmotic system with delayed onset. *European Journal of Pharmaceutics and Biopharmaceutics, 42***,** 74-81.

Hardy, J. G., Wilson, C. G. & Wood, E. (1985). Drug delivery to the proximal colon. *Journal of Pharmacy and Pharmacology, 37***,** 874-877.

Harland, R. S., Gazzaniga, A., Sangalli, M. E., Colombo, P. & Peppas, N. A. (1988). Drug/Polymer Matrix Swelling and Dissolution. *Pharmaceutical Research, 5***,** 488-494.

Hebden, J. M., Blackshaw, P., E, Perkins, A., C, Wilson, C., G & Spiller, R., C (2000). Limited exposure of the healthy distal colon to orally-dosed formulation is further exaggerated in active left-sided ulcerative colitis. *Alimentary Pharmacology & Therapeutics, 14***,** 155-161.

Hejazi, R. & Amiji, M. (2003). Chitosan-based gastrointestinal delivery systems. *Journal of Controlled Release, 89***,** 151-165.

Hinton, J. M., Lennard-Jones, J. E. & Young, A. C. (1969). A new method for studying gut transit times using radioopaque markers. *Gut, 10***,** 842-847.

Hodges, L. A., Connolly, S. M., Band, J., O'Mahony, B., Ugurlu, T., Turkoglu, M., Wilson, C. G. & Stevens, H. N. E. (2009). Scintigraphic evaluation of colon targeting pectin-HPMC tablets in healthy volunteers. *International Journal of Pharmaceutics, 370***,** 144-150.

Hodges, L. A., Stevens, H. N. E. & Mullen, A. B. (2004). Puncture test to simulate rapturing of ethylcellulose coat of a time-controlled delivery system. *AAPS Pharmaceutical Sciences* T3272.

Houghton, L. A., Mangnall, Y. F. & Read, N. W. (1990). Effect of incorporating fat into a liquid test meal on the relation between intragastric distribution and gastric emptying in human volunteers. *Gut, 31***,** 1226-1229.

Hu, Z., Kimura, G., Mawatari, S.-s., Shimokawa, T., Yoshikawa, Y. & Takada, K. (1998). New preparation method of intestinal pressure-controlled colon delivery capsules by coating machine and evaluation in beagle dogs. *Journal of Controlled Release, 56***,** 293-302.

Hu, Z., Mawatari, S., Shibata, N., Takada, K., Yoshikawa, H., Arakawa, A. & Yosida, Y. (2000a). Application of a biomagnetic measurement system (BMS) to the evaluation of gastrointestinal transit of intestinal pressure-controlled colon delivery capsules (PCDCs) in human subjects. *Pharmaceutical Research, 17***,** 160-167.

Hu, Z., Mawatari, S., Shimokawa, T., Kimura, G., Yoshikawa, Y., Shibata, N. & Takada, K. (2000b). Colon Delivery Efficiencies of Intestinal Pressure-

controlled Colon Delivery Capsules Prepared by a Coating Machine in Human Subjects. *Journal of Pharmacy and Pharmacology, 52***,** 1187.

Hunt, J. N. (1983). Mechanisms and Disorders of Gastric Emptying. *Annual Review of Medicine, 34***,** 219-229.

Hussain, M. S. H., York, P. & Timmins, P. (1992). Effect of commercial and high purity magnesium stearates on in-vitro dissolution of paracetamol DC tablets. *International Journal of Pharmaceutics, 78***,** 203-207.

Hussein, Z., Bialer, M., Friedman, M. & Raz, I. (1987). Comparative pharmacokinetic evaluation of sustained-release theophylline formulations in dogs and humans. *International Journal of Pharmaceutics, 37***,** 97-102.

Ibekwe, V. C., Liu, F., Fadda, H. M., Khela, M. K., Evans, D. F., Parsons, G. E. & Basit, A. W. (2006). An investigation into the in vivo performance variability of pH responsive polymers for ileo-colonic drug delivery using gamma scintigraphy in humans. *Journal of Pharmaceutical Sciences, 95***,** 2760-2766.

Ishibashi, T., Ikegami, K., Kubo, H., Kobayashi, M., Mizobe, M. & Yoshino, H. (1999). Evaluation of colonic absorbability of drugs in dogs using a novel colon-targeted delivery capsule (CTDC). *Journal of Controlled Release, 59***,** 361-376.

Ishino, R., Yoshino, H., Hirakawa, Y. & Noda, K. (1992). Design and preparation of pulsatile release tablet as a new oral drug delivery system. *Chemical and Pharmaceutical Bbulletin, 40***,** 3036-3041.

Itoh, T., Higuchi, T., Gardner, C. R. & Caldwell, L. (1986). Effect of particle size and food on gastric residence time of non-disintegrating solids in beagle dogs. *Journal of Pharmacy and Pharmacology, 38***,** 801-806.

Jamzad, S., Tutunji, L. & Fassihi, R. (2005). Analysis of macromolecular changes and drug release from hydrophilic matrix systems. *International Journal of Pharmaceutics, 292***,** 75-85.

Johnson, L. R. (2000). Gastrointestinal physiology In 5th (Ed.). St. Louis: Mosby

Jorgensen, F., Hesse, B., Tromholt, N., Hojgaard, L. & Stubgaard, M. (1992). Esophageal Scintigraphy: Reproducibility and Normal Ranges. *Journal of Nuclear Medicine, 33***,** 2106-2109.

Joseph, D., William, Spruill, William, Wade (2010). *Concepts in Clinical Pharmacokinetics*, (Editor ed.).

Joshi, S. C., Chen, B., Lim, C. T. & Goh, J. C. H. (2009). Swelling, Dissolution and Disintegration of HPMC in Aqueous Media. *13th International Conference on Biomedical Engineering*. Vol 23, Track 4 (pp. 1244-1247).

Kamba, M., Seta, Y., Kusai, A., Ikeda, M. & Nishimura, K. (2000). A unique dosage form to evaluate the mechanical destructive force in the gastrointestinal tract. *International Journal of Pharmaceutics, 208***,** 61-70.

Kamba, M., Seta, Y., Kusai, A. & Nishimura, K. (2001). Evaluation of the mechanical destructive force in the stomach of dog. *International Journal of Pharmaceutics, 228***,** 209-217.

Kamba, M., Seta, Y., Kusai, A. & Nishimura, K. (2002). Comparison of the mechanical destructive force in the small intestine of dog and human. *International Journal of Pharmaceutics, 237***,** 139-149.

Kararli, T. T. (1995). Comparison of the gastrointestinal anatomy, physiology, and biochemistry of humans and commonly used laboratory animals. *Biopharmaceutics & Drug Disposition, 16***,** 351-380.

Katori, N., Aoyagi, N. & Terao, T. (1995). Estimation of Agitation Intensity in the GI Tract in Humans and Dogs Based on Invitro-Invivo Correlation. *Pharmaceutical Research, 12***,** 237-243.

Katstra, W. E., Palazzolo, R. D., Rowe, C. W., Giritlioglu, B., Teung, P. & Cima, M. J. (2000). Oral dosage forms fabricated by Three Dimensional Printing. *Journal of Controlled Release, 66***,** 1-9.

Kavanagh, N. & Corrigan, O. I. (2004). Swelling and erosion properties of hydroxypropylmethylcellulose (Hypromellose) matrices--influence of agitation rate and dissolution medium composition. *International Journal of Pharmaceutics, 279***,** 141-152.

Khan, A. K. A., Piris, J. & Truelove, S. C. (1977). An Experiment To Determine The Active Therapeutic Moiety Of Sulphasalazine. *The lancet, 310***,** 892-895.

Khan, G. M. & Jiabi, Z. (1998). Formulation and in vitro evaluation of ibuprofen-carbopol® 974P-NF controlled release matrix tablets III: influence of co-

excipients on release rate of the drug. *Journal of Controlled Release, 54*, 185-190.

Khan, M. Z. I., Prebeg, Z. & Kurjakovic, N. (1999). A pH-dependent colon targeted oral drug delivery system using methacrylic acid copolymers: I. Manipulation of drug release using Eudragit® L100-55 and Eudragit® S100 combinations. *Journal of Controlled Release, 58*, 215-222.

Khosla, R. & Davis, S. S. (1989). Gastric emptying and small and large bowel transit of non-disintegrating tablets in fasted subjects. *International Journal of Pharmaceutics, 52*, 1-10.

Khosla, R. & Davis, S. S. (1990). The effect of tablet size on the gastric emptying of non-disintegrating tablets. *International Journal of Pharmaceutics, 62*, R9-R11.

Khosla, R., Feely, L. C. & Davis, S. S. (1989). Gastrointestinal transit of non-disintegrating tablets in fed subjects. *International Journal of Pharmaceutics, 53*, 107-117.

Kinget, R., Kalala, W., Vervoort, L. & van den Mooter, G. (1998). Colonic Drug Targeting. *Journal of Drug Targeting, 6*, 129-149.

Kleinebudde, P. (1993). Application of low substituted hydroxypropylcellulose (L-HPC) in the production of pellets using extrusion/spheronization. *International Journal of Pharmaceutics, 96*, 119-128.

Konrad, R., Christ, A., Zessin, G. & Cobet, U. (1998). The use of ultrasound and penetrometer to characterize the advancement of swelling and eroding fronts in HPMC matrices. *International Journal of Pharmaceutics, 163*, 123-131.

Körner, A., Larsson, A., Andersson, Å. & Piculell, L. (2010). Swelling and polymer erosion for poly(ethylene oxide) tablets of different molecular weights polydispersities. *Journal of Pharmaceutical Sciences, 99*, 1225-1238.

Korsmeyer, R. W., Gurny, R., Doelker, E., Buri, P. & Peppas, N. A. (1983). Mechanisms of solute release from porous hydrophilic polymers. *International Journal of Pharmaceutics, 15*, 25-35.

Kovacevic, D., Borkovic, S. & Pozar, J. (2007). The influence of ionic strength, electrolyte type and preparation procedure on formation of weak

polyelectrolyte complexes. *Colloids and Surfaces A: Physicochemical and Engineering Aspects, 302*, 107-112.

Krishnaiah, Y. S. R., Satyanarayana, S., Rama Prasad, Y. V. & Narasimha Rao, S. (1998). Gamma scintigraphic studies on guar gum matrix tablets for colonic drug delivery in healthy human volunteers. *Journal of Controlled Release, 55*, 245-252.

Krogel, I. & Bodmeier, R. (1998). Pulsatile Drug Release from an Insoluble Capsule Body Controlled by an Erodible Plug. *Pharmaceutical Research, 15*, 474-481.

Krogel, I. & Bodmeier, R. (1999). Evaluation of an enzyme-containing capsular shaped pulsatile drug delivery system. *Pharmaceutical Research, 16*, 1424-1429.

Kumar, D. & Phillips, S. (1987). The contribution of external ligamentous attachements to function of the ileocecal junction *Diseases of Colon Rectum, 13*, 410-416.

Kumar, R. & Majeti, N. V. (2000). A review of chitin and chitosan applications. *Reactive and Functional Polymers, 46*, 1-27.

Langer, R. S. & Peppas, N. A. (1981). Present and future applications of biomaterials in controlled drug delivery systems. *Biomaterials, 2*, 201-214.

Lapidus, H. & Lordi, N. G. (1968). Drug release from compressed hydrophilic matrices. *Journal of Pharmaceutical Sciences, 57*, 1292-1301.

Lerner, I. E., Flashner, M. & Penhasi, A. (2000). Local Delivery Of Drugs To The Colon For Local Treatment Of Colonic Diseases. *WO2000028974*. USA.

Li, H. & Gu, X. (2007). Correlation between drug dissolution and polymer hydration: A study using texture analysis. *International Journal of Pharmaceutics, 342*, 18-25.

Lin, S.-Y., Lin, K.-H. & Li, M.-J. (2001). Micronized ethylcellulose used for designing a directly compressed time-controlled disintegration tablet. *Journal of Controlled Release, 70*, 321-328.

Lin, S.-Y., Lin, K.-H. & Li, M.-J. (2004). Formulation design of double-layer in the outer shell of dry-coated tablet to modulate lag time and time-controlled

dissolution function: Studies on micronized ethylcellulose for dosage form design (VII). *The AAPS Journal, 6***,** 1-6.

Lin, S. Y. & Ayres, J. W. (1992). Calcium Alginate Beads as Core Carriers of 5-Aminosalicylic Acid. *Pharmaceutical Research, 9***,** 1128-1131.

Liu, J. & Cetinkaya, C. (2010). Mechanical and geometric property characterization of dry-coated tablets with contact ultrasonic techniques. *International Journal of Pharmaceutics, 392***,** 148-155.

Lui, C. Y., Amidon, G. L., Berardi, R. R., Fleisher, D., Youngberg, C. & Dressman, J. B. (1986). Comparison of gastrointestinal pH in dogs and humans: Implications on the use of the beagle dog as a model for oral absorption in humans. *Journal of Pharmaceutical Sciences, 75***,** 271-274.

Madhusudan, R. Y., Veni, J. K. & Jayasagar, G. (2001). Formulation and Evaluation of Diclofenac Sodium Using Hydrophilic Matrices. *Drug Development and Industrial Pharmacy, 27***,** 759-766.

Maggi, L., Segale, L., Ochoa Machiste, E., Faucitano, A., Buttafava, A. & Conte, U. (2004). Polymers-gamma ray interaction. Effects of gamma irradiation on modified release drug delivery systems for oral administration. *International Journal of Pharmaceutics, 269***,** 343-351.

Majid Khan, G. & Zhu, J.-B. (1999). Studies on drug release kinetics from ibuprofen-carbomer hydrophilic matrix tablets: influence of co-excipients on release rate of the drug. *Journal of Controlled Release, 57***,** 197-203.

Malaterre, V., Metz, H., Ogorka, J., Gurny, R., Loggia, N. & Mäder, K. (2009). Benchtop-magnetic resonance imaging (BT-MRI) characterization of push-pull osmotic controlled release systems. *Journal of Controlled Release, 133***,** 31-36.

Malveau, C., Baille, W. E., Zhu, X. X. & Marchessault, R. H. (2002). NMR imaging of high-amylose starch tablets. 2. Effect of tablet size. *Biomacromolecules, 3***,** 1249-1254.

Manning, T. S. & Gibson, G. R. (2004). Prebiotics. *Best Practice & Research Clinical Gastroenterology, 18***,** 287-298.

Marcela, H. y. d. l. P., Yolanda, V. A., Adriana, M. D.-R. & Alma, R. C. A. (2003). Comparison of Dissolution Profiles for Albendazole Tablets Using USP

Apparatus 2 and 4. *Drug Development and Industrial Pharmacy, 29***,** 777-784.

Maroni, A., Zema, L., Del Curto, M. D., Loreti, G. & Gazzaniga, A. (2010). Oral pulsatile delivery: Rationale and chronopharmaceutical formulations. *International Journal of Pharmaceutics, 398***,** 1-8.

Marvola, J., Kanerva, H., Slot, L., Lipponen, M., Kekki, T., Hietanen, H., Mykkanen, S., Ariniemi, K., Lindevall, K. & Marvola, M. (2004). Neutron activation-based gamma scintigraphy in pharmacoscintigraphic evaluation of an Egalet constant-release drug delivery system. *International Journal of Pharmaceutics, 281***,** 3-10.

Masazumi, K., Shuichi, A., Katsuo, K., Toyohiko, H., Kazuharu, A. & Hiroaki, N. (1998). Magnetic Resonance Imaging (MRI) Study of Swelling and Water Mobility in Micronized Low-Substituted Hydroxypropylcellulose Matrix Tablets. *Chemical & pharmaceutical bulletin, 46***,** 324-328.

Mastiholimath, V. S., Dandagi, P. M., Jain, S. S., Gadad, A. P. & Kulkarni, A. R. (2007). Time and pH dependent colon specific, pulsatile delivery of theophylline for nocturnal asthma. *International Journal of Pharmaceutics, 328***,** 49-56.

Maurer, A. H., Knight, L. C., Charkes, N. D., Vitti, R. A., Krevsky, B., Fisher, R. S. & Siegel, J. A. (1991). Comparison of left anterior oblique and geometric mean gastric emptying. *Journal of nuclear medicine, 32***,** 2176-2180.

McConnell, E. L., Liu, F. & Basit, A. W. (2009). Colonic treatments and targets: issues and opportunities. *Journal of Drug Targeting, 17***,** 335-363.

McConville, J. T., Hodges, L.-A., Jones, T., Band, J. P., O'Mahony, B., Lindsay, B., Ross, A. C., Florence, A. J., Stanley, A. J., Humphrey, M. J., Wilson, C. G. & Stevens, H. N. E. (2009). A pharmacoscintigraphic study of three time-delayed capsule formulations in healthy male volunteers. *Journal of Pharmaceutical Sciences, 98***,** 4251-4263.

McCrystal, C. B., Ford, J. L. & Rajabi-Siahboomi, A. R. (1999). Water distribution studies within cellulose ethers using differential scanning calorimetry. 2. Effect of polymer substitution type and drug addition. *Journal of Pharmaceutical Sciences, 88***,** 797-801.

McInnes, F. J., Clear, N., Humphrey, M. & Stevens, H., N, E (2008). In Vivo In Vitro Performance of an Oral MR Matrix Tablet Formulation in the Beagle Dog in the Fed and Fasted State: Assessment of Mechanical Weakness. *Pharmaceutical Research, 25***,** 1075-1084.

McInnes, F. J., Stevens, H. N., Humphrey, M. & Clear, N. (2005a). Preliminary evaluation of procedure for the gamma scintigraphic study of behaviour of oral dosage forms in the gastrointestinal tract of the beagle dogs. *32nd International Symposium on Controlled Release of Bioactive Materials.* Montreal, Canada.

McInnes, F. J., Stevens, H. N. E., Humphrey, M. & Clear, N. (2005b). Evaluation of Gastrointestinal Transit in the Dog Using Gamma Scintigraphy *American Association of Pharmaceutical Sciences*

Melia, C. D., A.R.Rajabi-Siahboomi, R.W. Bowtell (1998). Magnetic resonance imaging of controlled release pharmaceutical dosage form *Pharmaceutical Science Technology, Today, 1***,** 32-39.

Meshali, M. M. & Gabr, K. E. (1993). Effect of interpolymer complex formation of chitosan with pectin or acacia on the release behaviour of chlorpromazine HCl. *International Journal of Pharmaceutics, 89***,** 177-181.

Michailova, V., Titeva, S., Kotsilkova, R., Krusteva, E. & Minkov, E. (2000). Water uptake and relaxation processes in mixed unlimited swelling hydrogels. *International Journal of Pharmaceutics, 209***,** 45-56.

Mikac, U., Sepe, A., Kristl, J. & Baumgartner, S. (2010). A new approach combining different MRI methods to provide detailed view on swelling dynamics of xanthan tablets influencing drug release at different pH and ionic strength. *Journal of Controlled Release, 145***,** 247-256.

Mladenovska, K., Raicki, R. S., Janevik, E. I., Ristoski, T., Pavlova, M. J., Kavrakovski, Z., Dodov, M. G. & Goracinova, K. (2007). Colon-specific delivery of 5-aminosalicylic acid from chitosan-Ca-alginate microparticles. *International Journal of Pharmaceutics, 342***,** 124-136.

Mojaverian, P., Ferguson, R. K., Vlasses, P. H., Rocci, M. L., Jr., Oren, A., Fix, J. A., Caldwell, L. J. & Gardner, C. (1985). Estimation of gastric residence time

of the Heidelberg capsule in humans: effect of varying food composition. *Gastroenterology, 89***,** 392-397.

Moussa, I. S. & Cartilier, L. H. (1997). Evaluation of cross-linked amylose press-coated tablets for sustained drug delivery. *International Journal of Pharmaceutics, 149***,** 139-149.

Moustafine, R. I. & Bobyleva, O. V. (2006). Design of new polymer carriers based of Eudragit E PO/Eudragit L100-55 interpolyelectrolyte complexes using swellability measurements. *Journal of Control Release, 116***,** 35-36.

Moustafine, R. I., Salachova, A. R., Frolova, E. S., Kemenova, V. A. & Van den Mooter, G. (2009). Interpolyelectrolyte complexes of Eudragit® E PO with sodium alginate as potential carriers for colonic drug delivery: monitoring of structural transformation and composition changes during swellability and release evaluating. *Drug Development and Industrial Pharmacy, 35***,** 1439-1451.

Mullan, B. P., Camilleri, M. & Hung, J. C. (1998). Activated charcoal as a potential radioactive marker for gastrointestinal studies. *Nuclear Medicine Communications, 19***,** 237-240.

Munday, D. L., Fassihi, A. R. & De Villiers, C. (1991). Bioavailability study of a theophylline oral controlled release capsule containing film coated mini-tablets in beagle dogs. *International Journal of Pharmaceutics, 69***,** 123-127.

Muraoka, M., Hu, Z., Shimokawa, T., Sekino, S.-i., Kurogoshi, R.-e., Kuboi, Y., Yoshikawa, Y. & Takada, K. (1998). Evaluation of intestinal pressure-controlled colon delivery capsule containing caffeine as a model drug in human volunteers. *Journal of Controlled Release, 52***,** 119-129.

Murata, S., Ueda, S., Shimojo, F., Tokunaga, Y., Hata, T. & Ohnishi, N. (1998). In vivo performance of time-controlled explosion system (TES) in GI physiology regulated dogs. *International Journal of Pharmaceutics, 161***,** 161-168.

Nasmyth, D. G. & Williams, N. S. (1985). Pressure characteristics of the human ileocecal region--a key to its function. *Gastroenterology, 89***,** 345-351.

Nazzal, S., Nazzal, M. & El-Malah, Y. (2007). A novel texture-probe for the simultaneous and real-time measurement of swelling and erosion rates of matrix tablets. *International Journal of Pharmaceutics, 330***,** 195-198.

Neau, S. H., Chow, M. Y. & Durrani, M. J. (1996). Fabrication and characterization of extruded and spheronized beads containing carbopol® 974P, NF resin. *International Journal of Pharmaceutics, 131***,** 47-55.

Newhouse, M. T., Hirst, P. H., Duddu, S. P., Walter, Y. H., Tarara, T. E., Clark, A. R. & Weers, J. G. (2003). Inhalation of a Dry Powder Tobramycin PulmoSphere Formulation in Healthy Volunteers*. *Chest, 124***,** 360-366.

Nivatvongs, S. & Gordon, P. H. (1999). Principles and practice of surgery for colon, rectum, and anus. In 2nd (Ed.) (p. 1360). Informa Healthcare.

Nokhodchi, A., Ford, J. L., Rowe, P. H. & Rubinstein, M. H. (1996). The effects of compression rate and force on the compaction properties of different viscosity grades of hydroxypropylmethylcellulose 2208. *International Journal of Pharmaceutics, 129***,** 21-31.

Nott, K. P. (2010). Magnetic resonance imaging of tablet dissolution. *European Journal of Pharmaceutics and Biopharmaceutics, 74***,** 78-83.

Nunthanid, J., Huanbutta, K., Luangtana-Anan, M., Sriamornsak, P., Limmatvapirat, S. & Puttipipatkhachorn, S. (2008). Development of time-, pH-, and enzyme-controlled colonic drug delivery using spray-dried chitosan acetate and hydroxypropyl methylcellulose. *European Journal of Pharmaceutics and Biopharmaceutics, 68***,** 253-259.

Obeidat, W. M., Abu Znait, A. H. & Sallam, A. S. (2008). Novel combination of anionic and cationic polymethacrylate polymers for sustained release tablet preparation. *Drug Development and Industrial Pharmacy, 34***,** 650-660.

Obeidat, W. M., Abuznait, A. H. & Sallam, A. S. (2010). Sustained release tablets containing soluble polymethacrylates: comparison with tableted polymethacrylate IPEC polymers. *AAPS PharmSciTech, 11***,** 54-63.

Ozeki, Y., Ando, M., Watanabe, Y. & Danjo, K. (2004). Evaluation of novel one-step dry-coated tablets as a platform for delayed-release tablets. *Journal of Controlled Release, 95***,** 51-60.

Ozeki, Y., Watanabe, Y., Inoue, S. & Danjo, K. (2003). Evaluation of the compression characteristics and physical properties of the newly invented one-step dry-coated tablets. *International Journal of Pharmaceutics, 267***,** 69-78.

Pani, R., Pellegrini, R., Cinti, M. N., Trotta, C., Trotta, G., Scafè, R., Betti, M., Cusanno, F., Montani, L., Iurlaro, G., Garibaldi, F. & Del Guerra, A. (2003). A novel compact gamma camera based on flat panel PMT. *Nuclear Instruments and Methods in Physics Research Section A: Accelerators, Spectrometers, Detectors and Associated Equipment, 513***,** 36-41.

Papadimitriou, E., Buckton, G. & Efentakis, M. (1993). Probing the mechanisms of swelling of hydroxypropylmethylcellulose matrices. *International Journal of Pharmaceutics, 98***,** 57-62.

Park, H. M., Chernish, S. M., Rosenek, B. D., Brunelle, R. L., Hargrove, B. & Wellman, H. N. (1984). Gastric emptying of enteric-coated tablets. *Digestive Diseases and Sciences, 29***,** 207-212.

Parr, A., Jay, M., Digenis, G. A. & Beihn, R. M. (1985). Radiolabeling of intact tablets by neutron activation for in vivo scintigraphic studies. *Journal of Pharmaceutical Sciences, 74***,** 590-591.

Patel, P., Missaghi S, Fegely K, Tiwari S & Rajabi-Siahboomi, A. R. (2009). Investigation of the Effect of Tablet Geometry and Film Coating on Drug Release from Hypromellose Matrices at Constant Surface Area to Volume Ratio Using Two Model Drugs. *36thAnnual Meeting and Exposition of the Controlled Release Society.* Copenhagen, Denmark.

Pillay, V. & Fassihi, R. (1999). Electrolyte-induced compositional heterogeneity: a novel approach for rate-controlled oral drug delivery. *Journal of Pharmaceutical Sciences, 88***,** 1140-1148.

Pillay, V. & Fassihi, R. (2000). A novel approach for constant rate delivery of highly soluble bioactives from a simple monolithic system. *Journal of Controlled Release, 67***,** 67-78.

Pocock, G. & Richards, C. D. (2006). Human physiology: the basis of medicine. In 3rd (Ed.). Oxford University Press.

Podczeck, F., Course, N., Newton, J. M. & Short, M. B. (2007a). Gastrointestinal transit of model mini-tablet controlled release oral dosage forms in fasted human volunteers. *Journal of Pharmacy and Pharmacology, 59***,** 941-945.

Podczeck, F., Course, N. C., Newton, J. M. & Short, M. B. (2007b). The influence of non-disintegrating tablet dimensions and density on their gastric emptying in fasted volunteers. *Journal of Pharmacy and Pharmacology, 59***,** 23-27.

Podczeck, F., Course, N. J. & Newton, J. M. (1999). Determination of the gastric emptying of solid dosage forms using gamma-scintigraphy: a problem of image timing and mathematical analysis. *European Journal of Nuclear Medicine and Molecular Imaging, 26***,** 373-378.

Podczeck, F., Mitchell, C. L., Newton, J. M., Evans, D. & Short, M. B. (2007c). The gastric emptying of food as measured by gamma-scintigraphy and electrical impedance tomography (EIT) and its influence on the gastric emptying of tablets of different dimensions. *Journal of Pharmacy and Pharmacology, 59***,** 1527-1536.

Polentarutti, B., Albery, T., Dressman, J. & Abrahamsson, B. (2010). Modification of gastric pH in the fasted dog. *Journal of Pharmcy and Pharmacology, 62***,** 462-469.

Prekeges, J. (2009). Nuclear Medicine Instrumentation. In 1st (Ed.) (p. 313). Sudbury: Jones & Bartlett Learning.

Price, J. M. C., Davis, S. S., Sparrow, R. A. & Wilding, I. R. (1993). The Effect of Meal Composition on the Gastrocolonic Response: Implications for Drug Delivery to the Colon. *Pharmaceutical Research, 10***,** 722-726.

Prisant, L., Michael, E. & William, J. (2003). Drug Delivery Systems for Treatment of Systemic Hypertension. *Clinical Pharmacokinetics, 42***,** 931-940.

Rajabi-Siahboomi, A. R., Bowtell, R. W., Mansfield, P., Davies, M. C. & Melia, C. D. (1993). NMR microscopy studies of swelling and water mobility in HPMC hydrophilic matrix systems undergoing hydration. *Proceeding of international symposium of controlled release and bioactive materials.* 20, (pp. 292-293).

Rajabi-Siahboomi, A. R., Bowtell, R. W., Mansfield, P., Henderson, A., Davies, M. C. & Melia, C. D. (1994). Structure and behaviour in hydrophilic matrix

sustained release dosage forms: 2. NMR-imaging studies of dimensional changes in the gel layer and core of HPMC tablets undergoing hydration. *Journal of Controlled Release, 31*, 121-128.

Read, N. W., Cammack, J., Edwards, C., Holgate, A. M., Cann, P. A. & Brown, C. (1982). Is the transit time of a meal through the small intestine related to the rate at which it leaves the stomach? *Gut, 23*, 824-828.

Rees, W. D. W., Malagelada, J. R., Miller, L. J. & Go, V. L. W. (1982). Human interdigestive and postprandial gastrointestinal motor and gastrointestinal hormone patterns. *Digestive Diseases and Sciences, 27*, 321-329.

Remunan-Lopez, C. & Bodmeier, R. (1997). Mechanical, water uptake and permeability properties of crosslinked chitosan glutamate and alginate films. *Journal of Controlled Release, 44*, 215-225.

Reynolds, T. D., Gehrke, S. H., Hussain, A. S. & Shenouda, L. S. (1998). Polymer erosion and drug release characterization of hydroxypropyl methylcellulose matrices. *Journal of Pharmaceutical Sciences, 87*, 1115-1123.

Reynolds, T. D., Mitchell, S. A. & Balwinski, K. M. (2002). Investigation of the effect of tablet surface area/volume on drug release from hydroxypropylmethylcellulose controlled-release matrix tablets. *Drug Development and Industrial Pharmacy, 28*, 457-466.

Richardson, J. C., Bowtell, R. W., Mader, K. & Melia, C. D. (2005). Pharmaceutical applications of magnetic resonance imaging (MRI). *Advanced Drug Delivery Reviews, 57*, 1191-1209.

Rinaudo, M. (2006). Chitin and chitosan: Properties and applications. *Progress in Polymer Science, 31*, 603-632.

Ritger, P. L. & Peppas, N. A. (1987). A simple equation for description of solute release I. Fickian and non-fickian release from non-swellable devices in the form of slabs, spheres, cylinders or discs. *Journal of Controlled Release, 5*, 23-36.

Robinson, J. W., Frame, E. M. S. & Frame, G. M. (2005). Undergraduate instrumental analysis. In 6th (Ed.). CRC Press.

Rosenberg, J. C. & Didio, L. J. (1970). Anatomic and clinical aspects of the junction of the ileum with the large intestine *Diseases of Colon Rectum, 13*, 220-224.

Ross, A. C., Macrae, R. J., Walther, M. & Stevens, H. N. E. (2000). Chronopharmaceutical Drug Delivery from a Pulsatile Capsule Device based on Programmable Erosion. *Journal of Pharmacy and Pharmacology, 52***,** 903-909.

Rowe, R. C. (1980). The molecular weight and molecular weight distribution of hydroxypropyl methylcellulose used in the film coating of tablets. *Journal of Pharmacy and Pharmacology, 32***,** 116-119.

Rowe, R. C., Sheskey, P. J. & Quinn, M. E. (2009). Handbook of Pharmaceutical Excipients. In 6th (Ed.). London: Royal Pharmaceutical Society, UK.

Rubinstein, A., Nakar, D. & Sintov, A. (1992). Chondroitin sulfate: A potential biodegradable carrier for colon-specific drug delivery. *International Journal of Pharmaceutics, 84***,** 141.

Rujivipat, S. & Bodmeier, R. (2010a). Improved drug delivery to the lower intestinal tract with tablets compression-coated with enteric/nonenteric polymer powder blends. *European Journal of Pharmaceutics and Biopharmaceutics, 76***,** 486-492.

Rujivipat, S. & Bodmeier, R. (2010b). Modified release from hydroxypropyl methylcellulose compression-coated tablets. *International Journal of Pharmaceutics, 402***,** 72-77.

Saffran, M., Kumar, G. S., Savariar, C., Burnham, J. C., Williams, F. & Neckers, D. C. (1986). A new approach to the oral administration of insulin and other peptide drugs. *Science, 233***,** 1081-1084.

Sagawa, K., Li, F., Liese, R. & Sutton, S. C. (2009). Fed and fasted gastric pH and gastric residence time in conscious beagle dogs. *Journal of Pharmaceutical Sciences, 98***,** 2494-2500.

Sako, K., Sawada, T., Nakashima, H., Yokohama, S. & Sonobe, T. (2002). Influence of water soluble fillers in hydroxypropylmethylcellulose matrices on in vitro and in vivo drug release. *Journal of Controlled Release, 81***,** 165-172.

Samani, S. M., Montaseri, H. & Kazemi, A. (2003). The effect of polymer blends on release profiles of diclofenac sodium from matrices. *European Journal of Pharmaceutics and Biopharmaceutics, 55***,** 351-355.

Sangalli, M. E., Maroni, A., Zema, L., Busetti, C., Giordano, F. & Gazzaniga, A. (2001). In vitro and in vivo evaluation of an oral system for time and/or site-specific drug delivery. *Journal of Controlled Release, 73***,** 103-110.

Saravanan, M. & Rao, K. P. (2010). Pectin-gelatin and alginate-gelatin complex coacervation for controlled drug delivery: Influence of anionic polysaccharides and drugs being encapsulated on physicochemical properties of microcapsules. *Carbohydrate Polymers, 80***,** 808-816.

Sarisuta, N. & Mahahpunt, P. (1994). Effects of Compression Force and Type of Fillers on Release of Diclofenac Sodium from Matrix Tablets. *Drug Development and Industrial Pharmacy, 20***,** 1049-1061.

Sathyan, G., Hwang, S. & Gupta, S. K. (2000). Effect of dosing time on the total intestinal transit time of non-disintegrating systems. *International Journal of Pharmaceutics, 204***,** 47-51.

Sato, Y., Kawashima, Y., Takeuchi, H., Yamamoto, H. & Fujibayashi, Y. (2004). Pharmacoscintigraphic evaluation of riboflavin-containing microballoons for a floating controlled drug delivery system in healthy humans. *Journal of Controlled Release, 98***,** 75-85.

Sawada, T., Kondo, H., Nakashima, H., Sako, K. & Hayashi, M. (2004). Time-release compression-coated core tablet containing nifedipine for chronopharmacotherapy. *International Journal of Pharmaceutics, 280***,** 103-111.

Sawada, T., Sako, K., Fukui, M., Yokohama, S. & Hayashi, M. (2003a). A new index, the core erosion ratio, of compression-coated timed-release tablets predicts the bioavailability of acetaminophen. *International Journal of Pharmaceutics, 265***,** 55-63.

Sawada, T., Sako, K., Yoshihara, K., Nakamura, K., Yokohama, S. & Hayashi, M. (2003b). Timed-release formulation to avoid drug–drug interaction between diltiazem and midazolam. *Journal of Pharmaceutical Sciences, 92***,** 790-797.

Schiller, C., Frohlich, C. P., Giessmann, T., Siegmund, W., Monnikes, H., Hosten, N. & Weitschies, W. (2005). Intestinal fluid volumes and transit of dosage forms as assessed by magnetic resonance imaging. *Alimentary Pharmacology & Therapeutics, 22***,** 971-979.

Schott, H. (1992). Swelling kinetics of polymers. *Journal of Macromolecular Science, Part B, 31***,** 1-9.

Schulze, J. D., Peters, E. E., Vickers, A. W., Staton, J. S., Coffin, M. D., Parsons, G. E. & Basit, A. W. (2005). Excipient effects on gastrointestinal transit and drug absorption in beagle dogs. *International Journal of Pharmaceutics, 300***,** 67-75.

Segale, L., Giovannelli, L., Pattarino, F., Conti, S., Maggi, L., Grenier, P. & Vergnault, G. (2010). Thermogravimetric investigation of the hydration behaviour of hydrophilic matrices. *Journal of Pharmaceutical Sciences, 99***,** 2070-2079.

Shafik, A., El-Sibai, O. & Shafik, A. A. (2002). Physiological assessment of the function of the ileocecal junction with evidence of ileocecal junction reflexes. *Medical science monitor : international medical journal of experimental and clinical research, 8***,** CR629-635.

Shameem, M., Katori, N., Aoyagi, N. & Kojima, S. (1995). Oral Solid Controlled Release Dosage Forms: Role of GI-Mechanical Destructive Forces and Colonic Release in Drug Absorption Under Fasted and Fed Conditions in Humans. *Pharmaceutical Research, 12***,** 1049-1054.

Shapiro, M., Jarema, M. A. & Gravina, S. (1996). Magnetic resonance imaging of an oral gastrointestinal-therapeutic-system (GITS) tablet. *Journal of Controlled Release, 38***,** 123-127.

Shibata, N., Ohno, T., Shimokawa, T., Hu, Z., Yoshikawa, Y., Koga, K., Murakami, M. & Takada, K. (2001). Application of pressure-controlled colon delivery capsule to oral administration of glycyrrhizin in dogs. *Journal of Pharmacy and Pharmacology, 53***,** 441-447.

Siepmann, J. & Peppas, N. A. (2001). Modeling of drug release from delivery systems based on hydroxypropyl methylcellulose (HPMC). *Advanced Drug Delivery Reviews, 48***,** 139-157.

Siepmann, J., Podual, K., Sriwongjanya, M., Peppas, N. A. & Bodmeier, R. (1999). A new model describing the swelling and drug release kinetics from hydroxypropyl methylcellulose tablets. *Journal of Pharmaceutical Sciences, 88***,** 65-72.

Siepmann, J. & Siepmann, F. (2008). Mathematical modeling of drug delivery. *International Journal of Pharmaceutics, 364*, 328-343.

Simonsen, L., Hovgaard, L., Mortensen, P. B. & Brondsted, H. (1995). Dextran hydrogels for colon-specific drug delivery. V. Degradation in human intestinal incubation models. *European Journal of Pharmaceutical Sciences, 3*, 329.

Sinha Roy, D. & Rohera, B. D. (2002). Comparative evaluation of rate of hydration and matrix erosion of HEC and HPC and study of drug release from their matrices. *European Journal of Pharmaceutical Sciences, 16*, 193-199.

Sirkiä, T., Mäkimartti, M., Liukko-Sipi, S. & Marvola, M. (1994a). Development and biopharmaceutical evaluations of a new press-coated prolonged-release salbutamol sulphate tablet in man. *European Journal of Pharmaceutical Sciences, 1*, 195-201.

Sirkiä, T., Salonen, H., Veski, P., Jürjenson, H. & Marvola, M. (1994b). Biopharmaceutical evaluation of new prolonged-release press-coated ibuprofen tablets containing sodium alginate to adjust drug release. *International Journal of Pharmaceutics, 107*, 179-187.

Smith, H. J. & Feldman, M. (1986). Influence of food and marker length on gastric emptying of indigestible radiopaque markers in healthy humans. *Gastroenterology, 91*, 1452-1455.

Sriamornsak, P., Thirawong, N. & Korkerd, K. (2007). Swelling, erosion and release behavior of alginate-based matrix tablets. *European Journal of Pharmaceutics and Biopharmaceutics, 66*, 435-450.

Steed, K. P., Hooper, G., Monti, N., Strolin Benedetti, M., Fornasini, G. & Wilding, I. R. (1997). The use of pharmacoscintigraphy to focus the development strategy for a novel 5-ASA colon targeting system ("TIME CLOCK®" system). *Journal of Controlled Release, 49*, 115-122.

Stevens, H. N. E., Wilson, C. G., Welling, P. G., Bakhshaee, M., Binns, J. S., Perkins, A. C., Frier, M., Blackshaw, E. P., Frame, M. W., Nichols, D. J., Humphrey, M. J. & Wicks, S. R. (2002). Evaluation of Pulsincap(TM) to provide regional delivery of dofetilide to the human GI tract. *International Journal of Pharmaceutics, 236*, 27-34.

Strübing, S., Abboud, T., Contri, R. V., Metz, H. & Mäder, K. (2008). New insights on poly(vinyl acetate)-based coated floating tablets: Characterisation of hydration and CO2 generation by benchtop MRI and its relation to drug release and floating strength. *European Journal of Pharmaceutics and Biopharmaceutics, 69***,** 708-717.

Sugito, K., Ogata, H., Goto, H., Noguchi, M., Kogure, T., Takano, M., Maruyama, Y. & Sasaki, Y. (1990). Gastrointestinal transit of non-disintegrating solid formulations in humans. *International Journal of Pharmaceutics, 60***,** 89-97.

Sun, C. (2005). True density of microcrystalline cellulose. *Journal of Pharmaceutical Sciences, 94***,** 2132-2134.

Sundy, E. & Paul Danckwerts, M. (2004). A novel compression-coated doughnut-shaped tablet design for zero-order sustained release. *European Journal of Pharmaceutical Sciences, 22***,** 477-485.

Sungthongjeen, S., Puttipipatkhachorn, S., Paeratakul, O., Dashevsky, A. & Bodmeier, R. (2004). Development of pulsatile release tablets with swelling and rupturable layers. *Journal of Controlled Release, 95***,** 147-159.

Sutch, J. C., Ross, A. C., Kockenberger, W., Bowtell, R. W., MacRae, R. J., Stevens, H. N. & Melia, C. D. (2003). Investigating the coating-dependent release mechanism of a pulsatile capsule using NMR microscopy. *Journal of Controlled Release, 92***,** 341-347.

Synowiecki, J. & Al-Khateeb, N. A. (2003). Production, properties, and some new applications of chitin and its derivatives. *Critical Reviews in Food Science and Nutrition, 43***,** 145-171.

Tahara, K., Yamamoto, K. & Nishihata, T. (1995). Overall mechanism behind matrix sustained release (SR) tablets prepared with hydroxypropyl methylcellulose 2910. *Journal of Controlled Release, 35***,** 59-66.

Tajarobi, F., Abrahmsen-Alami, S., Carlsson, A. S. & Larsson, A. (2009). Simultaneous probing of swelling, erosion and dissolution by NMR-microimaging--effect of solubility of additives on HPMC matrix tablets. *European journal of pharmaceutical sciences, 37***,** 89-97.

Tajiri, S., Kanamaru, T., Yoshida, K., Hosoi, Y., Fukui, S., Konno, T., Yada, S. & Nakagami, H. (2010). Colonoscopic method for estimating the colonic

absorption of extended-release dosage forms in dogs. *European Journal of Pharmaceutics and Biopharmaceutics, 75***,** 238-244.

Takada, K. (1997). Controlled-release preparations. *5637319*. USA.

Takaya, T., Sawada, K., Suzuki, H., Funaoka, A., Matsuda, K.-I. & Takada, K. (1997). Application of a Colon Delivery Capsule to 5-Aminosalicylic Acid and Evaluation of the Pharmacokinetic Profile after Oral Administration to Beagle Dogs. *Journal of Drug Targeting, 4***,** 271-276.

Takayama, T., Goji, T., Taniguchi, T. & Inoue, A. (2009). Chemoprevention of colorectal cancer-experimental and clinical aspects. *The Journal of Medical Investigation, 56***,** 1-5.

Therien-Aubin, H., Baille, W. E., Zhu, X. X. & Marchessault, R. H. (2005). Imaging of High-Amylose Starch Tablets. 3. Initial Diffusion and Temperature Effects. *Biomacromolecules, 6***,** 3367-3372.

Thirawong, N., Nunthanid, J., Puttipipatkhachorn, S. & Sriamornsak, P. (2007). Mucoadhesive properties of various pectins on gastrointestinal mucosa: An in vitro evaluation using texture analyzer. *European Journal of Pharmaceutics and Biopharmaceutics, 67***,** 132-140.

Tiwari, S. B. & Rajabi-Siahboomi, A. R. (2009). Applications of complementary polymers in HPMC hydrophilic extended release matrices. *Journal of Drug Delivery Technology, 9***,** 20-27.

Tse, F. L. S. & Szeto, D. W. (1982). Theophylline bioavailability in the dog. *Journal of Pharmaceutical Sciences, 71***,** 1301-1303.

Tu, Y.-O. & Ouano, A. C. (1977). Model for the Kinematics of Polymer Dissolution. *IBM Journal of Research and Development, 21***,** 131-142.

Ueda, S., Hata, T., Asakura, S., Yamaguchi, H., Kotani, M. & Ueda, Y. (1994). Development of a Novel Drug Release System, Time-Controlled Explosion System (TES). I. Concept and Design. *Journal of Drug Targeting, 2***,** 35-44.

Ugurlu, T., Turkoglu, M., Gurer, U. S. & Akarsu, B. G. (2007). Colonic delivery of compression coated nisin tablets using pectin/HPMC polymer mixture. *European Journal of Pharmaceutics and Biopharmaceutics, 67***,** 202-210.

Varum, F. J. O., Merchant, H. A. & Basit, A. W. (2010). Oral modified-release formulations in motion: The relationship between gastrointestinal transit and drug absorption. *International Journal of Pharmaceutics, 395***,** 26-36.

Vassallo, M., Camilleri, M., Phillips, S. F., Brown, M. L., Chapman, N. J. & Thomforde, G. M. (1992). Transit through the proximal colon influences stool weight in the irritable bowel syndrome. *Gastroenterology, 102***,** 102-108.

Velasco, M. V., Ford, J. L., Rowe, P. & Rajabi-Siahboomi, A. R. (1999). Influence of drug:hydroxypropylmethylcellulose ratio, drug and polymer particle size and compression force on the release of diclofenac sodium from HPMC tablets. *Journal of Controlled Release, 57***,** 75-85.

Vergnaud, J. M. (1993). Liquid transport controlled release processes in polymeric materials: Applications to oral dosage forms. *International Journal of Pharmaceutics, 90***,** 89-94.

Vertzoni, M., Diakidou, A., Chatzilias, M., Söderlind, E., Abrahamsson, B., Dressman, J. & Reppas, C. (2010). Biorelevant Media to Simulate Fluids in the Ascending Colon of Humans and Their Usefulness in Predicting Intracolonic Drug Solubility. *Pharmaceutical Research, 27***,** 2187-2196.

Vervoort, L. & Kinget, R. (1996). In vitro degradation by colonic bacteria of inulinHP incorporated in eudragit RS films. *International Journal of Pharmaceutics, 129***,** 185.

Viridén, A., Abrahmsén-Alami, S., Wittgren, B. & Larsson, A. (2010). Release of theophylline and carbamazepine from matrix tablets - Consequences of HPMC chemical heterogeneity. *European Journal of Pharmaceutics and Biopharmaceutics, 78***,** 470-479.

Vlachou, M., Naseef, H. & Efentakis, M. (2004). Image analysis studies of dimensional changes in swellable hydrophilic polymer matrices. *Polymers for Advanced Technologies, 15***,** 683-689.

Walewijk, A., Cooper-White, J. J. & Dunstan, D. E. (2008). Adhesion measurements between alginate gel surfaces via texture analysis. *Food Hydrocolloids, 22***,** 91-96.

Wang, J., Wen, H. & Desai, D. (2010). Lubrication in tablet formulations. *European Journal of Pharmaceutics and Biopharmaceutics, 75*, 1-15.

Watson, D. G. (2005). Pharmaceutical analysis: a textbook for pharmacy students and pharmaceutical chemists. In 2nd (Ed.). Elsevier/Churchill Livingstone.

Wei, G., Xu, H., Ding, P. T., Li, S. M. & Zheng, J. M. (2002). Thermosetting gels with modulated gelation temperature for ophthalmic use: the rheological and gamma scintigraphic studies. *Journal of Controlled Release, 83*, 65-74.

Weitschies, W., Blume, H. & Mönnikes, H. (2010). Magnetic Marker Monitoring: High resolution real-time tracking of oral solid dosage forms in the gastrointestinal tract. *European Journal of Pharmaceutics and Biopharmaceutics, 74*, 93-101.

Wilding, I. (2002). Bioequivalence testing for locally acting gastrointestinal products: what role for gamma scintigraphy? *Journal of clinical pharmacology, 42*, 1200-1210.

Wilding, I. R., Coupe, A. J. & Davis, S. S. (1991). The role of [gamma]-scintigraphy in oral drug delivery. *Advanced Drug Delivery Reviews, 7*, 87-117.

Wilding, I. R., Coupe, A. J. & Davis, S. S. (2001). The role of gamma-scintigraphy in oral drug delivery. *Advance Drug Delivery Review, 46*, 103-124.

Wilson, C. G. (2010). The transit of dosage forms through the colon. *International Journal of Pharmaceutics, 395*, 17-25.

Wilson, C. G., Washington, N., Greaves, J. L., Kamali, F., Rees, J. A., Sempik, A. K. & Lampard, J. F. (1989). Bimodal release of ibuprofen in a sustained-release formulation: a scintigraphic and pharmacokinetic open study in healthy volunteers under different conditions of food intake. *International Journal of Pharmaceutics, 50*, 155-161.

Wilson, C. G., Washington, N., Greaves, J. L., Washington, C., Wilding, I. R., Hoadley, T. & Sims, E. E. (1991). Predictive modelling of the behaviour of a controlled release buflomedil HC1 formulation using scintigraphic and pharmacokinetic data. *International Journal of Pharmaceutics, 72*, 79-86.

Yakovlev, G. A. (2004). Accuracy of Measurement of Acidogenic Function of the Stomach by Intragastric pH-Metry *Biomedical Engineering, 38*, 292-295.

Yamada, K., Furuya, A., Akimoto, M., Maki, T., Suwa, T. & Ogata, H. (1995). Evaluation of gastrointestinal transit controlled-beagle dog as a suitable animal model for bioavailability testing of sustained-release acetaminophen dosage form. *International Journal of Pharmaceutics, 119***,** 1-10.

Yang, L., Johnson, B. & Fassihi, R. (1998). Determination of continuous changes in the gel layer thickness of poly(ethylene oxide) and HPMC tablets undergoing hydration: a texture analysis study. *Pharmaceutical Research, 15***,** 1902-1906.

Youngberg, C. A., Wlodyga, J., Schmaltz, S. & Dressman, J. B. (1985). Radiotelemetric determination of gastrointestinal pH in four healthy beagles. *American journal of veterinary research, 46***,** 1516-1521.

Youngson, R. (2000). Digestive system. *The Royal Society of Medicine Health Encyclopedia*. Bloomsbury Publishing Ltd.

Yuen, K.-H. (2010). The transit of dosage forms through the small intestine. *International Journal of Pharmaceutics, 395***,** 9-16.

Yuen, K. H., Deshmukh, A. A., Newton, J. M., Short, M. & Melchor, R. (1993). Gastrointestinal transit and absorption of theophylline from a multiparticulate controlled release formulation. *International Journal of Pharmaceutics, 97***,** 61-77.

APPENDIX I RIBOFLAVIN CALIBRATION CURVE AND LINEAR REGRESSION EQUATION

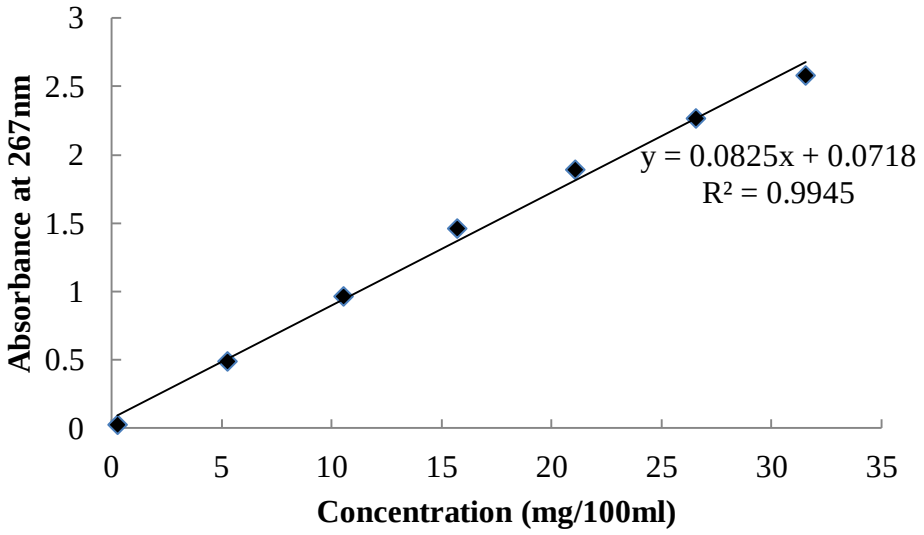

APPENDIX II THEOPHYLLINE CALIBRATION CURVE AND LINEAR REGRESSION EQUATION

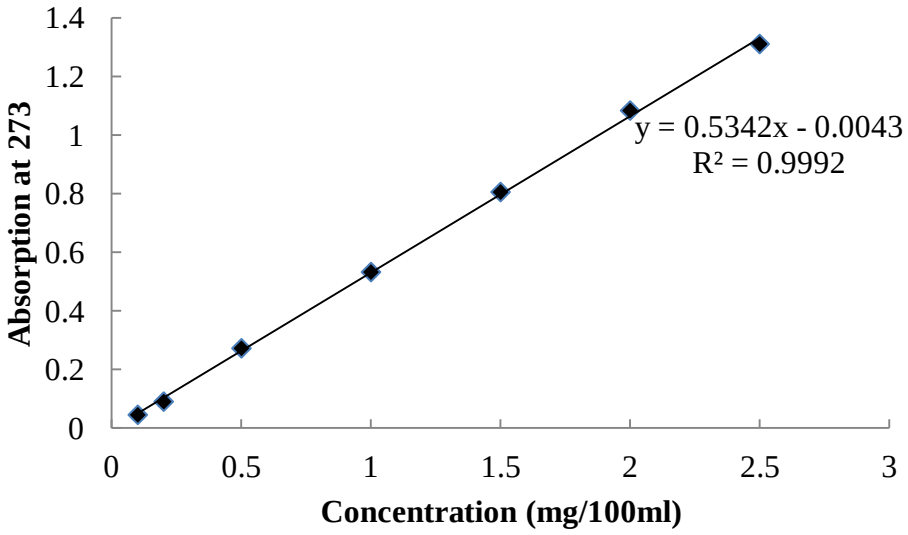

APPENDIX III **CHROMATOGRAM OF BLANK PLASMA SAMPLE (NO SPIKING) USING 18% METHANOL AND 82% PHOSPHATE BUFFER (pH 4.3) CONTAINING NO INTERFERECE PEAK AT RETETION TIME 8.5 MIN WHEN THEOPHYLLINE IS EXPECTED TO ELUTE.**

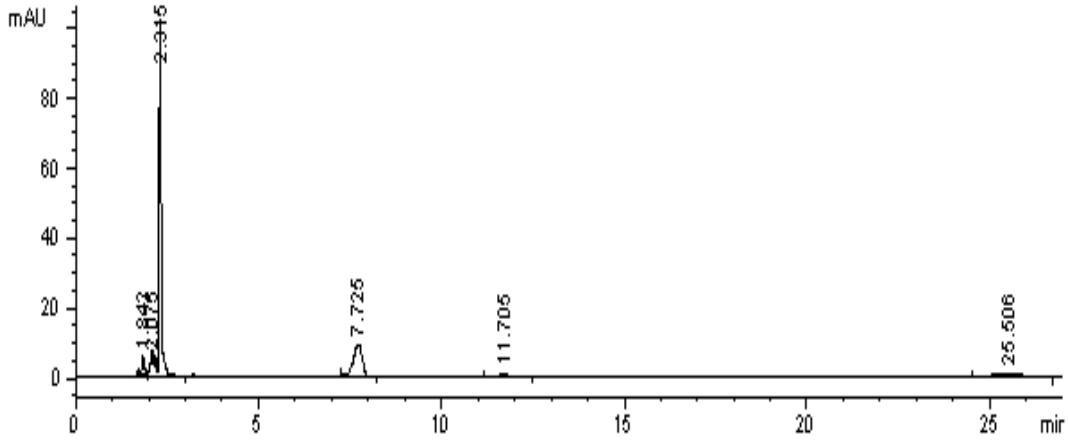

APPENDIX IV **CHROMATOGRAMS OF SPIKED PLASMA SAMPLE CONTAINING THEOPHYLLINE (5µg/ml) AND CAFFEINE (5µg/ml); APPROXIMATE RETENTION TIMES: THEOPHYLLINE = 8.5 MIN; CAFFEINE = 14.8 MIN**

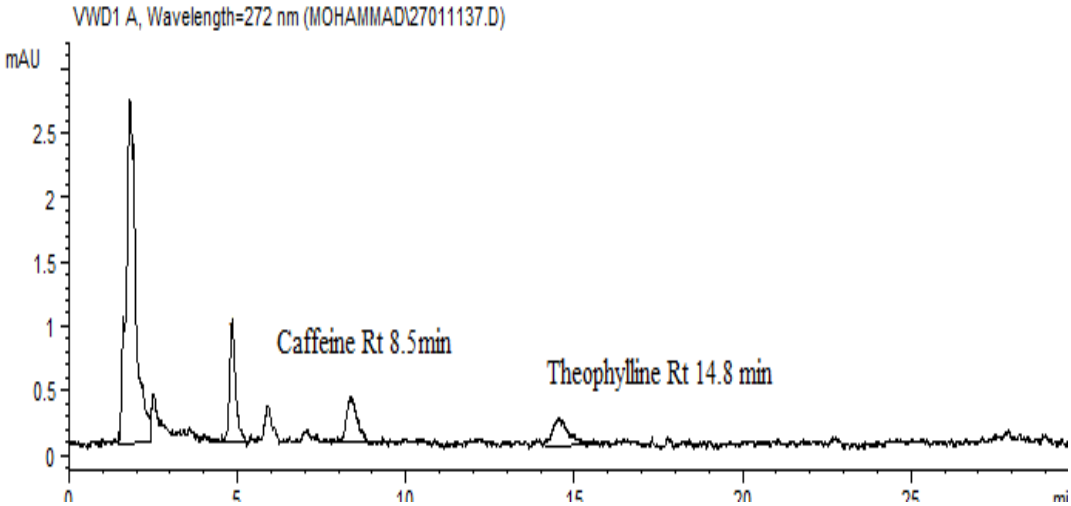

APPENDIX V CALIBRATION CURVE OF THEOPHYLLINE IN PLASMA